



City Research Online

City, University of London Institutional Repository

Citation: Badini, G E. (1995). Investigation of porous glass-like substrates for use in fibre-optic chemical sensors. (Unpublished Doctoral thesis, City, University of London)

This is the accepted version of the paper.

This version of the publication may differ from the final published version.

Permanent repository link: <https://openaccess.city.ac.uk/id/eprint/29327/>

Link to published version:

Copyright: City Research Online aims to make research outputs of City, University of London available to a wider audience. Copyright and Moral Rights remain with the author(s) and/or copyright holders. URLs from City Research Online may be freely distributed and linked to.

Reuse: Copies of full items can be used for personal research or study, educational, or not-for-profit purposes without prior permission or charge. Provided that the authors, title and full bibliographic details are credited, a hyperlink and/or URL is given for the original metadata page and the content is not changed in any way.

**INVESTIGATION OF POROUS GLASS-LIKE SUBSTRATES
FOR USE IN FIBRE-OPTIC CHEMICAL SENSORS**

by G. E. Badini

A thesis submitted for the degree of Doctor of Philosophy

City University

**Department of Electrical, Electronic and Information Engineering
Northampton Square
London EC1V 0HB**

April 1995

Papà - finalmente il tetto!

CONTENTS

	<i>Page</i>
LIST OF FIGURES	
LIST OF TABLES	
DECLARATION	
ACKNOWLEDGEMENTS	
GENERAL ABSTRACT	
CHAPTER 1: INTRODUCTION AND BACKGROUND	
1.1 Introduction	1-1
1.2 Aims and Objectives	1-2
1.3 Structure of The Thesis	1-3
CHAPTER 2: REVIEW OF FIBRE OPTICAL CHEMICAL SENSING	
2.0 Abstract	2-1
2.1 Principle of FOCS	2-1
2.2 Instrumentation in FOCS	2-2
2.2.1 Light Source	
2.2.1.1 Lasers	
2.2.1.2 Lamps	
2.2.1.3 Light Emitting Diodes	
2.2.2 Light Propagation in an Optical Fibre	
2.2.2.1 Total internal Reflection	
2.2.2.2 Number of Modes in a Fibre	
2.2.2.3 Losses in Fibres	
2.2.3 Types of Fibre Optic Configurations	
2.2.3.1 Single Fibre Configurations	
2.2.3.2 Multiple Fibre Configurations	
2.2.3.3. Bifurcated Fibres	
2.2.4 Optical Coupling and Frequency Separation	
2.2.5 Light Detectors	
2.2.5.1 Thermal Detectors	
2.2.5.2 Photon Devices	
2.2.5.3 Choice of Detectors	
2.2.6 Signal Processing	
2.3 Advantages and Disadvantages of FOCS	2-23
2.3.1 Advantages	
2.3.2 Disadvantages	
2.4 Types of Optical Sensors	2-26
2.4.1 Plain Fibre Sensors	
2.4.2 Reservoir Sensors	
2.4.3 Indicator Phase Sensors	
2.4.3.1 Extrinsic Sensors	
2.4.3.2 Intrinsic Sensors	
2.5 Modes of Operation in FOCS	2-30
2.5.1 Absorption-Reflection	
2.5.2 Fluorescence	
2.5.3 Time Resolved Fluorimetry	

2.5.4	Evanescant Wave Sensing	
2.5.5	FOCS based on Energy Transfer	
2.6	Fluorescence-Based FOCS for Measuring pH	2-46
2.6.1	Optical pH Sensing	
2.6.2	Choice of Indicator	
2.6.3	Choice of Substrate	
2.6.4	Methods of Immobilisation	
2.7	Summary	2-54
CHAPTER 3: DESIGN AND CONSTRUCTION OF THE OPTO-ELECTRONIC CONFIGURATIONS		
3.0	Abstract	3-1
3.1	Fibre-Optic Link to a Commercial Spectrophotometer	3-1
3.2	Opto-Electronic Arrangement for FOCS	3-4
3.3	Optical Fibre Bundle	3-5
3.3.1	Components	
3.3.2	Method of Construction	
3.3.3	Number of Fibres	
3.3.4	Mode of Excitation	
3.4	Computer Interface	3-8
3.4.1	Components	
3.4.2	Description of the Computer Interface	
CHAPTER 4: CHOICE OF pH SENSITIVE FLUORESCENT REAGENT		
4.0	Abstract	4-1
4.1	Structure of FITC	4-1
4.2	FITC Solution Spectra Versus Concentration	4-3
4.2.1	UV-VIS Absorbance Spectra	
4.2.1.1	Procedure	
4.2.1.2	Results and Discussion	
4.2.2	Fluorescence Spectra using Fibre-Optic Link to the Spectrophotometer	
4.2.2.1	Procedure	
4.2.2.2	Results and Discussion	
4.2.3	Sensitivity of the Fibre Optic Link to the Spectrophotometer	
4.3	FITC Solution as a Function of pH	4-9
4.3.1	UV-Absorbance Spectra	
4.3.1.1	Procedure	
4.3.1.2	Results and Discussion	
4.3.2	Excitation Spectra	
4.3.2.1	Procedure	
4.3.2.2	Results and Discussion	
4.3.3	Fluorescence Spectra using the Fibre-Optic Link to the Spectrophotometer	
4.3.3.1	Procedure	
4.3.3.2	Results and Discussion	
4.3.4	Fluorescence Spectra using Electro-Optic Arrangement Linked to Ar ⁺ Laser	
4.3.4.1	Procedure	
4.3.4.2	Results and Discussion	
4.4	Summary	4-16

CHAPTER 5: THE USE OF POROUS GLASS IN FOCS

5.0 Abstract	5-1
5.1 Background	5-2
5.1.1 Porous Glass	
5.1.2 Immobilisation of Dye onto Porous Glass	
5.1.2.1 Silane Coupling Agent	
5.1.2.2 Immobilisation Reaction Scheme	
5.2 Experimental Procedure	5-9
5.2.1 Materials and Equipment	
5.2.2 Pretreatment of Porous Glass	
5.2.2.1 Washing of Porous Glass	
5.2.2.2 Thermal Pretreatment of Porous Glass	
5.2.3 Stage 1 Reaction: Silylation of PG Surface	
5.2.4 Stage 2 Reaction: Immobilisation of FITC onto Silylated PG Surface	
5.2.5 Sample Labelling	
5.2.6 Thermal Analysis	
5.2.7 Fluorescence Analysis	
5.3 Results and Discussion	5-12
5.3.1 Appearance of Glass Samples	
5.3.2 Thermal Analysis	
5.3.2.1 Model for the Two-Stage Immobilisation Reaction	
5.3.2.2 Testing the Validity of the Model	
5.3.2.3 Effect of Refluxing PG in 3APTS	
5.3.2.4 Effect of FITC Concentration	
5.3.2.5 Effect of Thermal Treatment	
5.3.3 Fluorescence Analysis	
5.3.3.1 Excitation Spectra	
5.3.3.2 Emission Spectra	
5.4 Summary and Conclusions	5-32

CHAPTER 6: EVALUATION OF SOL-GEL TECHNOLOGY AS A MEANS OF PREPARING MATERIALS USEFUL IN FIBRE OPTIC CHEMICAL SENSING

6.0 Abstract	6-1
6.1 Introduction to Sol-Gel Technology	6-2
6.1.1 Historical Background	
6.1.2 Outline of Sol-Gel Process	
6.1.3 Mixing	
6.1.4 Hydrolysis and Condensation	
6.1.4.1 Hydrolysis	
6.1.4.2 Polymerisation	
6.1.4.3 Influence of Catalyst and pH	
6.1.4.4 Influence of Solvent	
6.1.4.5 Influence of Water	
6.1.5 Structural Evolution: Gelation and Aging	
6.1.6 Drying of Gels	
6.1.7 Heat Treatment of Dried Gels	
6.2 Experimental Investigation of Sol-Gel Formation	6-14
6.2.1 Preliminary Investigations	
6.2.1.1 Preparation of Derivatised Sol-Gel Granules	
6.2.1.2 Preparation of Derivatised Sol-Gel Coating	
6.2.1.3 Preparation of Sol-Gel Monoliths	
6.2.1.4 Use of Drying Control Chemical Additives to Facilitate the Preparation of Gel Monoliths	

6.3 Impregnation of FITC in already formed Gels	6-27
6.3.1 Objective	
6.3.2 Experimental Procedure	
6.3.3 Results and Discussion	
6.3.3.1 Gelation and Drying Stages	
6.3.3.2 Immersion in DMF Solution	
6.3.3.3 Impregnation of FITC into Gel	
6.3.3.4 Effect of Extent of Drying Prior to Impregnation of FITC into Gel	
6.3.3.5 Leaching of FITC from Gel	
6.3.3.6 Fluorescence Response to Varying pH	
6.3.3.7 Fluorescence Response to a Step Change in pH	
6.3.3.8 Effect of Drying Gels after Impregnation with FITC	
6.3.4 Summary	
6.4 Incorporation of FITC into Gel at Sol Stage	6-36
6.4.1 Objective	
6.4.2 Experimental Procedure	
6.4.3 Results and Discussion	
6.4.3.1 Gelation	
6.4.3.2 Difficulties Associated with the Incorporation of 3APTS	
6.4.3.3 Preparation of Gels with Lower Concentrations of H ₂ O - Long Term Observations	
6.4.3.4 Potential Problems Associated with Insufficient Aging or Too-Rapid Drying	
6.4.3.5 Immersing Gels in H ₂ O	
6.4.3.6 Effect of Dry-Wet-Dry Cycles on Gel Structures	
6.4.3.7 Leaching of FITC from Gel	
6.4.3.8 Dissolution of Gels in H ₂ O	
6.4.5 Summary and Conclusions	
6.5 Preparation of FITC Containing Coatings	6-57
6.5.1 Objective	
6.5.2 Experimental Procedure	
6.5.3 Results and Discussion	
6.5.3.1 Appearance of Coatings	
6.5.3.2 Visible Spectra	
6.5.4 Summary and Conclusions	

CHAPTER 7: GENERAL CONCLUSIONS

CHAPTER 8: RECENT ADVANCES IN SOL-GEL DERIVED PROCESSING

CHAPTER 9: SUGGESTIONS FOR FUTURE WORK

9.1 The identification and use of analyte sensitive dyes which exhibit a high quantum yield and low photofading ration.	9-1
9.2 Preparation of true glass substrate using sol-gel method, followed by immobilisation of sensor reagent.	9-1
9.3 Organic-Inorganic Polymer Blends to Improve Structural Stability	9-2
9.4 Alternative routes to immobilise analyte reagents in thin films prepared using sol-gel technology.	9-2
9.5 Investigate the effect of different pore sizes and particle size distributions of porous glass on fluorescence response.	9-3
9.6 Optimisation of optical fibre configuration.	9-4
9.7 Above all, focus on developing FOCS for applications where they are most needed.	9-4

REFERENCES

APPENDIX

LIST OF PUBLICATIONS AND PRESENTATIONS

LIST OF FIGURES

CHAPTER 2: REVIEW OF FIBRE OPTICAL CHEMICAL SENSING

- Figure 2.1 General scheme for a fibre-optic chemical sensor.
Figure 2.2 Typical outputs of some common laser dyes pumped by ion lasers.
Figure 2.3 Emission spectra of different LEDs.
Figure 2.4 Total internal reflection
Figure 2.5 Light propagation in a step index fibre.
Figure 2.6 Ray propagation and electric field distribution of modes in a step index fibre.
Figure 2.7 Attenuation in a typical 600 μm plastic-clad silica fibre.
Figure 2.8 Affect of attenuation factor on transmittance through optical fibres.
Figure 2.9 Single fibre Sensors.
Figure 2.10 Multiple fibre Sensors.
Figure 2.11 Fibre optic for measuring fluorescence emission.
Figure 2.12 (a) Sapphire ball optrode (b) Capillary optrode.
Figure 2.13 (a) Holed-mirror coupler (b) Small prism coupler
Figure 2.14 Idealised wavelength response curve for a photoconductive detector.
Figure 2.15 FOCS literature citations.
Figure 2.16 Example of reservoir sensor.
Figure 2.17 Examples of extrinsic FOCS.
(a) with semipermeable membrane.
(b) without semipermeable membrane.
Figure 2.18 Types of intrinsic FOCS.
(a) Reagent covalently bound to tip of fibre.
(b) Reagent immobilised in core of porous glass fibre.
(c) Reagent immobilised onto surface of fibre core.
(d) Reagent immobilised in fibre core and on fibre surface.
Figure 2.19 Example of TRF measurement cycle.
Figure 2.20 Illustration of the total internal reflection phenomenon: (A) for incident angle equal to the critical angle and (B) for incident angle greater than the critical angle (note the penetration of light across the interface).
Figure 2.21 The use of total internal reflection to probe indicator molecules which are immobilised on the core of an optical fibre.
Figure 2.22 Methods of FIA involving a solid support.
Figure 2.23 Monitoring donor fluorescence (D) in the cases where the acceptor fluorescence signal (a) decreases with analyte concentration or (b) the acceptor fluorescence signal increases with analyte concentration.
Figure 2.24 Overlap of FITC emission spectrum with Rhodamine absorption spectrum.
Figure 2.25 Chemical equilibrium between the acidic and basic forms of phenol red showing isosbestic points at 338, 367 and 480 nm.
Figure 2.26 Different methods of immobilisation of a reagent.

CHAPTER 3: DESIGN AND CONSTRUCTION OF THE OPTO-ELECTRONIC CONFIGURATIONS

- Figure 3.1 Schematic diagram of a fluorescence spectrophotometer.
Figure 3.2 Optical-fibre link to spectrophotometer.
Figure 3.3 Opto-electronic arrangement for FOCS.
Figure 3.4 Number of fibres in fibre optic bundle.
Figure 3.5 Mode of excitation.
Figure 3.6 (a) DATALOG program.
(b) Initialisation and input parameters routine (general)
(c) Data menu routine (general).
Figure 3.7 (a) Manual log data routine.
(b) Auto log data routine.

CHAPTER 4: CHOICE OF pH SENSITIVE FLUORESCENT REAGENT

- Figure 4.1 Structure of FITC (lactoid configuration).
Figure 4.2 Protolytic forms of fluorescein.
Figure 4.3 (a) Absorbance spectra of FITC at different concentrations.
(b) Maximum absorbance values at different concentrations.
Figure 4.4 (a) Fluorescence spectra of FITC at different concentrations using fibre-optic link to spectrophotometer.
(b) Total FITC at different concentrations.
Figure 4.5 Absorbance spectra for FITC at different pH values.
Figure 4.6 Excitation spectra of FITC at different pH values.
Figure 4.7 (a) FITC fluorescence spectra at different pH values.
(b) Total FITC fluorescence at different pH values.
Figure 4.8 (a) FITC fluorescence response to wide pH range.
(b) FITC fluorescence response in critical pH range.
(c) Plot of residuals from regression of linear portion of FITC fluorescence response in critical pH range.

CHAPTER 5: THE USE OF POROUS GLASS IN FOCS

- Figure 5.1 Three component glass system.
Figure 5.2 Porous glass structure.
Figure 5.3 Heat treatment versus pore diameter.
Figure 5.4 Postulated types of hydroxyl groups on amorphous silica surface.
Figure 5.5 Affect of curvature of the silica surface on dehydroxylation.
Figure 5.6 Immobilisation of FITC onto glass.
Figure 5.7 Stage 1 observed weight percents for C and N.
Figure 5.8 Stage 1 calculated carbon and nitrogen loading values.
Figure 5.9 Stage 2 observed weight percents for C and N.
Figure 5.10 Effect of refluxing on the measured carbon and nitrogen contents after stage 1 reaction.
Figure 5.11 Effect of refluxing on the measured carbon and nitrogen contents after stage 2 reaction.
Figure 5.12 Effect of concentration of FITC solution on observed carbon and nitrogen contents.
Figure 5.13 Effect of experimental method on stage 1 on a) PC_{1obs}, b) PN_{1obs}.
Figure 5.14 Comparison of excitation spectra of PG-FITC and FITC.
Figure 5.15 Emission spectrum of dry derivatised PG-FITC.
Figure 5.16 Emission spectrum of PG-FITC at different pHs.
Figure 5.17 (a) Fluorescence response of PG-FITC and FITC between pH 2 and pH 8.
(b) Fluorescence response of PG-FITC and FITC between pH 2 and pH 12.
Figure 5.18 Fluorescence response of PG-FITC to a step change in pH.
Figure 5.19 Fluorescence response of PG-FITC samples.

CHAPTER 6: EVALUATION OF SOL-GEL TECHNOLOGY AS A MEANS OF PREPARING MATERIALS USEFUL IN FIBRE OPTIC CHEMICAL SENSING

- Figure 6.1 Preparation of shaped glasses by the sol-gel process.
Figure 6.2 Acid- and base-catalysed mechanisms for hydrolysis of sol-gel mixture.
Figure 6.3 Inductive effect of substituents on the silicon atom.
Figure 6.4 Gelation in open and closed systems.
Figure 6.5 TGA and DTA of a dry gel.
Figure 6.6 Photograph showing patterns on sol-gel coated slides.
Figure 6.7 Absorption spectra of glass slides through sol-gel coated and uncoated areas.
Figure 6.8 Impregnation of FITC into already formed gel.
Figure 6.9 Graph of weight changes during drying of gel prior to impregnation with FITC solution.
Figure 6.10 Photograph of gels at different stages of drying.
Figure 6.11 Schematic representation of drying of gel.
Figure 6.12 Emission spectra of gels prepared with and without 3APTS.
Figure 6.13 Fluorescence vs pH.
Figure 6.14 Incorporation of FITC into gel network.

- Figure 6.15 Photograph of aged and partially dried gels.
- Figure 6.16 Postulated structure of FITC incorporated into gel network.
- Figure 6.17 Photograph of gels prepared with different H₂O concentrations.
- Figure 6.18 Photographs of a gel immersed in water (illuminated under blue light).
- Figure 6.19 Effect of extent of drying on some gels.
- Figure 6.20 Photographs of gels incorporating FITC after different degrees of drying.
- Figure 6.21 Photographs showing cracking of dry gel on immersion in water.
- Figure 6.22 Microhardness of gels.
- Figure 6.23 Thermal analysis of gels.
- Figure 6.24 Absorbance spectra for pH 7 buffer solution surrounding powdered sol-gel samples impregnated with FITC prepared with and without 3APTS.
- Figure 6.25 Graph of AA of solutions surrounding gels.
- Figure 6.26 Photograph of gels prepared with different concentrations of 3APTS immersed in pH 7 buffer solution.
- Figure 6.27 Photograph of thick coating showing cracks.
- Figure 6.28 Photograph of cracked coating after heating.
- Figure 6.29 Absorption spectra of FITC-in-gel coatings after soaking in solutions of different pHs.

LIST OF TABLES

- Table 2.1 Covalent immobilisation onto polymer surfaces.
- Table 4.1 Absorption maxima of the different protolytic forms of fluorescing and the corresponding pKa values.
- Table 4.2 Data from excitation spectra of FITCaq at different pH values.
- Table 5.1 Effect of temperature on the surface of silica.
- Table 5.2 Thermal pretreatment of porous glass.
- Table 5.3 Summary of observed results compared to theoretical values.
- Table 6.1 Sol-gel coating methods.
- Table 6.2 Appearance of sol-gel coated slides.
- Table 6.3 Compositions of sol-gel mixtures.
- Table 6.4 Influence of reaction parameters on the sol-gel system.
(a) Uncatalysed
(b) Acid Catalysed
(c) Basic Catalysed
- Table 6.5 Composition of FITC-containing sol-gel coating mixtures.
- Table 6.6 Appearance of coatings on microscope slides.

ACKNOWLEDGEMENTS

The Author wishes to express sincere recognition to Professor K.T.V. Grattan of City University for his unrelenting support and encouragement throughout the period FO research and especially in the final stages. Sincere appreciation is also extended to Professor A.C.C. Tseung, presently at the University of Essex, for initiating this study and for his encouragement and motivation throughout.

The writing of this thesis would have been an impossible task without the persistent reassurance of many friends and colleagues and staff at both City University and the University of Essex, and more recently those at Dow Chemical Europe. Friends and family in London and Italy have also been a great source of encouragement throughout the final stage, which would have been a completely unbearable task without the patience and support from my wife, Lucia.

DECLARATION

The Author hereby grants powers of discretion to the City University Librarian to allow the thesis to be copied in whole or in part without further reference to the author. This permission covers only single copies made for study purposes, subject to normal conditions of acknowledgements.

GENERAL ABSTRACT

Fibre optic chemical sensors (FOCSs) are reviewed and a general scheme of a typical sensor is given with details of the various component sections. The interest in FOCSs is presented from the stand-point of the potential advantages which they can offer, but reasons are also proffered for the hitherto small presence of these instruments in the market place. The subject is further developed by considering the types of optical sensors which have been described in the literature. Attention is focussed on the types of sensing materials which have been investigated with particular reference to pH sensing.

A description is given of two opto-electronic configurations which were developed specifically for this investigation. The first consists of a fibre-optic link to a commercial spectrophotometer. The second involved the use of an argon ion laser and was constructed to illustrate some of the other design principles which feature in FOCS. The arrangement of fibres in a simple fibre optic bundle is considered and its optimum configuration is illustrated by experiment.

A data acquisition program which was designed specifically for this work is outlined and, in practice, the use of this program greatly facilitated the acquisition and evaluation of data from the opto-electronic configurations described.

The fluorophore **fluorescein isothiocyanate (FITC)** is discussed and its fluorescence properties are assessed. The suitability of FITC as a pH sensitive reagent is confirmed using the opto-electronic configurations developed for this study.

The use of **porous glass (PG)** as a support for the analyte-sensitive reagent in FOCS is investigated in order to gain further understanding regarding the advantages and disadvantages of the use of PG for such applications. Microanalysis was used in an attempt to assess the effect of certain reaction parameters on the efficiency of each of the two steps involved in immobilising FITC onto the glass surface. The low organic content of the derivatised samples limits the overall usefulness of this analytical approach. Nevertheless, a model is presented which, with some modification, can explain most of the observations concerning the two step immobilisation reaction involving **3-aminopropyltriethoxysilane (3APTS)** and FITC.

It is found that refluxing in 3APTS in the first step significantly improves the loading of the fluorophore on the porous glass, but that the type of porous glass pretreatment and the concentration of the FITC solution do not result in differences which can be measured by conventional microanalysis.

The fluorescence response of the derivative porous glass, both dry and in solution, was recorded. The fibre optic configuration described resulted in strong fluorescent signals but a longer than desirable response time. Generally, it was found that the fluorescence intensity of the dry PG was greater when lower concentrations of FITC had been used in the immobilisation step.

The **sol-gel** process is introduced and its potential applicability to preparing glass-like structures which can be used in FOCS is reviewed and further explored.

The main features of sol-gel processing which are potentially relevant to the preparation of a high surface area solid support for use as a sensor substrate are presented. From the literature reviewed it was not possible clearly to define an ideal sol composition which would lead to a material with properties that could best be tailored to FOCS. Nevertheless, there was much evidence that such a material could be prepared and work was conducted in order to investigate this approach with a view of the possible application of such materials in FOCS.

FITC containing monoliths were prepared by two routes; impregnation of the FITC into already formed gels and the incorporation of FITC into the gel at the sol stage. The properties of these materials are discussed with respect to the applicability in FOCS and their stability, both from the point of view of a wet-dry-wet cycle and in terms of storage stability over a number of years.

The preparation of FITC containing coatings is also discussed and appears to offer the best opportunity for use of this technology in FOCS.



Chapter 1

INTRODUCTION AND BACKGROUND

1.1 INTRODUCTION

The measurement and monitoring of specific compounds plays a significant role in most, if not all, areas of industry and scientific research. For instance, in medicine clinically important parameters such as pH, oxygen and carbon dioxide provide essential information regarding the physiological condition of a patient. The monitoring of species which could have an environmental impact also continues to grow and examples include chlorine and trichloroethylene in drinking water, oil in water, SO₂ in air and a number of other compounds. Other areas where chemical sensing is important include the nuclear industry and, of course, the chemical industry itself.

Sophisticated research in all scientific disciplines provides a background for the development of reliable, accurate and powerful instrumentation for the quantitative analysis of species to a sensitivity in the parts per billion range. Existing analytical methods rely on the transducing effect generated when a parameter is subjected to a physical, chemical or electrical disturbance or a combination of these. In the majority of cases, these methods have been refined over a number of years and give satisfactory performance in good operating conditions, especially for the electronics involved.

Optical methods are widely employed and light ranging from the ultra violet (UV) to the infra-red (IR) is frequently used to detect the presence of specific compounds or to measure the concentration of a particular species. Notwithstanding the well established nature of some of these methods, limitations still exist. For example, most optical-based analysis is done off-line requiring sample collection and precluding a high degree of automation and real-time analysis. Sample preparation is also a critical element in many existing optical techniques and may limit the versatility and convenience of some of the methods as well as having a direct impact on the value of the analyte being measured due to changes occurring between sampling and measurement.

The advent of the laser in the early sixties provided a driving force for further developments and research. Communications, which were at the that time dominated by wire transmission, were the first to take advantage of moving to the optical medium which, in turn, led to technological advances in the fabrication processes of optical glass fibres and the associated opto-electronics.

This opened up the potential for the implementation of many new fibre-optic based analytical methods and also lowered the price of many related components.

Fibre optic chemical sensors (FOCSs) were first developed in the early eighties and have been actively investigated as a result of the many potential advantages they can offer over traditional spectroscopic or electrochemical methods. These advantages centre primarily on their ability to be used invasively and remotely and, potentially, in environments where electrical-based sensors would suffer electromagnetic interference or pose a serious explosion or fire hazard.

FOCSs can be used to monitor chemical conditions, such as the pH of a solution, by monitoring the changes in the optical properties of substances which vary in their optical properties according to the particular chemical condition. Perhaps the simplest examples of such systems are the dyes commonly referred to as indicators. Such indicators change in colour depending upon the pH of the surrounding environment, so that this can be measured by observing this change by simple inspection. Fibre-optic arrangements can be used to quantify the change in colour of a surrounding solution by measuring the absorbance of light of specific wavelengths and in such instances the optical arrangement performs essentially the same task as a spectrometer, except that it performs these operations remotely. Luminescence, rather than absorbance, can also be measured using the same principle and offers an intrinsically more sensitive approach.

Although FOCSs which perform as remote spectrometers could find use in controlled environments, for example laboratories, in practice it is much more desirable to immobilise the sensing chemistry at the distal end of the fibre or on the fibre core and hence eliminate the need for a change in the colour or the fluorescence of the bulk solution itself. Various methods exist to contain an analyte-sensitive reagent at the end of the fibre, the majority of which depend on chemically binding the reagent onto an appropriate organic or inorganic polymeric support. This work focuses on factors affecting the immobilisation of a pH-sensitive fluorophore, fluorescein isothiocyanate (FITC), onto glass and glass-like substrates. Specifically, it looks at aspects relating to the derivatisation of FITC onto commercially available porous glass and the incorporation of this dye into a sol-gel network as the basis of a sensor system.

1.2 AIMS AND OBJECTIVES

The overall objective of this work was to consider aspects which could lead to the development of a FOCS which gives a fast response and high signal intensity. A high signal intensity is important since it enables the use of relatively simple detection equipment and one way to achieve a high signal intensity is to immobilise a large volume of sensing reagent at the end of

the fibre. Unfortunately, depending on the type of immobilisation which is used and the nature of the substrate, a high reagent volume can result in a relatively long response time since mass transfer kinetics rather than actual chemical reaction kinetics will govern the rate-determining step. Since the substrate support plays a critical role in both the amount of reagent which can be immobilised and the rate of response, the main focus of the work which is presently reported relates to its interaction with the dye in the sensing process.

It was decided to consider the measurement of pH since this provided a convenient method to study specific aspects of the substrate support and associated dye properties. It is anticipated, however, that the results of this work can readily be extended to other analytes of interest. The main goals for this work may be summarised as follows:-

- To review the development of FOCS.
- To evaluate and confirm the usefulness of FITC as a suitable reagent for pH FOCS.
- To consider in detail the immobilisation of FITC onto a porous glass substrate and determine the influence of a number of the processing parameters on the final measured fluorescence and potential sensor response.
- To investigate the preparation by the sol-gel method of glass-like substrates and the usefulness of this approach in the making pH sensitive materials for sensor purposes.

1.3 STRUCTURE OF THE THESIS

This thesis is comprised of the work carried out by the author in the course of an investigation of the attainment of the goals given above. Chapter 2 provides a thorough review of the literature concerning FOCS including an overview of the instrumentation used, the advantages and disadvantages of FOCS and the types and modes of operation of FOCS. Particular attention is given to fluorescence-based FOCS for measuring pH.

In Chapter 3, the instrumentation developed and employed for the course of this study is described. Specific aspects of the development work are illustrated using the instruments presented.

Chapter 4 describes and characterises FITC, the pH-sensitive fluorescent reagent which was used throughout this work. Solution spectra as a function of concentration and pH were measured using the instrumentation described in chapter 3 and the dynamic range of FITC is presented for sensor use.

The use of porous glass in FOCS is investigated in Chapter 5. A two step immobilisation reaction is described in detail and a model developed to describe it. The influence of a number

of experimental parameters is investigated and the analysis of the resulting material is also covered.

In Chapter 6, sol-gel technology is introduced and its potential applicability in FOCS described. This chapter contains a review of the sol-gel process and highlights how the properties of the final materials depend on a number of inter-related experimental conditions. The incorporation of FITC into monolithic structures and coatings is described with particular emphasis on their stability both from the point of a wet-dry-wet cycle and in terms of storage stability over a number of years.

The conclusion of this work is presented in Chapter 7, and in Chapter 8, the author's views on the aspect of future work and further developments in this field are given.



Chapter 2

REVIEW OF FIBRE OPTICAL CHEMICAL SENSING

2.0 ABSTRACT

This introduction will cover the general area of fibre optic sensing with a thorough review of the literature and with particular emphasis on fibre optic chemical sensors (FOCSs). A general scheme of a typical sensor is given with details of the various component sections. The interest in FOCSs is argued from the stand-point of the potential advantages which they can offer, but reasons are also proffered for the hitherto small presence of these instruments in the market place. The subject is further developed by considering the types of optical sensors which have been described in the literature. Attention is focussed on the types of sensing materials which have been investigated with particular attention to pH sensing.

2.1 PRINCIPLE OF FOCS

When light interacts with matter a variety of phenomena may occur between the photons of the electromagnetic radiation and the atoms and molecules comprising the material. These interactions involve an exchange of energy and may lead to absorption, transmission, emission, scattering or reflection of the light. Any phenomenon which can cause a change in one of the properties of light can, in theory, be exploited to construct an optical fibre sensor. Consequently, both physical and chemical parameters can be investigated by fibre optic techniques. This review is not concerned with the former group, typical examples of which include sensors for temperature, pressure, flow rates, liquid level and voltage^{1,2}.

Continuous sensing of chemical analytes is a matter of growing interest, especially with the increasing environmental concerns and the economic incentive for real-time analysis. Strictly speaking, a sensor is a device that is able to indicate continuously and reversibly the concentration of an analyte or physical parameter. The term, however, has occasionally been used to describe devices which do not sense continuously, but rather allow only a single, 'one-off', determination. For the sake of distinction the latter shall be referred to as a 'detector', although some authors also use the name 'probe'.

A typical scheme for a FOCS is shown in figure 2.1.

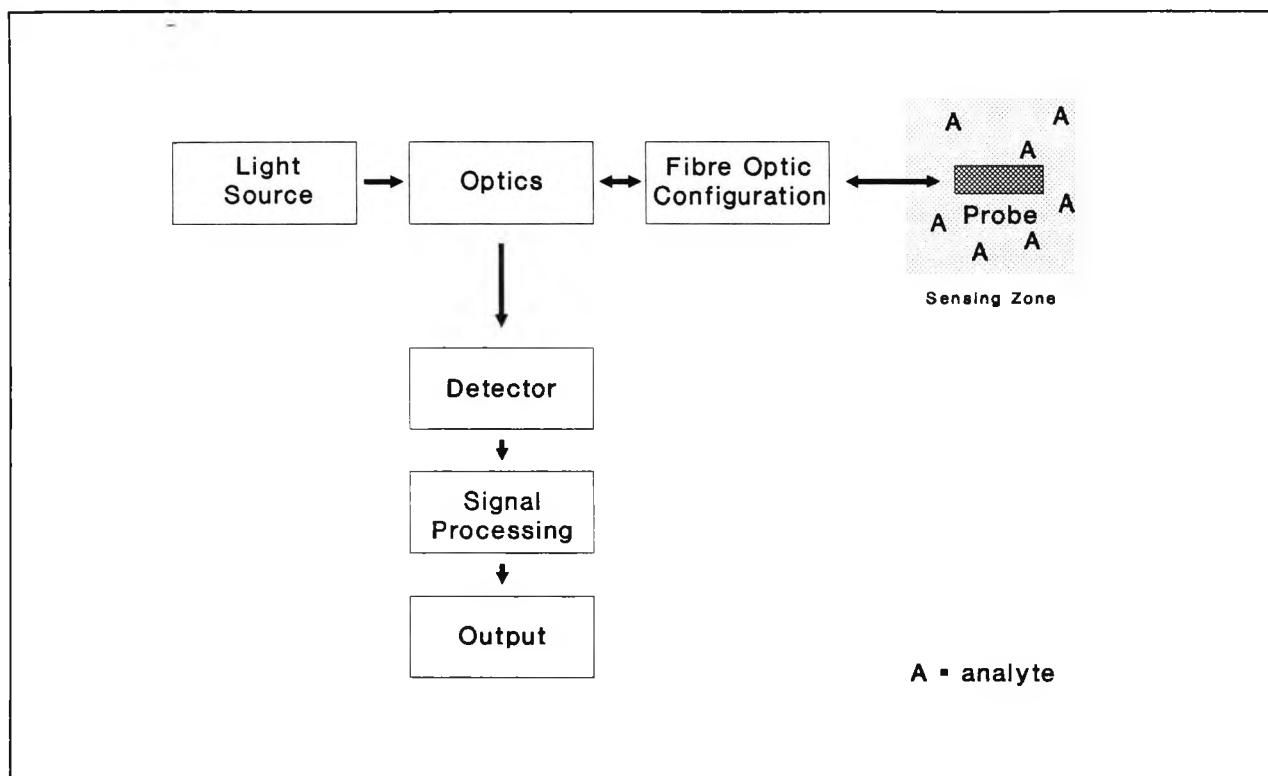


Figure 2.1 General scheme for a fibre-optic chemical sensor.

A FOCS essentially consists of one or more of the following devices: a light source, optical filters and/or beam splitters, a fibre light guide including light couplers and decouplers, a sensing zone or layer, and a light detector which transforms the optical signal into voltage. This voltage can then undergo further signal processing to give the desired and hopefully a meaningful output. In operation, interaction with the analyte leads to a change in the optical properties of the reagent phase, which is probed and detected through the fibre optic.

2.2 INSTRUMENTATION IN FOCS

As has been shown, a FOCS typically consists of a number of specific components and in this section, these components are considered separately.

2.2.1 LIGHT SOURCE

The primary factors to consider when selecting a light source for luminescence instrumentation are the intensity of the radiation available (also known as radiance or brightness), the wavelength distribution of the emitted light and the stability of the emission over time. The following light sources have been reported with use in FOCS: lasers; xenon

lamps, hydrogen, deuterium, mercury, tungsten and halogen lamps; and light-emitting diodes (LEDs).

2.2.1.1 LASERS

All the main classes of lasers have been investigated in conjunction with FOCSs. Perhaps the most arresting feature of laser light is its directionality. Apart from some semiconductor junction lasers, lasers emit radiation in a highly directional, collimated beam with a low angle of divergence. This makes coupling to the fibre optic configuration much more efficient. Lasers typically have radiation of a higher brightness than other light sources which makes them extremely useful for transmission of light over long distances. Another feature of lasers is that they emit light which is monochromatic, which in FOCS facilitates the spectral separation between the excitation and emission radiations.

In FOCSs, lasers are employed in two very distinct ways. In the first case, they are used as a means of providing a convenient light beam, where the value of the wavelength is not relevant, alternatively they are used to provide excitation radiation for absorbance or fluorescence analysis in which case the value of the wavelength is quite critical.

The most commonly used lasers in FOCSs are *gas lasers* of the types He-Ne (wavelength: 633, 543, 1153nm; typical continuous wave (CW) power: 1.0-10.0 mW; price: low) and argon ion (wavelengths 488, 514nm; typical CW power: 10.0 mW-1.0 W; price: low-medium). The He-Ne laser invariably falls into the first type of application³ or alternatively is used as a means for aligning the optical arrangement. The Argon ion laser is widely used in conjunction with the dye fluorescein, which absorbs strongly at 488nm^{4,5}. It must also be said that another reason for using the argon ion laser, especially in situations where such brightness is not required and must often be reduced, is that there have traditionally been no convenient powerful alternatives, for example such as blue LEDs, although this field is developing rapidly.

Semiconductor lasers are quite similar in principle to LEDs. There are two main categories depending on the form of the junction between the semiconducting p-type or n-type materials. The *homojunction semiconductor diode lasers* (e.g. GaAs) can usually only be operated in pulsed mode at room temperature because the threshold pumping current density required is so high, being typically of the order of 400 mm⁻². Also, the narrow width of the junction causes a large fan-shaped beam, which render these types of laser diodes difficult to couple to fibres. Recent reports⁶, however, suggest that this problem might be overcome by producing smooth-surfaced hyperbolic lens on the tips of optical fibres. *Heterojunction semiconductor laser diodes* permit the use of low threshold currents and continuous wave (CW) operation. The stripe geometry of the different types of semiconducting materials has the further advantages that the radiation is produced from a small area, so coupling to fibres is

much more efficient. However, laser diodes are severely limited in their application in FOCSs because they typically emit at wavelengths above 700nm. Frequency doubling may be one approach to overcome this restriction.

The final class of lasers that shall be mentioned are the *dye lasers* in which the active medium is an organic dye dissolved in a solvent. The dye is excited by short wavelengths, normally by other laser lines. Many dyes have been used as the laser media so that it is possible to cover the complete spectral range (figure 2.2). Furthermore, significant tuning can be achieved using a prism, wedge filter or a diffraction grating, by employing only a single dye. Rhodamine 6G in methanol is a good example with a tuning range from 570 to 600nm. Apart from the cost, a limitation of these types of lasers is that they must normally be driven by high frequency pulses or powerful CW lasers e.g. argon ion. Dye lasers have not been widely reported in the literature in connection with FOCS, but their use should become more common should their cost be reduced.

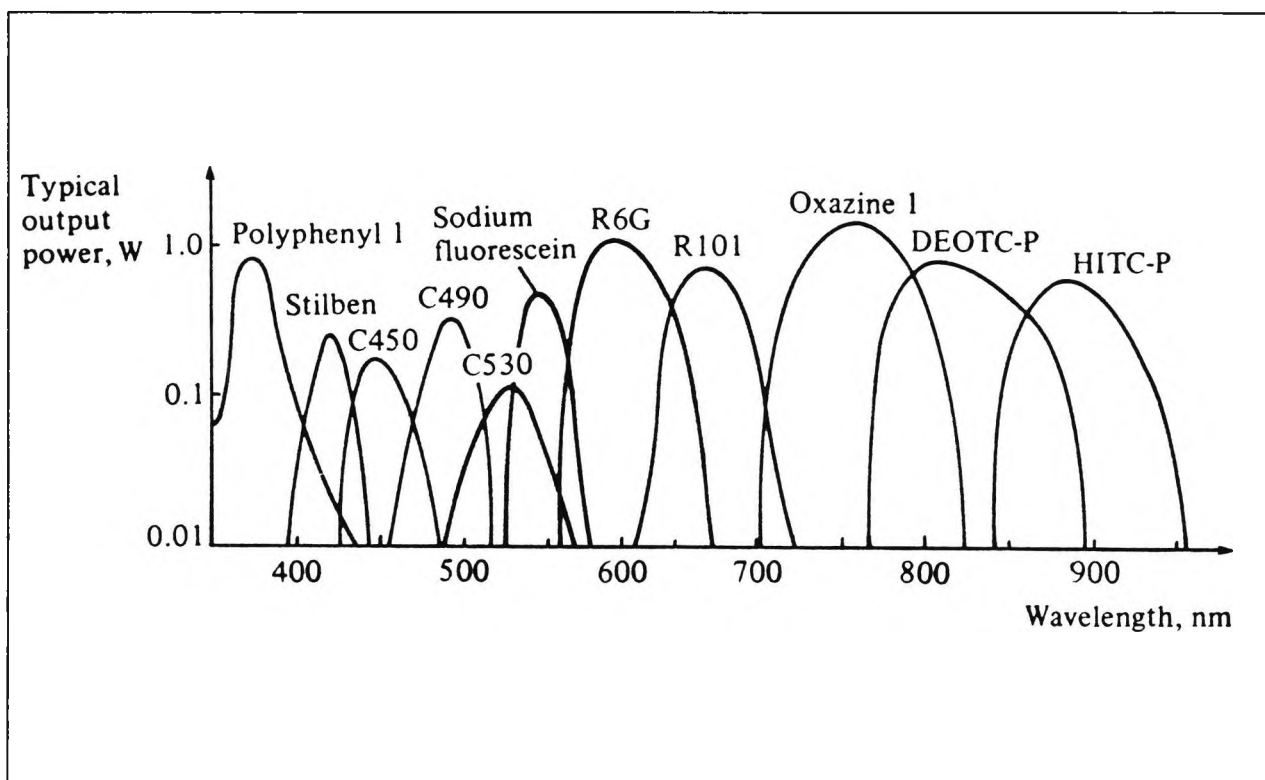


Figure 2.2 Typical outputs of some common lasers dyes pumped by ion lasers⁷.

2.2.1.2 LAMPS

Lamps fall into two broad groups; arc discharge lamps and incandescent filament lamps and are by far the most commonly reported light sources for FOCS.

Incandescent tungsten-halogen filament lamps give continua over the range 350nm to 2.5 μ m, are relatively cheap and their output is normally very stable around the maxima. They

suffer from the fact that they produce a lot of heat, have short lifetimes and a low intensity in the spectral range below about 400nm. Nevertheless, their spectral range above 500nm is of sufficient intensity to excite even weak fluorophores and so their use tends to be reported quite widely in the literature^{e.g.8,9}.

Of the discharge lamps, the xenon, or occasionally krypton, lamp is the most common. The former type is often used in commercial spectrophotometers. Their spectral range, extending from UV (where intensity is low) to the IR, is almost ideal for FOCS. Continuously burning xenon and krypton lamps have several drawbacks in that they are expensive, have limited lifetimes and require higher electrical power than do other conventional sources. Pulsed xenon lamps overcome some of these short-comings but may require signal averaging to overcome the variation in pulse characteristics such as are caused by arc-wandering.

Hydrogen and deuterium discharge lamps are very useful sources for UV excitation. However, since UV-transparent fibres are expensive and because the cost of the associated UV spectroscopy itself is generally higher, these lamps are infrequently used in FOCS.

2.2.1.3 LIGHT EMITTING DIODES

LEDs are semiconductor devices which possess many of the properties desirable for FOCS. They are run at low voltage and current, typically 2.5-3.5V at 20mA, and are therefore ideal for portable instrumentation. Although they produce small light intensities (about 2 millicandela, where 1 candela = 1.5mW sr^{-1} at $\lambda = 550\text{nm}$) they have extremely long life-times, good spectral constancy and a high mechanical stability. The materials that are frequently used are group III-V compounds such as gallium arsenide phosphide ($\text{GaAs}_{1-x}\text{Px}$), gallium phosphide (GaP), gallium aluminium arsenide ($\text{Ga}_{1-x}\text{Al}_x\text{As}$) and silicon carbide (SiC). Typical emission spectra are shown below.

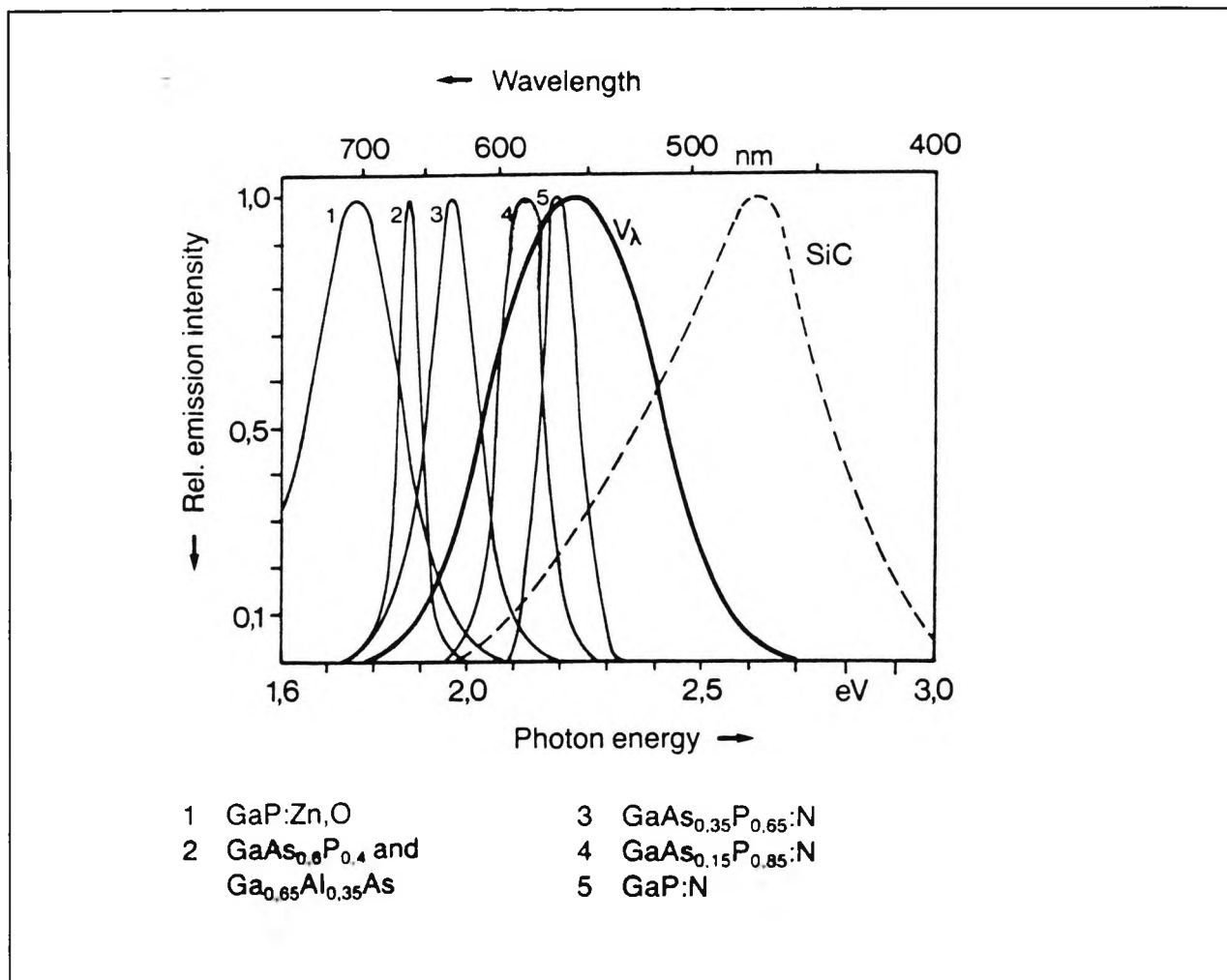


Figure 2.3 Emission spectra of different LEDs¹⁰

LEDs have been used as simple, low-cost light sources¹¹. However, another very attractive feature of LEDs is that they have very short response times (typically 1-10 μ s) and can be driven by simple electronic circuitry so that their modulation in the kHz to MHz frequency domain is comfortably attainable. In FOCSs, this is important because it means that mechanical "chopping" or modulation of the light can be avoided. Consequently, LEDs are ideal for use in fluorescence decay time applications¹². In recent years, blue LEDs have been developed which emit light many times the intensity of the brightest SiC and this should further increase their usage in sensor applications.

2.2.2 LIGHT PROPAGATION IN AN OPTICAL FIBRE

2.2.2.1 TOTAL INTERNAL REFLECTION

When an electromagnetic wave is incident upon the boundary between two dielectric media whose refractive indices are n_1 and n_2 ($n_1 > n_2$) then the refracted ray (ray 1) makes an angle θ_2 with the normal to the surface where $n_1 \sin \theta_1 = n_2 \sin \theta_2$ (Snell's Law). At the critical angle

($\theta_1 = \theta_c$), $\theta_2 = 90^\circ$ (ray 2) and the refracted ray emerges along the interface. (The relationship between the two reflection indices and θ_c simply reduces to $\sin\theta_c = n_2/n_1$). At angles greater than θ_c (ray 3), the ray is totally internally reflected into the first medium. (In fact, light is not instantaneously reflected when it reaches the interface, instead the light just penetrates the optically rare phase giving rise to an evanescent wave.)

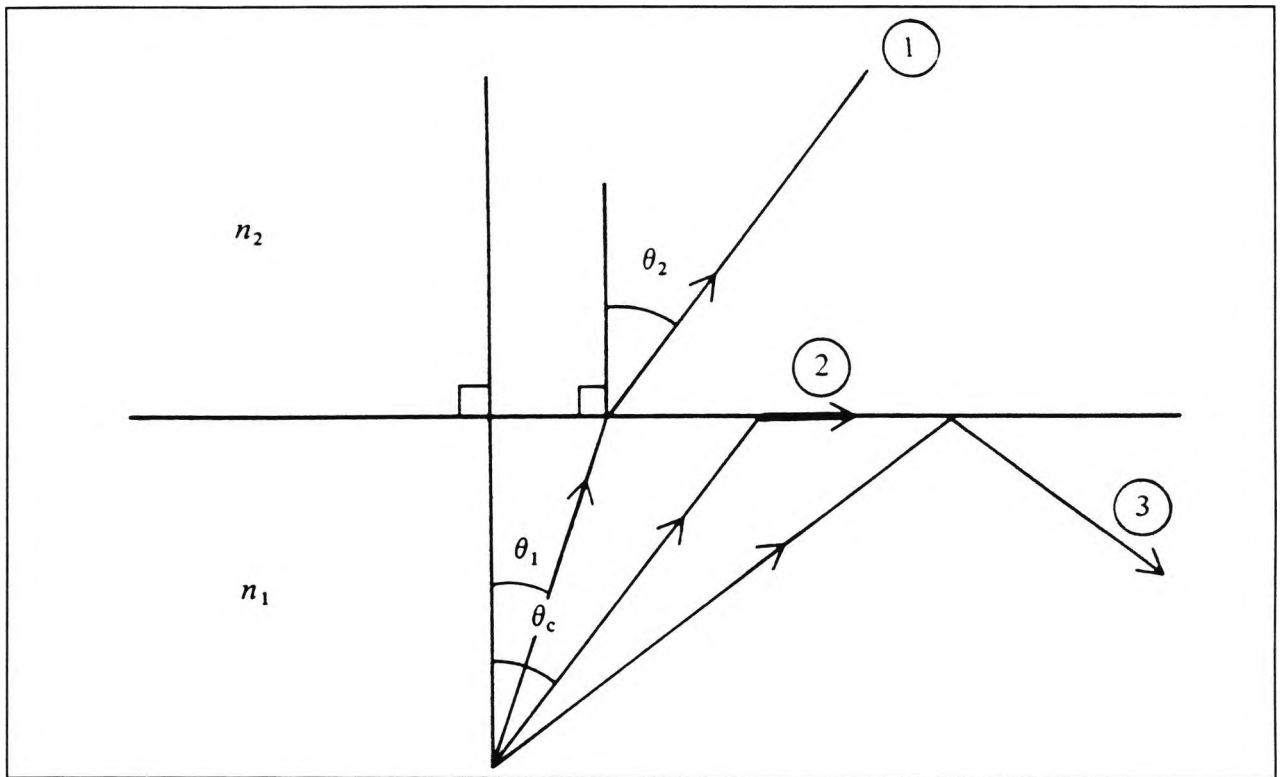


Figure 2.4 Total internal reflection

The principle of total internal reflection is fundamental to the light-guiding properties of optical fibres. One type of optical fibre consists of a central core of transparent material such as high purity silica or plastic and a concentric outer cladding of a lower refractive index. This construction, known as a step-index type fibre, causes light which is launched in at one end to be totally internally reflected at the core-cladding interface, thus trapping the light in the core which then acts as an optical waveguide. Figure 2.5 considers a ray that passes through the centre of the guide.

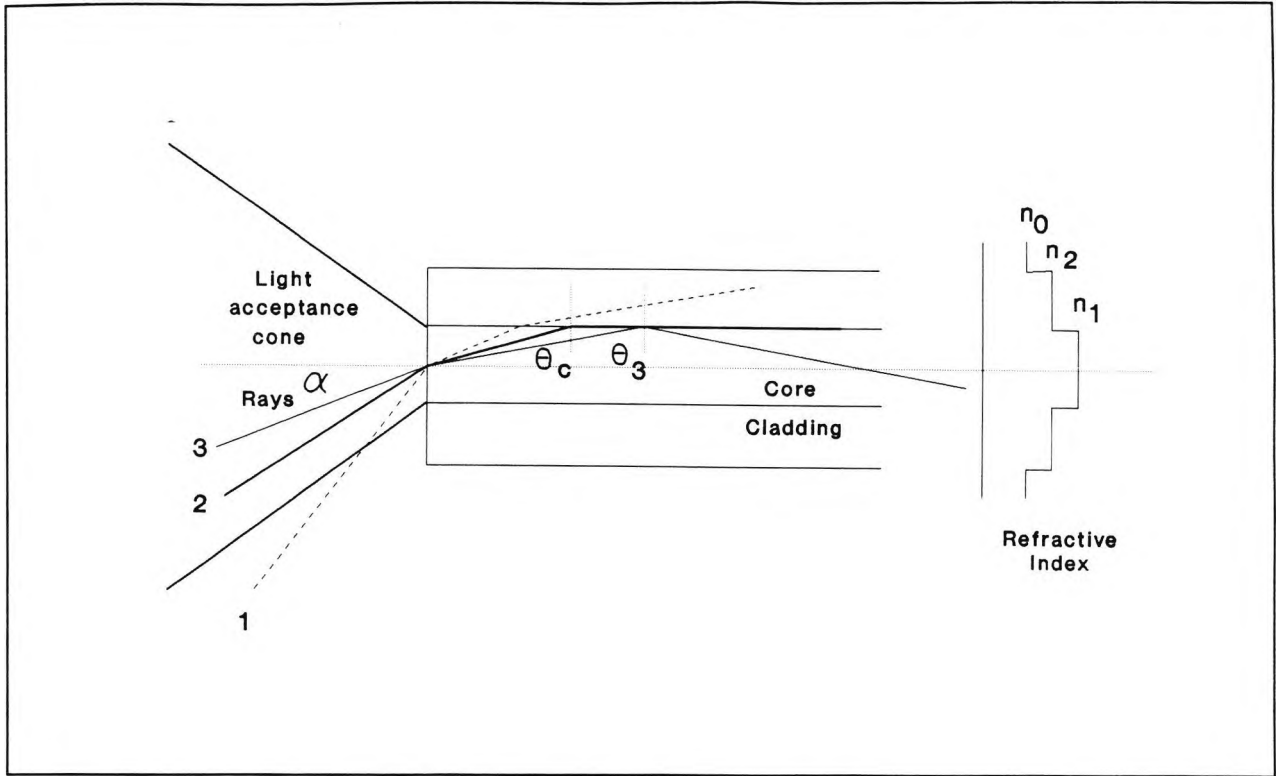


Figure 2.5 Light propagation in a step index fibre.

When the angle α that the ray in the external medium (usually air) makes with the normal to the end of the guide results in an internal angle, θ_3 , which is greater than the critical angle for the core-cladding interface, then total internal reflection will take place (ray 3). α is related to θ_3 by Snell's law such that:

$$n_0 \sin \alpha = n_1 \sin(90 - \theta_3)$$

The maximum value that α can take which will result in light propagation along the fibre is determined by the minimum value that θ_3 can take which, of course, is the critical angle i.e. $\theta_3 = \theta_c$ (ray 2).

$$\begin{aligned} \sin \alpha_{\max} &= \frac{n_1 \sin(90 - \theta_c)}{n_0} \\ &= \frac{n_1 \cos(\theta_c)}{n_0} \end{aligned}$$

This gives

$$\begin{aligned} n_0 \sin \alpha_{\max} &= n_1 (1 - \sin^2 \theta_c)^{1/2} \\ &= (n_1^2 - n_2^2)^{1/2} \end{aligned}$$

The quantity $(n_1^2 - n_2^2)^{1/2}$ is known as the *numerical aperture (NA)* of the fibre and hence (since for air $n_0=1$)

$$\alpha_{\max} = \sin^{-1} \text{NA}$$

The NA describes the cone within which light is accepted and guided by the fibres. α_{\max} is known as the *fibre acceptance angle* and $2\alpha_{\max}$ is sometimes used and is called the *total acceptance angle*. When $\alpha > \alpha_{\max}$ (ray 1), the light strikes the core-cladding boundary at an angle greater than θ_c and then only partial reflection takes place and some of the energy is lost by refraction into the cladding. After several successive reflections, very little energy is left in the core and guidance is lost. This factor, the NA, is important in selecting a fibre for a specific sensor application.

2.2.2.2 NUMBER OF MODES IN A FIBRE

When entrapped in a fibre, light propagates in different *modes*. Waveguide modes represent the radial (or transverse) electric and magnetic field intensity distributions of standing electromagnetic waves within the fibre cross-section. The modes arise as a result of constructive and destructive interference of the electromagnetic fields associated with each family of rays that have the same angle and propagate simultaneously along the fibre in a zig-zag motion as a result of successive reflections at the core-cladding interface.

The phase shift which is introduced between the incident and reflected rays is a function of the angle of incidence, α , therefore it follows that for a particular set of fibre parameters, only certain values of α will be supported and each of these will give rise to a distinct wave pattern or mode. In fact, the mode of propagation is determined by the angle of light entry, characteristics of the waveguide and light wavelength⁷.

Figure 2.6 shows the rays for the three lowest modes (mode number $N = 0, 1$ and 2), and the corresponding electric field distributions in the transverse direction. π represents the distance along the diameter of the fibre between two successive nodes formed as a result of the interference of two rays travelling down the fibre with the same angle of incidence. It can be noted that the exponentially decreasing electric fields extend beyond the surface of the light guide and into the cladding and that the higher order modes have a greater intensity at a given distance than do the lower order modes. This evanescent tail represents an electromagnetic field that oscillates at the frequency of the incident light but does not propagate along the second medium. The field is strong only near the interface between the core and the outer medium and in FOCS this feature has been used to induce the fluorescence of an absorbed indicator or analyte and hence provide the sensing region. FOCSs which use this evanescent mode are described in more detail in a later section.

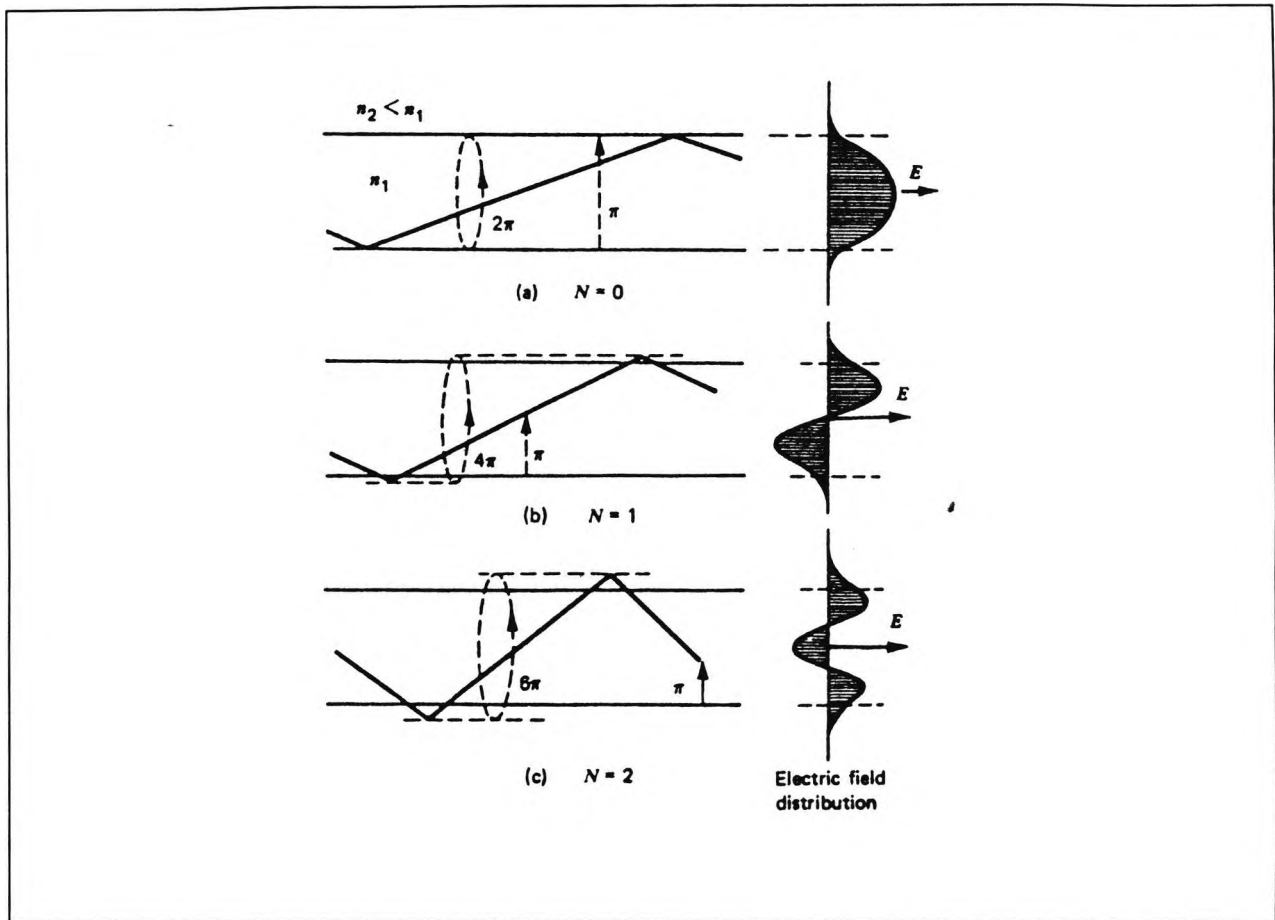


Figure 2.6 Ray propagation and electric field distribution of modes in a step index fibre.

The approximate total number of modes which can be propagated can be calculated by the equation⁷:

$$N = \frac{V^2}{2}$$

where

$$V = \frac{2\pi a(n_1^2 - n_2^2)^{1/2}}{\lambda_0}$$

where a = radius of fibre core
 λ_0 = wavelength of the radiation

For $V < 2.405$ only one mode may be propagated. Such so-called single mode fibres have very small diameters and can only accommodate the propagation of light along one path. Coupling

useful in some sensor applications where the measurand may act directly on the fibre to change properties such as refractive index, path length or plane of polarization. These intrinsic-type sensors can be applied to measuring a variety of physical parameters for example pressure, temperature or electric fields.

Modal dispersion can also be partly alleviated by having a core with a refractive index decreasing with distance from the centre of the core to the core/cladding interface. This arrangement ensures that the further away from the centre the light strays, the faster it will travel and the more it is refracted back to the centre. This has the overall effect of speeding up the slower modes and hence reducing the overall dispersion of the light signal. Fibres having a refractive index gradient are known as graded index fibres.

Although modal dispersion in certain types of FOCSs (e.g. evanescent wave) can lead to reduced accuracy in the prevention of source modal integrity is not a prerequisite in all cases. This means that large diameter fibres can be used. These are able to carry more energy and are much easier to utilise. Typical sizes range from 200 to 1000 μm and are thus capable of allowing the propagation of many hundreds of modes, although the larger fibres tend to be quite inflexible and relatively costly.

2.2.2.3 LOSSES IN FIBRES

Some losses in radiation arise as a result of the very nature of the fibres themselves. One of the causes of this intrinsic attenuation is Rayleigh scattering, which is caused by micro-fluctuations (small compared to the light wavelength) in the index of refraction of the fibre. The attenuation coefficient for Rayleigh scattering increases as the inverse of the fourth power of the wavelength. Losses also occur due to the microscopic compositional irregularities and "impurities" (intentional or unintentional) which are present in the fibre down to ppb levels. IR absorption at the longer wavelength arises due to SiO_2 molecular resonance. As a consequence, although silica fibres are a good choice in the 0.2 to 2 μm range, operation in the 3 to 10 μm range (within which lies the C-H vibrational band) requires glasses composed of more exotic materials such as fluoride, ZnCl and KCl^{139,140}. Figure 2.7 illustrates the attenuation behaviour in a typical multimode silica fibre.

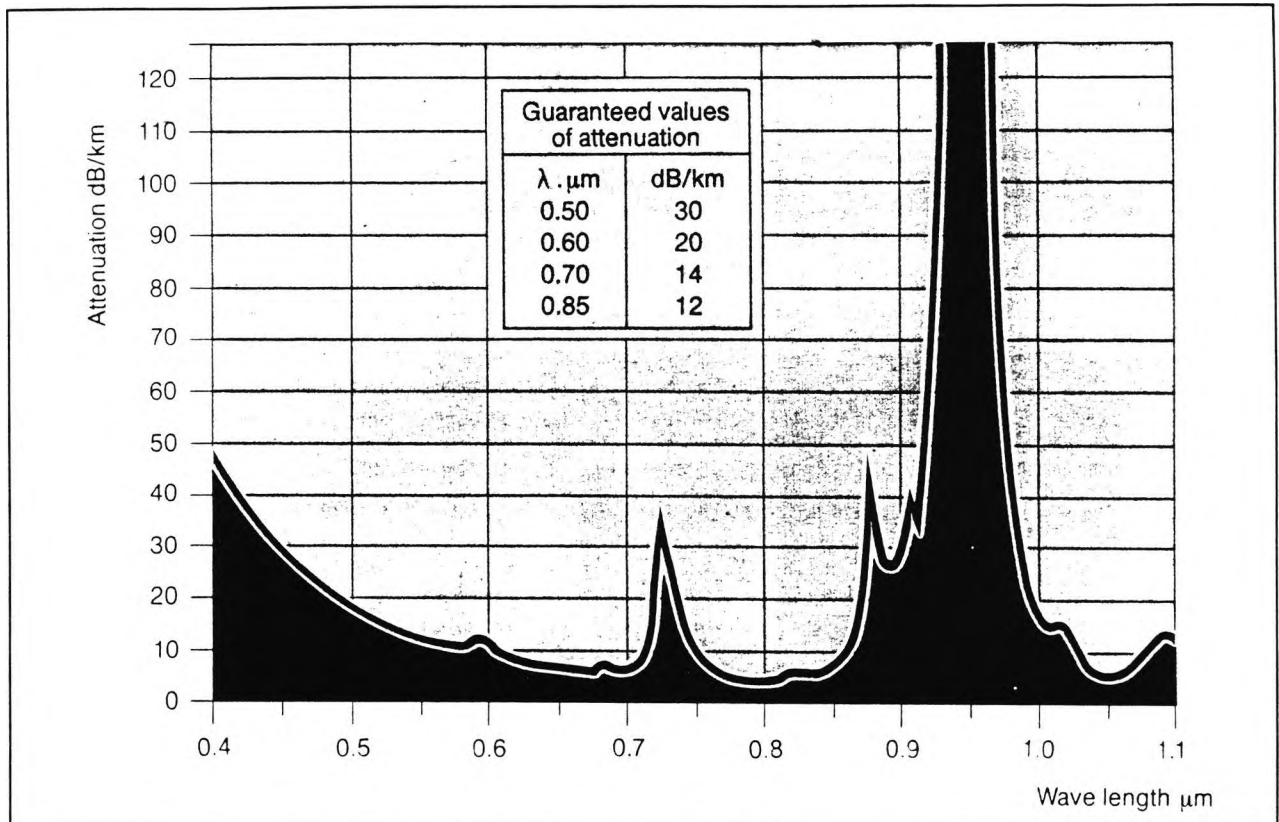


Figure 2.7 Attenuation in a typical 600μm plastic-clad silica fibre¹⁴.

The extent to which an optical fibre absorbs light power may be expressed as an attenuation factor A , independent of wavelength in such a way that

$$A = \frac{10 \log_{10}(P_i/P_f)}{L}$$

- where
- A = attenuation in dB km^{-1}
 - P_i = power of launched light
 - P_f = power of exit light
 - L = distance the ray travels through the medium (km)
(\approx length of fibre)

Fibres with losses between 0.1 and 0.05 dB/km are "state of the art", especially for long range communication purposes, but lower loss fibres are under development in particular for the short (UV) and longer ($\lambda \geq 2\mu\text{m}$) regions. For FOCSs, the optical fibres have to carry what is usually visible light or UV to and from the measuring zone. From figure 2.7, for the fibre discussed, it can be seen that at a $\lambda = 500 \text{ nm}$ the attenuation is around 20 dB/km. Figure 2.8 shows the effect of such an attenuation on the transmittance (P_f/P_i) through the fibre and this is compared with the effect of an attenuation at $\lambda = 800\text{nm}$ of 3 dB/km. FOCS based on visible

light and involving long distances is obviously much less efficient than the infra-red wavelengths used for telecommunication purposes.

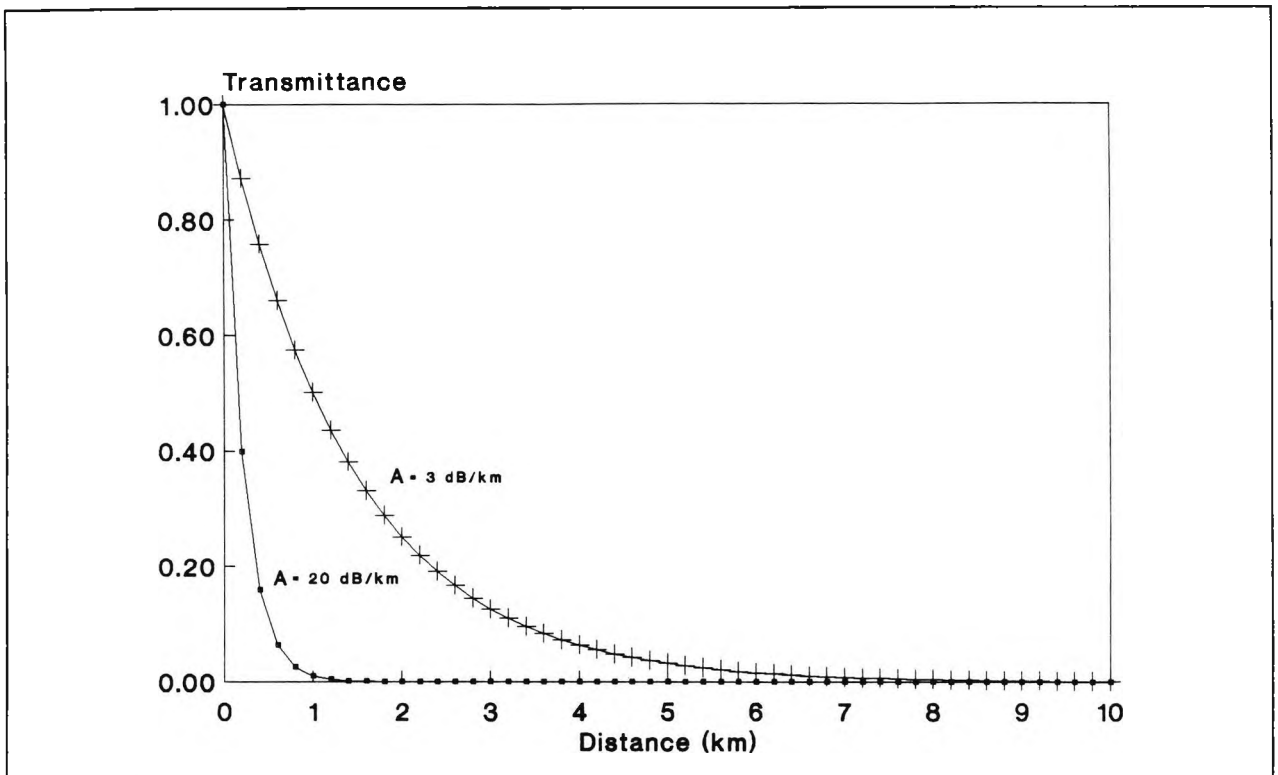


Figure 2.8 Affect of attenuation factor on transmittance through optical fibres

2.2.3 TYPES OF FIBRE OPTIC CONFIGURATIONS

Since it determines the complexity of the optical coupling required, the fibre optic configuration has a great influence on the overall efficiency of the sensor. The different types of configurations are discussed below.

2.2.3.1 SINGLE FIBRE CONFIGURATIONS

There are at least two very different ways of utilizing a single fibre in a FOCS. In the first type (figure 2.9a), excitation light is emitted from the distal end of the fibre and interacts with the analyte which is present in the measuring zone. The modulated light is reflected back along the same fibre to the detector.

The second type (figure 2.9b) is based on evanescent wave sensing and has seen much interest in a number of types of studies^{15,16,17}. The measuring zone in this case is restricted to about 50 to 1200nm above the fibre core surface, but this configuration provides a spatially selective means for very analyte-selective detection. In order to prevent an interfering signal from the bulk measuring zone it may be necessary to terminate the distal end with an opaque cap.

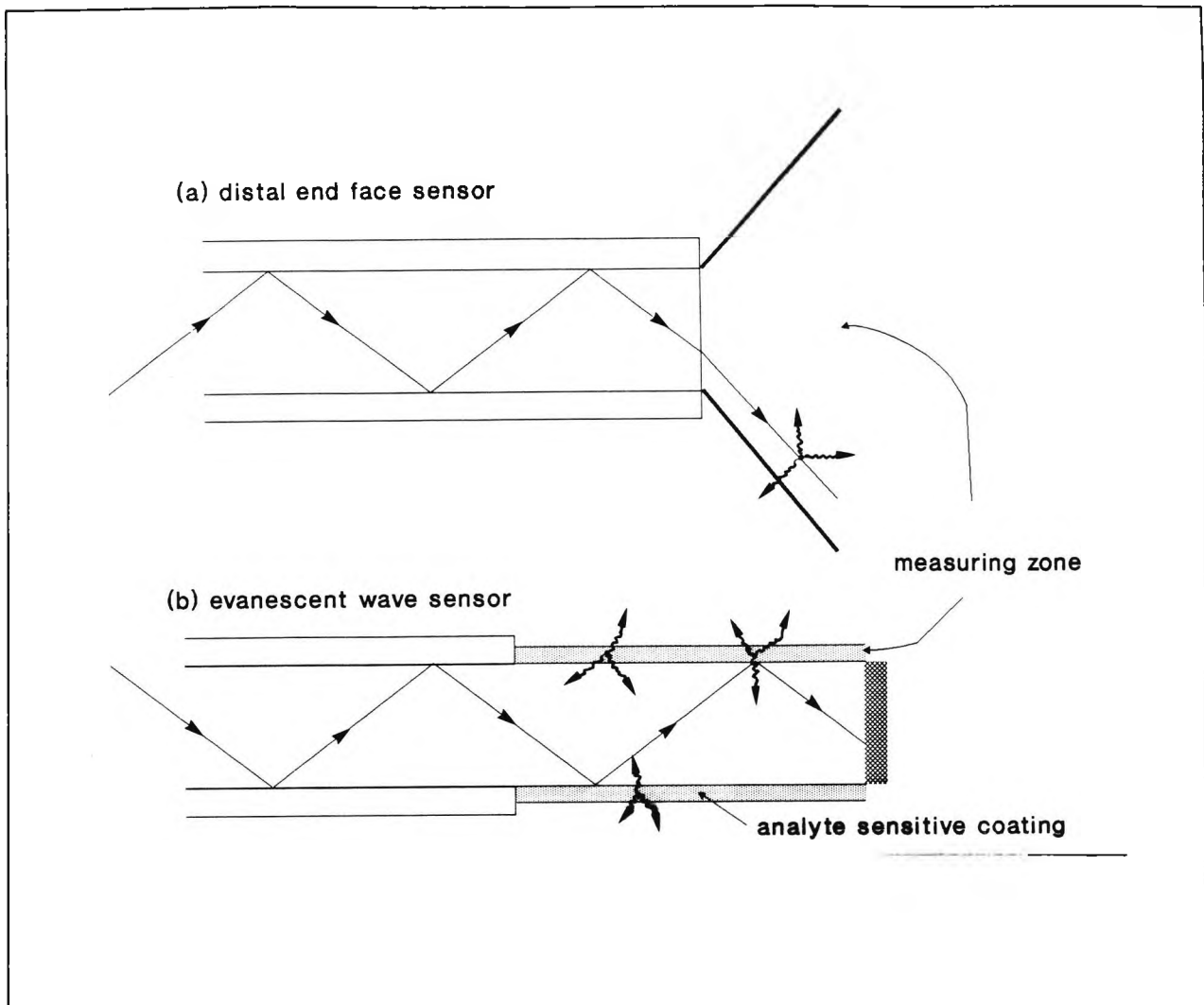


Figure 2.9 Single fibre Sensors

It is also possible to detect and identify different constituents in a gaseous or liquid mixture by using a number of fibres in a single sensor configuration. Smardzewski¹⁸ describes the concept of such a multi-elemental FOCS consisting of eight optical waveguides, each coated with a thin film known to react specifically with one or more components in a multicomponent system.

When a single fibre is used, some form of frequency separation will normally be required in order to reduce the intensity of the reflected excitation signal and so separate excitation light from sensor or emitted signal.

2.2.3.2 MULTIPLE FIBRE CONFIGURATIONS

Multiple fibre systems often allow more light to be transmitted to and obtained from the system under study. Various types of multiple fibre optic configurations are shown in figure 2.10.

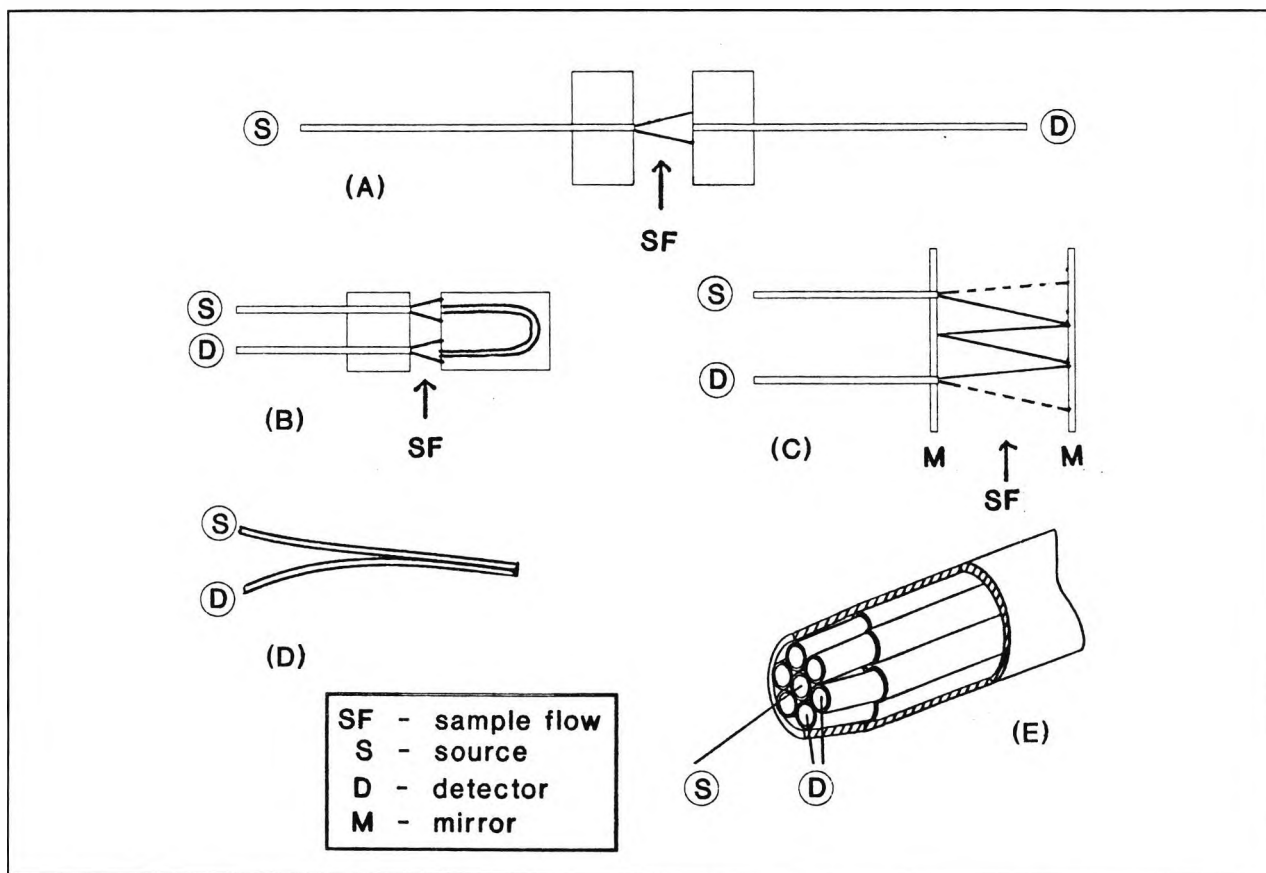


Figure 2.10 Multiple fibre Sensors

The arrangements (a) to (c) are applicable where the analyte of interest has an intrinsically measurable optical property. The path length increases in going from (a) to (c) and the latter is often used to sense gases which have low absorbance in the near infra-red. These configurations provide a means of remote spectroscopy and although they can be an important class of sensor, they are outside the scope of this study. The main difference between type (c) and type (d) is that with (d) there is reflection or fluorescence from an immobilized reagent into the return fibre. Configuration (e) is similar to in principle to (d) but is much more efficient in gathering reflected light. A probe similar to the last type was used for in the present study (section 3.3). Wolfbeis¹⁷ also describes a fibre optic specifically designed for measuring fluorescence emission (figure 2.11).

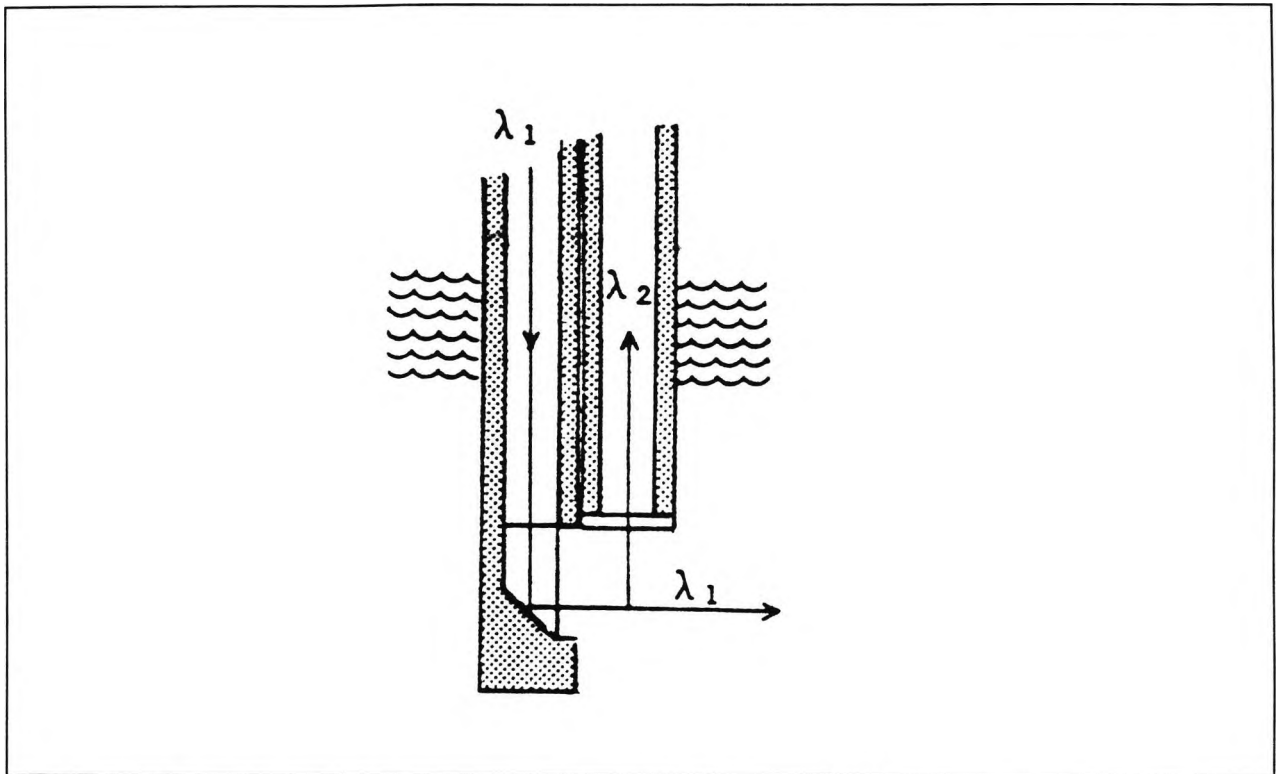


Figure 2.11 Fibre optic for measuring fluorescence emission.

Although somewhat more complicated than the previous examples, this configuration has the advantage of eliminating much of the incident radiation (λ_1) from the return signal (λ_2) and leads to an enhancement of the overall sensitivity of the device to the desired radiation.

Multiple fibre-optic configurations can also be used for the detection and identification of individual constituents of gaseous or liquid mixtures¹⁸ and this can increase the economic efficiency of a FOCS.

2.2.3.3 BIFURCATED FIBRES

These are fibre arrangements in which there are two fibres or fibre bundles leading to a single common end. One example of such a configuration is really an extension of the fibre bundles discussed above. It consists of a bundle of small diameter fibres arranged in such a way that the common end of the two arms are randomly mixed so that there is the most effective overlap of input and output radiations^{19,20}. Another type is where the two arms of the bifurcated fibre lead into a single fibre common end^{12,21}. Both kinds have the advantage that they are easy to use in many applications, although they can be larger than some of the sensor constructions previously considered and may still not be the most efficient type.

2.2.4 OPTICAL COUPLING AND FREQUENCY SEPARATION

One low cost modification that has been used to improve the efficiency of FOCS is the positioning of a small sapphire ball at the distal end of a single fibre²².

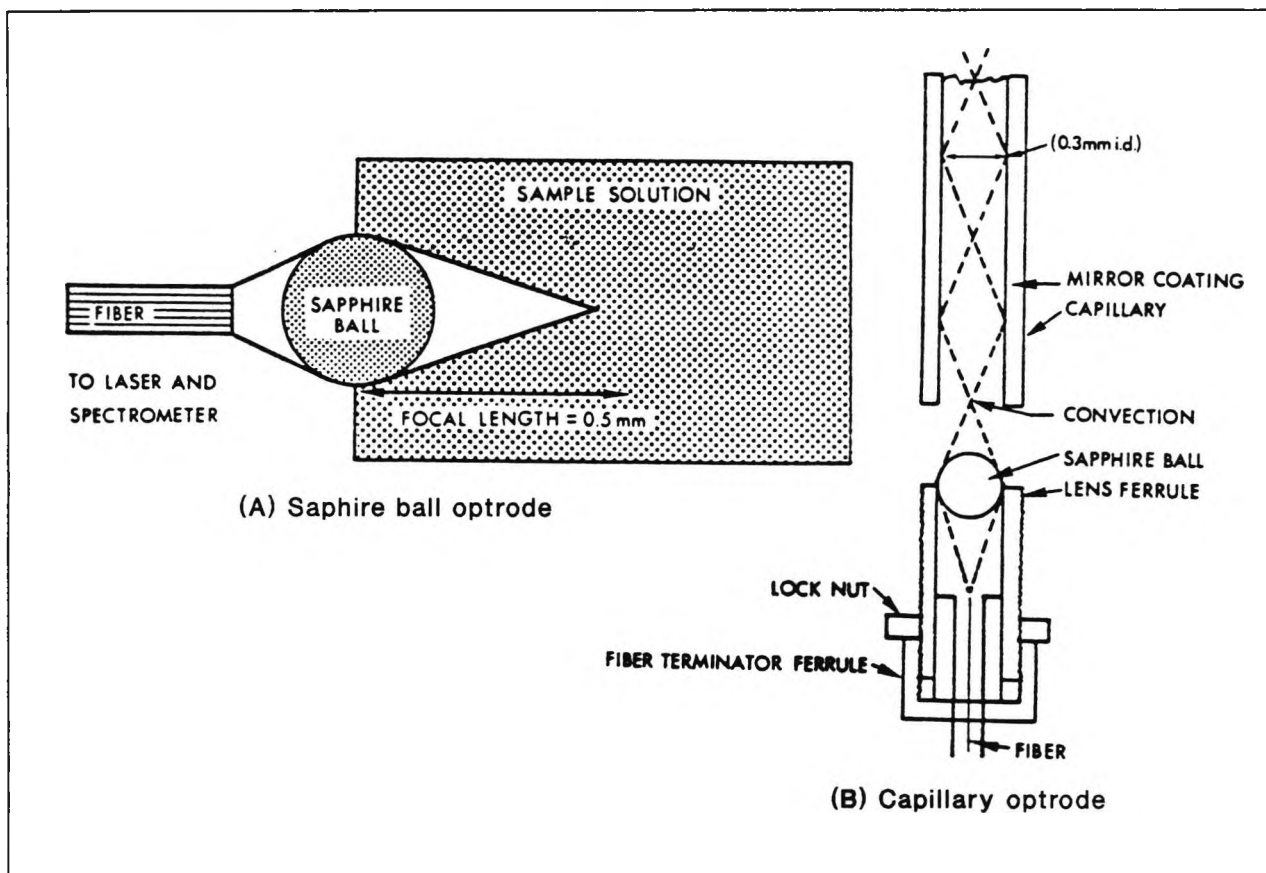


Figure 2.12 (a) Sapphire ball optrode (b) Capillary optrode

The sapphire ball simply acts as a compact focussing lens and is able to increase the sensitivity by about a factor of two. An extension of this concept incorporates an internally mirrored capillary tube (fig 2.12(b)), which confines the excitation and fluorescence radiation throughout the tube length resulting in a six- to seven-fold signal enhancement. Unfortunately, not all FOCS types can benefit from such simple improvements.

The ability of an optical arrangement to discriminate between the excitation and signal radiations will also greatly influence the overall efficiency of the instrument. The simplest type of light separation can be accomplished by a beam splitter, but this is not very efficient and a number of other approaches have been widely reported.

One method uses a mirror which has a long or short pass characteristic (dichroic mirror)²³. Bandpass filters which transmit a discrete band of wavelengths and reflect all others could also be used. In another technique, a mirror with a small hole is used to separate a highly collimated excitation beam from the divergent returning beam (figure 2.13(a))¹⁷. A more costly

but more effective solution would be to use a monochromator which would then transmit only the light of the required frequency range.

The separation of concentric outgoing and returning beams can also be accomplished using a small prism (shown in figure 2.13(b))²⁴.

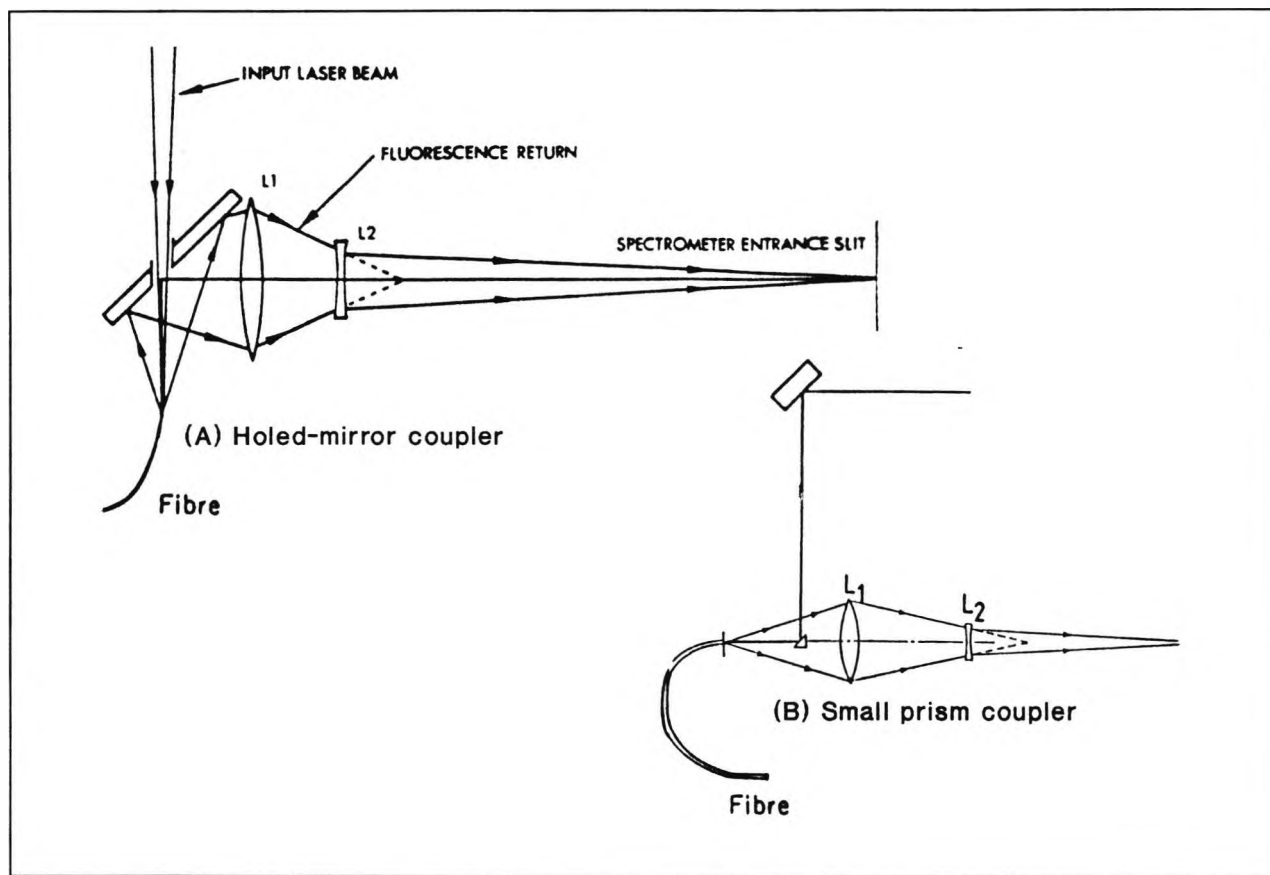


Figure 2.13 (a) Holed-mirror coupler (b) Small prism coupler.

The prism is used to turn the focused laser beam onto the fibre while the divergent returning fluorescence is collected out of the fibre at its numerical aperture. The presence of a prism causes minimal interference on the signal and almost no loss of signal intensity. Another common approach has already been mentioned and involves the use of the bifurcated fibre bundles.

2.2.5 LIGHT DETECTORS

So far, the transmission of light to and from the distal end of a fibre optic configuration has been considered. In this section the various types of detectors which are available to convert the return light signal into an electrical signal are outlined. There are two broad groups. The first of these are the so called thermal detectors and because of their relative unimportance in the field of optoelectronics due to their sensitivity being optimised for the longer wavelength regions ($\lambda \geq 1\mu\text{m}$), they shall be dealt with only briefly. The second types are the photonic devices, which are much more commonly employed.

2.2.5.1 THERMAL DETECTORS

In thermal detectors the absorption of light raises the temperature of the device and this in turn results in changes in some temperature-dependent parameters. Essentially, some of these common devices use the principle of the thermocouple whereby the heating of one junction between two dissimilar metals relative to the other causes a current to flow which is proportional to the difference in temperature between the junctions. In the *bolometer* the resistance of the temperature- (hence light-) sensitive element is affected by the intensity of the radiation. By using the appropriate material and with cooling to eliminate thermal noise, this type of detector can be constructed to measure very weak signals and has proved successful in far-infrared astronomy. *Pneumatic thermal detectors* are also able to measure extremely small power (down to 10^{-11} W), but because they work on the principle of light deflection due to changes in the tension of a thin silvered membrane contained in an air-tight chamber (Golay cell), they are more fragile and difficult to set-up than other devices. Another type of thermal detector is the *pyroelectric detector*. This is a comparatively recent development which does not have the sensitivity of the Golay cell. However, pyroelectric detectors can be made with response times in the nanosecond region and have proved very useful as low cost, robust infrared devices often employed in such areas as fire detection and intruder alarms. They are all, however, optimised for infra red detection.

Fibre optic sensing is a growing field and more and more applications are being investigated. It may be that thermal detectors will find favour in some of these new spheres but to date they have rarely been reported, largely due to the wavelengths utilised in this work.

2.2.5.2 PHOTON DEVICES

(a) Photomultiplier Tubes

When radiation with a frequency greater than a critical value is incident upon a metal surface electrons are emitted; this is called the *photoemissive* or *photoelectric effect* and the devices based on this phenomenon include the *vacuum photodiode* and *photomultiplier tubes* (PMTs). In both types there is a photoemissive surface which forms the cathode in a vacuum tube. When an electron is emitted from this surface it is accelerated by a high voltage towards the anode where it recombines to give a current signal. Vacuum photodiodes normally have no internal gain and require external amplification. For this reason they are not often encountered in FOCS work. PMTs on the other hand possess secondary emission electrodes called dynodes. The dynodes are maintained at successively higher potentials with respect to the cathode. On striking a dynode surface each electron causes the emission of several more electrons which in turn are accelerated to the next photoemissive surface. This multiplication process is repeated

for each electrode so that if there are N dynodes overall, then the total current amplification factor between the cathode and the anode will be given by:

$$G = \delta^N$$

where δ is the average number of electrons emitted at each dynode surface for each incident electron. Considerable amplification is thus possible, for example, $\delta=5$ and $N=9$ gives $G=2 \times 10^6$.

The PMT responds to light input by delivering charge to the anode. Individual pulses may also be examined and this feature is utilized in photon-counting techniques which allows the detection of very low level signals (typical minimum detectable signal is approximately $10^{-15}W$). PMTs have often been reported in FOCS^{e.g.23,24} but size, price and the high voltage required for the operation may be limiting factors for certain applications. However, recent work has resulted in the development of compact, lower voltage devices than those used traditionally in UV spectroscopy which could have significant impact on future FOCS studies and developments.

(b) Photoconductive Devices

Photoconductive detectors rely on the change of conductivity that occurs when semiconductor material is radiated with light of below a certain wavelength.

$$\lambda_g = \frac{hc}{E_g}$$

E_g is the energy gap in the semiconductor which must be overcome for an electron to be raised from the valence band to conduction band. When light of $\lambda \geq \lambda_g$ shines on a photoconductive detector, the resistance changes as the light level increases giving an idealized response expressed in terms of output per unit of incident energy as shown in figure 2.14. Beyond λ_g the output falls to zero since the photons have insufficient energy to excite carriers across the bandgap.

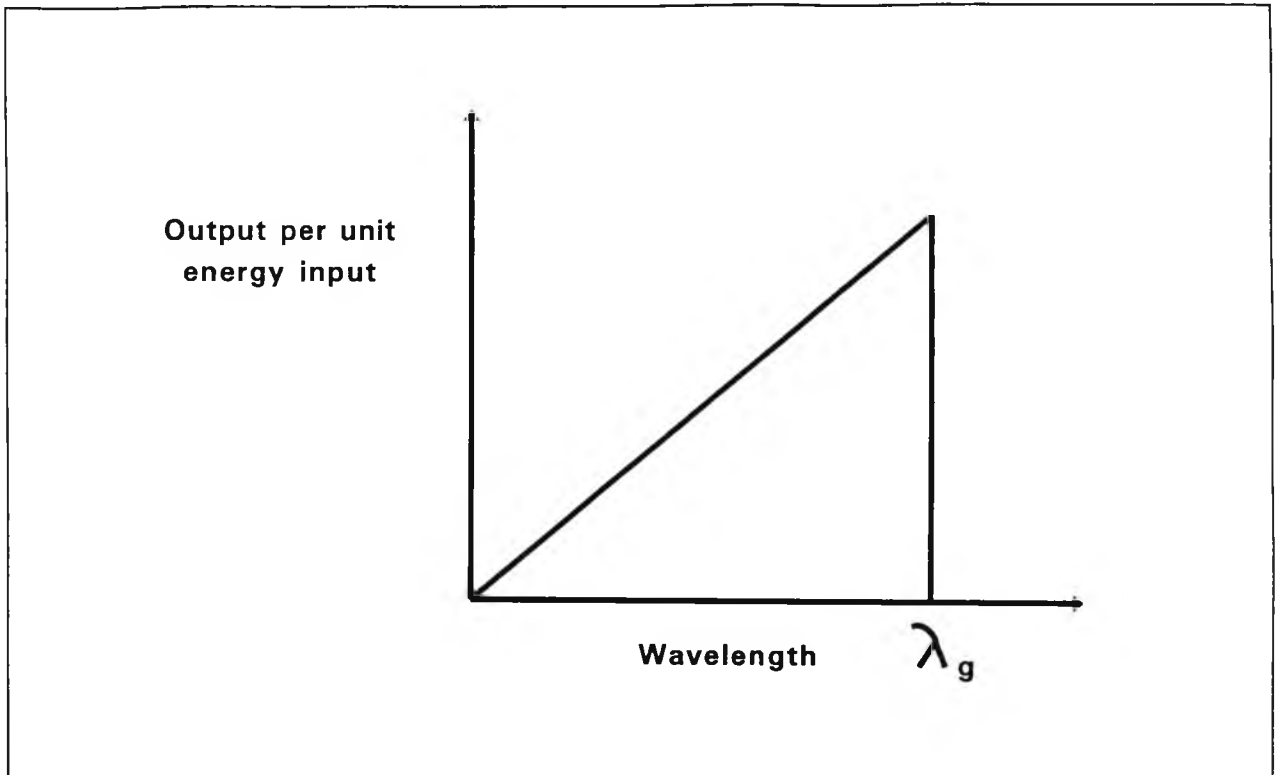


Figure 2.14 Idealised wavelength response curve for a photoconductive detector⁷

The most common examples of such detectors are the cadmium sulphide and cadmium selenide types, both used for low cost visible radiation sensors, for example light meters for cameras. These devices usually have high photoconductive gains (some 10^3 to 10^4) but poor response times (about 50 ms). Moreover, the response time is strongly dependent on the illumination level, being much reduced at higher illuminations. Given the dependence of the response on wavelength and intensity of radiation, such photoconductive devices are not typically used in FOCS.

(c) Junction Detectors

Semiconductor photodiodes are often used in FOCS because they are easy to incorporate into a sensor design, are relatively inexpensive and compact. When light is incident on a the depletion region of a semiconductor-semiconductor junction, an electron-hole pair can be generated which then separates due to the equilibrium junction contact potential. This charge separation can be measured in two ways. If the device is left on open circuit an externally measurable potential will appear between the p and n regions. This is known as the *photovoltaic* mode of operation. On the other hand, if the device is short circuited externally (zero biased) or, as is more usual, operated under reverse bias, an external current flows between the p and n regions. This is known as the *photoconductive* mode of operation and an output voltage can be measured across a load resistor.

In the photovoltaic mode, the external voltage is a logarithmic function of the incidence light irradiance whereas this response is linear when the diode is operate in the photoconductive mode. In addition to its inherently linear response, the photoconductive mode usually offers the advantages of faster response, better stability and greater dynamic range. In both modes, the ultimate sensitivity of the device will be limited by the presence of a dark current, although this problem is greater in the photoconductive mode.

The most common semiconducting material used for photodiodes is silicon, and this type of detector is one of the most popular of all-purpose radiation detectors in the wavelength range 400 to 1000nm. It has the virtues of high quantum efficiency, small size, good linearity of response, high response speed, simple biasing requirements and relatively low cost.

Variations of the photodiode principle include the so-called PIN detector which has an intrinsic semiconducting zone sandwiched between p-type and n-type material and results in good long-wave response with only modest bias levels. PIN photodiodes are ideally suited for detecting ultrashort pulses in the order of 50-100ps in the range 300-1100nm and often reported for fibre optic sensing, as they are cheap and widely available. The avalanche photodiode is able to provide useful internal amplification by being able to be operated under very high reverse bias. As a result, carriers traversing the depletion region gain enough energy to enable further carriers to be developed by impact excitation. The phototransistor also affords internal amplification.

2.2.5.3 CHOICE OF DETECTORS

The detectors described so far do not represent the total list of available detectors, but they are the most commonly reported ones in the field of FOCS. The final choice will depend on various technical and economic factors but should be made in the light of certain parameters which can be applied to all types of detectors. These parameters include responsivity, spectral response, response (rise) time, cut-off frequency, noise equivalent power (NEP), and sensitivity. In the present investigation, a general purpose PIN photodiode was used (BPX 65, RS Components Limited). This diode has a peak spectral response of 850 nm which is beyond that required for the sensing application considered but it was selected because it exhibited an adequate performance and it was simple to use.

2.2.6 SIGNAL PROCESSING

The detector provides a current or voltage signal which corresponds to the intensity of the radiation which is incident on it. This radiation, however, consists not only of the signal arising from the sensor-analyte interaction but interfering inputs such as the noise from the detector and background light. Also, the intensity of the signal may be affected by the efficiency of the

sensor which might change with time, or the presence of absorbing species other than the analyte of interest. By using readily available technology it is possible to reduce or eliminate many of the conflicting signals and dramatically improve the performance of the FOCS. Examples include the use of optical reference channels²⁵, multidimensional fluorescence analysis²⁶, lock-in-amplifier techniques²⁷ and internal electronic referencing²⁸. Many of the short-comings of FOCS that are discussed in the next section can be overcome with appropriate signal processing.

2.3 ADVANTAGES AND DISADVANTAGES OF FOCS

2.3.1 ADVANTAGES

Between 1967 and October 1993 there were 711 citations in *Chemical Abstracts* containing the combination of key words {FIBER? AND OPTIC? OR FIBRE? AND SENSOR?} AND {SENSOR? OR INSTRUMENT?} AND {CHEMIC? OR ANALY?} (?=string). The graph below clearly illustrates how this topic has attracted more and more attention over the years shown.

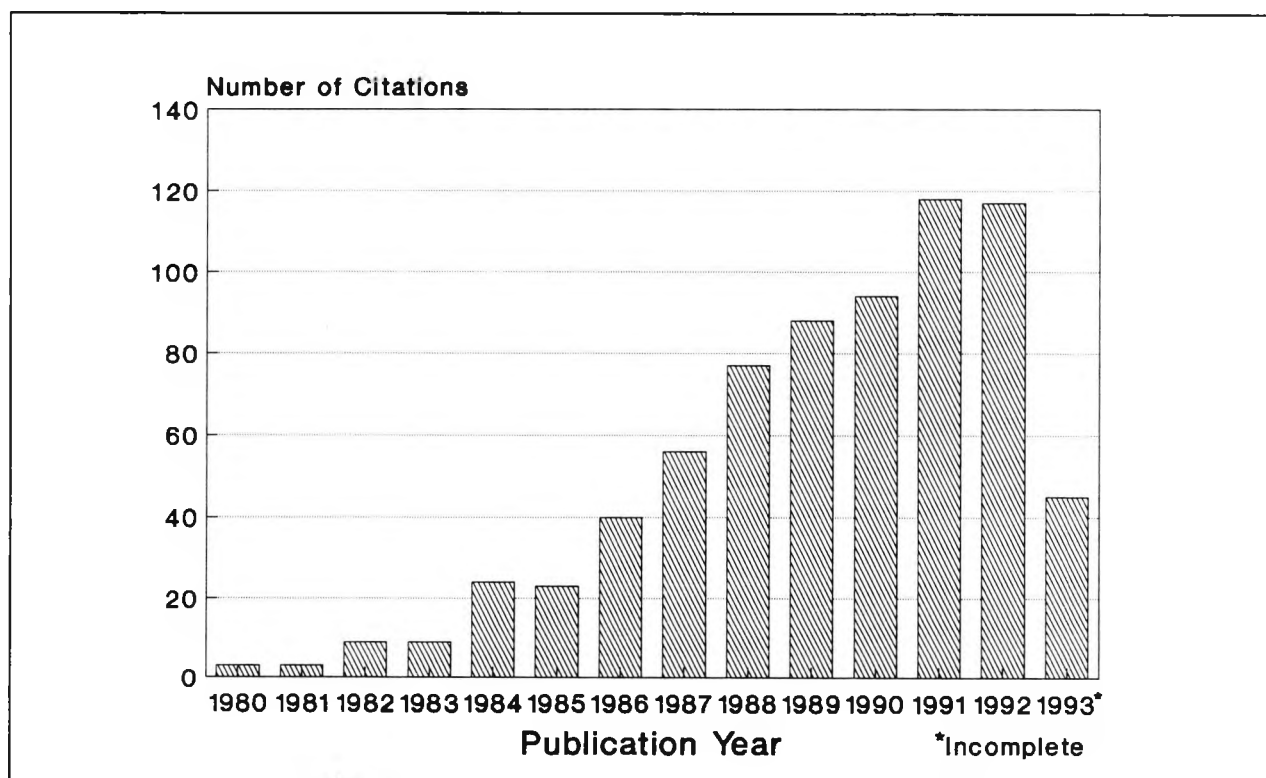


Figure 2.15 FOCS literature citations.

There were only three references found prior to 1980 and the slightly lower value in 1992 may be because not all relevant publications had been registered at the time of searching. Of the

711 citations, 87 referred specifically to pH in the title or key words, reflecting the high degree of interest in the subject.

References to fibre optic based *chemical* sensors make-up nearly 40 per cent of the references to all the types of fibre optic sensors. The driving force behind much of this effort appears to have been has been the inherent advantages associated with the use of optical fibres in sensing, compared to conventional voltage-based systems.

In FOCS, since there is an absence of electric current or voltage at the sensor head, there is no risk of electrical interference. In practice this means that the sensor can be operated near zones of high electrical or magnetic power. Furthermore, because the primary signal is optical, FOCS do not present a spark or fire risk and so can be operated safely in hazardous environments. Sensors can be designed to be sensitive to current and voltage but these are usually based on phase or polarization changes which are not often utilized in chemical analysis.

The typical dimensions of optical fibre cables with cladding are in the order of 0.5 to 1.0mm. This facilitates the ease of miniaturisation of the systems allowing the development of very small, light and flexible fibre devices.

Fibres are able to behave as simple "light pipes", carrying radiation to and from the measuring zone. Consequently, they lend themselves admirably to applications where remote sensing is of benefit. The often cumbersome and delicate instrumentation can be well removed from the analyte-containing environment.

When considered together, the three advantages mentioned so far combine to provide what must surely be the most powerful feature of this type of sensing: the ability to probe both invasively and remotely. This is obviously important for *in vivo* medical or clinical applications. But it is also important in applications such as process control, where an industrial reaction needs to be monitored continuously, or for performing analysis in hostile or difficult to access areas.

Signal multiplexing is possible with optical fibres since the signals can differ with respect to wavelength, phase, decay profile, polarization or intensity modulation. Thus, for example, a single fibre can guide green and red light in one direction, and blue and yellow light in the other. Therefore, a single fibre can, in principle, guide a large number of signals simultaneously which in practice means that several analytes with different spectral characteristics could be assayed at the same time although the complexity of such a system may outweigh any cost benefits to be gained.

This feature of multiple analysis can also be attained by using a combination of fibres to form a so-called hybrid or multi-elemental sensor (section 2.3.2.2). The advantage in this instance is that a single electro-optic instrument can be used in conjunction with many fibres, thus increasing the economic efficiency of the instrument.

Optical sensors have been developed which respond to chemical analytes or physiochemical parameters for which electrodes or other sensing methods are not available. In such areas, and in areas where they stand to replace less convenient approaches (e.g. fluorescence immunoassaying), FOCS show great promise. Fibre sensors with indicator layers are less prone to inner filter effects caused by interfering analytes with similar absorption. Many probe heads are simple in design and mass production can be readily envisaged. This opens the way for disposable sensors, especially of interest for the medical market.

2.3.2 DISADVANTAGES

Notwithstanding the considerable ongoing interest in FOCS and the fact that a large number of related concepts have been successfully demonstrated in the laboratory, only a few FOCS are commercially available. Part of the reason for this limited success is that many FOCS possess one or more of the disadvantages discussed below.

To begin with, optical sensors, in general, will be affected in different ways by ambient light. This necessitates the use of appropriate filters or the modulation of the optical signal so that it can be resolved from the background light. Ideally, the measurements should be conducted in optically-isolated environments but this is often not practicable.

Many indicators are not selective enough toward the analyte of interest and are affected by other chemical species. Many indicators also suffer a reduction of sensitivity after immobilization or when dissolved in a polymer. Sensors with immobilized pH indicators have limited dynamic ranges compared to electrodes. This may mean needing to use more than one sensor to measure across the required range.

Quite often in the design of FOCS there has to be a compromise between the response time and the signal intensity. This is because when the quantity of indicator exceeds a certain amount then the response will enter a mass transfer limited domain rather than one which is governed simply by the kinetics of the analyte-indicator reaction.

Almost certainly the most serious disadvantage of FOCS with indicator phases is that they are likely to have limited long-term stability because of photofading or because the indicators slowly leach out into the surrounding environment. This results in a signal drift which must be compensated for in order to obtain reliable results. In practice, this can sometimes be

achieved by having a suitable reference signal, for example, the intrinsic Raman scatter in the fibre itself. However, this adds to the complexity of the instrument and is sometimes not possible. Also, since the extent of reagent photobleaching increases with increasing irradiation intensity, the use of powerful light sources should be avoided and this leads to reduced signal strengths.

No doubt, part of the reason for the limited prominence of FOCS is due to these drawbacks. It is also appropriate to bear in mind, however, that this type of sensing is still a fairly new technology and in many instances it is competing with tried-and-tested methods. Many novel FOCS continue to be patented^{e.g.29,30} and it is likely therefore that certain types of FOCS will become more widely available in the future but at the end of this thesis some reasons are offered as to why their eventual commercial penetration may not become as prolific as was maybe originally anticipated.

2.4 TYPES OF OPTICAL SENSORS

2.4.1 PLAIN FIBRE SENSORS

Plain fibre sensors utilize the intrinsic fluorescence or absorbance of the analyte or an added indicator and do not have a reagent phase at the end of the fibre. The possible configurations include all those illustrated in figures 2.9 and 2.10. These types of devices are effectively just forms of remote sensing. They are especially useful in systems with poor access, for example, for the remote detection of inflammable gases in refineries, petrochemical plants and fuel tanks³¹ or simply as a replacement of more costly spectrophotometric equipment¹¹.

Plain fibre sensors are simple in design and manufacture so that if it is possible to develop a device based on this principle, then many potential problems can be avoided. However, in practice it is not widely acceptable to add reagent to the measuring zone and any method based on a purely spectrophotometric criterion will be limited by the applicability of the approach itself (e.g. non-specificity).

2.4.2 RESERVOIR SENSORS

Only a limited number of inorganic and organic analytes display a native fluorescence that is sufficiently intense to be utilized in FOCS. In the majority of cases, then, the plain fibre approach will be inoperative and it has therefore become necessary to make analytes fluorescent or to bring the analytes into contact with a fluorescing system such that the

concentration of the analyte will be related to the fluorescence of the reagent. The most obvious approach is simply to contain a small volume of an indicator in solution at the end of the fibre optic within a semi-permeable membrane that allows two-way diffusion of the analyte. This is illustrated schematically in figure 2.16.

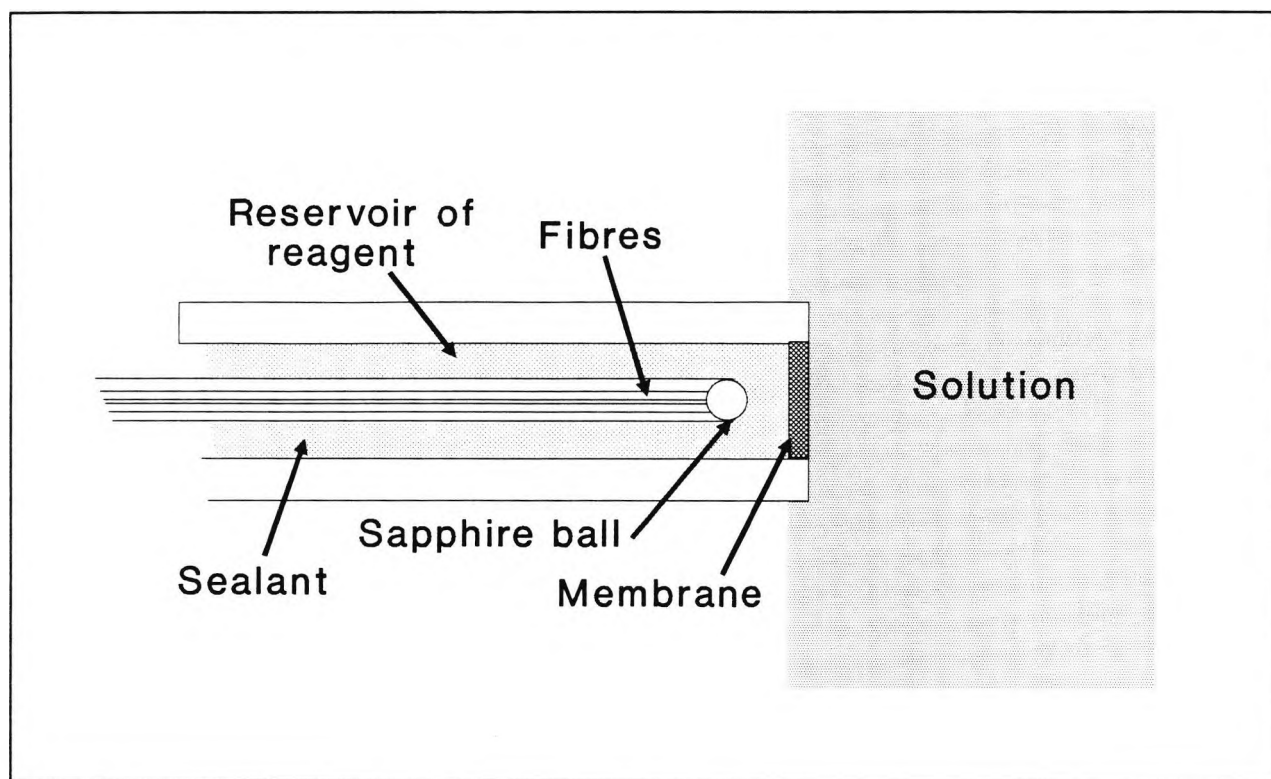


Figure 2.16 Example of reservoir sensor¹⁷.

The fluorogenic reaction takes place at the membrane surface or close to it, resulting in improved selectivity and sensitivity over plain fibre sensors. Furthermore, because of the relatively large amount of reagent compared to the size of the fibre tip, the usage rate of the reagent can be quite small, thus making long-lived FOCSs a possibility. Unfortunately this approach has its limitations. For example, the rate of response will be governed by both the mass transfer kinetics of the analyte through the membrane and the amount of reagent present and so it could be quite slow. Also, the membrane itself may restrict the ruggedness of the sensor and generally these devices tend to be more difficult to construct and maintain than those of simple fibre sensors. As a consequence of these restraints, reservoir sensors have only occasionally been reported^{8,32} although there are more recent developments that claim to overcome these limitations²⁹.

2.4.3 INDICATOR PHASE SENSORS

Broadly speaking, indicator phase sensors belong to one of two groups, *extrinsic* or *intrinsic* type sensors. The classification depends on whether the change in the property of light which is

to be measured occurs due to changes of the fibre itself (intrinsic) or due to some external transducer (extrinsic).

2.4.3.1 EXTRINSIC SENSORS

These are by far the most commonly reported sensor type. An indicator is immobilized on a solid support and held at the distal end of the fibre optic configuration. The types of indicator and the mode of immobilization vary widely from sensor to sensor, but essentially the principle of use is similar. When the reagent is brought into contact with the analyte, its optical properties are altered and this change can be detected through the fibre.

There are two basic designs of an extrinsic sensor probe head (figure 2.17). In the first, the indicator is separated from the analyte-containing fluid by a semi-permeable membrane. The first optical sensor with an indicator phase responding to a chemical analyte was described in 1974³³ and was based on oxygen-sensitive tryptaflavin adsorbed onto silica gel attached to the end of a fibre optic set-up and covered with a semi-permeable membrane. A reference sensor not in contact with the sample was used to account for photobleaching and temperature effects. This sensor design comprises most of the features of a modern instrument. The other type of sensor is more recent and normally involves a high surface area substrate (e.g. porous glass) being attached to the end of the fibre. No membrane is present and response times may be faster. However, there may be problems with selectivity and also loss of dye material.

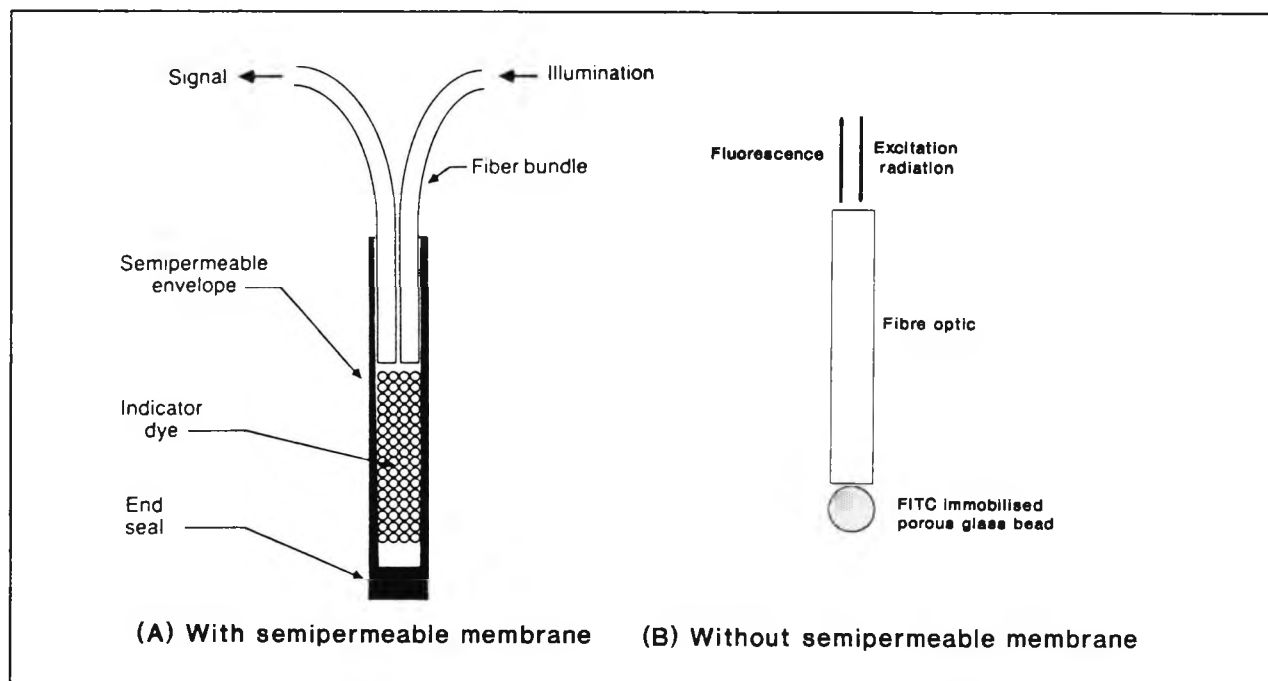


Figure 2.17 Examples of extrinsic FOCS

(a) with semipermeable membrane²²

(b) without semipermeable membrane³⁴

2.4.3.2 INTRINSIC SENSORS

In the strictest sense of the definition, it is almost impossible to have intrinsic chemical sensors since the sensitive reagent phase will not form a part of the original fibre. However, if one allows the definition to incorporate designs in which the indicator phase is found in a thin layer on the surface of the fibre core or on the bare fibre tip, then it is acceptable to classify certain FOCSs under this heading. Three types of intrinsic fibres have been reported in the literature (figure 2.18). The simplest is where an indicator is covalently bound to the tip of the fibre³⁴. The problem with this system is that the resulting signal is very weak and although the response time is fast, the long term stability is poor. A major incentive for the present investigation was to consider ways to resolve this short-coming. Recent advances in which the sensor dye is contained in the fibre core (which may be porous^{36,37}) have resulted in significantly higher signal-to-noise ratios. Unfortunately this has often been at the cost of longer response times. The third approach involves coupling of the evanescent field arising from the fibre core-modes to a reagent immobilised in a coating on the surface of the fibre core³⁸. Since the field extends only a short distance into the material surrounding the fibre core, the intensity of the signal will tend to be low. Evanescent wave sensing is described in more detail in the next section. Lieberman *et al*³⁹ combine some features from these last two systems and have described a configuration which claims to have attained relatively high signals with short response times. A fluorescent sensor dye is contained in a permeable fibre coating and a second fluorescent compound whose excitation spectrum overlaps with the emission spectrum of the first dye is contained in the (non-porous) fibre core (Figure 2.18(d)). Light incident on the fibre coating at a wavelength (λ_1) causes molecules in the coating to fluoresce isotropically emitting light at a longer wavelength (λ_2). A portion of the coating emission which is directed into the fibre is absorbed by the fluorophore in the core, causing a secondary emission (at wavelength (λ_3). This secondary emission is guided by the fibre to the detector and can result into a more than 100-fold increase in the coupling energy compared to other intrinsic designs.

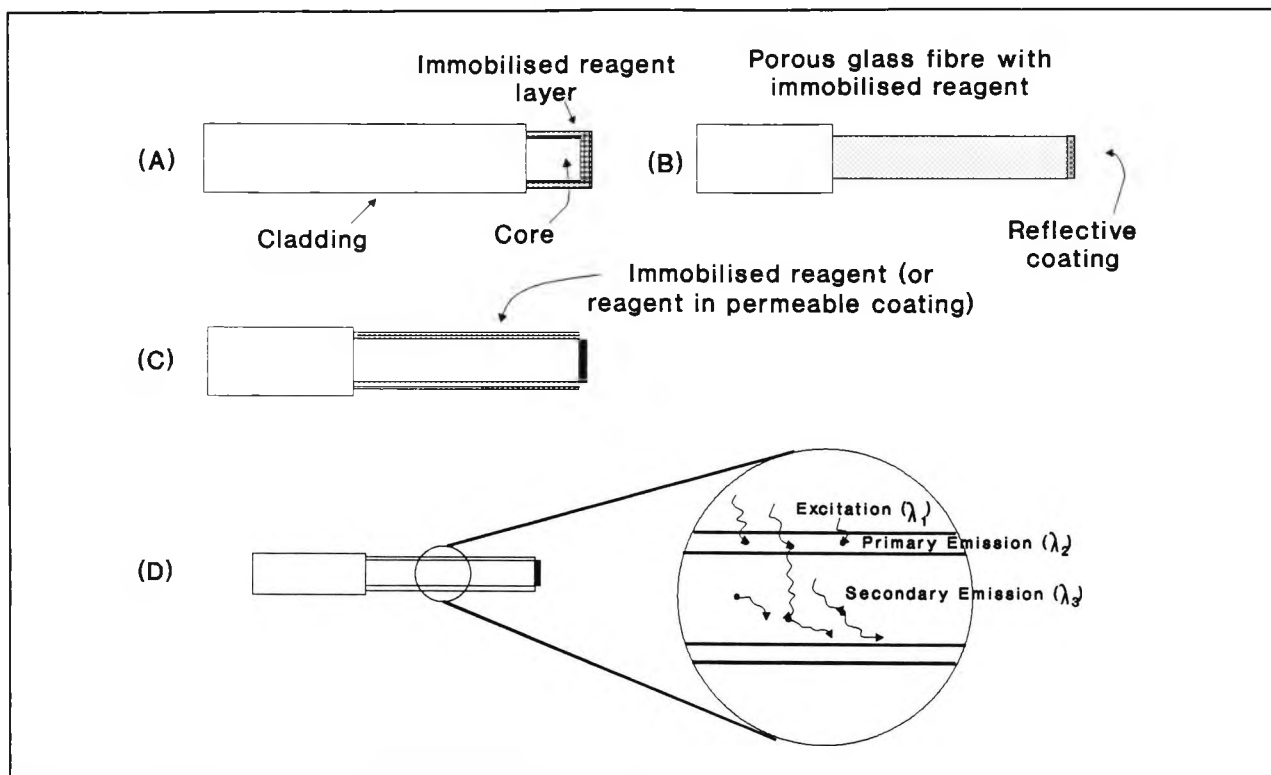


Figure 2.18 Types of intrinsic FOCS.

(a) Reagent covalently bound to tip of fibre.

(b) Reagent immobilised in core of porous glass fibre.

(c) Reagent immobilised onto surface of fibre core.

(d) Reagents immobilised in fibre core and on fibre surface.

2.5 MODES OF OPERATION IN FOCS

There are four major phenomena which can occur when light interacts with matter: absorption, reflection, scattering and luminescence. Based on these effects, the following approaches have been used to extract information from a FOCS system: absorbance/reflectance, fluorescence, time resolution, energy transfer and evanescent wave coupling. In this section, each of these methods shall be considered with some examples.

2.5.1 ABSORPTION-REFLECTION

When a beam of light impinges on a transparent layer of a solid, liquid or gas, certain frequencies of the radiation can be selectively removed by the process of absorption. The decrease in light intensity is determined by the number of absorbing species in the light path, and is related to the concentration of the absorbing species through the Beer-Lambert equation.

$$\ln(I_0/I_t) = kCd$$

I_0 = intensity of incident radiation
 I_t = intensity of transmitted radiation
 k = a proportionality constant
 C = conc. of absorbing species (in mol litre⁻¹ or g litre⁻¹)
 d = optical path length (normally expressed in cm)

Absorbance, A , is defined as the base-ten logarithm of the ratio of incident and transmitted radiations, i.e.

$$A = \log(I_0/I_t)$$

or $A = \epsilon Cd$

where $\epsilon = 2.303k$

The absorptivity, ϵ , (previously called the extinction coefficient) is a characteristic of the analyte substance at a given wavelength. The units of ϵ depend on the units used for concentration (i.e. litre g⁻¹ cm⁻¹, or, litre mol⁻¹ cm⁻¹). This relationship can be directly applied to the analysis of the type of configurations illustrated in figures 2.11 (a) to (c). When considering indicator phase sensors, however, the signal is normally reflected from the indicator surface and absorption process can no longer be modelled according to the Beer-Lambert law.

There are two types of reflection processes. The first is the mirror-type or specular reflection which occurs at the interface of a medium with no transmission through it. The other type is diffuse reflection, in which the radiation penetrates the indicator phase and subsequently reappears at the surface of the system following partial absorption and multiple scattering within the system. In FOCSs, it is often desirable to minimise the former type and hence maximise the latter and this can be achieved by proper sample preparation or optical engineering⁴⁰.

The model most widely used to describe diffuse reflectance is the *Kubelka-Munk* theory. A thick semi-infinite scattering layer is assumed and the reflectance, R , is related to the concentration, C , of the absorbing species on the scattering layer through the molar absorptivity, ϵ , and the scattering coefficient S , as follows:

$$F(R) = \frac{(1-R)^2}{2R} = \frac{\epsilon C}{S}$$

F(R) is the Kubelka-Munk function. This relates the reagent concentration to the reflected light intensity and can be corrected to take into account the contribution of the reagent independent of the substrate. When this model was used to characterize a pH sensor based on the use of bromothymol blue adsorbed onto amberlite XAD-2 (a macroporous cross-linked polystyrene-divinylbenzene copolymer) it was found that the theory could be applied to this system and that it could also be used to predict the performance of the sensor²⁸.

Scheggi and co-workers⁴¹ have carried out many investigations concerning the preparation of a pH sensor also based on bromothymol blue adsorbed onto amberlite XAD-2 copolymer. Part of their studies included suspending the derivatised XAD-2 microspheres in an hydrophilic gel in order to try and achieve a higher sensitivity. Response time and reproducibility became more problematic with this design.

A reflectance sensor for oxygen based on immobilized hemoglobin has been described by Zhujun⁴². An ion exchange resin was used as the substrate and the reagent was separated from the sample by a semi-permeable membrane. A similar set-up was utilized to measure ammonia⁴³. An approach based on an intrinsic sensor design incorporating a porous fibre section with adsorbed cobalt chloride was used to measure humidity⁴⁴. In this instance the scheme was quite different in that the sensitive region was contained not at the distal end of the fibre but along its axis, probably limiting potential applicability of such a sensor.

Reflectance-absorbance type FOCS are normally based on the spectral shifts which arise as a result of the interaction of the analyte with the reagent, in other words the reagent will change colour depending on the concentration of the analyte. Such systems inherently possess more information than is available from sensors where the measured parameter is solely a change in intensity (e.g. fluorescence quenching), but in order to take full advantage of this effect, measurements at more than one wavelength must be performed. Reflectance sensors are normally less prone to interfering species than fluorescence-based sensors but also intrinsically less sensitive.

2.5.2 FLUORESCENCE

Fluorescence analysis has assumed a major role in conventional spectroscopy because for applicable compounds it gives high sensitivity (up to low parts per trillion⁴⁵ and high specificity). High sensitivity arises from the difference in wavelengths between exciting and fluorescence radiation which governs a signal contrasted with essentially zero background (not normally true in FOCS). This is easier to measure than a signal which arises from the difference between two inputs as is done in absorption spectroscopy. High specificity is observed because the relationship between the absorption and emission spectra of an analyte will be specific to that analyte. That is not to say that there are no interfering mechanisms. One very common source of interference is oxygen, which quenches the fluorescence. This phenomenon is well characterized and is utilised in some oxygen sensors^{46,47}. Also, a fluorescent compound in the presence of one or more non-fluorescent compounds is readily analysed even when the compounds have overlapping absorption spectra. In fact, even if there are other fluorescent compounds present in the sample, methods exist to discriminate between the various signals (e.g. time resolved fluorimetry). Even non-fluorescent or weakly fluorescent compounds can often be reacted with strong fluorophores enabling them to be determined quantitatively (e.g. energy transfer systems). Taking into account all these applications it is not surprising that fluorescence techniques constitute the majority of fibre optic based chemical sensors.

There are two predominant equations of special importance for the description of the relations between analyte concentration and emission intensity. The first is *Parker's law*, which relates the fluorescence of a fluorescing reagent to its concentration in low absorbing media and can be applied to plain fibre sensors which utilize the intrinsic fluorescence of analytes in the measurement zone. The other type of expression is based on the *Stern-Volmer* equation describing the relationship between emission intensity and quencher (analyte) concentration and can be applied to sensors with immobilised indicators.

For weakly absorbing solutions the relationship between absorbance (i.e. Beer-Lamber law, section 2.5.1) and fluorescence is given by Parker's law^{17,40}:

$$I_f = 2.303\phi I_0 \epsilon C d$$

where	I_f	=	intensity of fluorescence radiation
	I_0	=	intensity of incident radiation
	ϵ	=	molar absorptivity
	ϕ	=	luminescence quantum yield (power ratio of emitted versus absorbed radiation for the reagent species)
	C	=	concentration of luminescent species

- d = optical path length
- g = fraction of emission observed (this takes into account the geometrical arrangement of the instrument)

This equation holds with sufficient precision for most fluorosensors applied in optically thin media such as ground water or air although in practice most samples exhibit considerable absorption at the wavelength of excitation, leading to the so-called *inner filter effect*. In such cases Parker's law is no longer applicable. Errors resulting from the inner filter effect depend on how deep exciting light has to penetrate the sample and are most serious at high fluorophore concentration.

A second type of inner filter effect is observed when there is considerable overlap between the excitation and emission spectra. It is therefore desirable to have indicators with large Stokes shifts and this is another useful criterion when choosing a suitable fluorophore.

Inner filter effects are not so pronounced in FOCS as they are under conventional right angle fluorimetric analysis because at high concentrations the excitation light can be totally absorbed by the sample which in turn leads to higher emission intensities. However, non-linear calibration curves do arise over wide concentration ranges because of the varying penetration depth of the excitation light¹⁷ and this will be illustrated in a subsequent chapter (section 4.2.2.2).

In sensors with immobilised indicator phases the measured fluorescence is that of the indicator and not that of the analyte -hence Parker's law cannot be employed. In such cases an equilibrium is established between the concentrations of the analyte [A], the reagent [R] and associated complexes [AR]. In *static quenching*, the fluorescent reagent interacts with the analyte (quencher) in the ground state to form an associated complex:



The fluorescence efficiency of the analyte will be governed by the efficiency of the quenching reaction which is described by the binding constant:

$$k = \frac{[AR]}{[A][R]} \quad (2)$$

The total amount of immobilised indicator (C) remains constant and is the sum of the free (R) and complexed (AR) molecules:

$$[C] = [R] + [AR]$$

This can be re-written, considering equation (2) as:

$$[C] = [R](1 + k[A])$$

If only AR is fluorescent, the resulting signal will depend only on the analyte concentration since both k and C are constant i.e.

$$[AR] = \frac{k[A][C]}{1 + k[A]} \quad (3)$$

For this type of response the fluorescence will decrease with increasing analyte concentration. Typical sensors for which this relation is valid are represented by those in which an immobilised reagent is quenched by an analyte such as a transition metal ion. A similar relation holds when a non-fluorescent reagent combines with a non-fluorescent ion to form a fluorescent complex. In this case however, the fluorescence will increase with increasing analyte concentration.

Dynamic quenching occurs when the quenching species and the fluorescent molecule undergo a collision process during the lifetime of the excited state of the fluorescent molecule. This relationship is mathematically represented by the Stern-Volmer equation:

$$\frac{F}{F_0} = \frac{1}{1 + K_{SV}[A]} \quad (4)$$

where F = the measured fluorescence intensity,
 F_0 = the fluorescence intensity in the absence of any quencher,
 K_{SV} = the Stern-Volmer constant which considers the diffusion of the analyte to the fluorescent species and the fluorescence lifetime of the latter.

Although the nature of the static and dynamic quenching processes are quite different, equations (3) and (4) are completely analogous to each other and intensity measurements alone cannot distinguish between dynamic and static quenching. A number of approaches exist in order to discriminate between these two processes, including lifetime measurements, dependence of temperature and viscosity on the quenching efficiency and analysis of absorption spectrum⁴⁸. Typical examples for sensors based exclusively on dynamic quenching are those for oxygen and or halothane⁴⁹.

For the situation in which a pH indicator is immobilised a similar mathematical approach can be made to relate fluorescence intensity with pH. When an immobilized fluorophore is immersed into a solution, an equilibrium will be established in the immobilised phase according to the actual pH value and the equilibrium constant can be represented by:

$$K = \frac{[H^+][F^-]}{[HF]} \quad (5)$$

where $[H^+]$ is the activity of hydrogen ions (for dilute solutions this is approximately the same as concentration since interactions between the H^+ ions themselves are unlikely) and $[HF]$ and $[F^-]$ are the number of moles of acid and base form of the fluorophore, respectively. Because the total number of immobilised fluorophores in the reagent phase ($[C]$) is fixed,

$$[C] = [F^-] + [HF] \quad (6)$$

By introducing equation (6) into equation (5), the following expressions for $[HF]$ and $[F^-]$ can be derived.

$$[HF] = \frac{[H^+][C]}{K + [H^+]}$$

$$[F^-] = \frac{K[C]}{[H^+] + K}$$

In the investigations which will be subsequently described, both the acid (HF) and conjugate base $[F^-]$ species of the fluorophore which was used were absorbing and fluorescent. For such cases, the ideal fluorescence response would be described by

$$F_{\text{total}} = k_1[HF] + k_2[F^-]$$

where k_1 and k_2 represent constant factors that relate fluorescence intensity to the concentrations of HF and F^- respectively. In reality, however, a number of correction factors have to be introduced e.g. to account for the inner filter effect and to consider the nature of the solid medium, and this renders such quantitative treatments difficult and often unrealistic.

2.5.3 TIME RESOLVED FLUORIMETRY

Time-resolved fluorimetry (TRF) is another example of a fluorescence mode of operation of a FOCS but because it encompasses some quite distinct concepts, it is useful to deal with it in a separate section. In TRF, the difference between the fluorescence lifetimes of the analyte signal and the non-specific background is utilised to increase the signal-to-noise ratio and thus the sensitivity and specificity of the measurement⁵⁵. When the fluorescence lifetimes due to the analyte are sufficiently longer than the average background decay, the specific signal can be integrated after the background fluorescence has tailed-off. This approach is especially useful where a single fibre needs to be used (for example if *in vivo* measurements are to be made) since the significant amount of radiation reflected at the fibre face is not easily removed by spatial filtering.

Fibre-optic sensors based on TRF have been described for the measurement of biological analytes,^{50,51,52} industrial species such as dissolved uranyl⁵³ and even pH⁵⁴. Their use has been patented for these and more general applications⁴⁷. Measurement of typical fluorescent lifetimes, which are in the order of 10^{-8} seconds, would require expensive and bulky instrumentation due to the speed of response required. Rare earth metal chelates, on the other hand, have emission life-times of around 0.1-1.0ms and are those quoted in the above examples. The working principle of a lifetime sensor is quite straightforward. The long-lived fluorescence of the dye is repeatedly excited by a modulated light source and appropriate measurements are made such that an amplitude-independent relation between lifetime and measurand is provided. Many of the advantages of a lifetime sensor rely on the fact that lifetime measurements do not depend on the absolute intensity of the luminescence which is transmitted through the fibre to the detector. For example, the lifetime measurement will not suffer any losses due to the flexing of the fibre-optic even though a reduction in the signal intensity will be observed⁷. Furthermore, such systems will not be as markedly influenced by the "drift" which arises due to the slow photodegradation or bleaching of the luminescent indicator.

One type of measurement that can be made to determine lifetime values is that of measuring the integral under a typical fluorescence decay curve (figure 2.19).

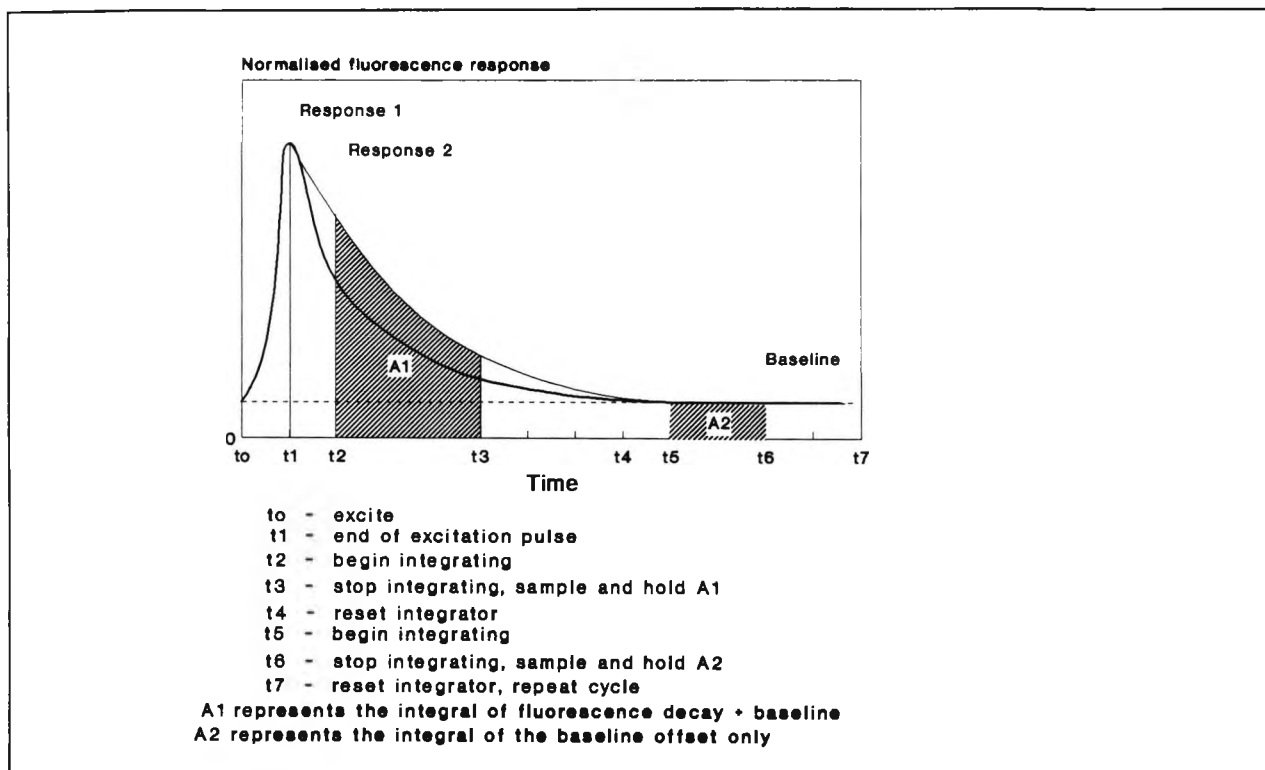


Figure 2.19 Example of TRF measurement cycle⁴⁷.

Integration of the area under the curve is only initiated after a fixed time has elapsed from the end of the excitation pulse. This enables the scattered light arising from the excitation to be ignored. Appropriate signal processing converts the difference in integral measurements A1 and A2 to a lifetime value based on the realistic assumption that the decay is a true exponential. By this method, the baseline signal which arises from detector characteristics and which may not be constant (e.g. PMT dark current) can be accounted for. The lifetime signal is then related to the quencher concentration according to a modified Stern-Volmer relationship and hence a change in the quencher concentration will result in a corresponding change in the lifetime of the sensor (as long as the quenching mechanism is predominantly dynamic).

2.5.4 EVANESCENT WAVE SENSING

In section 2.2.3.1 the concept of an evanescent wave sensor was introduced. This technique is similar in principle to total internal reflection spectroscopy (TIRF) which has provided sensitive, real-time, interfacial methods for detecting the fluorescence of proteins as they adsorb from solution to the solid/liquid interface. As has already been described, the total internal reflection phenomenon occurs when two transparent dielectric media of different optical densities share a common boundary. When light propagating through the more optically dense medium (n_1) strikes the boundary with the less dense medium (n_2) at an incident angle greater than critical angle, all of the incident light is eventually reflected back into the more dense medium (hence the term *total internal reflection*). However, the electromagnetic boundary conditions (a full analysis of which would require finding the appropriate solutions of the

Maxwells equations) require a small fraction of the incident intensity to penetrate the interface into the less dense medium before rejoining the totally reflected beam (figure 2.20).

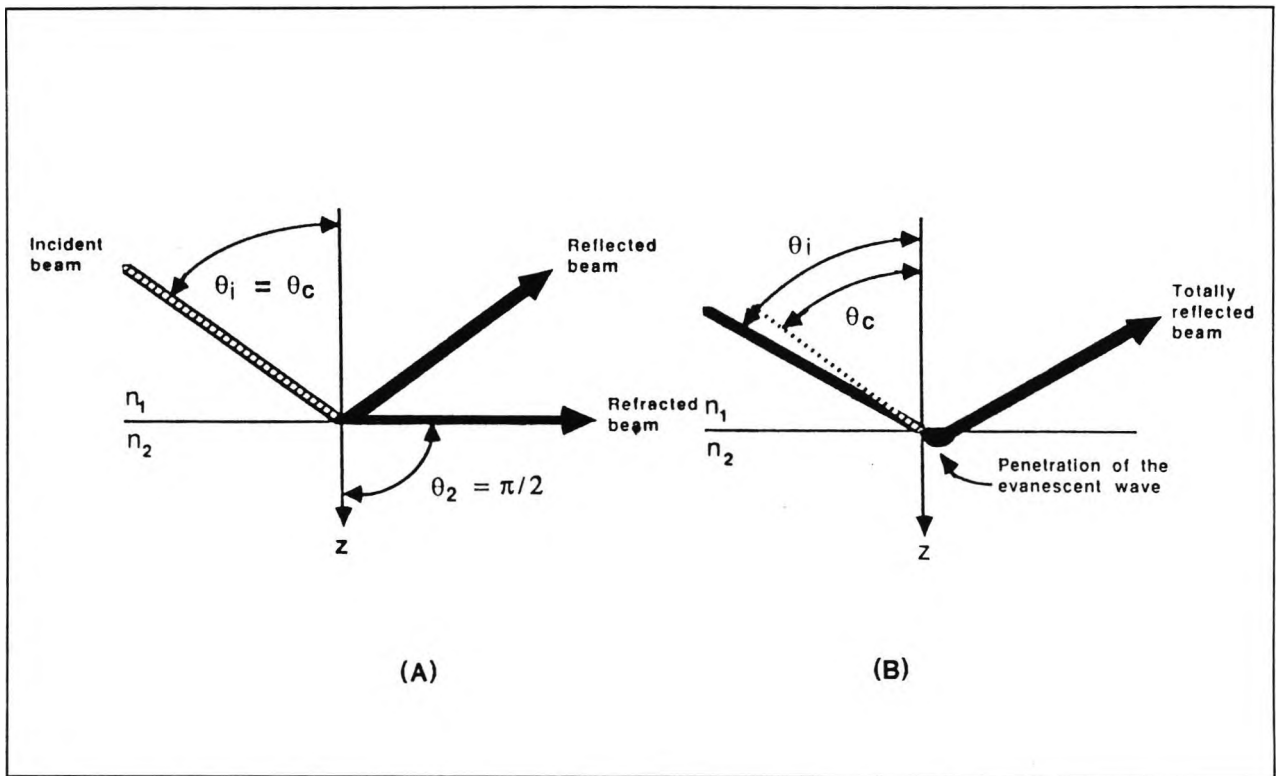


Figure 2.20 Illustration of the total internal reflection phenomenon:⁵⁶ (A) for incident angle equal to the critical angle and (B) for incident angle greater than the critical angle (note the penetration of light across the interface).

The intensity of this interfacial field, called the *evanescent wave*, decays exponentially with distance from the totally reflecting interface into the less dense medium. The absorption or scattering of the evanescent wave within the interfacial region of the less dense medium is the basis of all total internal reflection spectroscopy.

Figure 2.21 shows a schematic of a single interfacial reflection. At a given angle of incidence, the depth of penetration (d_p) of the light into the optically rarer phase (n_2) is defined as the distance within which the electric field of the wave falls to $1/e$ of its value, E_0 , at the interface:

$$\mathbf{E} = E_0 \exp(-z/d_p)$$

where \mathbf{E} is the amplitude of the electric field at depth z . d_p depends on the wavelength of the light and the refraction indices of the two media:

$$d_p = \lambda / [2\pi n_1 (\sin^2 \theta - \sin^2 \theta_c)^{1/2}]$$

Increasing the incident angle beyond the critical angle will lead to a decrease in the intensity transmitted across the interface into medium n_2 and an increase in the decay rate of the evanescent wave in medium n_2 . The polarization of the incident light will also affect the evanescent wave so it can be seen that this type of sensor is rather dependent on the nature of the incident light employed and the geometry of the optical arrangement.

Typically, d_p ranges from 50nm to 1200nm for visible light¹⁷. This can be more than the thickness of an indicator immobilized on the surface and light protruding into this phase is able to induce fluorescence in a fluorophore, or be absorbed or scattered. This feature has been especially utilized in developing fibre-optic based immunosensors (figure 2.21).

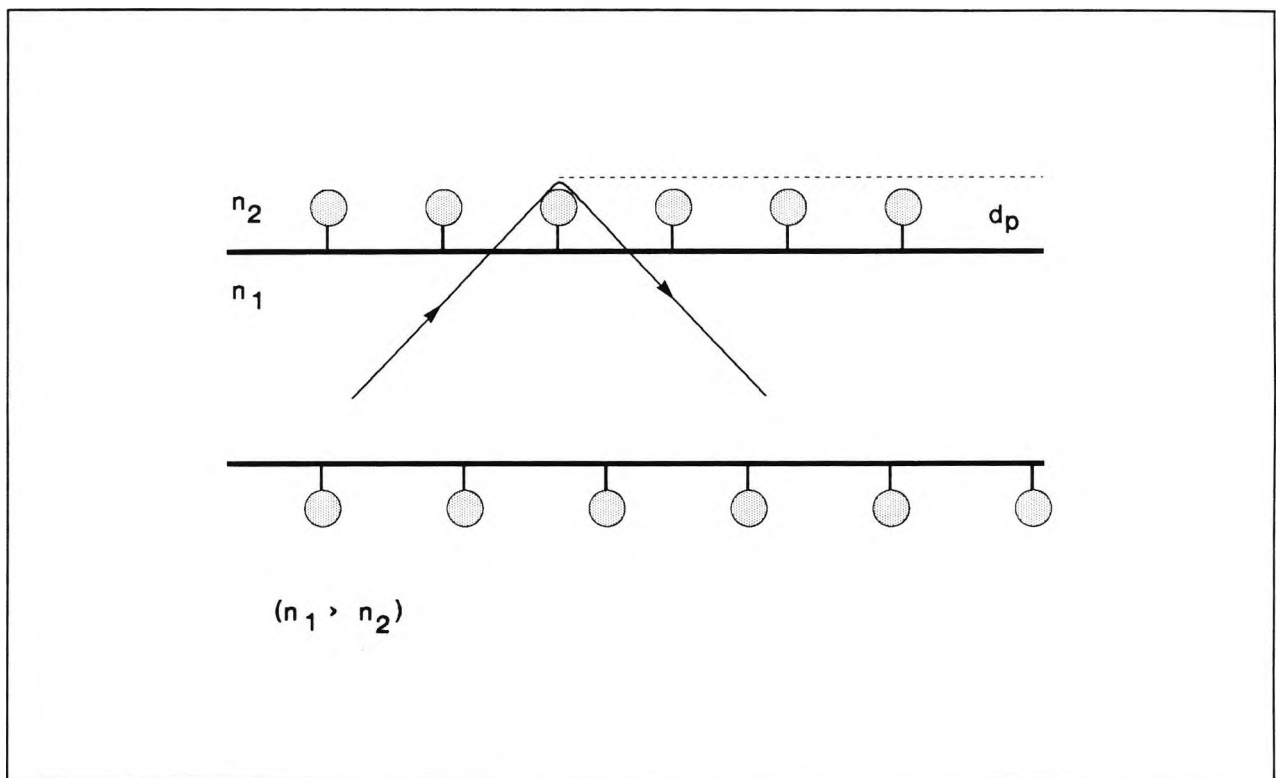


Figure 2.21 The use of total internal reflection to probe indicator molecules which are immobilised on the core of an optical fibre.

In some of the conventional fluoroimmunoassaying (FIA) methods, either the antibody or antigen species are bound to a solid substrate in such a way that their chemical specificity is retained such that a particular antibody will react with a particular antigen. For these solid-phase FIA, there are four commonly employed approaches, three of which are illustrated in figure 2.22.

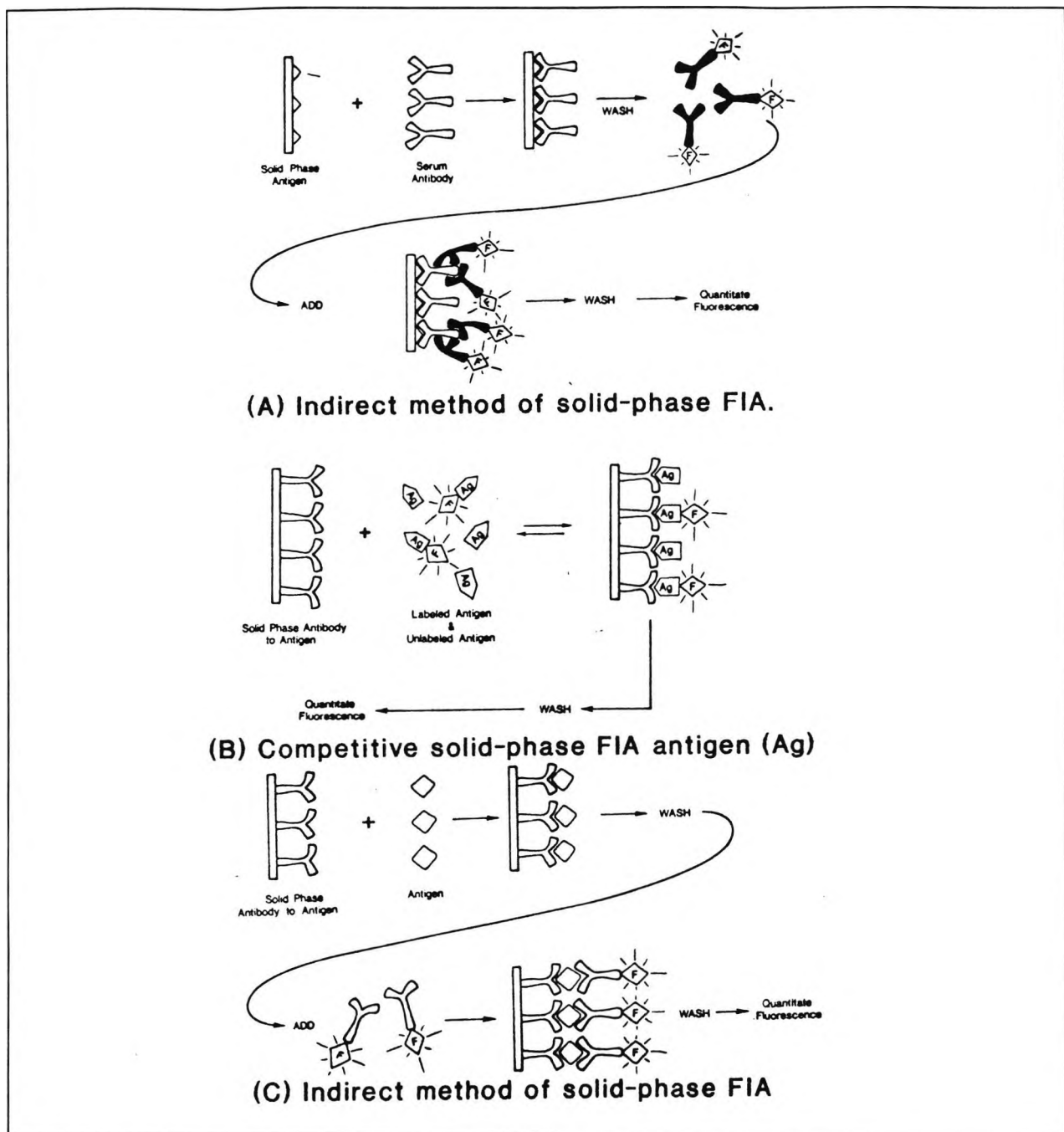


Figure 2.22 Methods of FIA involving a solid support.

In the indirect method (figure 2.22a), a specific antibody in the sample binds to a solid-phase antigen. The matrix is washed and reacted with fluorophore-labelled antibody and after a second wash, the fluorescence is quantified. Figure 2.22b shows a competitive method in which labelled and unlabelled analytes compete for a limited number of antibody sites. The solid matrix is then washed and the fluorescence measured. In the sandwich method (figure 2.22c), the analyte antigen reacts with matrix-bound antibody. The solid phase matrix is washed and reacted with fluorophore-labelled antibody and after a second wash the fluorescence is measured. In the final example, the fluoroimmunochemical method, the analyte reacts with a labelled antibody in solution. Residual labelled antibody binds to excess solid-phase bound antigen, the solid matrix is then washed and the fluorescence measured.

In fibre optic based FIA similar approaches to the above are used. Laser excitation of antibody-bound analyte produces a fluorescence signal which is either directly proportional (as in the case of the sandwich assays) or inversely proportional (as in the case of the competitive-binding assays) to analyte concentration. Since the penetration depth of an evanescent wave is small, fluorescence occurring on the fibre surface is preferentially collected over bulk solution fluorescence, thereby significantly reducing the problem of background fluorescence from biological fluids such as serum which has severely limited the sensitivity of early FIA techniques. A sensor for detecting chemical and physical parameters based on evanescent wave excitation has been patented (e.g. EU Pat Appl 61,884 (Oct. 1982)) and Love *et al*⁵⁷ developed a system which was able to measure the concentration of the fluorophore B-phycoerythrin in solution down to 10^{-12} molar free solution. An evanescent wave technique was used to follow the adsorption of an antigen to the surface of an antibody-derivatised optical waveguide without the use of a fluorescent label: the growing antibody-antigen layer resulted in an increase of scattered light which was monitored continuously. A number of other applications have also been investigated for use with evanescent FOCSs^{58,59,60}.

Evanescent wave sensing systems are prone to low signal-to-noise ratios, mainly because the quantity of fluorophore that can be immobilised is quite small and the evanescent coupling itself is not as efficient as conventional fibre distal end methods. Bhatia *et al*⁶¹ found that in general, the noise (and not the signal strength) limited detectability and that an important source of noise was background photoluminescence from the optical components themselves. One redeeming approach they used was to place the optical chopper (light modulator) just in front of the proximal end of the fibre (it is more commonly placed just after the light source). This simple modification ensured that light affected by the components in front of the fibre could be strongly rejected by the lock-in amplifier.

Optical waveguides offer great potential for studying immunoreactions and performing immunoassays and the use of evanescent wave sensing in this area seems promising and continues to receive wide attention in the literature. .

2.5.5 FOCS BASED ON ENERGY TRANSFER

Most FOCS are fluorescence-based because fluorescence is easily measured with high sensitivity. It is often difficult, however, to find appropriate fluorescent indicators for all analytes of interest. This problem can sometimes be overcome by the use of sensors based on an energy transfer mechanism. The concept is simple: two species are chosen such that the emission spectrum of one of them (i.e. the fluorophore (donor)) overlaps with the absorption spectrum of the other (acceptor). The spectrum of the acceptor is in turn affected by the concentration of the analyte. In this manner, it is possible to combine the more general

availability of colorimetric reagents with the convenient features of fluorescent measurement.

There are two direct pathways for non-collision transfer of electronic energy between a fluorescent donor molecule and an energy acceptor. Radiative transfer occurs via the reabsorption of donor emission by acceptor molecules. This process is not very efficient because it requires an optically dense absorber and long path lengths, which is not suitable for small optical fibre sensors. Exchange of electronic energy between a donor-acceptor pair can also take place without the emission of a photon and is then termed non-radiative transfer. When a molecule undergoes electronic excitation there is usually a change in its polarity. Interaction between the transition dipoles in the donor and those in the acceptor can lead to radiationless energy transfer. Förster, in a quantum mechanical treatment of resonance transfer which takes place between two well-separated molecules, derives expressions for the transfer rate K_t for radiationless electronic energy transfer between donor and acceptor and the efficiency (E) of the process²²:

$$K_t = \frac{AK^2JK_f}{r^6n^4}$$

$$E = \frac{r^{-6}}{(r^{-6} + R_0^{-6})}$$

$$R_0 = \text{distance at which the transfer efficiency is 50\%}$$

$$= B.(JK^2Q_0n^{-4})^{1/6}$$

- where r = the distance between the molecules
 K^2 = orientative factor (=2/3 for random distribution)
 J = the spectral overlap integral
 K_f = the rate constant for fluorescence emission by the donor molecule
 n = refractive index of medium
 A, B = numerical constants
 Q_0 = quantum yield of fluorescence emission by the donor in the absence of acceptor

The equations illustrate the strong dependence on molecular separation to efficient energy transfer, the practical distance being limited to about 7 nm or a few molecular lengths.

Also, the dependence on the spectral overlap integral (J) means that it is necessary for the donor-acceptor molecules to be in resonance; that is, the emission spectrum of the donor molecule must overlap the absorption spectrum of the acceptor molecule. The fluorescence molecule should also have a high quantum yield so that a high proportion of the excitation energy is transferred to the absorber species.

There are four basic absorption-emission optrode designs. In all cases, a donor molecule is initially excited and transfers its energy to an acceptor molecule, which may or may not be fluorescent. In the cases in which the donor fluorescence is monitored, the intensity might increase or decrease with increasing analyte concentration, depending on whether the acceptor absorption decreases (figure 2.23a) or increases (figure 2.23b). If the acceptor fluorescence is monitored, the analytical curves will show the opposite behaviour.

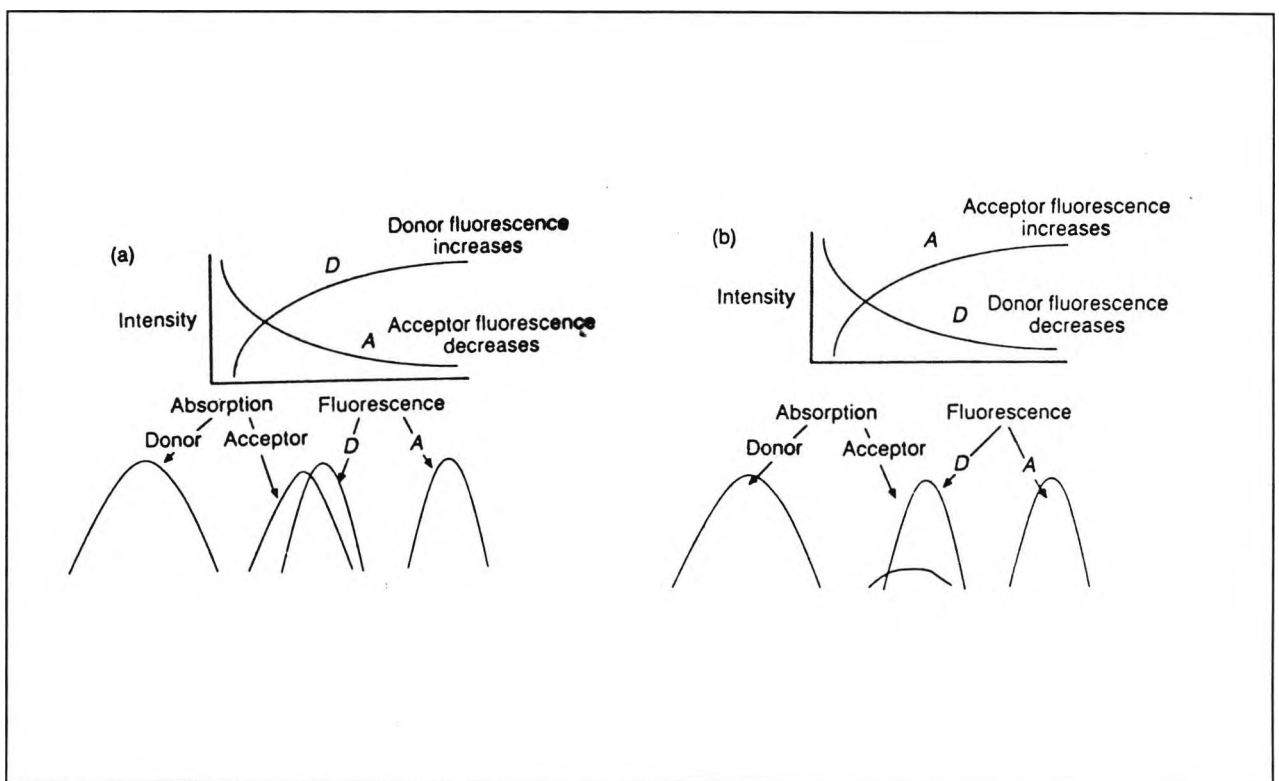


Figure 2.23 Monitoring donor fluorescence (D) in the cases where the acceptor fluorescence signal (A) decreases with analyte concentration or (B) the acceptor fluorescence signal increases with analyte concentration.

[Adapted from ref 22]

A physiological pH FOCs has been described in which energy is transferred from a pH-insensitive fluorophore, eosin, to a pH-sensitive absorber, phenol red⁶². Phenol red was selected because, in the pH range 6.0-8.0, it absorbs in the same region as eosin fluoresces. Protonation of phenol red shifts its absorbance maximum to shorter wavelengths and thus causes diminished absorptivity in the overlap region. Therefore, as the pH decreases, the

amount of energy transfer will be diminished, and eosins emission spectrum should show diminished quenching.

Another example of this type of sensor is one designed for the assay of glucose^{63,64}. Fluorescence energy is transferred between a glucose analogue labelled with fluorescein isothiocyanate (FITC-dextran), and a glucose receptor protein, rhodamine-labelled Concanavalin A (Rh-ConA). When FITC-dextran binds to Rh-ConA and is light activated, the FITC label transfers its absorbed energy to the rhodamine label, which then emits light according to its own characteristic spectrum. When glucose is added to the solution, it competes with the labelled dextran for the Rh-ConA causing the FITC-dextran to be released. Thus it is possible to determine glucose concentrations directly from the level of FITC fluorescence. Figure 2.24 shows the spectra of FITC and rhodamine with the overlap.

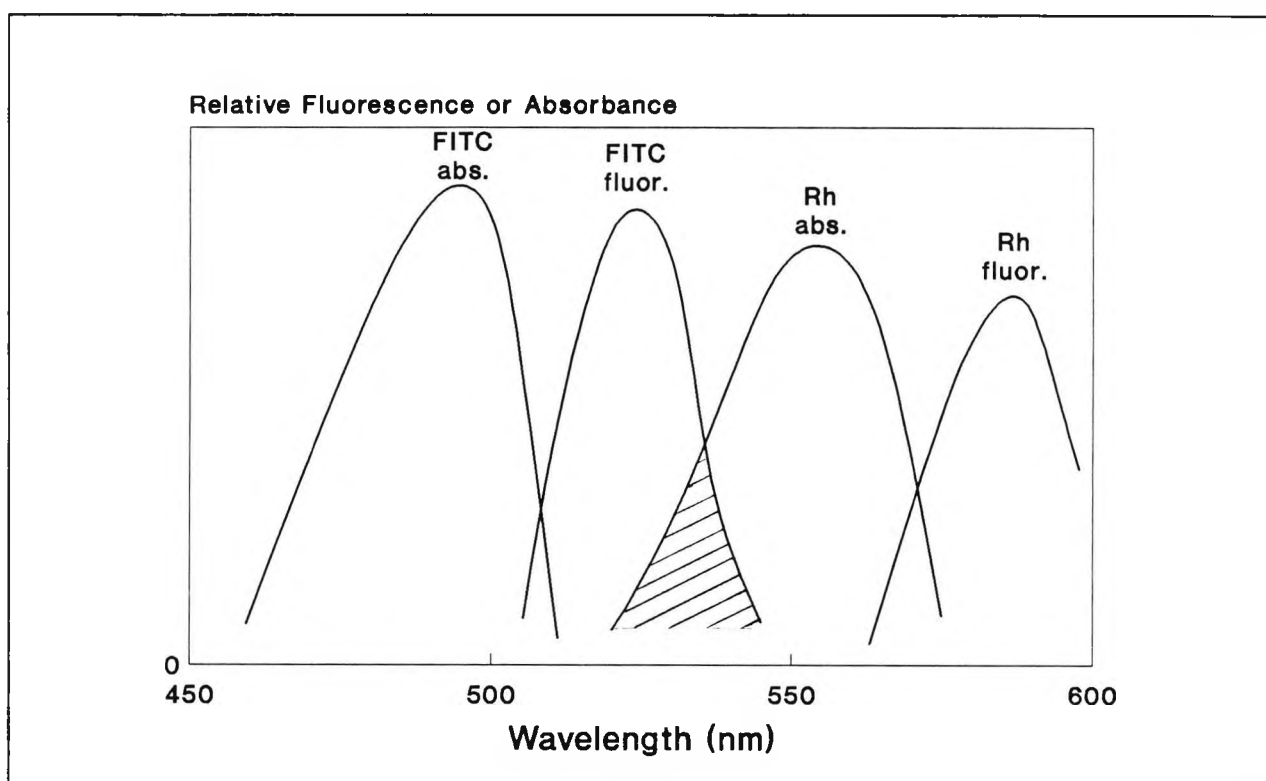


Figure 2.24 Overlap of FITC emission spectrum with Rhodamine absorption spectrum⁶³.

The advantage of this approach over some previous glucose sensor designs, is that it does not require a reagent-immobilization step. This is because in this case the fluorophore emission can be eliminated by the reversible reaction with an acceptor species, and need not be physically removed from the measuring zone. Consequently, the variables which depend on the immobilization step are completely circumvented. Moreover, if as in this example, the absorber fluorescence signal is not significantly affected by the energy transfer, it can be used to provide an internal reference to correct for light source and detector sensitivity fluctuations. In essence, then, FOCSs based on energy transfer mechanisms can lead to an increase in the versatility of these sensors and eliminated some of their deficiencies.

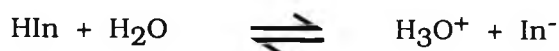
Approaches to FOCS other than the ones discussed are possible, although less common. These include sensors based on Raman spectroscopy and refractometry. Other applications may be found in the excellent reviews which are available^{17,65,22}.

2.6 FLUORESCENCE-BASED FOCS FOR MEASURING pH

2.6.1 OPTICAL pH SENSING

pH sensing is one of the most frequently described applications of fibre-optic based systems. In the author's opinion there are three main reasons for this. Most importantly, pH is a critical parameter for the monitoring of many systems, for example ground-water quality, human physiological stability and the extent of a chemical reaction. Secondly, there are many established methods for measuring pH and these provide good standards for comparison although they often suffer from inaccuracies leading to a desire for simpler methods. Thirdly, the colorimetric reagents used for following changes in pH are inexpensive and widely available.

There are essentially two approaches to optical pH sensing: colorimetric (absorbance) and fluorescence. Conventionally, fluorescence spectroscopy is more sensitive than absorbance methods and can be utilized, for example, in turbid mixtures. Nevertheless, absorbance methods in FOCSs are still widely reported because of the simpler instrumentation that is normally involved and because they can be less prone to chemical interference⁶⁶. Fundamental to both approaches is the use of acid-base indicators. An acid-base or hydrogen ion indicator is a substance which, within certain limits, varies its absorption or fluorescence spectrum according to the hydrogen ion activity of its environment. The indicator is invariably a weak acid, HIn , which differs in colour from its conjugate base, In^- ; the equilibrium between the two forms may be expressed by



To a good approximation, the hydrogen ion concentration is given by

$$[H^+] = \frac{K_a[HIn]}{[In^-]}$$

where K_a is simply the acid dissociation constant, sometimes called the *indicator constant*.

This leads to:

$$\text{pH} = \text{pK}_a + \log \frac{[\text{In}^-]}{[\text{HIn}]}$$

Colour changes can usually be detected as the ratio of $[\text{In}^-]/[\text{HIn}]$ varies between 0.9 and 9 which means that the useful range of an indicator is approximately given by $\text{pH} = \text{pK}_a \pm 1$. This is the reason that, as already has been mentioned, some FOCS have limited dynamic ranges. The types of reagents reported for pH FOCS have quite often been those with pK_a values around the normal physiological pH value of 7.4. This is again an indication of the perceived importance of this field. A wide range, simple, low cost fibre-optic device has been reported for use in clinical applications⁶⁸. The system is based on an indicator dye which is a mixture of equal volumes of bromothymol blue, phenol red and cresol red and when it is used with computer processing, the measuring range is between 5.1 and 9.0 pH units with an accuracy of 0.01 pH.

The first glass-bound pH indicators were accidentally discovered by Weetal of Corning Glass⁶⁹. In the process of activating high-surface area glass in the binding of enzymes, a pale orange sintered funnel was observed. Not only were attempts to wash-out the colour unsuccessful, but when washed with acids the funnel turned reversibly red. This observation led to the immobilization of a selection of indicators onto porous glass. In 1980, a fibre optic pH probe for physiological use was reported⁷⁰. It was based on the use of a dye indicator bound to polyacrylamide microspheres and was able to measure pH over the range 7.0 to 7.4. A high intensity tungsten lamp source was used and the reflected radiation was selected into two wavelengths - one which changes with pH and the other which does not which was used for reference purposes. The ratio of these two values was used to calculate the pH of the solution. The performance of the pH probe was compared with that of a commercial laboratory glass electrode. Tests were carried out to assess the temperature coefficients (probe better than electrode), ionic strength coefficients (electrode better than probe), response time (depended on the size of the probe and the duration of the test), effective cell path (only a few mm of probe dyestuff packing was required) and the stability of the probe (which at around 2 hours was quite good considering it was intended to be of inexpensive disposable construction). In-vivo monitoring of blood pH was carried out on an anaesthetized ewe sheep. Both the probe and the microelectrode used gave results which compared well with pH values determined on blood samples by a laboratory blood gas analyser. The probe was only half the size of the electrode, which could be considered a good reason for pursuing this type of investigation.

The first FOCS based on fluorescence was reported in 1982⁷¹ and this involved fluoresceinamine covalently coupled to cellulose and glass. Fluorescence measurements were made by attaching the immobilised fluoresceinamine to the end of the fibre and immersing the fibre in the analyte solution. The intensity of the fluorescence varied as the immobilised dye was changed from acid to base. The study demonstrated the feasibility of chemical sensors

based on fluorogenic materials though the authors did state that they thought it best to concentrate further efforts toward developing sensors for metal ions that cannot be measured by potentiometric means rather than attempting to improve the pH sensor.

These early probes contained the most important features of their most recent analogues. The latter-day emphasis has been placed on developing sensors which exhibit extended stability, short-response times, greater economic efficiency, increased ease of use and high signal to noise ratios. The variety of approaches that have been described focus on the choice of indicator, type and configuration of substrate, method of immobilisation of indicator onto the substrate and various aspects of the instrumentation.

2.6.2 CHOICE OF INDICATOR

Depending on the specific end-use application, a suitable pH indicator must meet certain criteria. Naturally, its spectral properties must exhibit the greatest degree of change over the range of interest and have a high molar absorptivity in order to make optimum use of incident light. It should also lend itself to facile immobilisation onto a substrate of choice.

Photochemical stability is another important feature. The lower the photodecomposition rate of the reagent, the longer the potential life-time of the sensor. Indicators with strong responses to a particular analyte, or with high quantum efficiencies, may be completely useless because their stability under illumination is too low.

The excitation wavelength of an indicator should favourably be beyond 420 nm to allow the use of inexpensive fibres. Ideally, it should be at 480 nm or higher to make it LED-excitabile, but with fluorophores in particular, this is often unlikely for high efficiency materials.

Some of the problems associated with photolability of a reagent can be overcome by having a reference signal. This increases the complexity of the instrument but may be able to provide an enhanced longevity. If referencing is useful, then an indicator which has an *isobestic point* may be preferred. An isobestic point is a wavelength where the molar absorptivity is the same for the acid and conjugate base species of the reagent, and is independent of the equilibrium position of the reaction between them. Figure 2.25 shows the conversion of phenol red ($pK_a = 7.9$) from the yellow (acidic) to the red (basic) form. Isobestic points are recorded at 338, 367 and 480 nm.

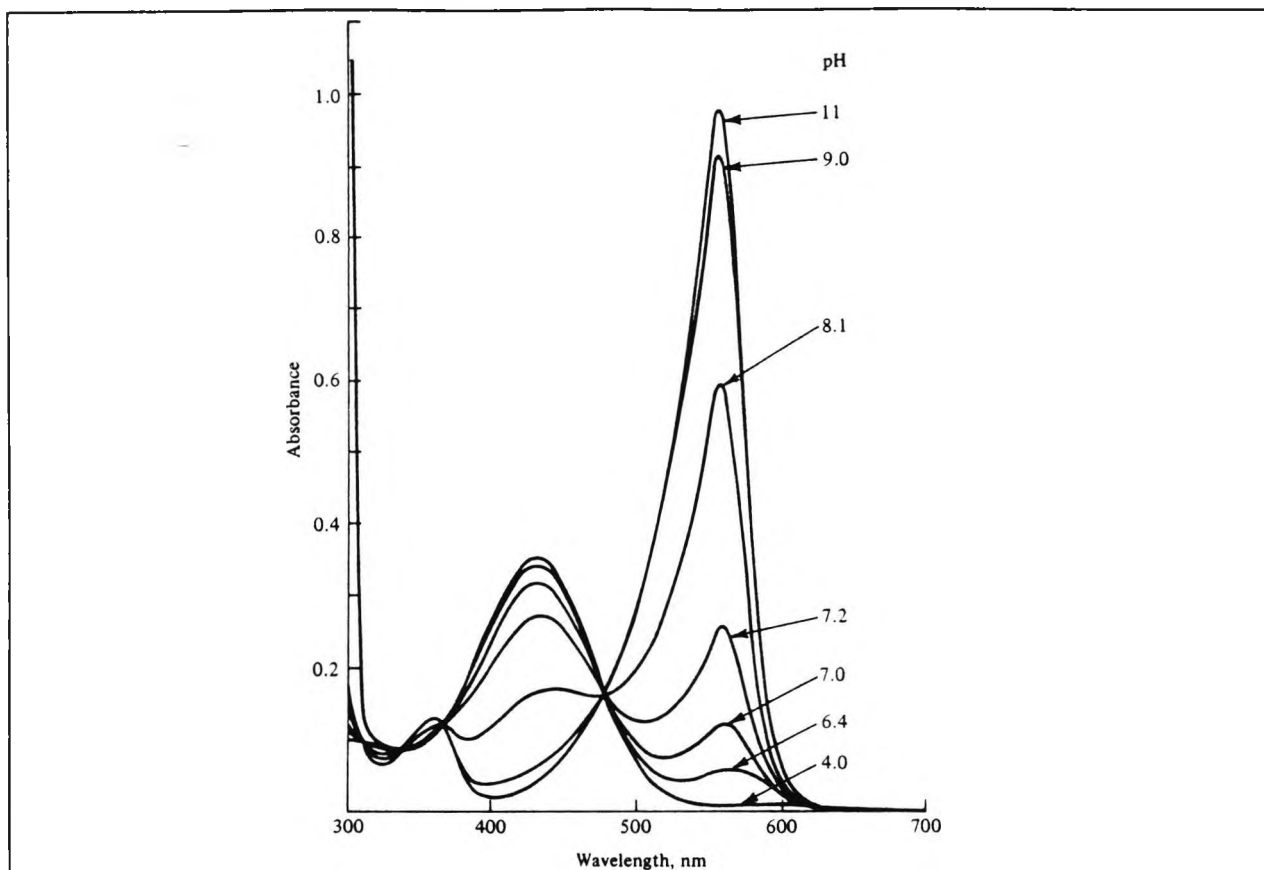


Figure 2.25 Chemical equilibrium between the acidic and basic forms of phenol red showing isosbestic points at 338, 367 and 480 nm⁴⁵.

A commonly used fluorescence indicator in pH FOCSS is fluorescein⁷² and the isocyanate version of fluorescein was the preferred indicator of the present study.

2.6.3 CHOICE OF SUBSTRATE

An indicator is usually immobilized on a rigid solid support which can then be attached to the end of the fibre. Ideally, for a material to be useful as a substrate it should be (a) optically transparent (b) rugged (c) chemically inert in the sampling environment (d) configured to a shape which enhances the optical signal (e) suffer no volume change when wetted or dried (f) have a high surface area in order to maximize the amount of indicator that can be immobilized (g) possess an open network of large volume pores so that the response time is minimized (h) be able to strongly adsorb the indicator without adversely affecting its optical properties.

The choice of support is governed by the requirements predicted by the analyte-indicator reaction and has a pronounced effect on the overall sensor performance. The solid supports can be broadly divided into two main groups: inorganic networks (mainly glass) and organic polymers. Polymers may offer a higher degree of processability which will allow the sensing material to be most favourably immobilized to the fibre. However they may have other

limitations, such as hydrophobicity, a tendency to swell or an intrinsic and interfering fluorescence. Polystyrene and polythene both fluoresce strongly in the blue, for example, and cellulose is not very rigid. Glass has the advantage of being rugged, transparent and resistant to bacterial attack. Porous glass (which will be discussed in more detail later) can provide the desired high specific surface and is available in various forms, even with surfaces which have already undergone chemical modification and are thus ready to be reacted to the indicator. On the other hand, it is prone to attrition when stirred or shaken and is not as efficiently bound directly to a fibre optic as are some polymers. *It has been one of the goals of the present investigations to develop polyorganic systems which synergetically combine the properties of polymers and glass-like substrates.*

2.6.4 METHODS OF IMMOBILISATION

The knowledge base accumulated on immobilisation techniques has arisen from protein-related studies but can be effectively applied to problems associated with dye immobilisation. Essentially there are four approaches covering both physical and chemical means^{73,40,140}, as is illustrated in figure 2.26.

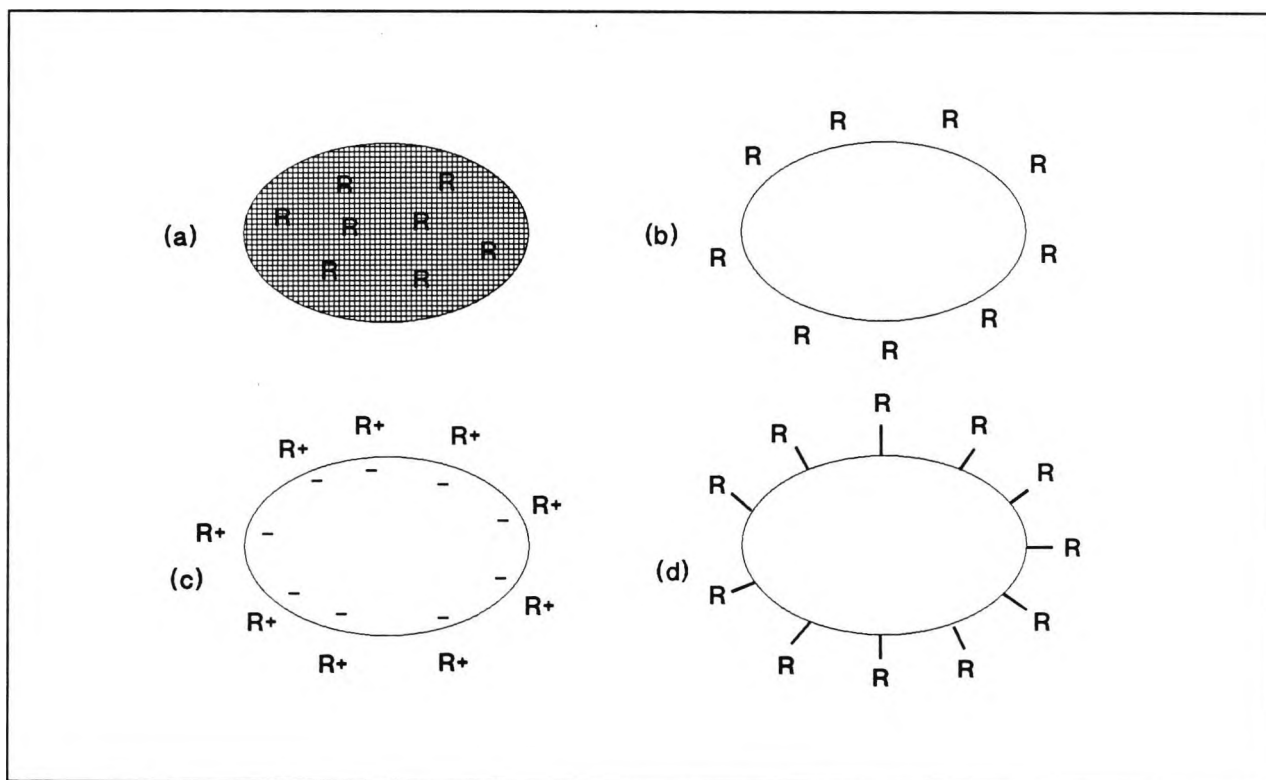


Figure 2.26 Different methods of immobilisation of a reagent⁴⁰.

The physical methods of immobilisation include gel entrapment, adsorption and electrostatic attraction. In gel entrapment (figure 2.26a), the reagent is immobilised within the interstitial space in the lattice of a polymeric network. In some cases the dye is entrapped mainly by virtue of its bulkiness, for example, microspheres of polyacrylamide containing non-diffusible phenol

red have been prepared by emulsion polymerisation⁷⁰. Another example is where sensing membranes are prepared by dissolving a polymer in an appropriate solvent (e.g. isoprene in chloroform, PVC in tetrahydrofuran), adding the indicator in solution and then coating the mixture onto the surface of a glass which allows the solvent to evaporate and gives the desired analyte sensitive film⁴⁹.

Entrapment can also be a result of adsorption phenomena (figure 2.26b), for example, FITC has been incorporated in the polar cages of a polysiloxane fibre-optic cladding prepared by the sol-gel by the addition of the FITC at the precursor stage¹⁴². The polar nature of the silica cage was demonstrated by pH studies conducted using entrapped bromocresol green and bromocresol purple which exhibited red or blue shifted absorption maxima compared to aqueous and alcoholic solutions of the dye, under acidic or basic conditions respectively. In general, adsorption involves the attachment of a reagent onto the support surface which has not been specifically functionalised for covalent or electrostatic bonding. Binding results from weak electrostatic or van der Waals interactions, hydrogen bonding and the formation of charge transfer complexes. Kirkbright *et al*¹⁹, used this latter approach to immobilise bromothymol blue to beads of a styrene-divinylbenzene copolymer by simply soaking the beads in a solution of the dye. Adsorption techniques are the most simple methods of immobilisation, but just like certain forms of gel entrapment, the binding strength to the solid surface is not very high and may be particularly susceptible to changes in pH, temperature or ionic strength.

Dyes can be immobilised onto solid supports which contain ionic groups by electrostatic attraction. Such solids are usually ion exchange resins which exist with a wide variety of functional groups for either anion or cation exchange. These resins can be classified into "strong" and "weak" ion exchangers, depending on the binding strength with the counter ion. Electrostatic immobilisation is possible with indicators that are charged in both the acid and the conjugate form. Typical examples¹⁴⁰ include bromothymol blue (on anionic polystyrene) and hydroxypyrene-trisulphate, HPTS, (on cationic quaternized aminostyrene). A major advantage of this material results from the fact that immobilisation occurs only at positions that are accessible to the indicator solution and, consequently, to the analyte as well. Therefore, high indicator blanks resulting from analyte-inaccessible indicator fractions are unlikely to occur. Unfortunately, the commonly available polystyrene-derived ion-exchange membranes exhibit a strong intrinsic fluorescence in the blue-green, which can strongly interfere with the signal from a number of important indicators.

Chemical immobilisation (figure 2.26d) is performed by covalently binding the indicator to a polymer surface. Both physical and covalent immobilisation have been applied to enzymes, antigens, antibodies and even whole bacteria and much information regarding immobilisation techniques can be found in the literature concerning these fields^{73,142}. The approaches

described are often applicable to the immobilisation of sensor indicators. Covalent bonding can be the most irreversible of the immobilisation techniques, but requires several steps in the synthesis of the immobilised reagent phase. It can involve the activation of the support material for reaction with the indicator, or the use of a coupling reagent for linkage of the indicator and support matrix, or the activation of the indicator for binding to the support. Consequently, the first step can involve the modification of the substrate surface in order to provide it with a sufficiently reactive function and similar procedure may also be required if the indicator does not possess chemical functions suitable for linkage to the modified surface. The subsequent stage involves the reaction of the modified solid substrate with the functionalised dye. Glass-like substrates have been employed in the present study and conventionally, these are modified with silylating agents. The topic of immobilisation onto glass is discussed in more detail in a later section. Table 2.1 (modified from reference 17) summarises the main routes for covalent immobilisation onto polymer substrates.

Although immobilisation techniques offer some obvious and decisive advantages, there are certain effects which must be considered. In the immobilisation of biosensing materials such as proteins or enzymes, care must be taken to retain the active conformation in order to avoid deactivation or denaturing effects. When a material is immobilised onto a solid surface, the conditions which immediately surround it will most likely not be the same as those in the external bulk solution. This phenomenon, referred to as the microenvironmental effect, can be the result of charges or physicochemical properties of the supporting matrix or may be caused by diffusional limitations⁷³. The effect has been exploited to develop a fluorescence sensor for monitoring ionic strength or pH⁷⁶ but can sometimes lead to unexpected results. Harper⁶⁹ noticed that in all the cases he studied, the colours of the bound pH indicators differed from those of the free indicators. Similarly, in the adsorption of a series of indicators on XAD-2, the dynamic response ranges were shifted to slightly higher pH values. It has also been observed that the value of the Stoke's shifts of different classes of dyes adsorbed on porous glass decrease as the molecules pass from solution to the solid matrix. This has been explained qualitatively based on a model of potential curves⁷⁵.

Table 2.1. Covalent Immobilisation onto Polymer Surfaces

Polymer	Reactive Group on Surface	Produced by Reaction with (e.g.):	Suitable for Coupling to:	
Cellulose (Agarose)	Hydroxyl	(Naturally occurring)	Triazine derivatives	
	Aminoethyl	(i)BrCN (ii)Ethylenediamine	Carboxylates, sulphonic acids, proteins, imidoesters	
	Epoxy	Epichlorohydrin/NaOH	Carboxylates, phenols, thiols, amines	
	Dichlorotriazinyl	Cyanuric chloride	Alcohols, amines, thiols	
	Glass (silica gel, quartz, porous glass)	Amine	Triethoxysilylpropyl-amine	Isocyanates, isothiocyanates, acids, acid chlorides
		Chloroethyl	Triethoxysilylpropyl-chloride	Alcohols, phenols, amines, carboxylates
		Mercaptopropyl	Triethoxysilylpropane-thiol	Thiols, acids, mercurials, diazoacetyls
Epoxy		Glycidyloxypropyl-trimethoxysilane	Carboxylates, phenols, thiols, amines	
	Vinyl	Triacetoxyvinylsilane	Strong nucleophiles	
	Methacryloyl	3-methacryloxy-propyltrimethoxysilane	Strong nucleophiles	
Poly(acrylic acid)	Carboxyethyl CH ₂ CH ₂ COCl	(Naturally occurring) SOCl ₂ , POCl ₃	Amines, proteins Amines, alcohols, thiols	
Polyacrylamide	Carboxyethyl	(i) strong alkali (ii) strong acid	Amines, proteins	
	Long-chain amine	Long-chain diamine	Carboxylic acids, isothiocyanates, proteins	
Polystyrene	Chloromethyl	Chloromethylation or by copolymerisation with vinyl-benzene chloride	Amines, alcohols, carboxylates, thiols	
Acrylic acid-vinyl chloride copolymer	Carboxyethyl CH ₂ CH ₂ COCl	(Naturally occurring) SOCl ₂ , POCl ₃	Amines, proteins Amines, alcohols, thiols	

2.7 SUMMARY

In conclusion, the notion of immobilising a suitable indicator onto a solid substrate for fibre optic pH sensing has been demonstrated in the literature and it is clear that consideration must be given to the choice of not only the indicator, but also of the substrate and method of immobilisation. For this study, the initial investigation dealt with the immobilisation of fluorescein isothiocyanate onto glass because the literature indicated that such an approach could be useful. These aspects are dealt with in some detail in subsequent chapters, which discuss a practical approach to the development of FOCSs.



Chapter 3

DESIGN AND CONSTRUCTION OF THE OPTO-ELECTRONIC CONFIGURATIONS

3.0 ABSTRACT

A description is given of two opto-electronic configurations which were developed specifically for this investigation. The first consists of a fibre-optic link to a commercial spectrophotometer. The second involved the use of an argon ion laser and was constructed to illustrate some of the other design principles which feature in FOCS. The arrangement of fibres in a simple fibre optic bundle is considered and its optimum configuration is illustrated by experiment.

A data acquisition program which was designed specifically for this work is outlined and a full listing is given in an appendix. In practice, the use of this program greatly facilitated the acquisition and evaluation of data from the opto-electronic configurations described.

3.1 FIBRE-OPTIC LINK TO A COMMERCIAL SPECTROPHOTOMETER

The main purpose of the work done for this study was to investigate certain aspects of specific substrates used to support a fluorescing reagent. It is clear from the previous Chapter that considerable effort could be invested into designing and optimising an opto-electronic configuration suitable for FOCS. Since this was not the primary objective of the present investigation a fibre-optic link was constructed to a Perkin Elmer (PE) Fluorescence Spectrophotometer MPF-4. This enabled the accumulation of reliable and reproducible measurements of optical fluorescence of the systems under investigation with little concern, at this early stage, for the details of the instrumentation. The PE MPF-4 is typical of such instruments and the basic components are illustrated in figure 3.1.

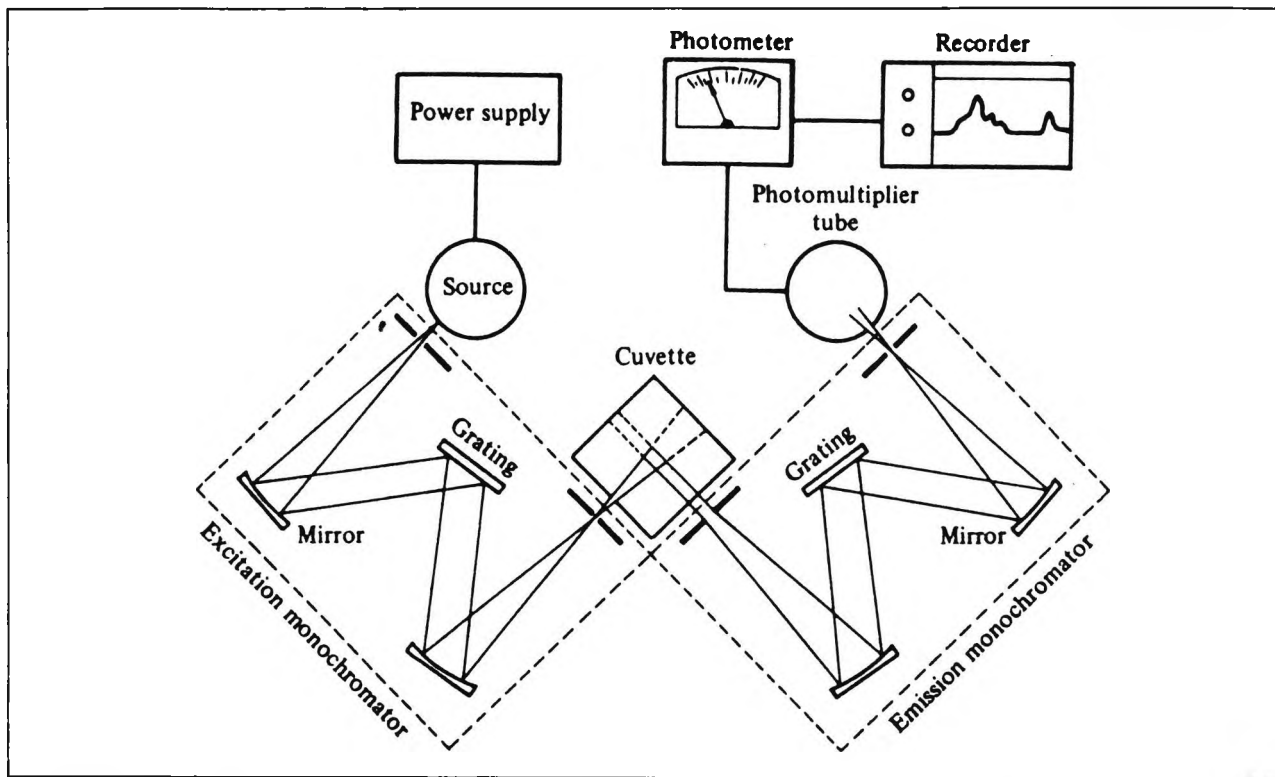


Figure 3.1 Schematic diagram of a fluorescence spectrophotometer⁴⁵

In the PE MPF-4, the configuration of the sample chamber can be changed so that, for example, phosphorescence studies can be performed. In practice, this entails removing the plate on which the lenses are set and replacing it with one of another design. This feature was exploited for the present investigation so that a fibre-optic link could be established; the original set-up was replaced with the one illustrated in figure 3.2.

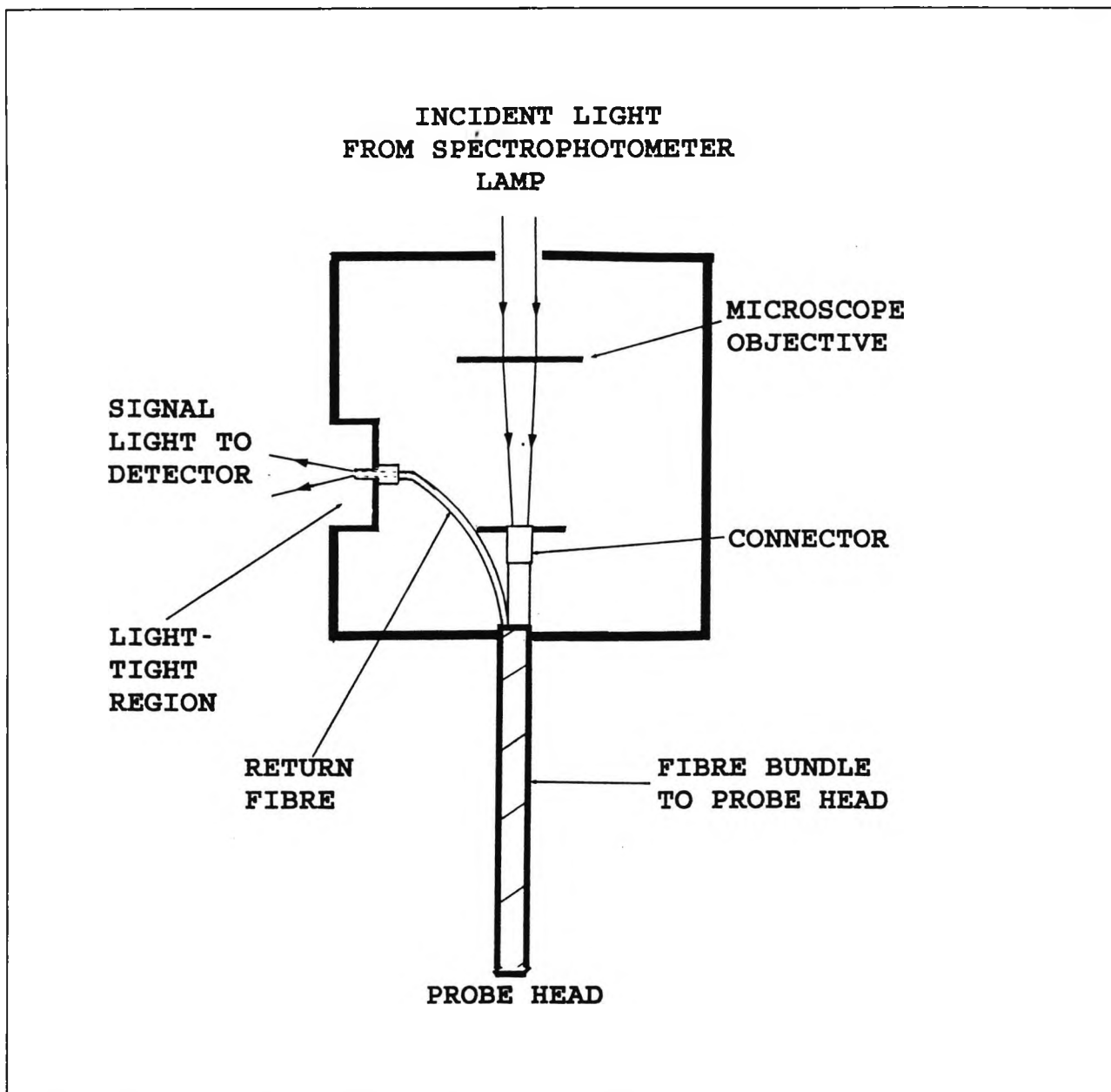


Figure 3.2 Optical-fibre link to spectrophotometer.

Light from the spectrophotometer lamp is focussed into the central fibre of the fibre bundle (described below) and propagated down its length to the distal end. The reflected or fluorescence radiation emerging from the sample under study is gathered by the seven surrounding fibres and carried back to the fluorometer. The plate into which the return fibres are set is butted up against the opening in the optical chamber which leads to the fluorometer detector. Although this is probably not the optimum arrangement in terms of the optical alignment, it was effective in that it ensures that there is minimal pick-up of background light and light signals from the sample were readily measurable. Essentially, this arrangement is tantamount to representing a spectrophotometer with a remote sensing capability.

3.2 OPTO-ELECTRONIC ARRANGEMENT FOR FOCS

This instrument (figure 3.3) was designed in order to assess further some features of the fluorophore and FOCS. The argon ion laser is a convenient source of 488 nm radiation and its collimated output is easy to couple to an optical fibre⁵.

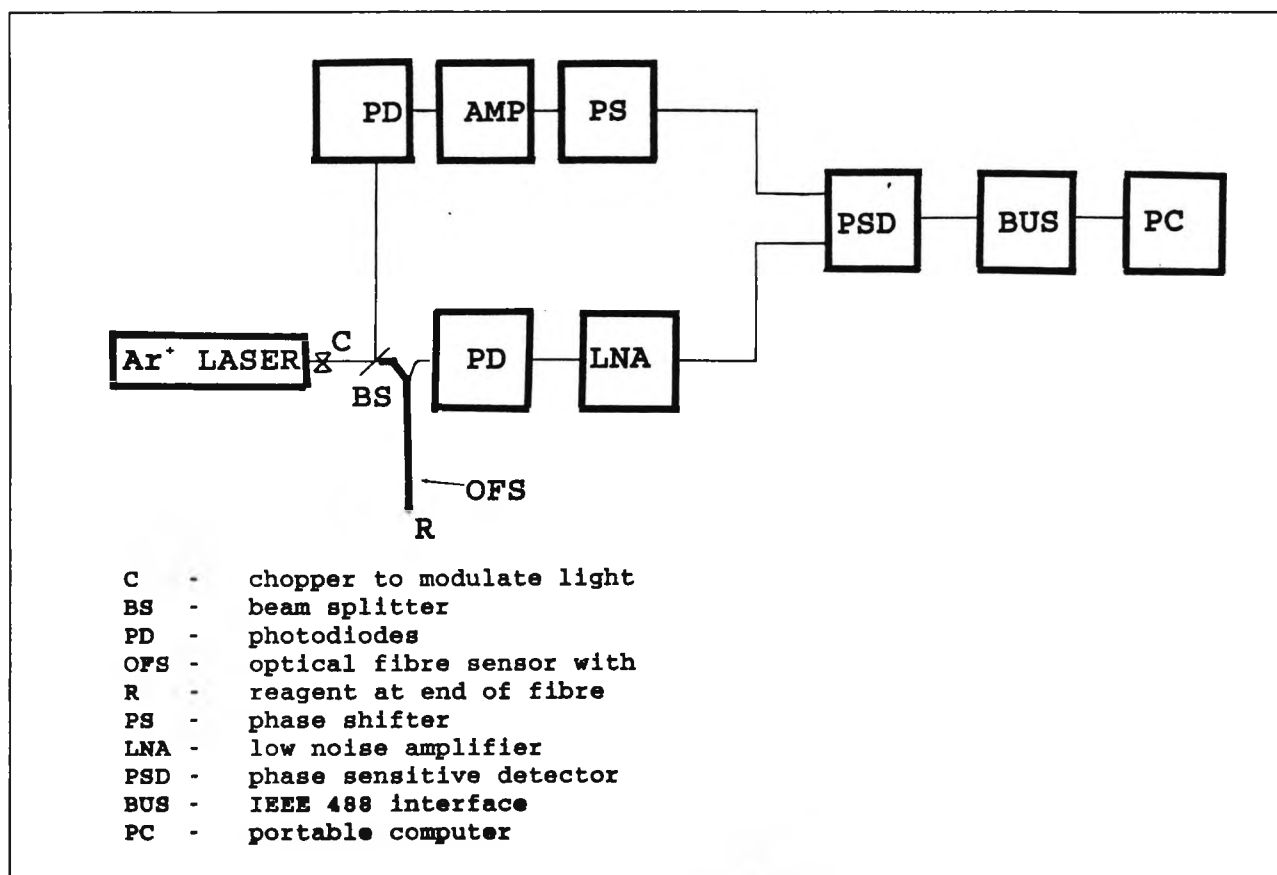


Figure 3.3 Opto-electronic arrangement for FOCS⁵

There are two main sources of error which will interfere in the measurement of weak light signals. The first is unwanted radiation from objects surrounding the measurement apparatus and the second is noise in the photodetector and its amplifier. In the configuration illustrated in figure 3.3, the light emerging from the argon ion laser is modulated by a "chopper" and then is split, to give an excitation and reference signal. Since the optical signal is modulated resulting in an output which is alternating current (a.c.), the direct current (d.c.) component due to background light may be eliminated by using a.c.-coupled amplification in the detection circuit. In essence, the light signal arising from the sample is related in frequency and phase to the reference signal and by using a phase-sensitive detector maximum readings will be obtained when the reference and signal voltages are in-phase. This enables the resolution of small signals and significantly reduces the sources of error mentioned above. The detection circuit has been optimised by the manufacturer and details of the components used can be found in the associated literature⁷⁷.

3.3 OPTICAL FIBRE BUNDLE

The arrangement of the fibres in the fibre-optic bundle was investigated in order to determine a convenient and efficient configuration.

3.3.1 COMPONENTS

The following components were used in its construction:

8 x 1 m lengths of 600 μm core fibres (Quartz & Silice)

Two component epoxy adhesive (Ciba Geigy)

Heat-shrink sleeving (RS Components)

PVC sleeving (RS Components)

3.3.2 METHOD OF CONSTRUCTION

The optical fibre bundle was constructed with **eight** fibres, for reasons as discussed below. Seven of the fibres were stripped of six centimetres of their protective coating. Epoxy adhesive was applied to the eighth fibre (which was not stripped of its outer coating) and the other fibres were carefully placed around it. Polyolefin tubing was positioned at the end of the fibre bundle and reduced in diameter by thermal irradiation using a heat gun. Adequate time was allowed for the adhesive to set.

Normally, the fibres are polished using diamond paper. In this case, however, this was not possible due to the presence of the plastic heat shrink material. Instead, a glass cutter was used. The fibre bundle was tightly clamped into position and its end cleanly cut-off by the rotating blade. The final result was quite suitable for the required application.

3.3.3 NUMBER OF FIBRES

In order to maximise the intensity of both the excitation and emission light signals consideration was given as to how best to arrange a small number of optical fibres in a bundle. The number of fibres of total radius r which can be arranged around a central fibre of total radius R is given by:

$$N = \frac{360}{2a}$$

$$\text{where } \sin a = \frac{r}{r + R}$$

The fibres used had the following specifications (appendix III.1):

Core diameter	=	600 ± 24 μm
Cladding diameter	=	750 ± 60 μm
Coating diameter	=	1060 ± 85 μm

If the protective coating is retained on all of the fibres (figure 3.4a), N is calculated as exactly 6 and the closest packing configuration consists of 6 fibres arranged in a hexagon around a central fibre. By retaining the coating on only the central fibre, N is calculated to be just greater than 7 and hence an eight-fibre configuration is possible (figure 3.4b).

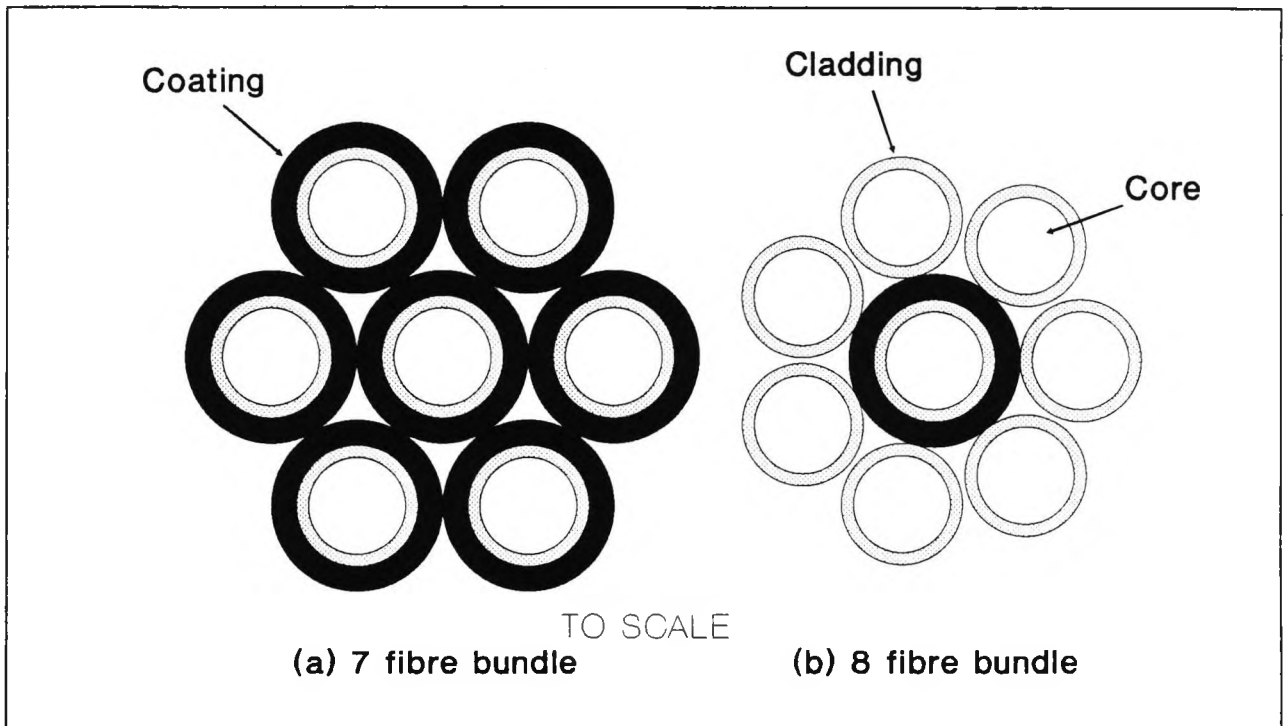


Figure 3.4 Number of fibres in fibre optic bundle.

If the **active** area is defined as the sum of the areas of the cores of the outer fibres (reflected or fluorescent light is launched along the return fibres through this area), and the **total** area is that which encloses the complete fibre optic arrangement (i.e. that circular area which will be illuminated from the reflected light of the central fibre) then the (theoretical optimum) **efficiency** of the fibre optic bundle is simply the ratio of active to total area. For the seven fibre

arrangement where all the fibres have an outer coating, the efficiency is calculated as 0.21. For the eight fibre arrangement, as described, the efficiency is 0.39 and thus this arrangement is to be preferred. (Note that if the coating is also removed from the central fibre, then the optimum efficiency increases to 0.43. This arrangement was not chosen because it was difficult to handle and since adhesive was used to hold the fibres together such close packing was in any case not possible).

3.3.4 MODE OF EXCITATION

The eight fibre bundle can be used such that the central fibre carries the excitation light from the light source to the sample and the surrounding fibres return the signal emission back to the detector (figure 3.5a, probe 1), or the outer fibres carry the excitation light and the central fibre returns the signal (figure 3.5a, probe 2). The intensity of reflected light as a function of the distance of the fibre bundle from a plane mirror was evaluated (figure 3.5b).

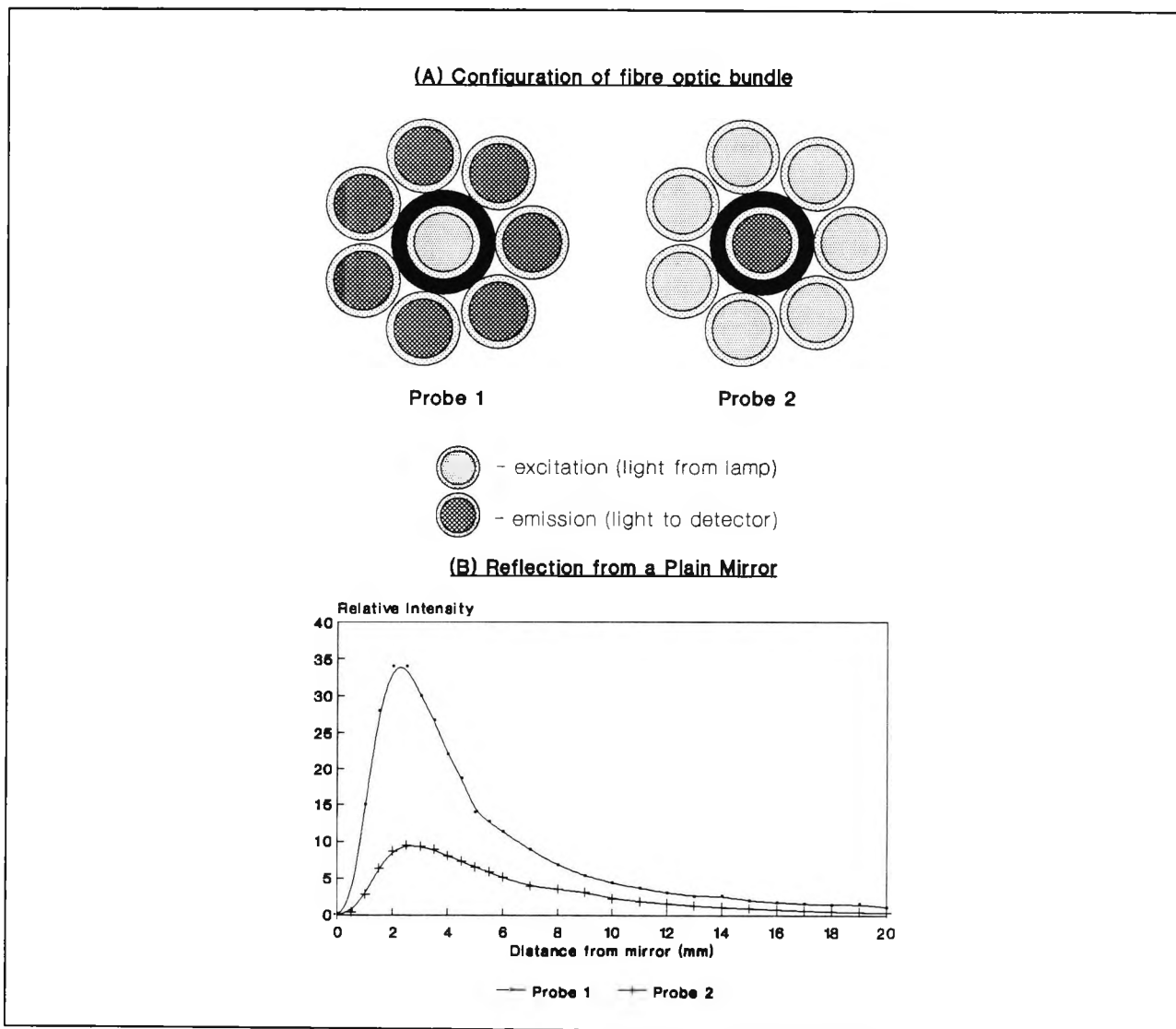


Figure 3.5 Mode of excitation.

The results indicated that probe 1 is the most efficient configuration and this arrangement was consequently used throughout the subsequently reported investigation.

Similar fibre arrangements to those described above have been reported by others⁷⁸ and are now also commercially available^{e.g. 79}.

In this section, a simple approach has been demonstrated for comparing the effectiveness of different configurations and have also drawn attention to the fact that the efficiency of a fibre arrangement can be readily predicted by considering its so-called 'active' area.

3.4 COMPUTER INTERFACE

Using commercially available components the data generated by the two electro-optical arrangements described earlier were interfaced to a computer. This was done in order to facilitate the data gathering procedure and the subsequent evaluation.

3.4.1 COMPONENTS

The instrumentation required for the computer interface incorporated the following components:

IEEE-488 General Purpose Instrument Bus (National Instruments)

IEEE-compatible Digital Multimeters (Hewlett Packard)

IEEE-compatible Cables (RS Components)

Data Acquisition Software (Lotus MeasureTM)

Portable Personal Computer (IBM)

3.4.2 DESCRIPTION OF THE COMPUTER INTERFACE

An IEEE-488 GPIB was fitted to the portable IBM PC and the voltage output directed to it via a digital multimeter. A commercial software package (Lotus MeasureTM) was used to access the data, but the actual data acquisition routines were tailor-written for user friendliness and with particular reference to the instruments available.

The data acquisition program consisted of three separate files. Appendix III.2 has copies of screen-prints for the three program files illustrating what is actually seen on the computer monitor. For each program, there is additionally a full program listing by cell entry. Figure 3.6a shows the logic steps in the first file (DATALOG). To begin with the bus configuration file (which was supplied with the GPIB) was retrieved and then titles and instructions were displayed. At this stage, the user could choose to read data from a multimeter either manually (in which case the program then retrieves the MANUALOG file), or automatically (in which case the program

then retrieves the AUTOLOG file). In the manual mode each data reading had to be separately prompted whereas in the automatic mode a data acquisition rate was defined (maximum 1 reading per second) and then, once the run was initiated, data were input automatically.

Simultaneous measurement of two signals was also possible which enabled the recording of the output from a pH electrode and the opto-electronic configuration at the same time. Calibration runs (using the manual mode of operation) were performed prior to each series of evaluations using this method.

Although the manual and automatic data logging programs were stored in separate files they were very similar in logic design. In the set up routines, the user was asked to enter various parameters such as the type of multimeter(s) employed (subroutine: CHOOSE), title of the experiment, the name of the data file and the names of the X and Y ranges (subroutine: INFOIN). The date is displayed automatically. To make the program more user friendly, error messages would be displayed if the input parameters had not been entered in the corrected format (subroutines: ERR1 and ERR2). At this stage the subroutine CHECK gives the user the opportunity to check that the run parameters were entered correctly and make changes as required. If the command is given to PROCEED then the subroutine INIT is executed which clears the multimeter buffers and positions the cursor ready to begin reading data into spreadsheet.

Once the necessary information had been registered, the subroutine MENU is accessed. Again, the logic design of this part of the program is the same for both the manual and automatic data logging procedures and is illustrated in figure 3.6c. The main difference between the two procedures is contained in the subroutine DATAIN. The manual and automatic logging versions of this subroutine are given in figures 3.7a and 3.7b respectively and are self-explanatory.

The final output was in the form of data entry to a spreadsheet which was then converted to meaningful units from the previously determined calibration values.

Subsequent chapters describe the use of the instrumentation considered in this section and, in practice, the data acquisition programs were found to be very useful in particular because they greatly facilitated the data gathering step but also because subsequent data handling and data display were significantly simplified.

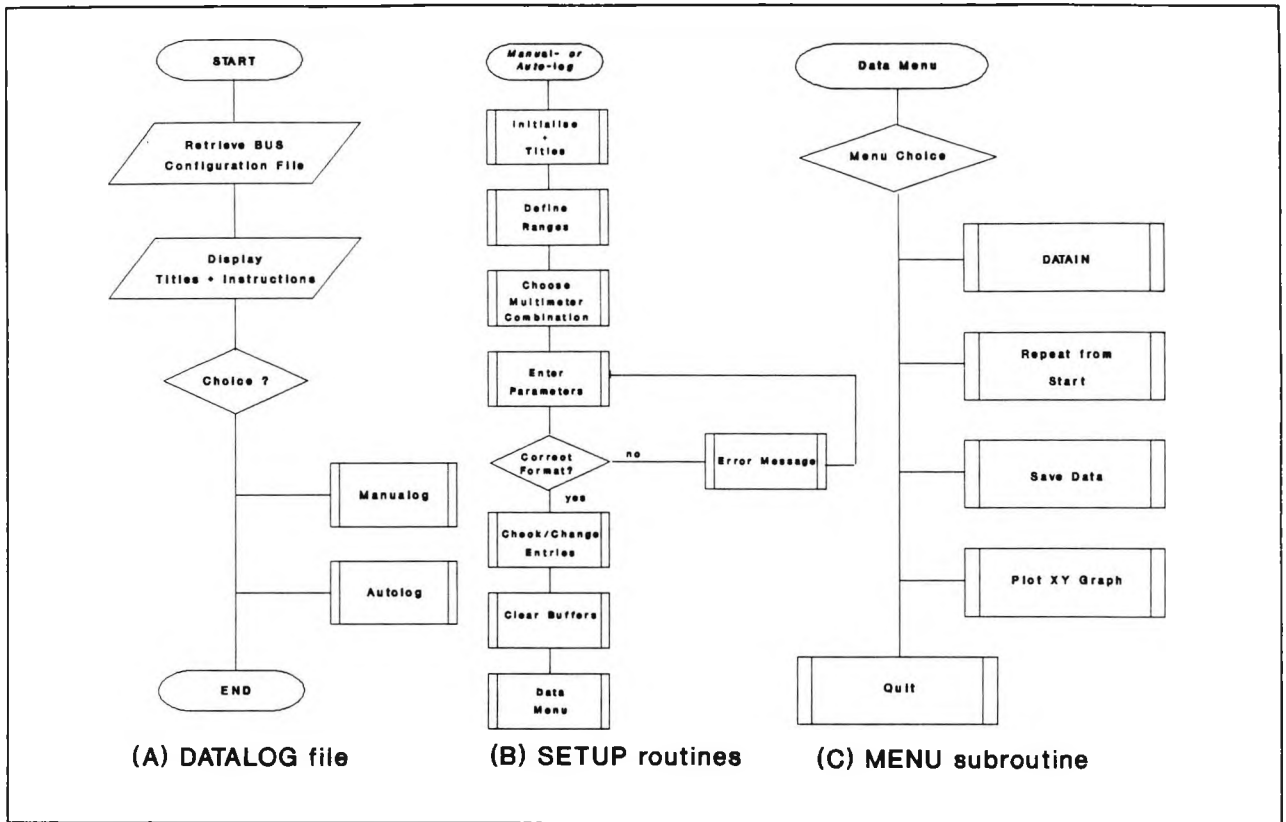


Figure 3.6. a) DATALOG program.
 b) Initialisation and input parameters routine (general).
 c) Data menu routine (general).

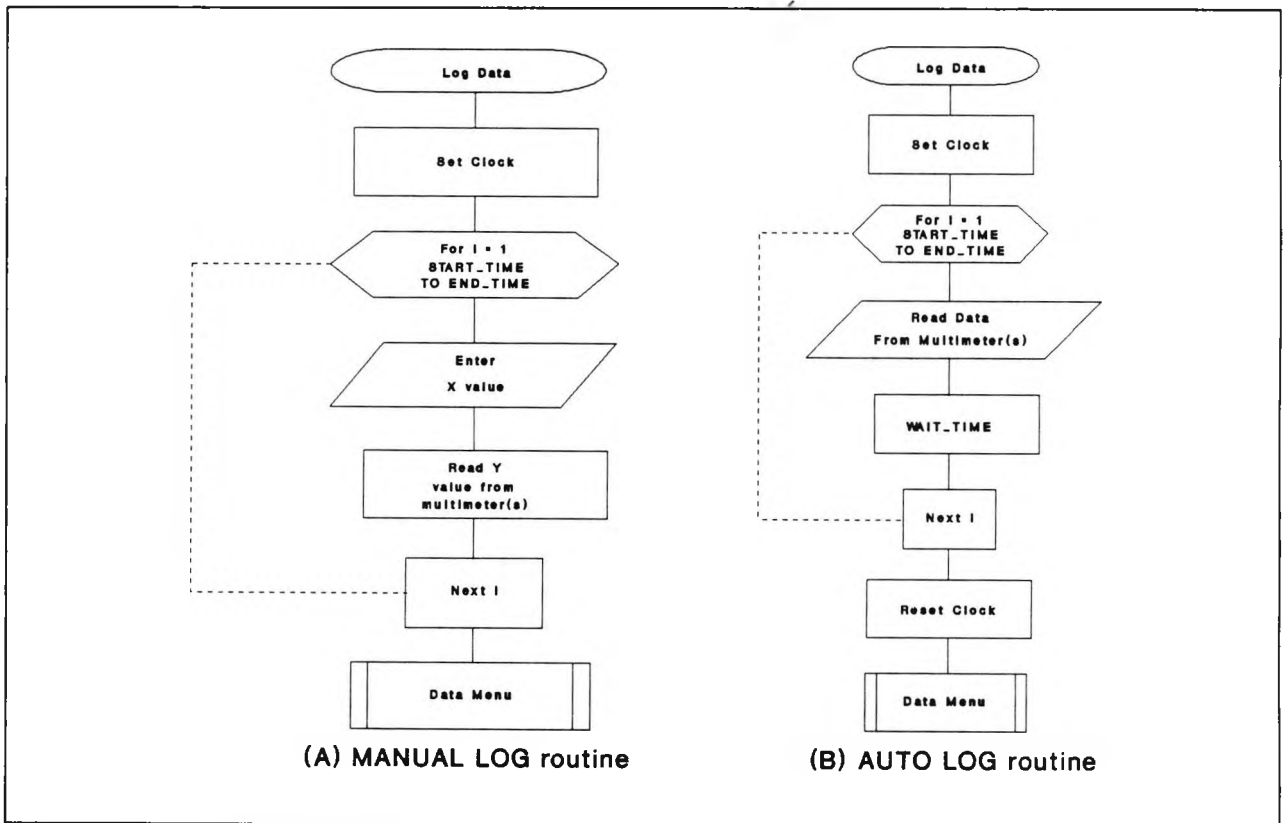


Figure 3.7. a) Manual log data routine.
 b) Auto log data routine.



CHOICE OF pH SENSITIVE FLUORESCENT REAGENT

4.0 ABSTRACT

The fluorophore fluorescein isothiocyanate (FITC) is discussed and its fluorescence properties are assessed. The suitability of FITC as a pH sensitive reagent is confirmed using the opto-electronic configurations developed for this study.

4.1 STRUCTURE OF FITC

The fluorescence indicator used in this study was fluorescein isothiocyanate (FITC) [3326-32-7].

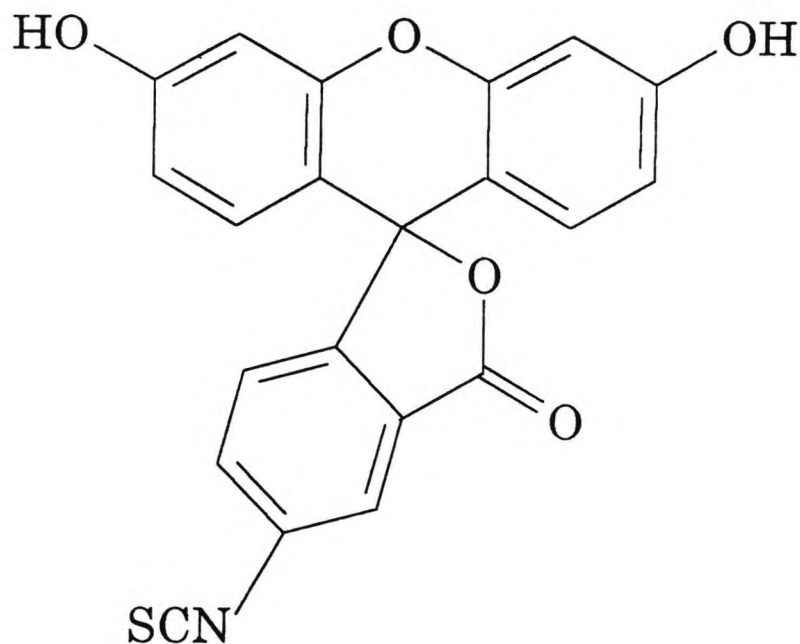


Figure 4.1 Structure of FITC (lactoid configuration).

FITC is the most widely used probe in fluorescent immunoassay techniques because fluorescein has an exceptionally high quantum yield, good photostability and a relatively low temperature coefficient. Also, the isothiocyanate group provides a site for easy immobilisation

of the molecule on to suitable substrates by reacting with amines to give thioureas and thiol groups to give dithiocarbamates. This group is much less sensitive towards water than the isocyanate group and is also safer to produce (since thiophosgene is used instead of phosgene)⁸². Another important practical feature of FITC is that it has convenient absorption and emission wavelengths^{73,81}.

FITC is attractive as a reagent for pH sensing because it can undergo rearrangement, deprotonation and protonation reactions which affect its resonance structure and consequently alter its fluorescence. The following scheme illustrates this point.

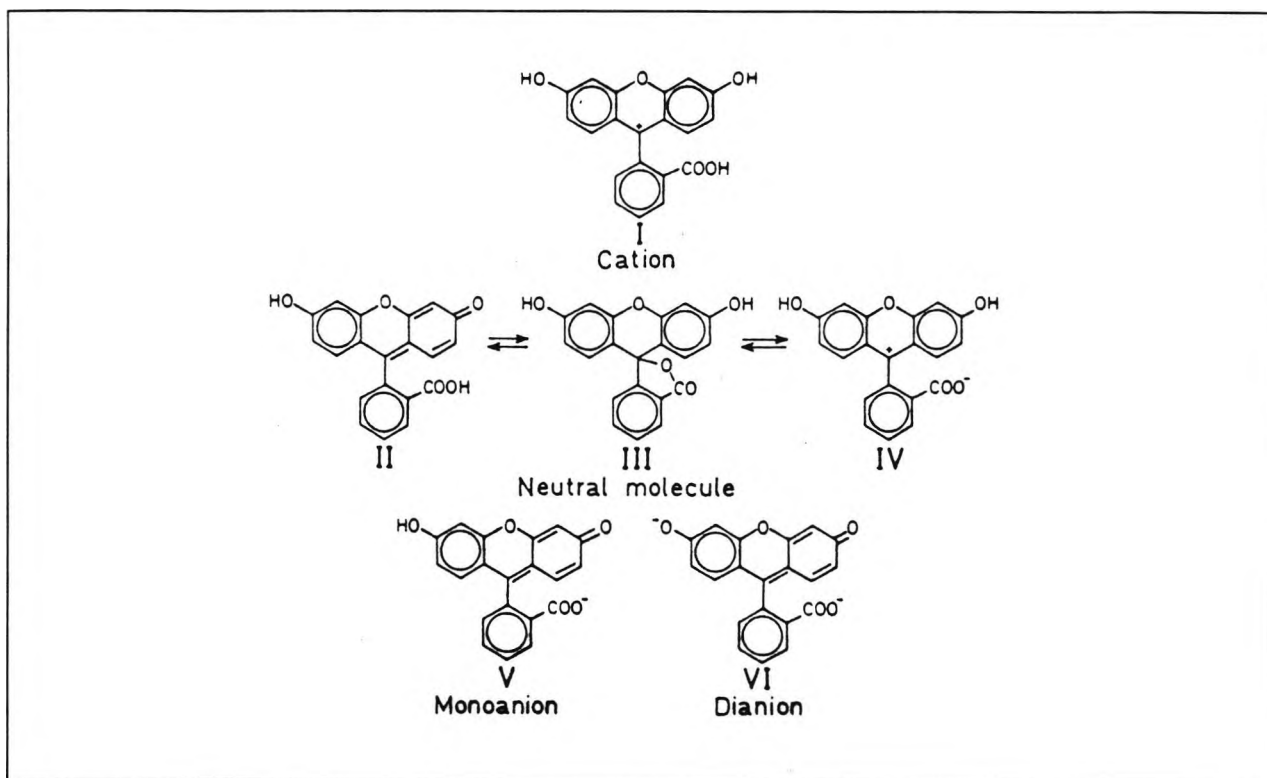


Figure 4.2 Protolytic forms of fluorescein⁸³.

The pK_a value of an indicator is equal to the pH value at which the transition occurs from one protolytic form to another. Fluorescein has three overlapping pK_a values which extend its analytically useful range from about pH 2 to pH 9, far beyond that of a conventional indicator. At the upper and lower pH limits, however, the response is non-linear which to some extent prevents the use of FITC for blood gas monitoring (pH of blood is 6.8 - 7.7)⁸⁰. Table 4.1 shows the absorption maxima of the different protolytic forms of fluorescein and the corresponding pK_a values⁸³.

Table 4.1 Absorption maxima of the different protolytic forms of fluorescein and the corresponding pKa values.

	Absorption Peaks		
	pK _a	λ (nm)	ε (mol dm ⁻³ cm ⁻¹)
cation (I)	2.2	437	55 000
neutral (II + III + IV)	4.4	437	16 000
monoanion (V)	6.7	437	30 000
		475	31 000
dianion (VI)		491	88 000

The fluorescence of fluorescein arises from the delocalised structure of the xanthenone part of the molecule. This structure is absent in the lactoid isomer of the neutral molecule. This partly explains why the fluorescence increases with increasing pH, since the anionic and dianionic forms are delocalised.

For fluorescein, the most useful transition in terms of FOCS occurs through pH 6.7. Firstly, this is because this pH range is of interest in many applications⁶⁷ and secondly because there is a significant increase in the molar absorptivity, ε, and hence a correspondingly large change in the fluorescence emission. The spectral properties of FITC are similar to those of fluorescein (see Appendix IV.1) although the relative fluorescence intensities are known to differ⁸⁴.

4.2 FITC SOLUTION SPECTRA VERSUS CONCENTRATION

4.2.1 UV-VIS ABSORBANCE SPECTRA

4.2.1.1 PROCEDURE

The UV-visible absorbance spectra of FITC were measured using a Perkin Elmer Lambda 5 UV-VIS spectrophotometer. FITC (5.2 mg) was dissolved in a pH 7 buffer solution (100 ml) to form a neat (N) mixture from which subsequent dilutions were prepared. Spectra were observed between 350 - 600µm using 1 cm quartz sample cuvettes and referenced versus air. The following settings were used:

Ordinate Mode	:	Absorbance
Slit Width	:	2 nm
Scan Speed	:	1000 nm
Response	:	0.5 s
Lamp	:	332.8 nm
Peak Threshold	:	0.020 A

4.2.1.2 RESULTS AND DISCUSSION

Figure 4.3a shows some of the UV-VIS spectra obtained. From concentrations of N/4 and lower, the maximum observed absorption wavelength was around 493nm. For N/2, λ_{\max} = 486 and for N, λ_{\max} = 471nm.

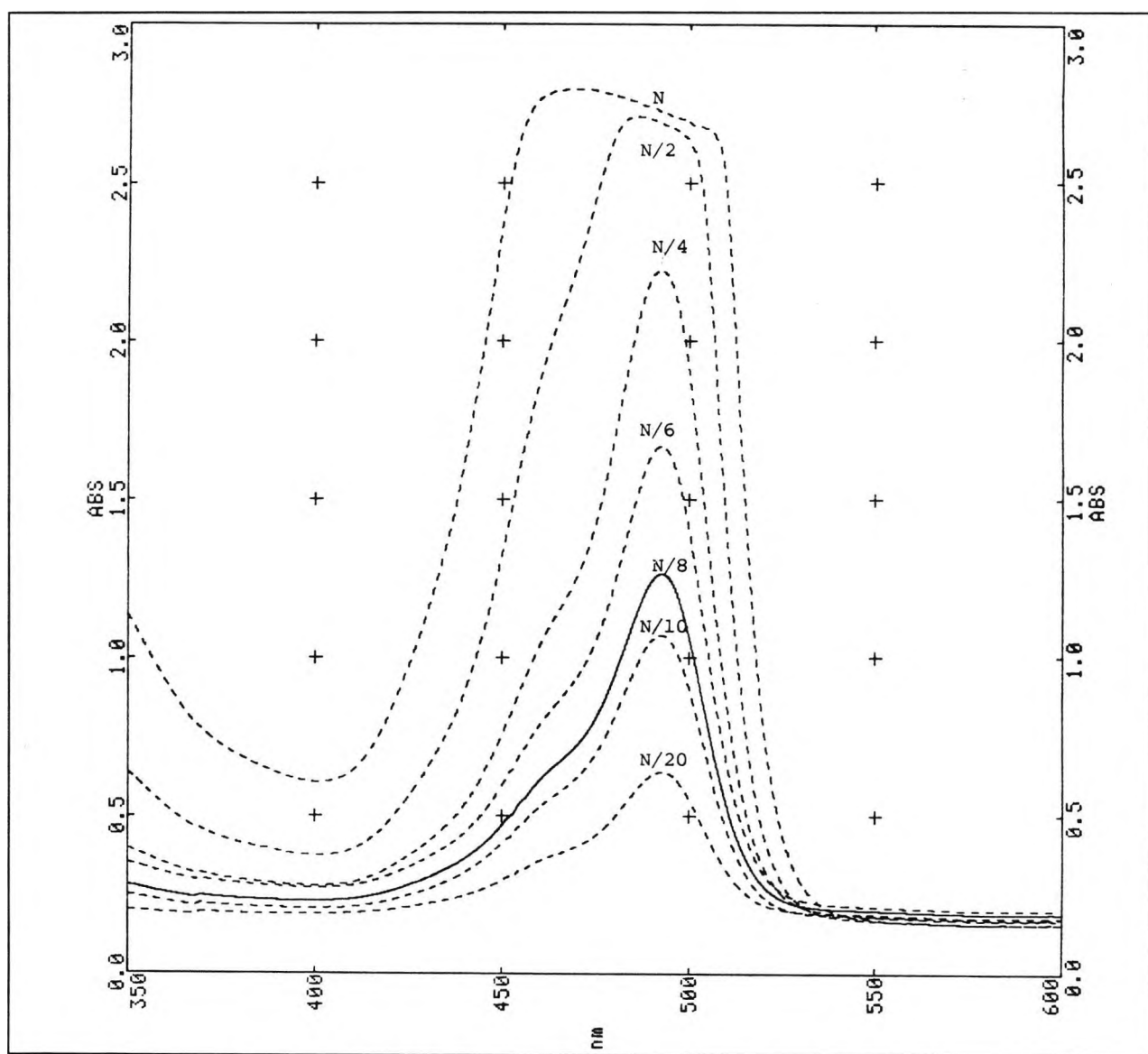


Figure 4.3(a) Absorbance spectra of FITC at different concentrations.

Figure 4.3b shows the peak absorbance values versus concentration. It can be seen that the relationship deviates from linearity at higher FITC concentrations. This is because the Beer-Lambert relationship (see section 2.5.1) only remains linear as long the refractive index of the solution does not change significantly i.e. at low concentrations⁴⁵.

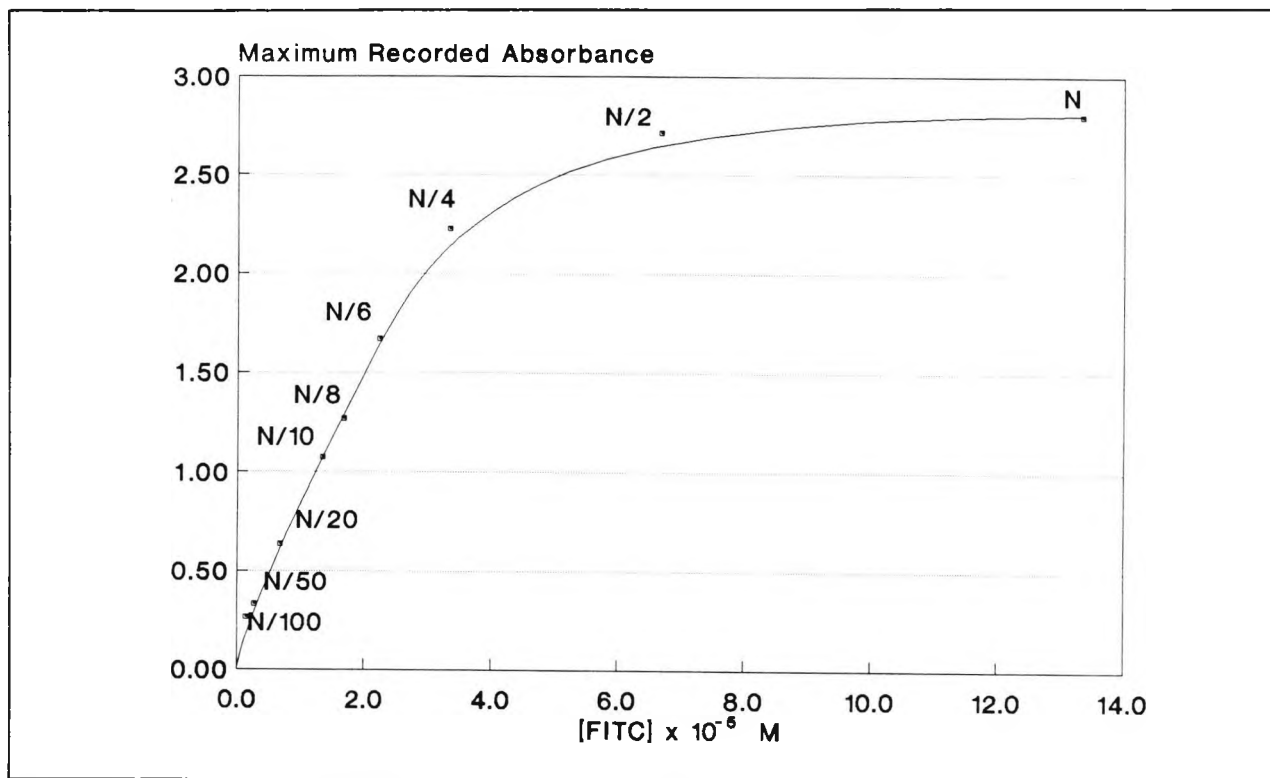


Figure 4.3(b) Maximum absorbance values at different concentrations.

4.2.2 FLUORESCENCE SPECTRA USING FIBRE-OPTIC LINK TO THE SPECTROPHOTOMETER

4.2.2.1 PROCEDURE

The fluorescence spectra were recorded using the fibre optic link described earlier (section 3.1).

Typical fluorometer settings used were:

Excitation Slit	:	6 nm
Emission Slit	:	6 nm
Excitation Shutter	:	"OPEN"
Scan Speed	:	30 nm min ⁻¹
Wavelength Drive	:	"EMISSION"
Excitation wavelength:		488 nm
Emission wavelength :		490 - 600 nm

The recorder settings were adjusted depending on the strength of the signal. From an analysis of the sensitivity settings of the fluorometer (see appendix IV.2) it was concluded that only the *coarse* gain setting could be varied during a series of measurements. The output response of the *fine* gain setting was non-linear at the high and low settings and consequently was kept constant for a particular set of measurements. In this case, the settings were adjusted from x30 to x100 (maximum) for concentrations at or below 3.6×10^{-6} M.

The distal end of the fibre bundle was fixed at a set height above the bottom of a black glossy container which held the FITC solution. Care was taken to shield the test solution from ambient light. The spectra were recorded using the automatic data logging routine described in section 3.4.2. In this case, the test mixtures were prepared from a stock solution concentration of $1.0 \text{ mg (100 ml pH 7 buffer)}^{-1}$.

4.2.2.2 RESULTS AND DISCUSSION

The maximum emission wavelengths for the recorded spectra (figure 4.4a) are around 510 nm, which is typical for this compound⁸⁴.

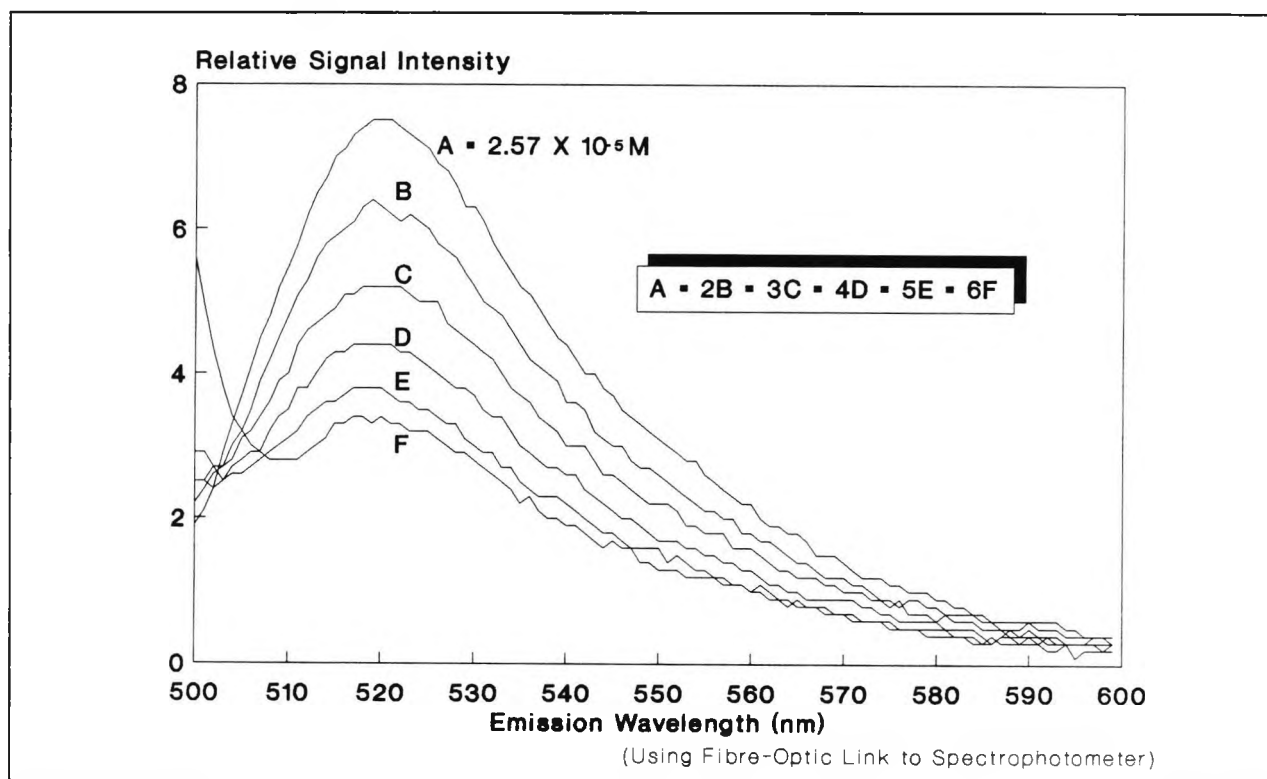


Figure 4.4(a) Fluorescence spectra of FITC at different concentrations using fibre-optic link to spectrophotometer.

Figure 4.4b shows the total fluorescence intensities (as calculated from the areas under the curves) plotted versus the concentration of the FITC solution. Some resemblance to the absorbance curve previously discussed is apparent but there is significant deviation from

linearity at both high and low concentrations and reasons for this are discussed below. It should also be noted that as the solutions become more dilute, the effect of the reflectance of the excitation radiation (at 488 nm) becomes more significant.

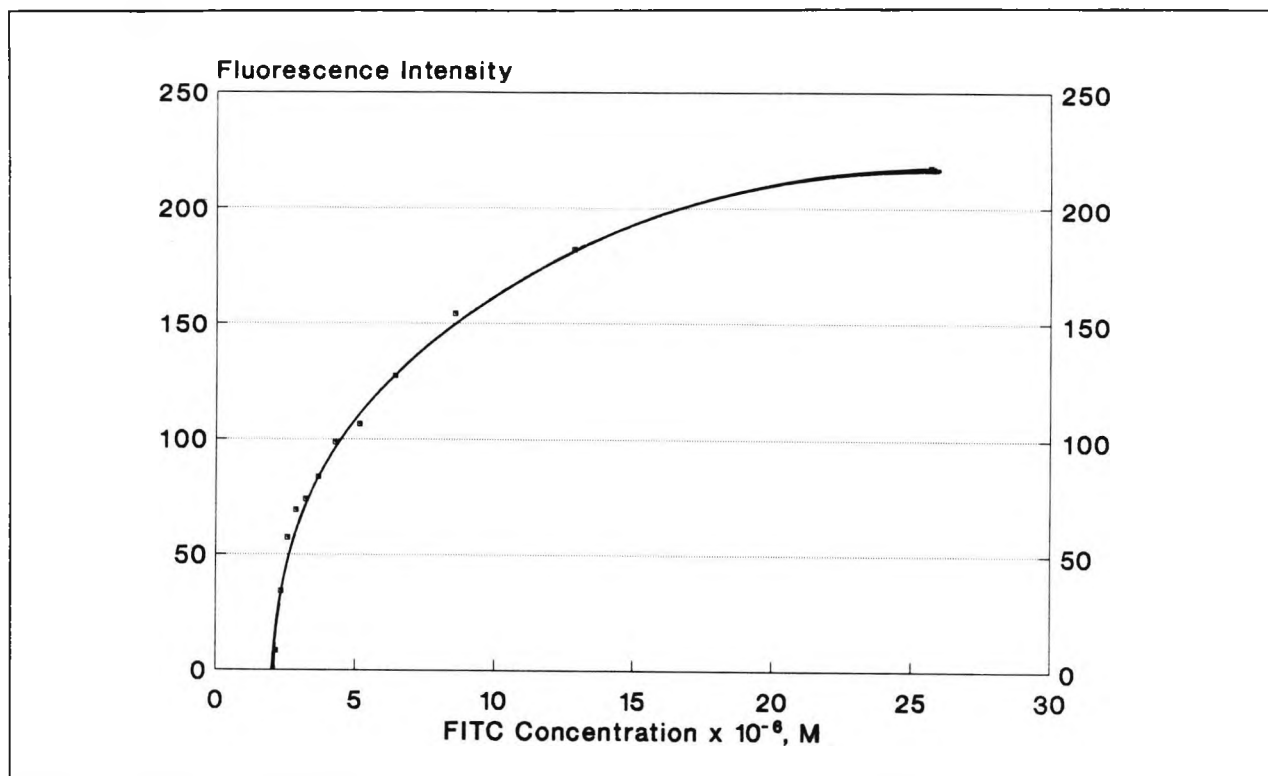


Figure 4.4(b) Total FITCaq fluorescence for different concentrations.

Some deviation from linearity toward the concentration axis is expected⁸⁵ since the unapproximated version of Parker's law (section 2.5.2) is given by:-

$$\frac{I_f}{I_o} = g\phi(1 - \exp^{-2.303\epsilon Cd})$$

- where
- I_f = intensity of fluorescence radiation
 - I_o = intensity of incident radiation
 - ϵ = molar absorptivity
 - ϕ = quantum yield
 - C = concentration of luminescent species
 - d = optical path length
 - g = fraction of emission observed

But, absorbance, $A = \epsilon Cd$ (section 2.5.1)

and hence,

$$\frac{I_f}{I_0} = g\epsilon(1 - \exp^{-2.303A})$$

Comparing this equation with the approximated version described in section 2.5.2:

$$\frac{I_f}{I_0} = g2.303\epsilon C d$$

it is apparent that significant deviations from linearity will occur at higher concentrations and will very much depend on the molar absorptivity of the system.

From the absorbance measurements previously described (figure 4.3b), the molar absorptivity at the maximum absorption wavelengths, ϵ , was calculated to be around $80\,000\text{ dm}^3\text{mol}^{-1}\text{cm}^{-1}$ for low concentrations of FITC solution (this is in line with the aforementioned references). For the standard 1 cm cuvettes which were used, this implies an expected deviation from linearity (> 5%) in the fluorescence curve at concentrations greater than about $6.4 \times 10^{-7}\text{ M}$. Figure 4.4b illustrates this feature.

Parker's law alone, however, does not account for the degree of deviation from linearity which was observed. Another reason for the departure from Parker's law is that the optical path length through which the absorption occurred was not 1 cm, but was less and varied depending on the concentrations of the solution. (This is a facet of the *inner filter* effect which was described in section 2.5.2). At higher FITC concentrations, most of the excitation radiation would have been absorbed very near the surface of the fibre-optic probe head and one would expect a reduction of the concentration dependence of the fluorescence¹⁷. At low concentrations, the absorbance of the solution will decrease significantly and hence the extent that fluorescence emission could be 'captured' by the return fibre will also decrease. This could explain the deviation from linearity observed at low concentrations, as illustrated in figure 4.4b. On the other hand, the excitation radiation will be able to pass through the lower absorbing liquid and be reflected back up through the return fibre, thus giving rise to the increased interference from the excitation peak that was observed in figure 4.4a. This could explain why, as the solutions become more dilute, the effect of the reflectance of the excitation radiation (at 488 nm) becomes more significant.

4.2.3 SENSITIVITY OF THE FIBRE OPTIC LINK TO THE SPECTROPHOTOMETER

A linear regression with a forced zero origin of the linear range of the fluorescence response (2.57×10^{-6} to $2.42 \times 10^{-6}\text{ M}$) resulted in a sensitivity value of about 55 ± 2 recorder units per

mg FITC. Although this is more sensitive than the absorbance measurements (approx. 0.2 units/mg) it does mean that the configuration used only gives meaningful output when the concentration of the FITC solution is in the p.p.m. range and not in the p.p.b. range as would be expected from traditional spectrophotometric techniques. In part, this is because the optical arrangement was not fully optimised and greater sensitivity is almost certainly possible. This is especially so in the case of the probe design, since fluorescence is isotropic so unless a means is devised to capture the radiation which is emitted in all directions, some losses in sensitivity are inevitable.

4.3 FITC SOLUTION SPECTRA AS A FUNCTION OF pH

4.3.1 UV-ABSORBANCE SPECTRA

4.3.1.1 PROCEDURE

A concentrated ethanolic solution of FITC (1 cm^3) was diluted to 50 cm^3 with standard buffer solutions (prepared as indicated in appendix IV.3). Absorbance measurements were run using the same settings as described in section 4.1.1., except that a wider wavelength range was investigated.

4.3.1.2 RESULTS AND DISCUSSION

The absorbance curves obtained for the different pH values (figure 4.5) are in line with literature examples⁸³ and clearly show the transitions through the different protolytic forms (pH 2: cation; pH 4 to pH 6: cation - neutral - monoanion). There appears to be an *isosbestic* point (wavelength of constant absorbance) at just over 350 nm between the neutral and anionic forms.

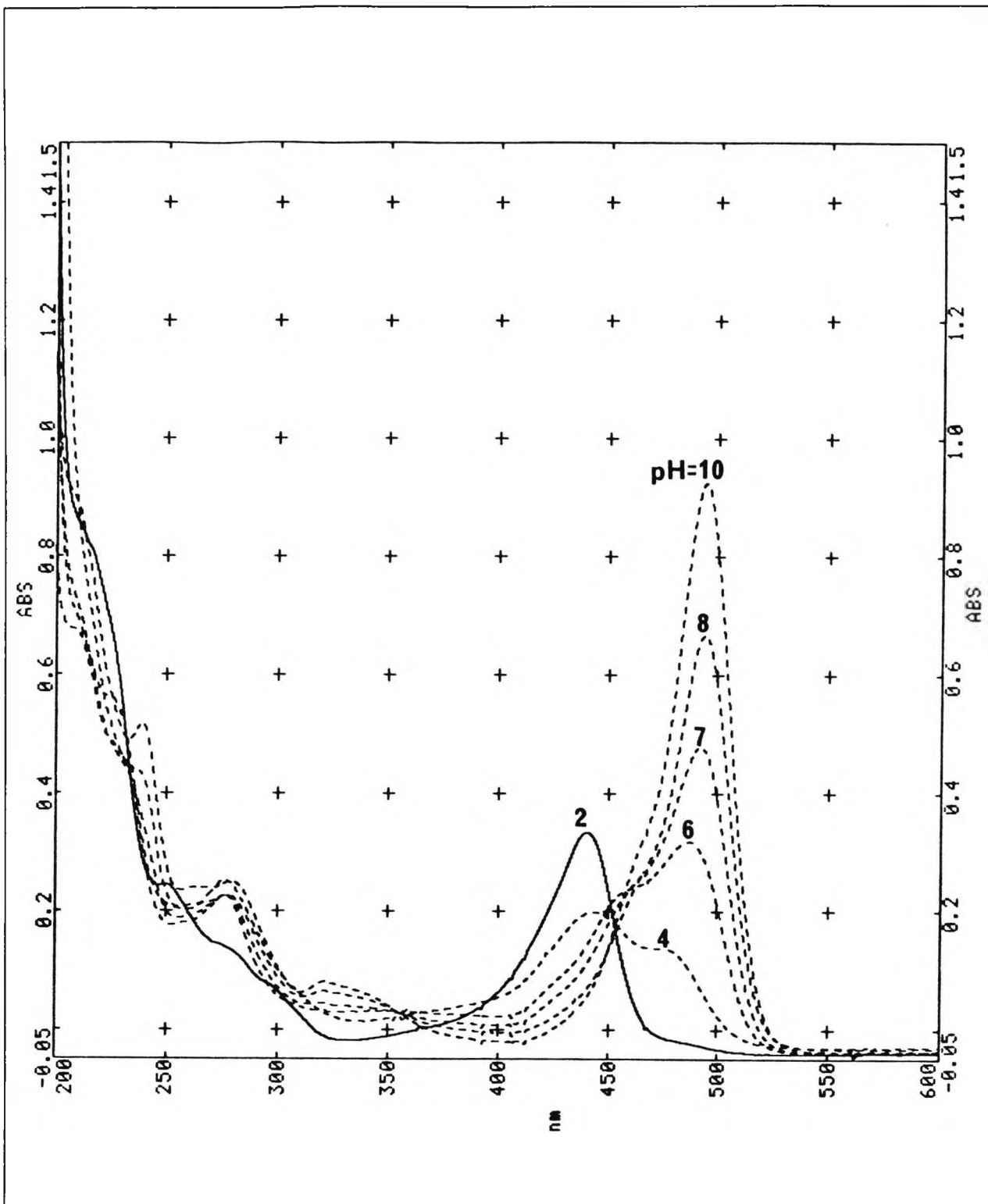


Figure 4.5 Absorbance spectra for FITCaq at different pH values.

4.3.2 EXCITATION SPECTRA

4.3.2.1 PROCEDURE

The emission wavelength of the Perkin Elmer fluorescence spectrophotometer was fixed at 525 nm and the excitation wavelength was varied from 200 nm to 510 nm.

4.3.2.2 RESULTS AND DISCUSSION

Figure 4.6 shows the excitation spectra of aqueous FITC solutions at different pH values.

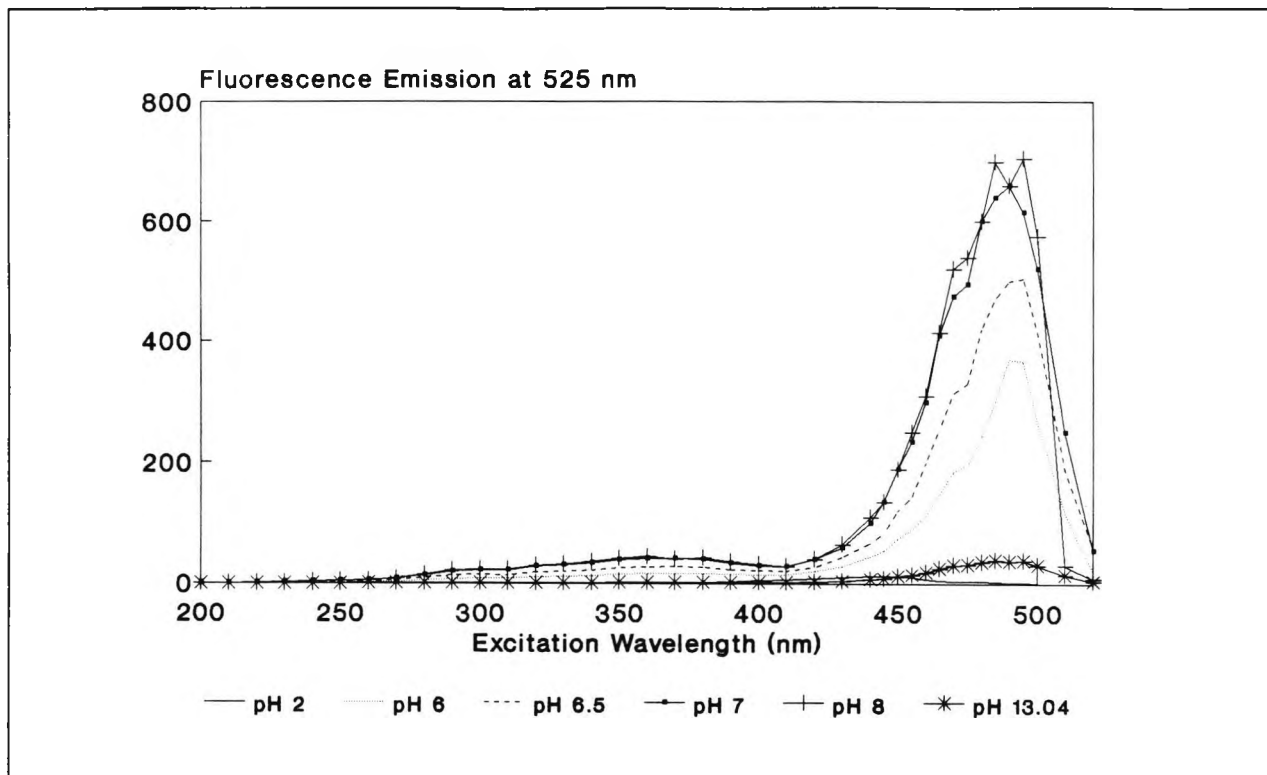


Figure 4.6 Excitation spectra of FITC at different pH values.

Table 4.2 Data from Excitation Spectra of FITC at different pH values.

pH	λ_{\max} , nm	I_{\max}
2	440	12.7
6	490	370.0
6.5	490	500.0
7	495	615.0
8	495	705.0
13.04	485	39.5

The λ_{max} values are consistent with those observed for the absorbance spectra, but the fluorescence intensity at pH 13.04 is lower than expected given the absorbance spectra. This could be due to the formation of dimers of the dianion³⁴.

4.3.3 FLUORESCENCE SPECTRA USING THE FIBRE-OPTIC LINK TO THE SPECTROPHOTOMETER

4.3.3.1 PROCEDURE

The set up shown in figure 3.2 was used for this part of the evaluation. A similar procedure was employed to that described in section 4.2.2 except that solutions of different pHs were used instead of solutions of varying concentration.

4.3.3.2 RESULTS AND DISCUSSION

The fluorescence spectra are shown in figure 4.7a. The emission maxima observed are around 525 nm as expected.

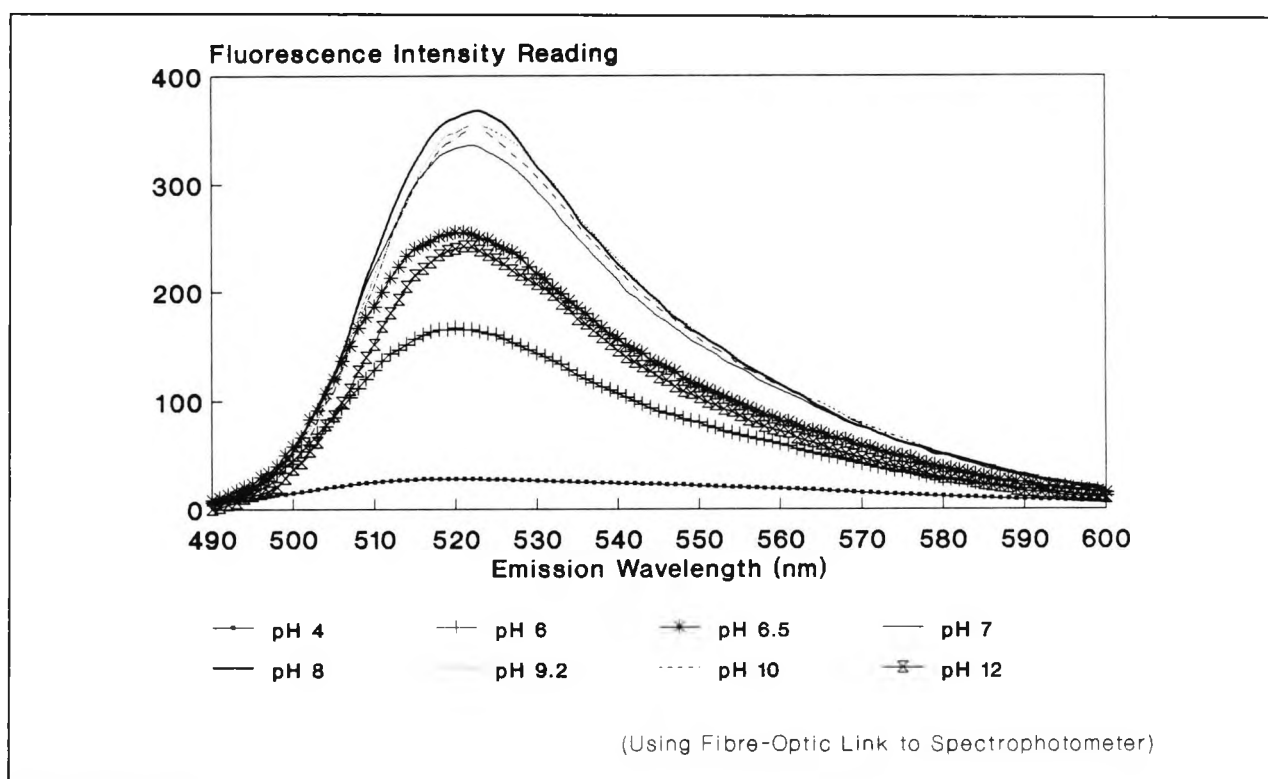


Figure 4.7(a) FITCaq fluorescence spectra at different pH values.

Figure 4.7b plots the total fluorescence emitted in the measured range of 490 to 600 nm (i.e. areas under curves) as a function of pH. A regression of the linear response range (by inspection: pH 5.5 to pH 7.0) gives the following equation:

$$I_f = 44.46 \text{ pH} - 216.57$$

$$R^2 = 0.998 \text{ (calculated from 3 points)}$$

$$\text{Std error of } I_f \text{ est} = 1.068$$

Within the linear range, the data suggest that the instrument as described is sensitive to pH changes of ≥ 0.025 units which is of the same order of magnitude of other FOCSs commonly reported.

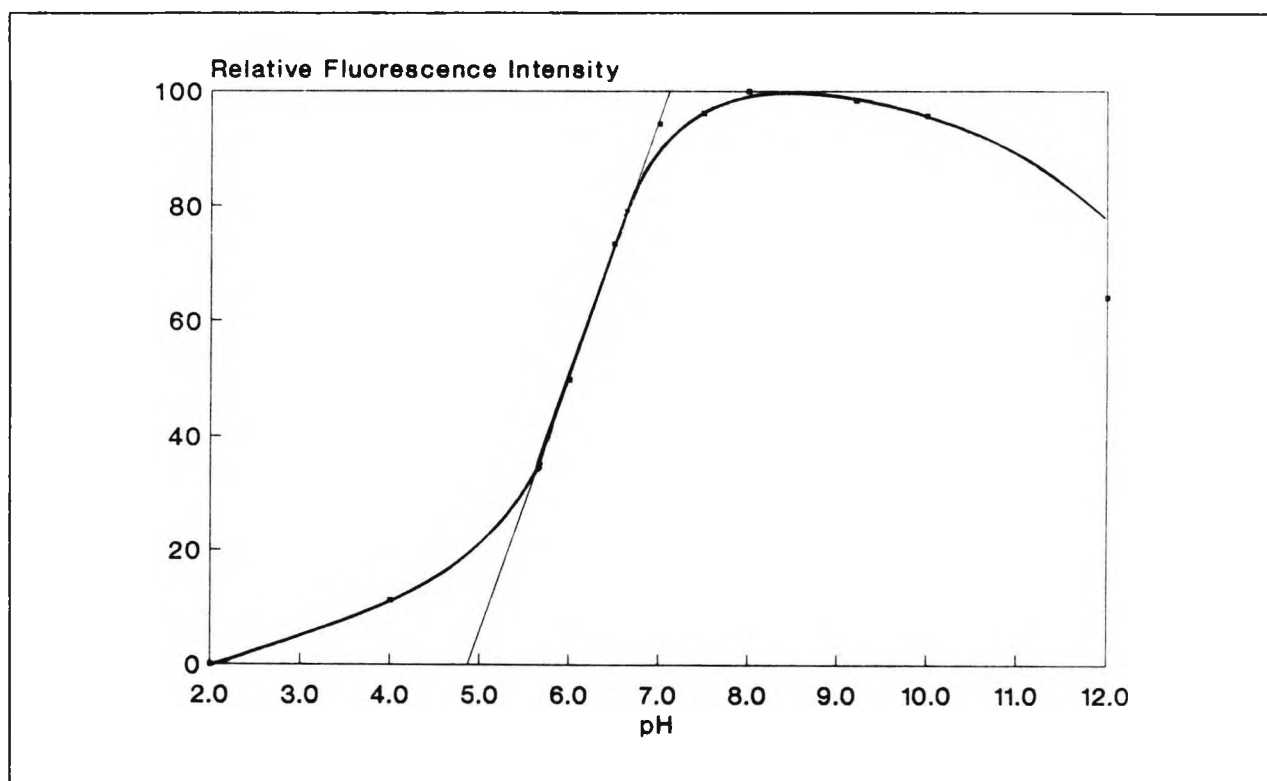


Figure 4.7(b) Total FITCaq fluorescence at different pH values.

4.3.4 FLUORESCENCE SPECTRA USING ELECTO-OPTIC ARRANGEMENT LINKED TO Ar⁺ LASER.

4.3.4.1 PROCEDURE

The electro-optic arrangement shown in figure 3.3 was used for this evaluation. The pH of a magnetically stirred solution of FITC was varied by adding small volumes of concentrated NaOH from a microsyringe to an acidified solution of FITC ($1\text{mg}/100\text{ml}^{-1}$). Using the *MANUAL LOG DATA* routine (section 3.4.2), fluorescence intensity readings and pH values were measured simultaneously (appendix IV.4). The pH was recorded using a previously calibrated pH electrode.

The evaluation was repeated in order to focus on the most sensitive pH range.

4.3.4.2 RESULTS AND DISCUSSION

The plotted data of fluorescence intensity (i.e. voltage output from the detector due to fluorescence intensity) versus pH shows a sigmoid-type curve as expected (figure 4.8a). Again, higher pH values led to a decrease in the fluorescence intensity but in this case the change may partly be explained by a dilution effect since relatively high amounts of NaOH were added at this stage. Generally, however, such high pH values are well outside of the linear range and the main range of interest for this study.

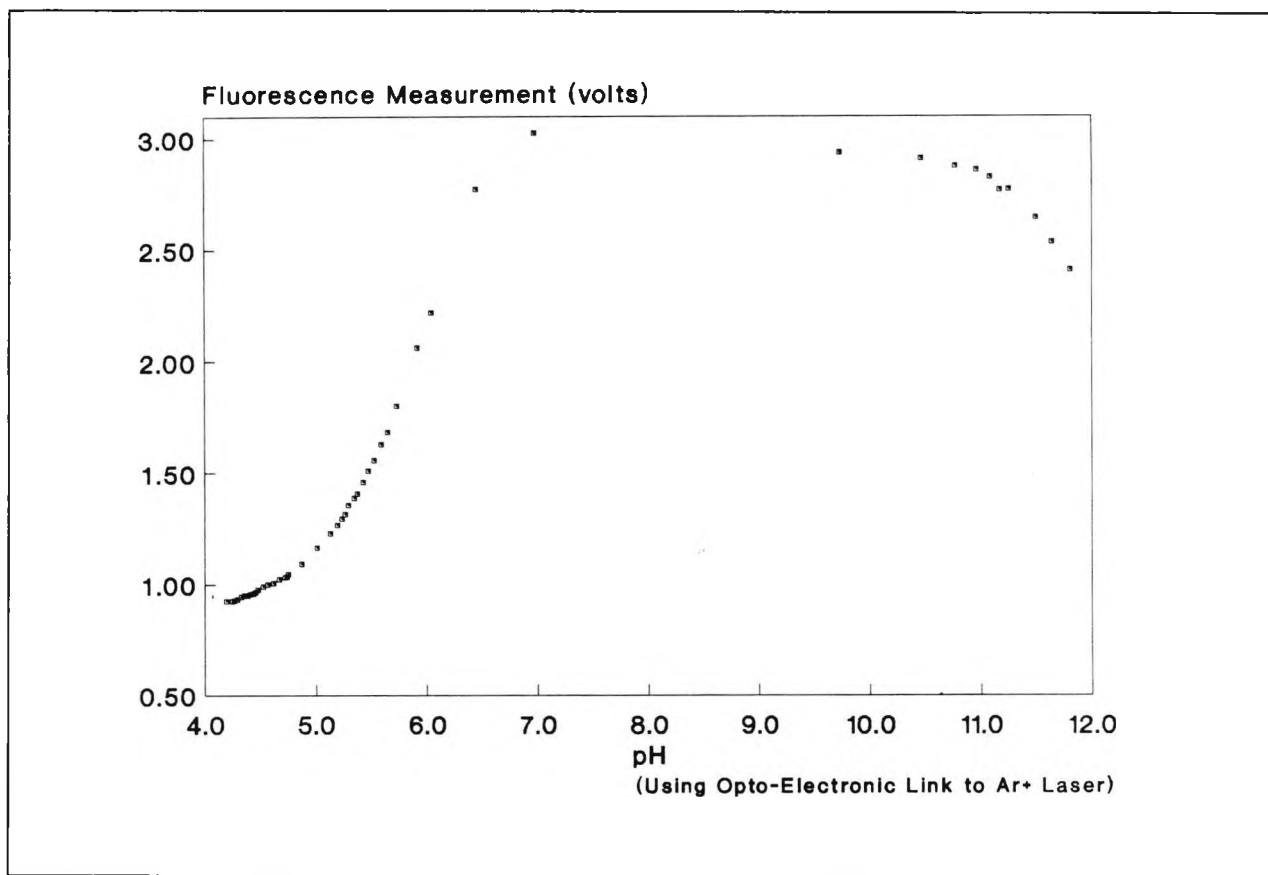


Figure 4.8(a) FITCaq fluorescence response to wide pH range.

In the second run (figure 4.8b) much smaller amounts of concentrated NaOH were added in order to focus on the most sensitive pH range. The addition was performed by dipping the needle tip of the syringe first into the base and then into the FITC solution.

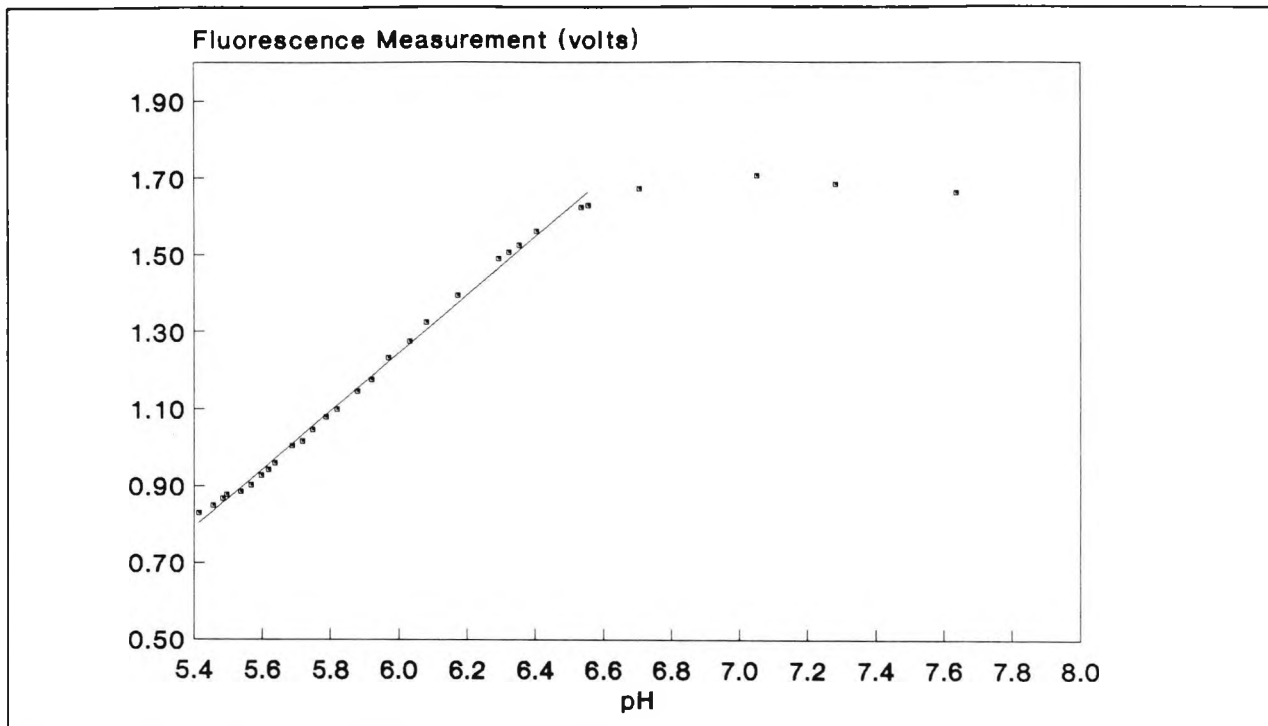


Figure 4.8(b) FITCaq fluorescence response in critical pH range.

From a plot of the residuals from the regression of the linear portion of the fluorescence response (figure 4.8c) it can be seen that the turning point lies between pH 5.9 and pH 6. This then is where the change of fluorescence is most sensitive to pH and is equivalent to the pK_a of the FITC (neutral to monoanion and dianion transition). It should be noted that it is somewhat lower than that of fluorescein⁸³.

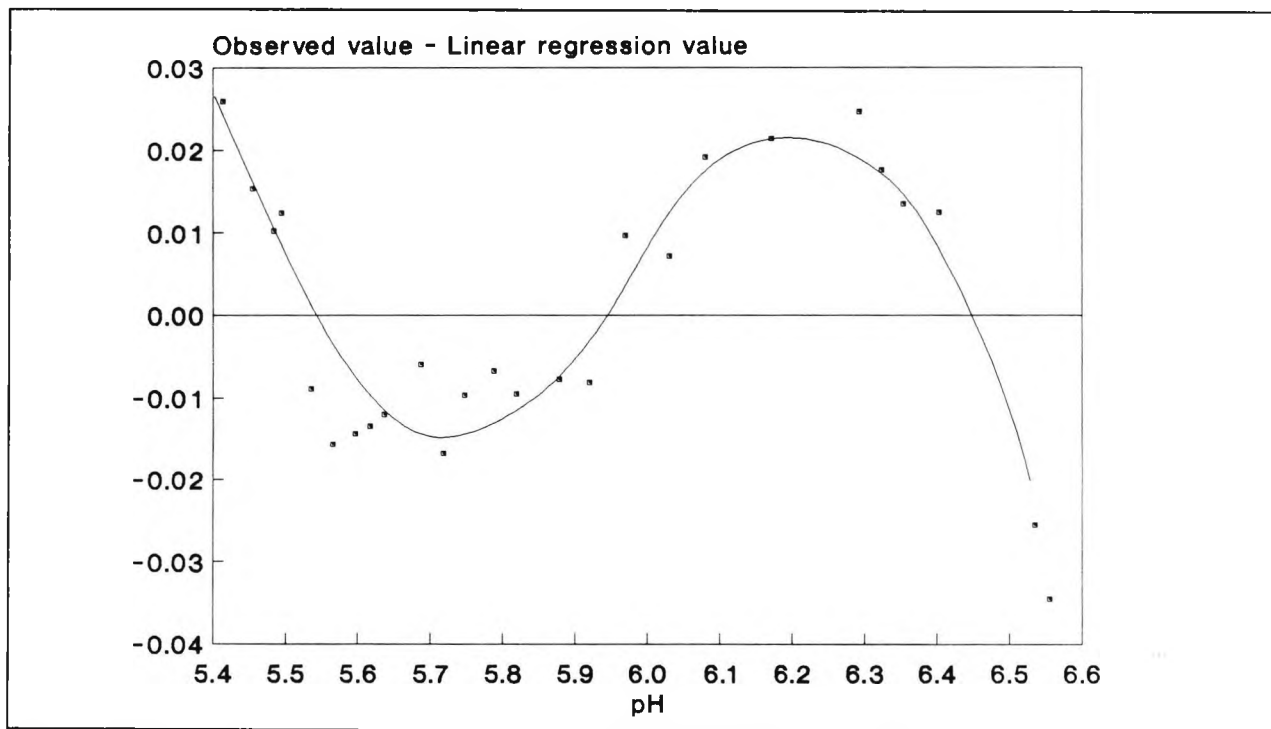


Figure 4.8(c) Plot of residuals from regression of linear portion of FITCaq fluorescence response in the critical pH range.

From inspection of the graph, the linear range is between pH 5.4 and pH 6.6. A linear regression of these data gives:

$$I_f = 0.75\text{pH} - 3.275$$
$$(R^2 = 0.9962)$$

This means that the sensitivity of the set-up used was 0.75 volts/pH unit. The percentage change in signal intensity over the linear range per unit change in pH works out to be about 87%, which is very similar to that obtained with the fibre-optic link to the spectrophotometer. In the opto-electronic arrangement linked to the Ar⁺ laser, however, readings in the 10 mV ranges were readily attainable which indicates that changes of the order of 0.01 pH units could be easily measurable. Such measurements were made without optimisation of the opto-electronic configuration or the phase sensitive detector amplification system, so it can confidently be predicted that the sensitivity of this arrangement could be further improved. For the link to the spectrophotometer, changes of less than about 1 unit at maximum amplification could not be considered as significant. As already mentioned, this gives a signal sensitivity limit of around 0.025 pH units and although some room for improvement also exists in this case it would appear that there is less scope for improvement than in the case of the laser-based opto-electronic arrangement.

4.4 SUMMARY

The fluorescence properties of FITC have been assessed using the fibre-optic based instrumentation previously described. The most sensitive fluorescence response takes place around pH 6 range and in the range pH 5.5 to pH 6.6. This is lower than for fluorescein which exhibits a pK_a value of 6.7. It is also lower than the limits of human blood hydrogen ion concentration compatible with survival (pH 6.8-7.7). Given that FITC was confirmed to be very sensitive to small changes in pH and that it is widely used in many areas of fluorometric analysis, FITC was chosen as the fluorescence reagent for these studies. This work has confirmed that both the instrumental arrangements developed could be put to practical use and provided useful data regarding the pH-response of FITC in solution. These data are referred to in subsequent Chapters where the emphasis is placed on the immobilisation of FITC onto glass and glass-like supports for use in FOCS, and this work is described.



THE USE OF POROUS GLASS IN FOCS

5.0 ABSTRACT

Porous glass (PG) is often used in fibre optic chemical sensors as a support for the sensitive reagent. The purpose of this investigation was to gain further understanding regarding the advantages and disadvantages of PG for such applications. Microanalysis was used in an attempt to assess the effect of certain reaction parameters on the efficiency of each of the two steps involved in immobilising FITC onto the glass surface.

The low organic content of the derivatised samples limits the overall usefulness of this analytical approach, nevertheless, a model is presented which, with some modification, can explain most of the observations.

It is found that refluxing in 3APTS in the first step significantly improves the loading of the fluorophore on the porous glass, but that the type of porous glass pretreatment and the concentration of the FITC solution do not result in differences which can be measured by conventional microanalysis.

The fluorescence response of the derivative porous glass, both dry and in solution, was recorded. The fibre optic configuration described resulted in strong fluorescent signals but a longer than desirable response time. Generally, it was found that fluorescence intensity of the dry PG was greater when lower concentrations of FITC had been used in the immobilisation step.

5.1 BACKGROUND

5.1.1 POROUS GLASS

Essentially, porous glass (PG) consists of pure silica with a microscopic system of interconnecting pores and channels. Hood *et al.* discovered that glass compositions in a certain region of the ternary system $R_2O-B_2O_3-SiO_2$ (R is an alkali metal such as Na, Li or K) will, on proper heat treatment, separate into two phases; one which is rich in alkali and boric oxide and the other which is rich in silica⁸⁶. Figure 5.1 shows a triaxial diagram representing a commonly used system.

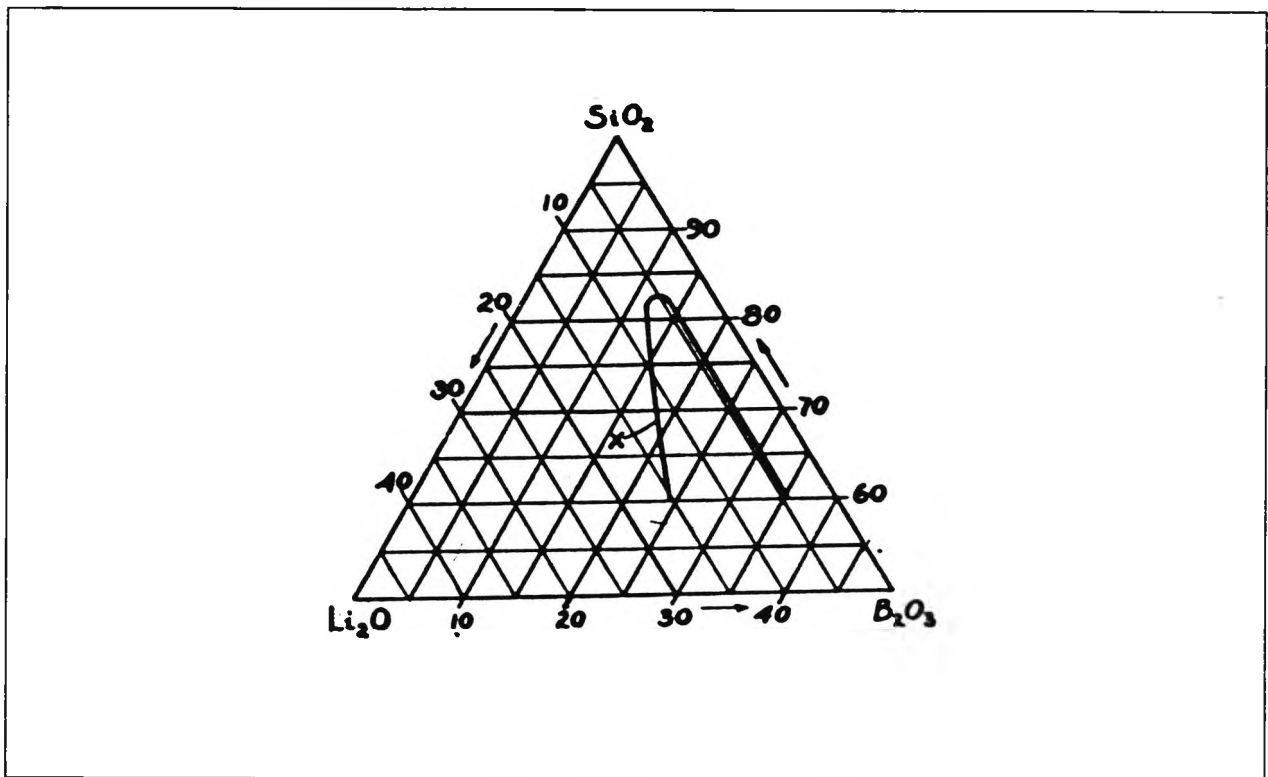


Figure 5.1 Three component glass system. The curve, X, outlines an area that includes the compositions in which phase separation takes place⁸⁶

After the glass has been heat treated at temperatures between about 500 and 700°C, it is immersed into hot concentrated acid for a few days. The acid dissolves the alkali-rich phase and penetrates into the glass. After rinsing, there remains an almost pure silica framework and it is this network which constitutes the porous glass (figure 5.2).

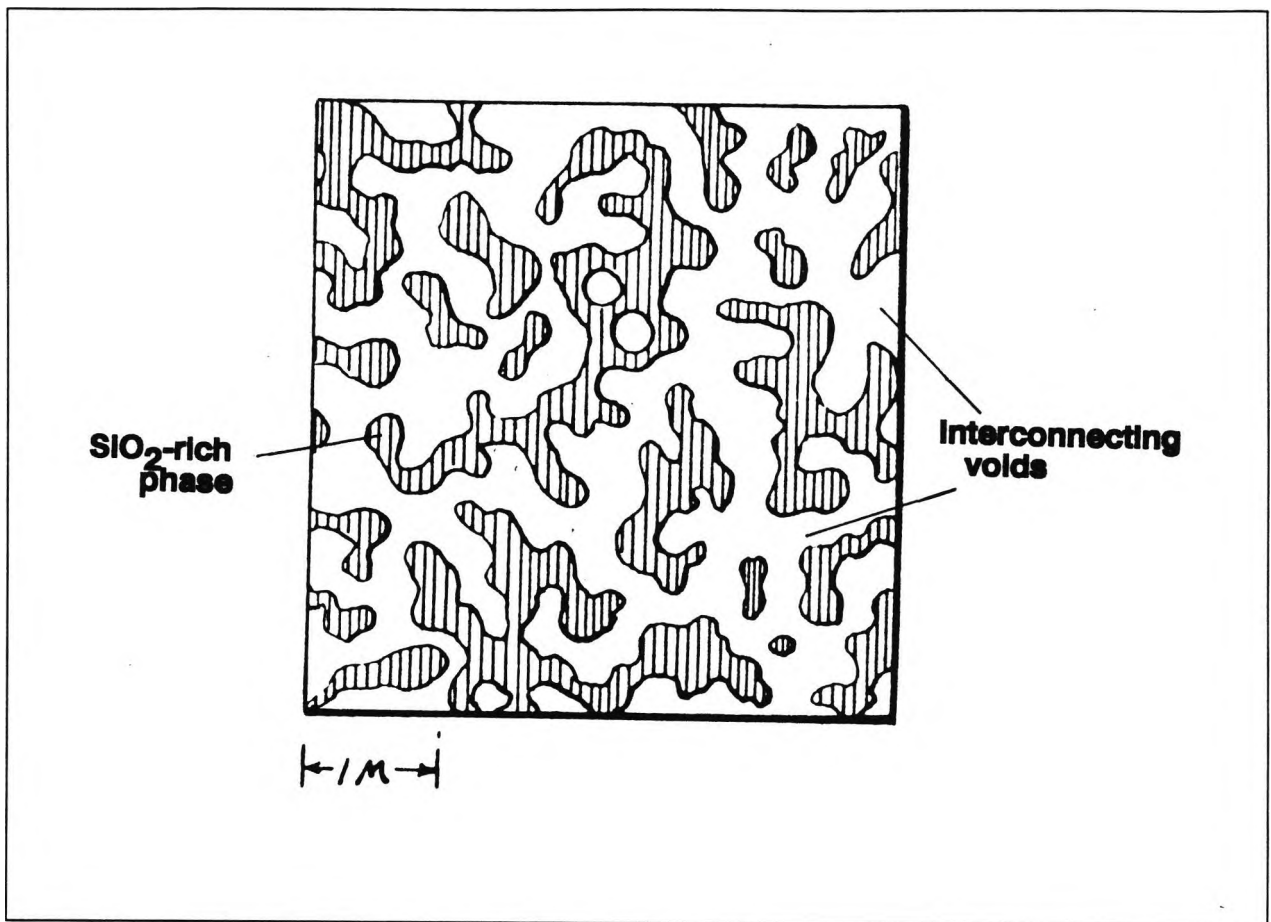


Figure 5.2 Porous glass structure⁸⁷.

By controlling the thermal history of the glass and by additionally having an alkali solution immersion step to dissolve any colloidal silica trapped in the pores, it was found that the pore volume could be accurately controlled (figure 5.3) and that, moreover, a narrow pore size distribution could be achieved⁸⁷. The material thus produced is named controlled pore glass (CPG) and is available commercially in a wide range of pore volumes and particle sizes (e.g. appendix V.1).

HEAT TREATMENT (TIME & TEMP.
VS PORE DIAMETER

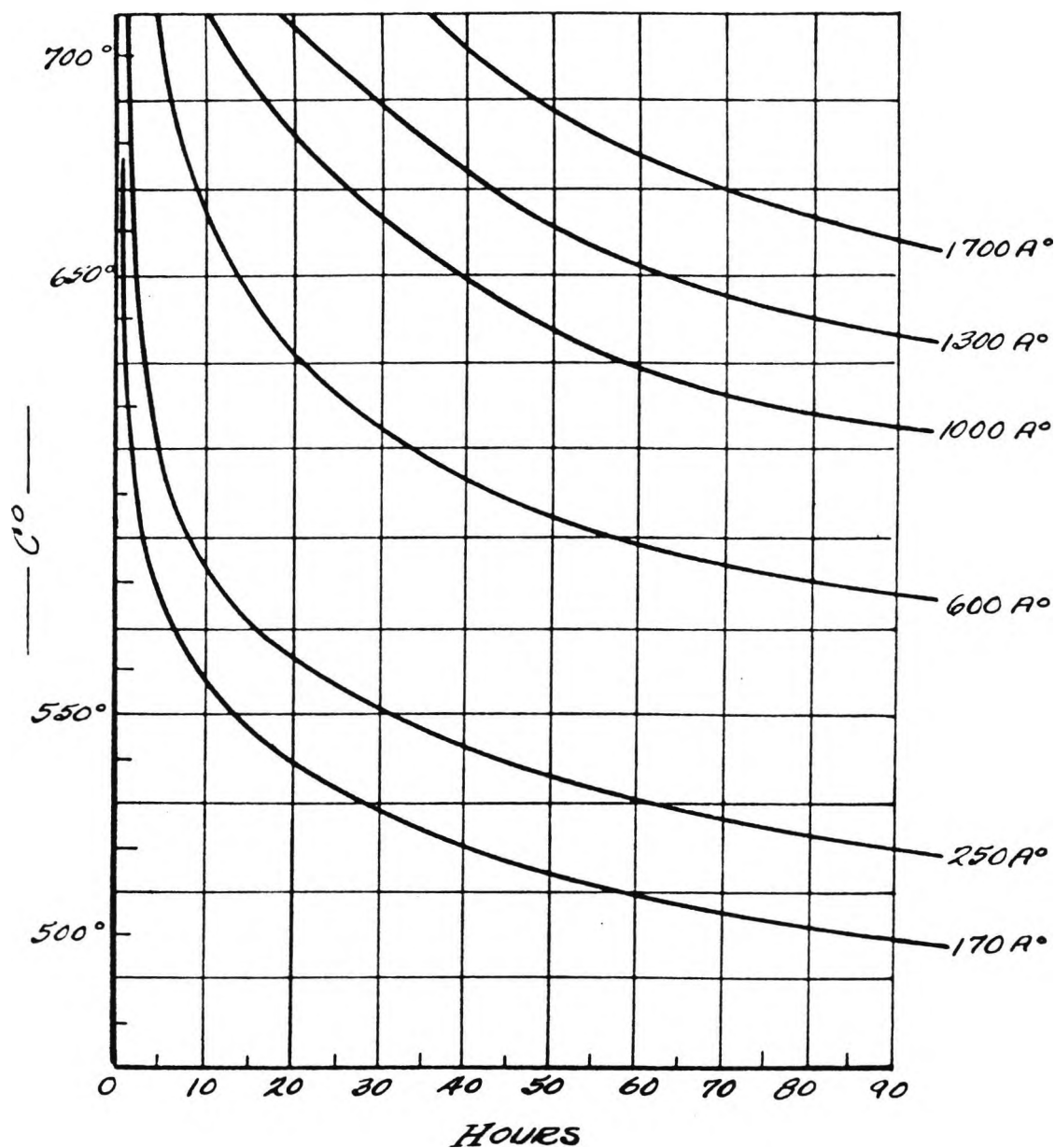


Figure 5.3 Heat treatment versus pore diameter⁸⁷.

PG is commonly used in permeation and affinity chromatographic methods where it has the useful properties of inertness, rigidity and a high surface area. Its surface chemistry also lends itself to facile modification and these qualities combined with that of transparency have also resulted in the wide use of PG as an indicator support in FOCS.

As with all silica structures the surface of PG can be thought of as being covered by silanol (SiOH) groups. Much work has been done in order to characterise the surface of silica. Iler devotes a whole chapter in his extensive treaty of silica to this topic⁸⁸. Silica has many polymorphs. Apart from the amorphous state, it is known to exist in many crystalline modifications. The most common is quartz and others include tridymite, cristobalite and

stishovite. In all the forms except for the latter each silicon atom is tetrahedrally surrounded by oxygen atoms. Stishovite has an octahedral rutile structure.

The silica surface becomes hydroxylated due to the unsaturated surface silicon atoms. Since the silicon atoms on the surface of amorphous silica are, by definition, not in an exactly regular geometrical arrangement, it is obvious that the distances between adjacent hydroxyl groups will not always be the same. Consequently there are quite a few types of postulated hydroxyl groups and these are illustrated in figure 5.4.

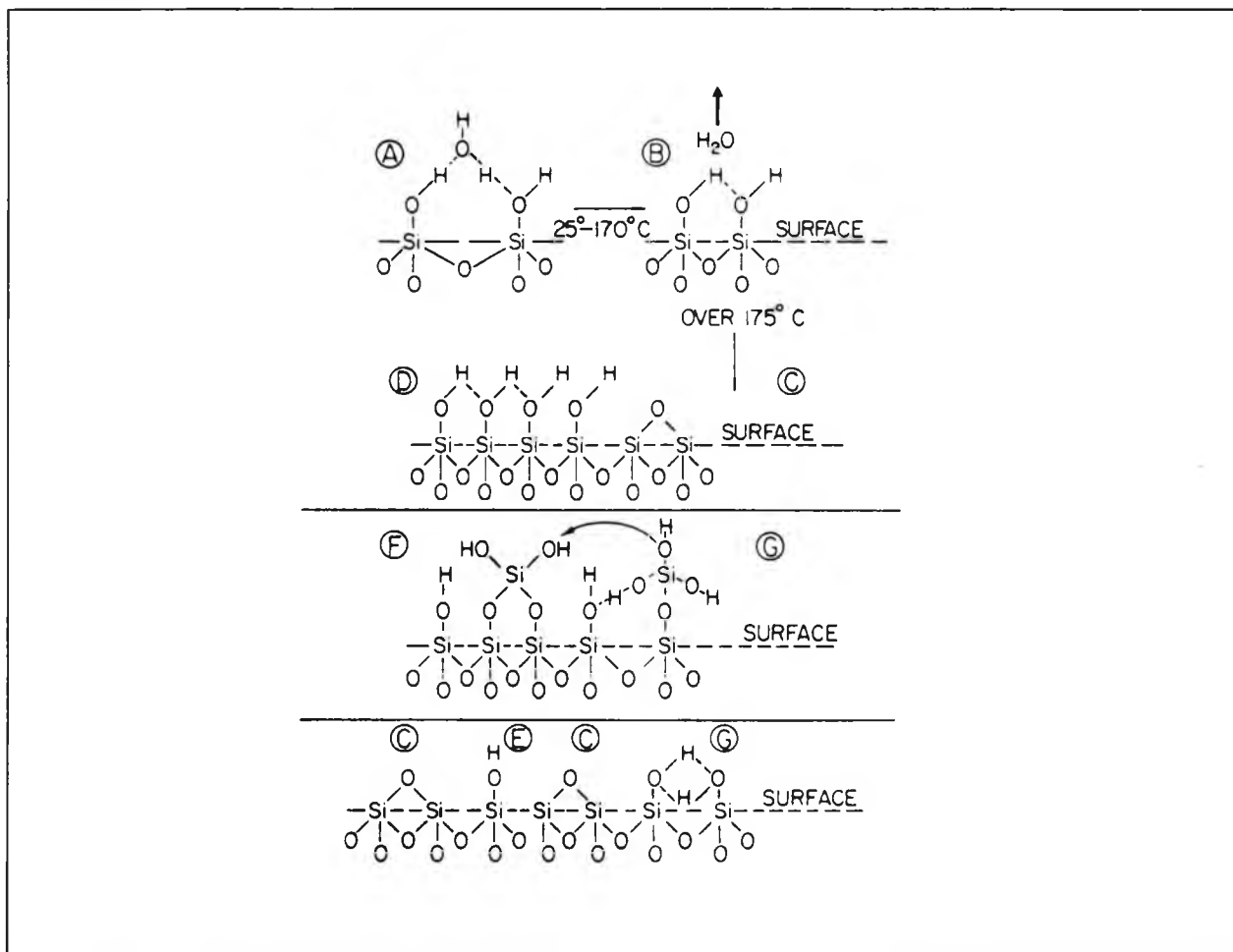


Figure 5.4 Postulated types of hydroxyl groups on amorphous silica surface. A, vicinal hydrated; B, vicinal anhydrous; C, siloxane-dehydrated; D, hydroxylated surface; E, isolated; F, geminal; G, vicinal, hydrogen bonded. Note: F and G probably do not actually exist on a dried surface⁸⁸

The number of silanol groups per unit area is of practical concern since it governs the amount of material that can be covalently immobilised onto the glass surface. Much work has been carried out into establishing the exact figure for the surface density using both chemical and physical methods. The main problems encountered in most of the approaches is that of differentiating between the hydroxyl groups due to adsorbed water and those due to the surface. The characteristic infrared absorption bands of different types of hydroxyl groups were used by many workers to overcome this problem (see 88 for references). It now seems generally accepted that on a smooth, non-porous heat-stabilised amorphous silica

surface that is maximally hydroxylated there are 4-5 SiOH groups nm^{-2} which remain when the sample is dried at 120-150°C.

In order to achieve the maximum number of SiOH groups on the silica surface various preparative techniques have been employed. Heat also plays an important role in determining the type of silica surface. Table 5.1 summarises the main effects.

Table 5.1 Effect of temperature on the surface of silica.

Temperature, K	Effect
393	Physically adsorbed water removed from silica surface.
423-573	Physically adsorbed water removed from silica surface of dispersed and porous silica.
473	Dehydration of amorphous silica will be accompanied by dehydroxylation of vicinal groups according to the scheme in figure 5.4.
773	Hydroxyl groups completely condensed.
>873	Dehydroxylation of isolated groups involving lateral movement of the silicon atoms. In porous glass this leads to sintering which is irreversible.
1473	Surface is nearly dehydroxylated and contains only surface siloxane (Si-O-Si) groups.

The above table is only an approximation of the affect of temperature on a silica surface. In reality, the temperature at which physisorbed water is completely removed and hydroxyl groups remain unreacted seems not to be well established⁸⁹ and varies over a wide range between 373 and 623K. As well as depending on the thermal history of the sample it is markedly effected by the morphology of the silica structure. On a small positive radius of curvature, as in small particles, there are fewer hydrogen bonds and so dehydration as well as dehydroxylation can probably occur at lower temperatures. For a large radius of curvature (large particles, flat surfaces) there will be more hydrogen bonds increasing the temperature required for desorption. In micropores, where there are negative radii of curvatures, higher energies are required to remove adsorbed water and surface hydroxyl groups. Figure 5.5 illustrates this effect.

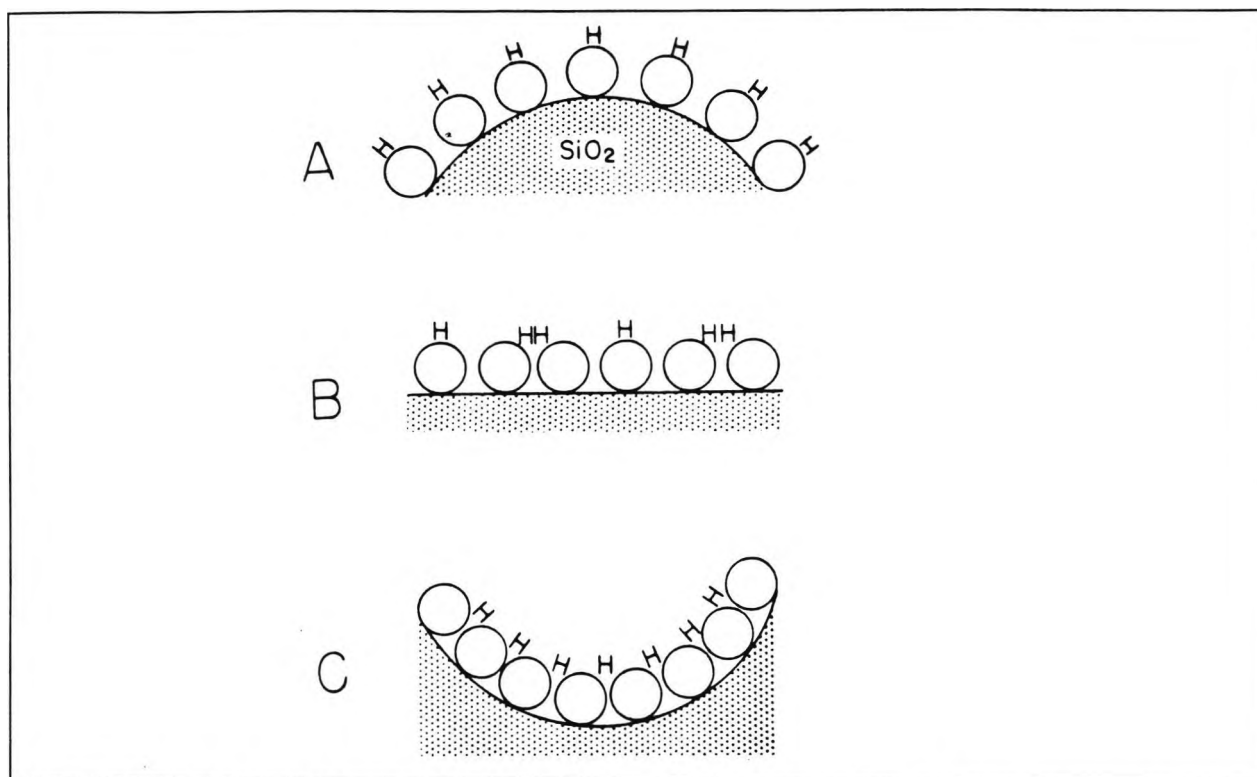


Figure 5.5 Affect of curvature of the silica surface on dehydroxylation. A, small positive radius of curvature (small particles) fewer hydrogen bonds, most easily dehydroxylated; B, large radius of curvature (large particles, flat surface) more hydrogen bonds, less readily dehydroxylated; C, small negative radius of curvature (in small pores), most hydrogen bonding, most difficult to dehydroxylate⁸⁸.

5.1.2 IMMOBILISATION OF A DYE ONTO POROUS GLASS

5.1.2.1 SILANE COUPLING AGENT

Much work has been done investigating chemically bonded stationary phases especially in the area of HPLC^{90,91}. Conventionally, bifunctional silanes are used to modify the SiO₂ surface. Their structures can be represented generally as:



where Y is typically a group consisting of amino, carbonyl, carboxy, isocyanato, diazo or isothiocyanato; R can be any lower alkoxy, phenoxy and halo; and R' can be a lower alkyl, lower phenyl or lower alkyl-phenyl. n is usually an integer having a value of 1-3. In FOCS, the main function of the silane coupling agent is to provide a bond between the indicator reagent (organic) and the substrate carrier (inorganic). Probably the most commonly used reagent and the one which was utilized for the present investigations is 3-aminopropyltriethoxysilane (3APTS), [919-30-2]. This shows excellent chemical affinity for the glass silanols and is less prone to hydrolysis and polymerisation during storage than other previously commonly used materials.

5.1.2.2 IMMOBILISATION REACTION SCHEME

The two step procedure which is commonly used to immobilize an organic species onto glass can be represented as follows^{35,81,95}:

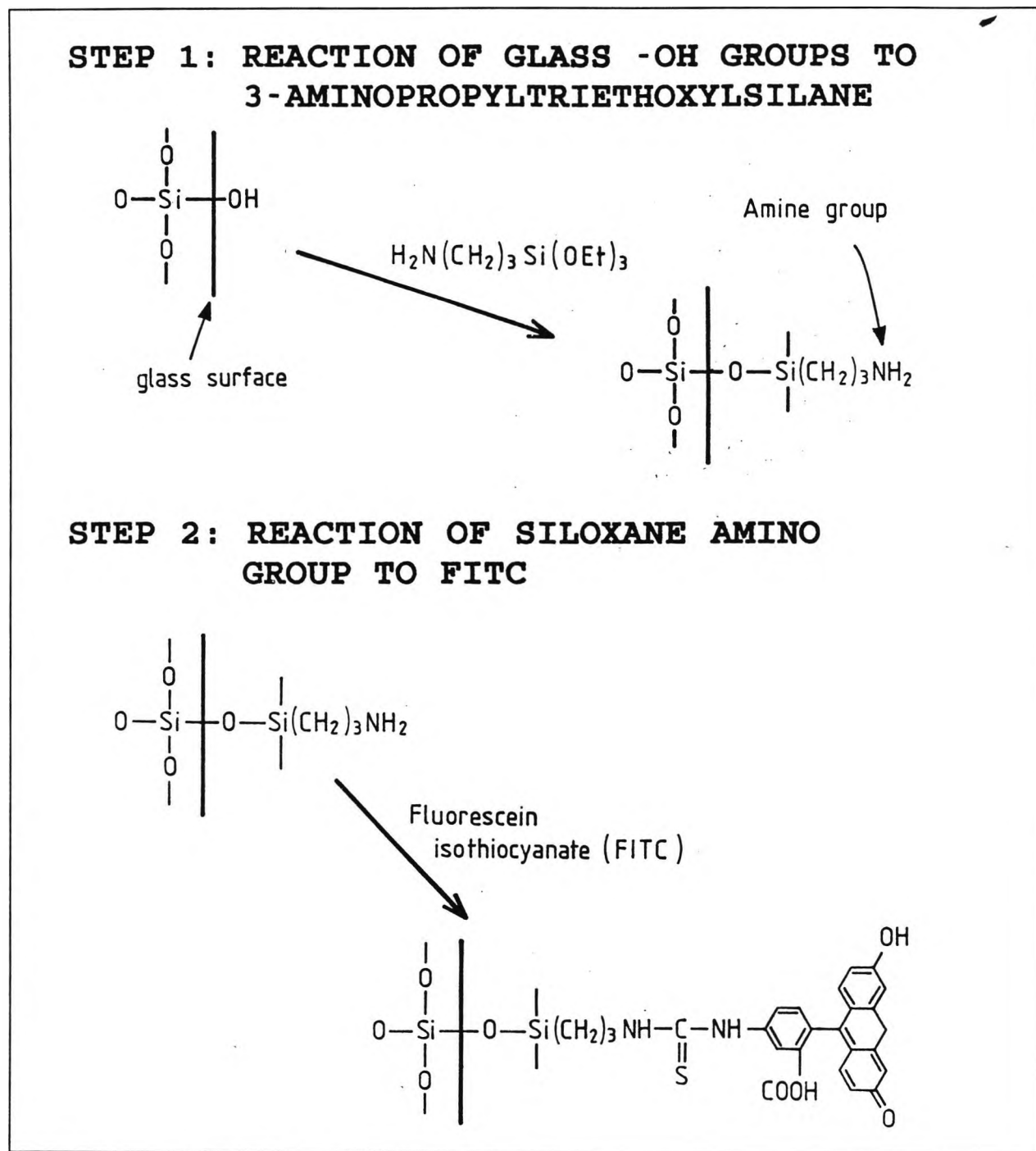


Figure 5.6 Immobilisation of FITC onto glass.

In the ideal case, stage 1 involves the condensation of three ethoxy groups with the glass hydroxyl groups to form stable siloxane bonds. The glass surface now carries an active amine functionality which, in stage 2 of the procedure, can undergo further reaction with the isothiocyanate group of the FITC. In reality, it is likely that coupling of the ethoxy group to the surface silanols is incomplete⁹⁶ and this can account for some the observations described in later sections.

5.2 EXPERIMENTAL PROCEDURE

5.2.1 MATERIALS AND EQUIPMENT

The porous glass (PG) used through-out this investigation was of unknown origin. The measured B.E.T.(Brunauer, Emmett, Teller) specific surface area was $32.4 \text{ m}^2\text{g}^{-1}$ (Micrometrics Surface Area Analyser). The particle size distribution (Malvern Instruments) was confirmed as 160-100 mesh (152-251 μm).

All other chemicals used in this work were obtained from either BDH Ltd., Poole, or Aldrich Chemical Co. Ltd., Gillingham, England.

Thermal analysis were performed on a Mettler Thermal Analyser 2.

5.2.2 PRETREATMENT OF POROUS GLASS

5.2.2.1 WASHING OF POROUS GLASS

Porous glass will turn brown on standing in room atmosphere due to absorption of organic materials from the air. Various methods are suggested in the literature to remove the contamination⁹². In the present investigation, the porous glass was gently stirred in a 1:1 v/v $\text{HNO}_3:\text{H}_2\text{SO}_4$ mixture for several hours, washed repeatedly with quantities of distilled water until the washings indicated a pH close to neutral on universal indicator paper, filtered, dried in an oven at 100°C and then stored in a vacuum desiccator over silica gel until used or stored under distilled water until thermally treated.

5.2.2.2 THERMAL PRETREATMENT OF POROUS GLASS

A number of thermal treatments were investigated to see if they had any significant effect on the extent of derivatisation of the PG. The following table summarises the methods used.

Table 5.2 Thermal Pretreatment of Porous Glass

Notation	Thermal Pretreatment					Comments
	Air(550)	O ₂ (450)	O ₂ (550)	N ₂ (150)	N ₂ (550)	
1						No heating
2				X		
3					X	
4		X				
5			X			
6					X	As for 3
7	X					
8		X				
9	X					As for 7
10	X					As for 7

The figures in brackets indicate the temperature of the thermal treatment in degrees Celsius.

5.2.3 STAGE 1 REACTION: SILYLATION OF PG SURFACE

Toluene (220 ml) was dried by refluxing over NaPb alloy for several hours followed by distillation.

Subsequent to the thermal pretreatment, each batch of porous glass (2-3 g) was treated by one of the following methods.

Notation	Method
1	Added immediately to a 1% v/v 3APTS solution in dry toluene (100 ml) and then left to stand for several hours.
2	Added immediately to a 1 % v/v 3APTS solution in dry toluene (100 ml) and then refluxed at 80-90 °C with gentle stirring for several hours.
3	Allowed to cool - then as for "2". (Performed on one sample only)

The PG was then filtered-off and washed in turn with MeOH, H₂O, MeOH, H₂O, MeOH and EtOH. The samples were dried in an oven at 80°C.

5.2.4 STAGE 2 REACTION: IMMOBILISATION OF FITC ONTO SILYLATED PG SURFACE

The aminopropylated porous glass samples were allowed to stand in solutions of FITC overnight, filtered, washed with copious quantities of distilled water and then dried in an oven at 80-100 °C. Four different concentrations of FITC were used.

Notation	[FITC] in mg(100ml) ⁻¹
1	4.0
2	2.0
3	1.0
4	0.5

5.2.5 SAMPLE LABELLING

Each sample is designated "x.y.z" where x is type of thermal pretreatment; y is method of silylation; z is concentration of FITC. For example 3.1.2 refers to a sample of PG which had been heated to 550°C in N₂ and then immersed immediately in the 3APTS solution with no refluxing. After solvent treatment, washing and drying the PG was left to stand in a 2.0mg(100ml)⁻¹ FITC solution overnight prior to drying. (The absence of a "z" value simply indicates that the samples were analysed without undergoing the stage 2 reaction.)

5.2.6 THERMAL ANALYSIS

Each sample was analysed for carbon, hydrogen and nitrogen. The results are expressed as percentages of the total sample weight.

5.2.7 FLUORESCENCE ANALYSIS

The excitation spectrum on a sample of the dry derivatised porous glass was measured using the fibre-optic link to the spectrophotometer described in section 3.1.

The fluorescence response to pH of the sensor was also measured using the same equipment. The probe was dipped into an aqueous solution of known pH and the spectrum was recorded using the program MANUALOG (section 3.4.2) once the emission intensity at a wavelength of 530 nm had reached a steady value. The probe was rinsed thoroughly with distilled water between each two measurements.

The response time of the probe configuration to a step change in pH was determined using the fibre optic link to the argon ion laser described in section 3.2. Distilled water was

acidified by addition of a small amount of HCl. The FITC probe was immersed in the solution (which was magnetically stirred). After 5 minutes the program AUTOLOG (section 3.4.2) was initiated and recordings of the pH of the solution and fluorescence intensity were made versus time. Once a the voltage reading was stable, a small amount of conc. NaOH was added. The recordings were continued until a total of 5 minutes had elapsed.

5.3 RESULTS AND DISCUSSION

5.3.1 APPEARANCE OF POROUS GLASS SAMPLES

Samples which had undergone the two-step derivatisation procedure were yellow to dark orange in colour (depending mainly on the concentration of FITC used) and this colour was retained even after a number of days immersion in water (although some leaching of dye into solution did occur). This contrasted with samples which had only been immersed in the FITC solution without undergoing the silylation reaction or which had been immersed in 3APTS solution without any refluxing or thermal pretreatment - these samples adopted a pale colouration which was readily washed out.

5.3.2 THERMAL ANALYSIS

5.3.2.1 MODEL FOR THE TWO-STAGE IMMOBILISATION REACTION

Appendix V.2 summarises the data from the thermal analysis. From the reaction scheme previously presented for the two step immobilisation of FITC onto porous glass it is possible to derive the two following relationships (see appendix V.3 for details):

Weight percent of species i , P_i , w.r.t. to the weight of the sample is given by:

$$P_i = \frac{10^{20} L_G (n_{i1} + X_{\text{FITC}} \cdot n_{i2}) M_i A}{N_A + 10^{18} L_G (M_{G1} + X_{\text{FITC}} \cdot M_{G2}) A} \quad (1)$$

and

Loading of the average surface group:

$$L_i = \frac{0.01 P_i N_A}{(1 - 0.01 (P_{G1} + X_{\text{FITC}} \cdot P_{G2})) M_i A 10^{18}} \quad (2)$$

so that

$$L_G = \frac{0.01P_iN_A}{(1 - 0.01(P_{G1} + X_{FITC} \cdot P_{G2}))M_iA10^{18}(n_{i1} + X_{FITC} \cdot n_{i2})} \quad (3)$$

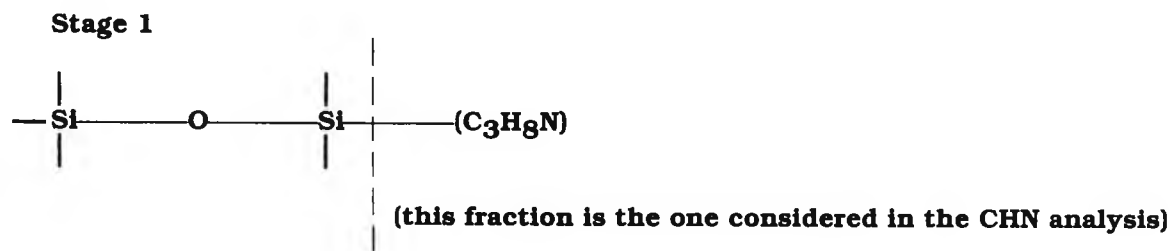
where

- L_i = loading of species i per nm^2
 n_i = number atoms of species i present in the average surface group.
 N_A = Avogadro constant ($= 6.023 \times 10^{23}$).
 A = specific surface area of porous glass ($= 32.4 \text{m}^2 \text{g}^{-1}$).
 X_{FITC} = mole ratio of FITC present on the surface ($= [\text{FITC}]/[\text{3APTS}]$)
 L_G = loading of the average surface group per nm^2 .
 M_i = relative molecular weight of species i .
 P_G = calculated weight percent of theoretical group $= P_iMG/(n_iM_i)$

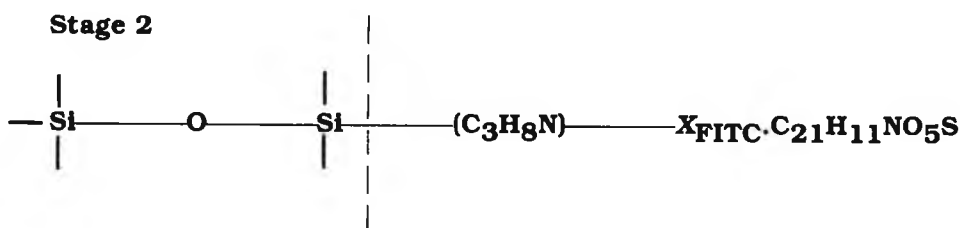
and the subscripts denote:-

- 1 - values after stage 1 of immobilisation reaction.
 2 - values after stage 2 of immobilisation reaction.
 $2'$ - values arising from components added during stage 2 of immobilisation reaction.
 G - average surface group $= G_1 + X_{FITC} \cdot G_2'$
 i - a surface species i.e. carbon (C), hydrogen (H), nitrogen (N), FITC, 3APTS or G.

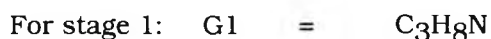
In the present case, the theoretically maximally hydroxylated surface is firstly amine functionalised with the silane coupling agent, 3APTS, to give:



This is followed by the partial addition of FITC to the amine groups:



Hence, according to the model, the surface groups are:



The limiting cases according to the model are when $X_{FITC} = 0$ and when $X_{FITC} = 1$. When $X_{FITC} = 0$, $G2 = G1$ i.e. no addition of FITC has taken place. The closer to unity is the value of X_{FITC} , the greater the extent of FITC addition to 3APTS. When $X_{FITC} = 1$, all of the available amine groups from the 3APTS have been derivatised with FITC.

From equation 1:

$$\frac{P_C}{P_N} = \frac{\left\{ \frac{10^{20} L_G (n_{C1} + X_{FITC} \cdot n_{C2}') M_{CA}}{N_A 10^{18} L_G (M_{G1} + X_{FITC} \cdot M_{G2}') A} \right\}}{\left\{ \frac{10^{20} L_G (n_{N1} + X_{FITC} \cdot n_{N2}') M_{NA}}{N_A 10^{18} L_G (M_{G1} + X_{FITC} \cdot M_{G2}') A} \right\}}$$

This reduces to:

$$\frac{P_C}{P_N} = \frac{(n_{C1} + X_{FITC} \cdot n_{C2}') M_C}{(n_{N1} + X_{FITC} \cdot n_{N2}') M_N} \quad (4)$$

So for the limiting cases:

when $X_{FITC} = 0$;

$$\begin{array}{lcl} n_{C1} & = & 3; \quad n_{N1} = 1 \\ n_{C2}' & = & 0; \quad n_{N2}' = 0 \end{array}$$

when $X_{FITC} = 1$;

$$\begin{array}{lcl} n_{C1} & = & 3; \quad n_{N1} = 1 \\ n_{C2}' & = & 21; \quad n_{N2}' = 1 \end{array}$$

$$\text{so } n_{C2} = 24; \quad n_{N2} = 2$$

It is worth noting that expression (4) could also have been derived from first principles by simply considering the ratio of masses of C and N based on the molecular formulae of the

surface groups. This confirms that expression (1) is indeed an accurate expression for the model as described, but it is not evidence that the model itself is correct.

5.3.2.2 TESTING THE VALIDITY OF THE MODEL

The reaction model can be tested by comparing the derived relationships with the experimental data. Table 5.3 summarises the observed data and compares them to the theoretical values predicted by the model given certain assumptions.

Table 5.3 Summary of Observed Results Compared to Theoretical Values

Values	Theoretical wt%	Observed wt%
<i>Stage 1:</i>		
P_{C1}	0.954	1.253
P_{N1}	0.371	0.388
slope (P_{C1} vs P_{N1})	2.573	2.634
P_{C1} vs P_{N1} Regression intercept	0	0.23040
<i>Stage 2:</i>		
P_{C2}	6.920	0.907
P_{N2}	0.673	0.263
slope (P_{C2}/P_{N2})	10.290	2.7142
P_{C2} vs P_{N2} Regression intercept	0	0.19193

where

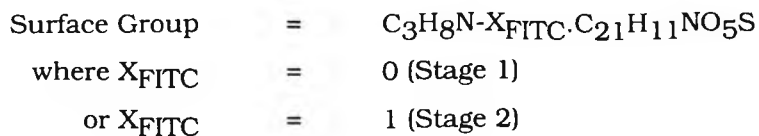
P_{C1} = weight percent of carbon on the surface of the porous glass after stage 1 of the immobilisation reaction.

or, in general terms,

P_{i1} or P_{i2} = weight percent of species i (i.e. C, H or N) on the surface of the porous glass after stage 1 or stage 2 of the immobilisation reaction respectively.

Assumptions:

L = 5 surface groups/nm²



(a) Stage 1 Loading Values

Figure 5.7 plots the observed carbon weight percentage values versus those of nitrogen (data given in appendix V.4).

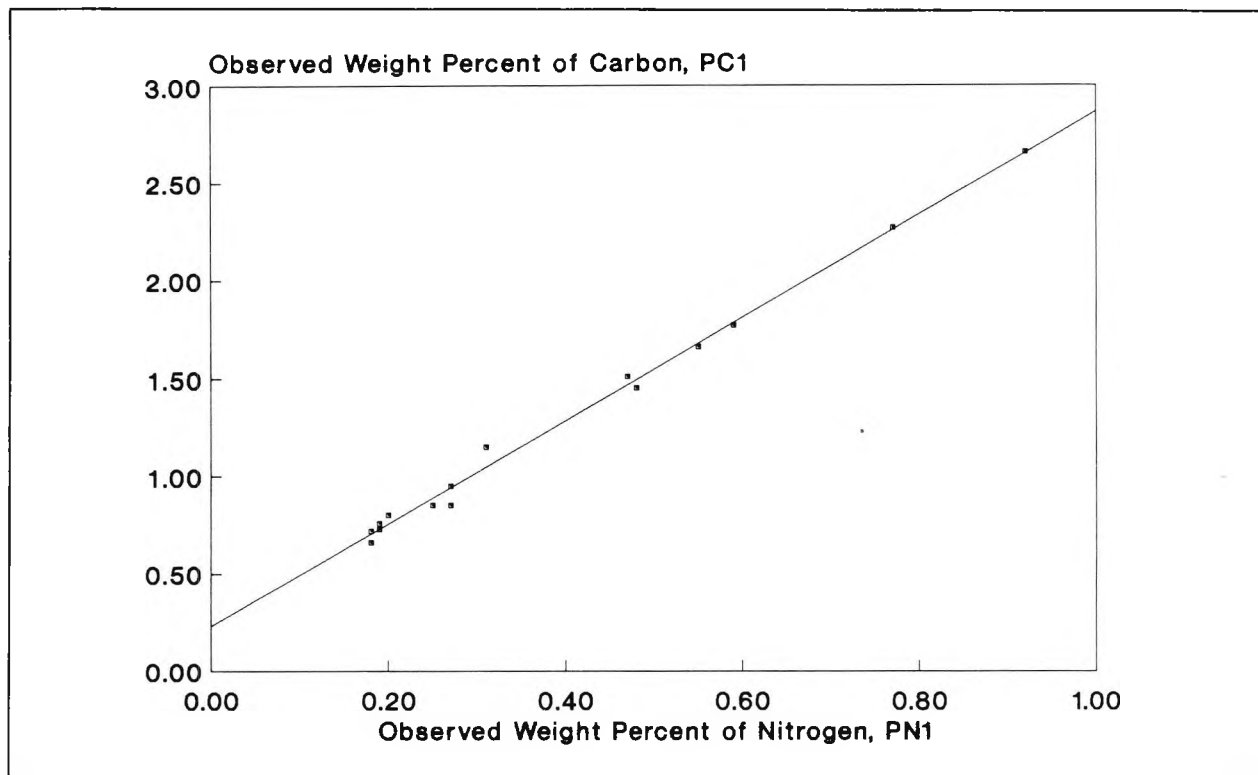
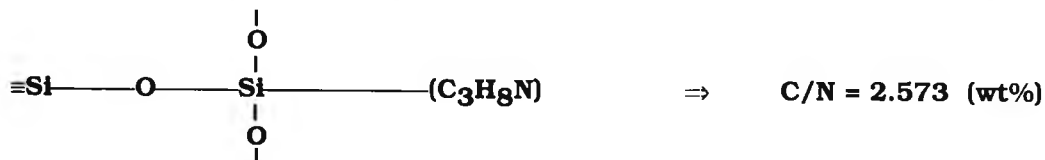


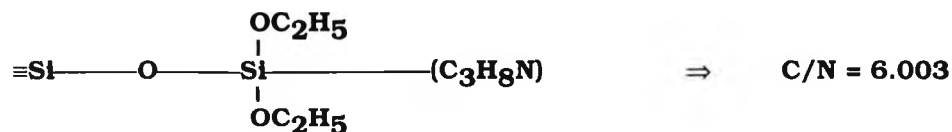
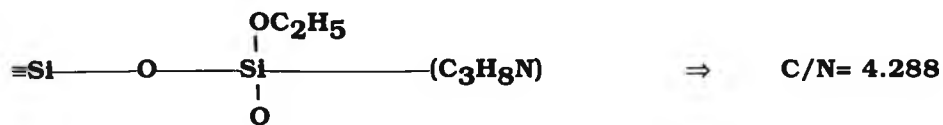
Figure 5.7 Stage 1 observed weight percents for C and N.

The regression analysis of the observed carbon and nitrogen gives the following equation:

Stage 1: $PC1 = 2.634(PN1) + 0.2304$

The model reaction predicts a slope of PC1 versus PN1 of 2.573 (i.e. weight ratio of C to N in the de-ethoxylated 3APTS) which is significantly smaller than the observed 2.634 (see appendix V.4 for values of standard errors). It is likely that this excess carbon content arises from some unreacted ethoxy groups⁹⁶, however, we can presume that the concentration of these groups is small. This is because significantly higher C:N weight% slopes would be observed if unreacted ethoxy groups were widely present, as is shown below:





A PC1:PN1 weight% slope of 2.634 (as observed) implies a C:N mole ratio of 3.07:1 (instead of 3:1). Assuming that this extra carbon content can be attributed only to additional ethoxy groups, this in turn implies that an equivalent of 3.6% of the immobilised 3APTS groups retain an ethoxy group.

The average carbon and nitrogen weight percent data are in reasonably good agreement with the values predicted assuming a group loading of 5 groups/nm², although the carbon data are somewhat high.

Moreover, in the experimental data a positive intercept value (= 0.2304) was recorded whereas the model predicts that this should be zero.

If we consider the PC1:PN1 weight% slope to be 3.07 and take into account the above mentioned intercept value, then equation 1 yields PC1 and PN1 values which match the observed data when a loading of 5.24 groups.nm⁻² is assumed. This is broadly in line with expectations.

Loading values for C, N and H (L_{C1}, L_{N1} and L_{H1} respectively) can also be calculated using equation 2 where X_{FITC} = 0 and where it is assumed that the total weight percent of the surface group, PG1 = the sum of the individual weight percents of C, H and N, PG1_{obs} (see appendix V.5 for explanation of this assumption).

The average calculated loading values are:

$$\text{LC1} = 19.91 \text{ nm}^{-2}$$

$$\text{LN1} = 5.29 \text{ nm}^{-2}$$

$$\text{LH1} = 95.16 \text{ nm}^{-2}$$

which gives an derived empirical formula for the stage 1 loading group of:

$$\text{C1} = 3.76$$

$$\text{N1} = 1.00$$

$$\text{H1} = 17.98$$

The model predicts a stage 1 surface group formula of:

$$C_1 = 3$$

$$N_1 = 1$$

$$H_1 = 8$$

So the results are in reasonably good agreement for C and N, but not H.

The constant in the observed regression equation means that carbon containing material is present even when the nitrogen content is zero. This information, together with the previously mentioned higher-than-predicted hydrogen content, suggest some hydrocarbon contamination on the surface of the porous glass.

The loading of the surface group (as opposed to the loadings of the individual surface atoms) can be found using equation 3, which for the stage 1 model reaction is given simply by:

$$L_{G'} = L_i/n_{i1}$$

If we consider the average of all the carbon and nitrogen loading values, then the calculated group loadings are:

$$L_{G'} = 19.91/3 = 6.63\text{nm}^{-2} \text{ (based on the carbon data)}$$

$$L_{G'} = 5.29/1 = 5.29\text{nm}^{-2} \text{ (based on the nitrogen data)}$$

Figure 5.8 shows the histograms of the carbon and nitrogen calculated loading values. It can be seen that over 50 per cent of the observations occur in the lowest interval range. So most of the calculated group loading values will be slightly lower than those given above.

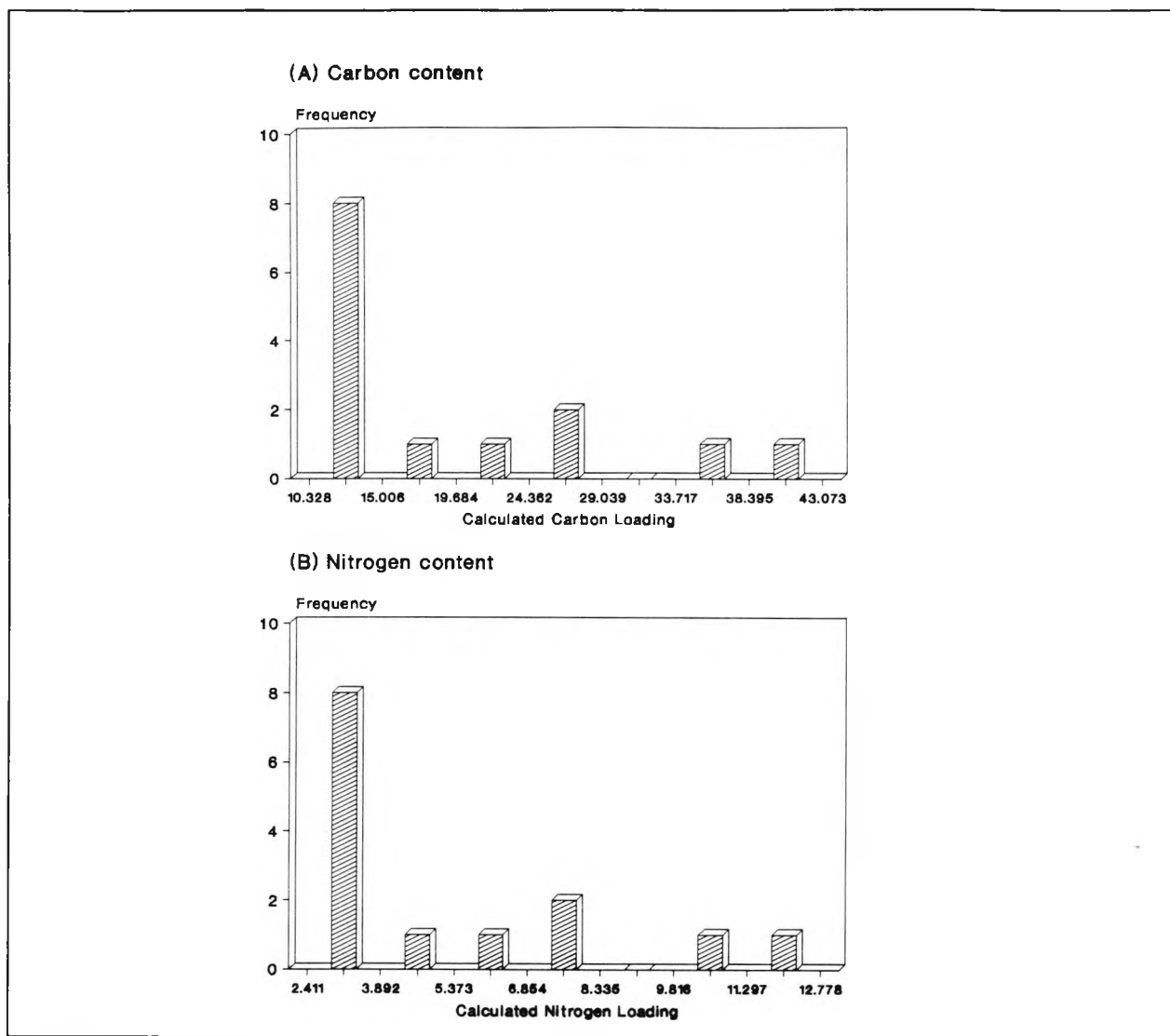


Figure 5.8 Stage 1 calculated carbon and nitrogen loading values.

To summarise, the results for stage 1 of the immobilisation reaction, the carbon and nitrogen data are in good agreement with the values predicted by model reaction and literature values for the concentration of reactive groups on silica surface. The hydrogen values were found to be less reliable and will not be considered in further calculations. The presence of some hydrocarbon contamination is also indicated.

(b) Stage 2 Loading Values

Now let us also consider the analysis of the samples which also underwent the stage 2 reaction. Appendix V.6 summarises the observed data and figure 5.9 plots P_{C2} versus P_{N2} .

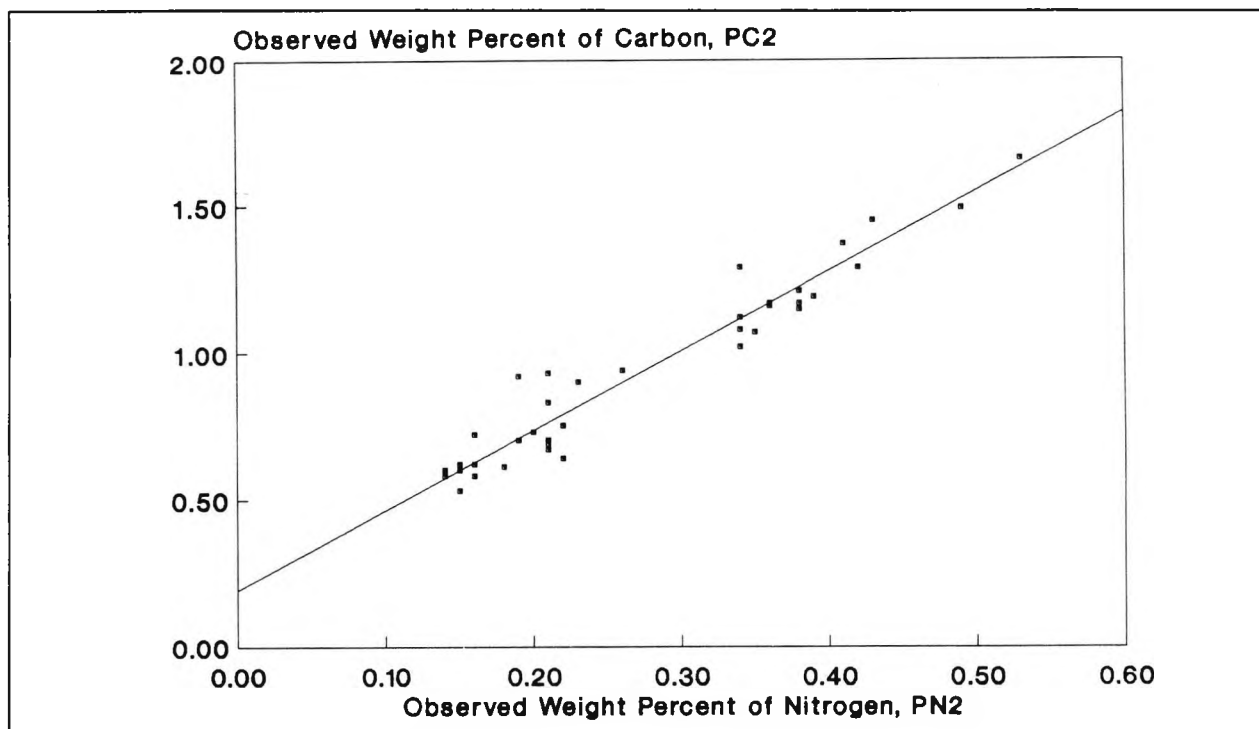


Figure 5.9 Stage 2 observed weight percents for C and N.

Referring also to table 5.3, the first thing to note is that lower weight percentage values for C, H and N were recorded for the stage 2 samples than for stage 1. This was unexpected and contrary to the model outlined earlier.

Regression analysis performed on the observed weight percentage data from stage 2 reactions generates the following equations:-

$$\text{Stage 2:} \quad PC2 = 2.713(PN2) + 0.1920$$

The second thing to note is that the stage 1 and stage 2 regression equations are not significantly different from each other. One problem with the technique used in this approach was that the absolute levels of percentage weight losses were themselves very low, especially in the case of the stage 2 samples. This may make the analysis prone to instrumental error, nevertheless, the measurements from the untreated porous glass sample suggest that the values recorded are significant. The biggest problem is that without explainable values for hydrogen, and without any data for the oxygen and sulphur content, it is difficult to reach any unambiguous conclusions relating to the immobilisation of the FITC onto the silylated porous glass.

Notwithstanding the shortcomings of the method for this application, some tentative conclusions can still be reached. Firstly, the extent of derivatisation of the FITC *must* be quite low. From the evaluations of the stage 1 results, it is reasonable to assume an average loading of 3APTS of around 5 groups/nm². Table 5.3 compares calculated versus observed data and assuming the loading of 5 groups per nm², we would still expect to record carbon values of around 6.92 wt% if all the aminopropyl groups reacted with an FITC group (i.e. $X_{\text{FITC}} = 1$). Such values are readily measurable by the instrumental method used. Also, the ratio of recorded wt% carbon to wt% nitrogen (slope of PC2 versus PN2) is much lower than predicted. Only when we assume values of $X_{\text{FITC}} = 0.0092$ and a loading of 3.505, do the calculated and observed data become comparable. This would suggest that just under 1 3APTS group in 100 undergoes subsequent reaction with FITC.

The intercept value indicates the presence of species on the surface of the porous glass which contain carbon but not nitrogen. There are at least two possible origins of this material. The first and most obvious is that it is residual toluene from the stage 1 reaction. The second possibility is that it is ethanol, either from the final rinsing procedure or as a result of the condensation reaction between ethoxy groups of the 3APTS and the surface silanol groups and or trace amounts of water. Whatever its precise origin, the intercept value does not decrease significantly from stage 1 to stage 2 products and cannot be used to explain the loss of material observed.

Although care was taken to exclude water from the stage 1 reaction, it is not inconceivable that some residual water was present on the surface of the porous glass and that this resulted in a degree of polymerisation of the 3APTS. Not all of the 3APTS molecules in this case would be attached to the silica surface. Under the influence of acids or bases the hydrolysis of siloxane bonds proceeds easily in the surface monomolecular polyorganosiloxane films⁹³. If we assume that the amine functionality on the 3APTS affects the pH of the microenvironment on the surface of the porous glass⁷⁶ then it is possible for the polysiloxane bonds formed in stage 1 of the reaction to undergo subsequent cleavage in stage 2. This could explain the significant reduction in the observed carbon and nitrogen contents in the stage 2 samples but also has implications regarding the stability of this reagent system for FOCS applications which will be discussed in a later section.

The calculation of stage 2 loading values for C and N is not as straightforward as with stage 1 loadings since the assumption that the total weight percent of the surface group is equal to the sum of the individual C, H and N weight percents recorded (i.e. $\text{PG2} = \text{PG2}_{\text{obs}}$) cannot be made without knowingly introducing some error. This is because no measurements were made for O and S and hence PG2_{obs} cannot be equal to the theoretical value of PG2, the latter of which must require an assumption as to the empirical formula of the surface group. This leads to the calculation of slightly different loading values for C, N and H depending on whether PG2 or PG2_{obs} are used. But the *ratio* of LC2 and LN2 can also be calculated without considering PG2

(as is suggested by equation 4). When $X_{\text{FITC}} = 0.0092$ (i.e. assuming an empirical formula for the surface group) the value of LC2/LN2 derived in this manner is close to the observed value.

To summarise, we observed that the stage 2 reaction procedure resulted in an overall loss of material present on the PG surface, even though it was obvious from inspection that derivatisation of FITC had occurred. We concluded that there was a very low extent of FITC derivatisation (low X_{FITC} value) and that some non-nitrogen containing species were also present on the PG surface (intercept values).

The microanalysis resulted in values for carbon and nitrogen content which could be explained by the reaction model proposed, however, because of lack of reliable hydrogen data and unavailable sulphur and oxygen measurements the model could not be tested exhaustively. Moreover, in the determination of X_{FITC} for stage 2 we effectively assumed that the stage 1 reaction proceeded as proposed by the reaction model, even though we have generated no independent evidence for this assumption. On the other hand, many "what-if" calculations using different molecular formulae for the stage 1 group lead to much higher carbon to nitrogen ratios than those observed and so the model does appear to be able to provide a reasonable explanation for the observations.

5.3.2.3 EFFECT OF REFLUXING PG IN 3APTS

Figures 5.10 and 5.11 compare the measured carbon and nitrogen contents for samples which were refluxed in 3APTS with samples which were simply immersed in the 3APTS solution. From the graphs it can be seen that for both stage 1 and stage 2 reaction steps, refluxing leads to an increase in the carbon and nitrogen content.

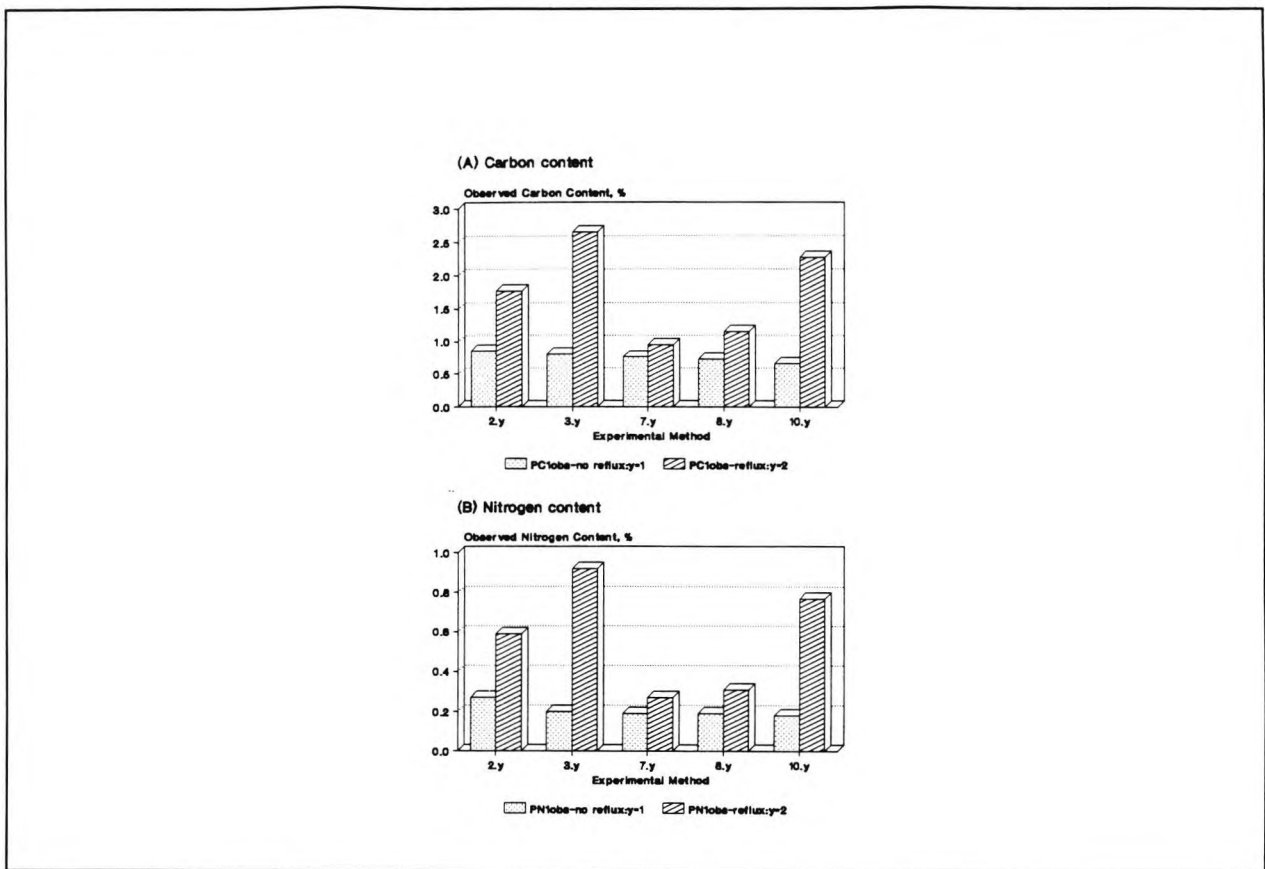


Figure 5.10 Effect of refluxing on the measured carbon and nitrogen contents after stage 1 reaction.

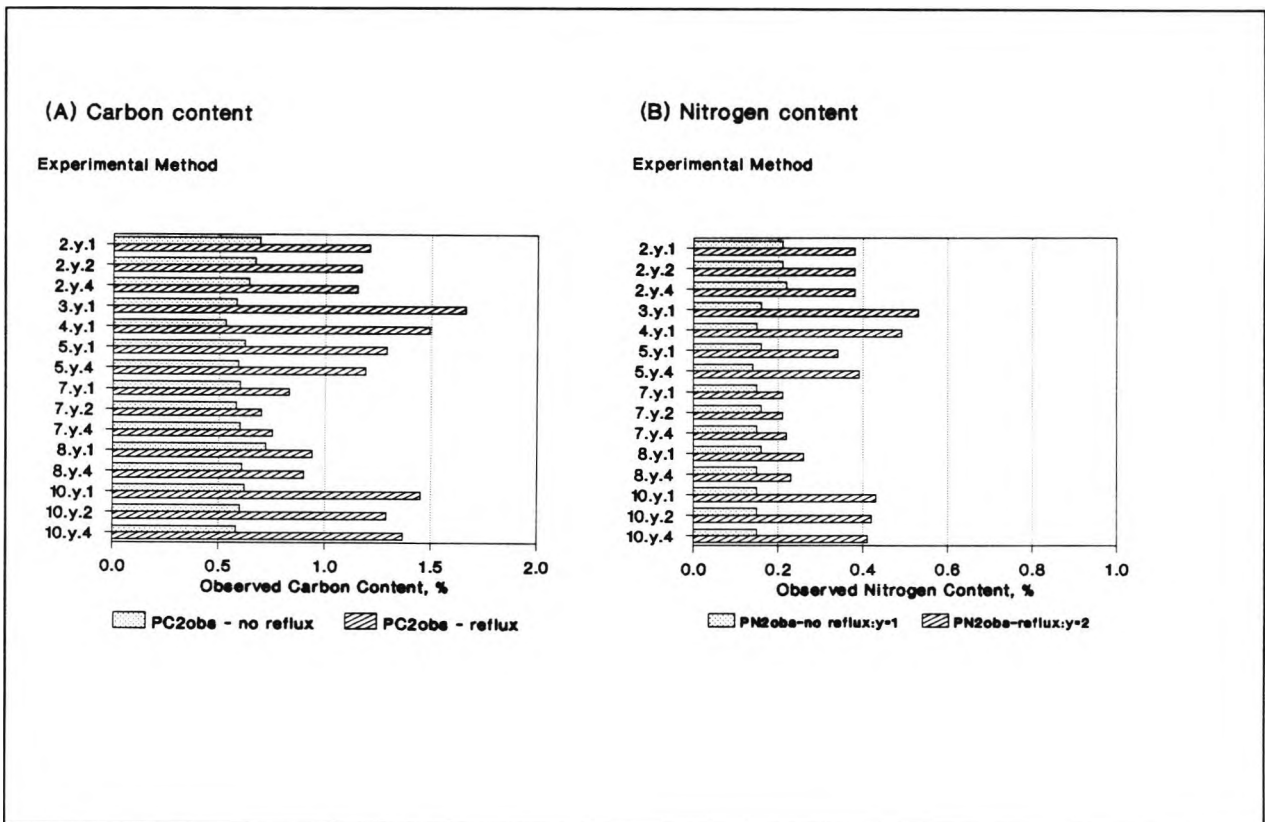


Figure 5.11 Effect of refluxing on the measured carbon and nitrogen contents after stage 2 reaction.

5.3.2.4 EFFECT OF FITC CONCENTRATION

Figure 5.12 illustrates that there is a correlation between stage 2 and stage 1 carbon and nitrogen contents. The relationships deviate from linearity at the higher stage 1 concentrations. The effect of using different concentrations of FITC solution does not lead to a significant difference in the measured quantities even though the appearance of the samples were different in some cases.

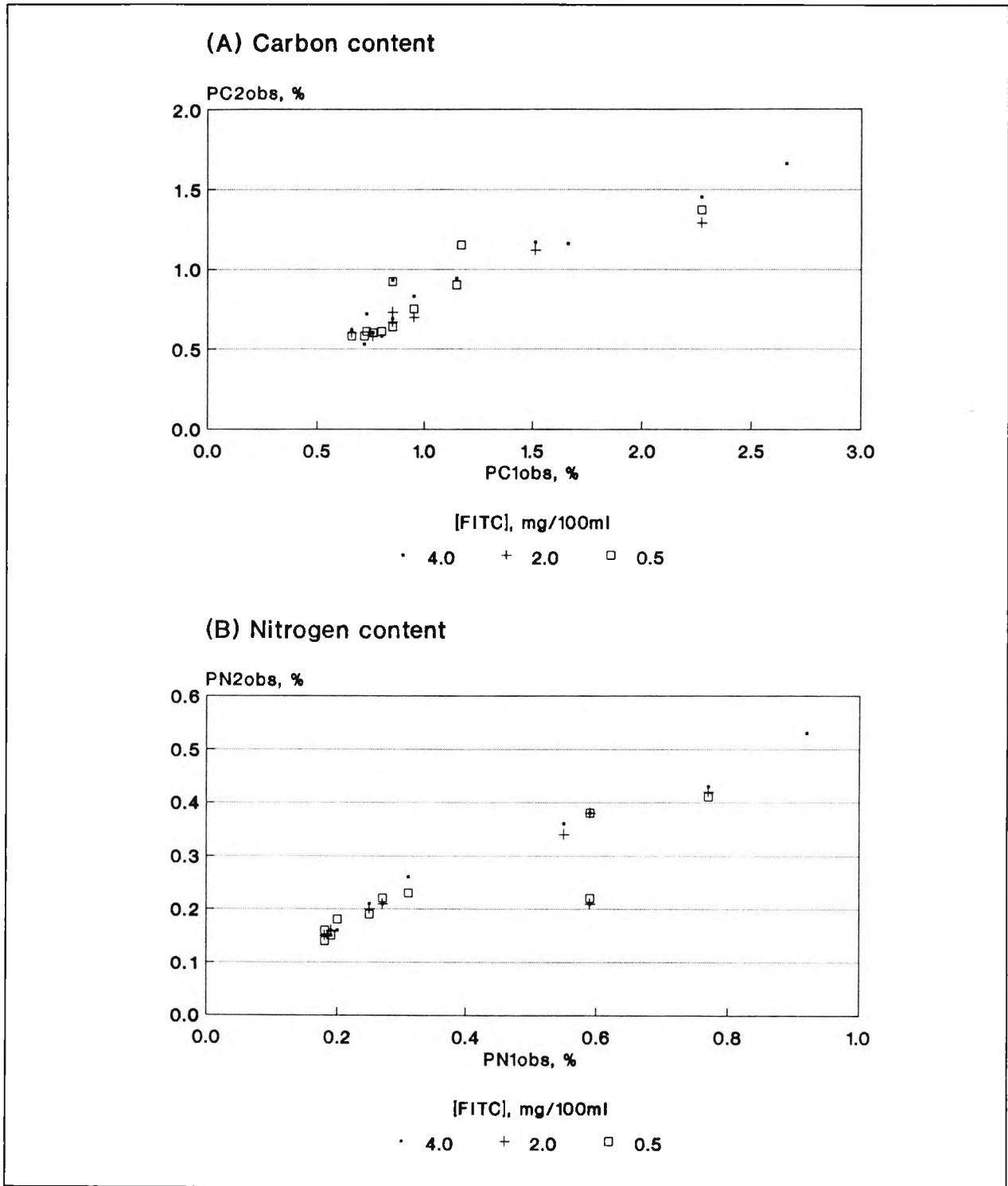


Figure 5.12 Effect of concentration of FITC solution on observed carbon and nitrogen contents.

5.3.2.5 EFFECT OF THERMAL TREATMENT

Figure 5.13 summarises the stage 1 data for the different methods used. The differences observed in the repeat experiments (3 and 6; 7, 9 and 10) were of a such a magnitude as to prohibit any deduction regarding the effect of the experimental method used. These differences cannot be readily explained but may be due to the different lots of cleaned porous glass being used. In any case, the effect of refluxing was often more significant than the effect of the thermal pretreatment.

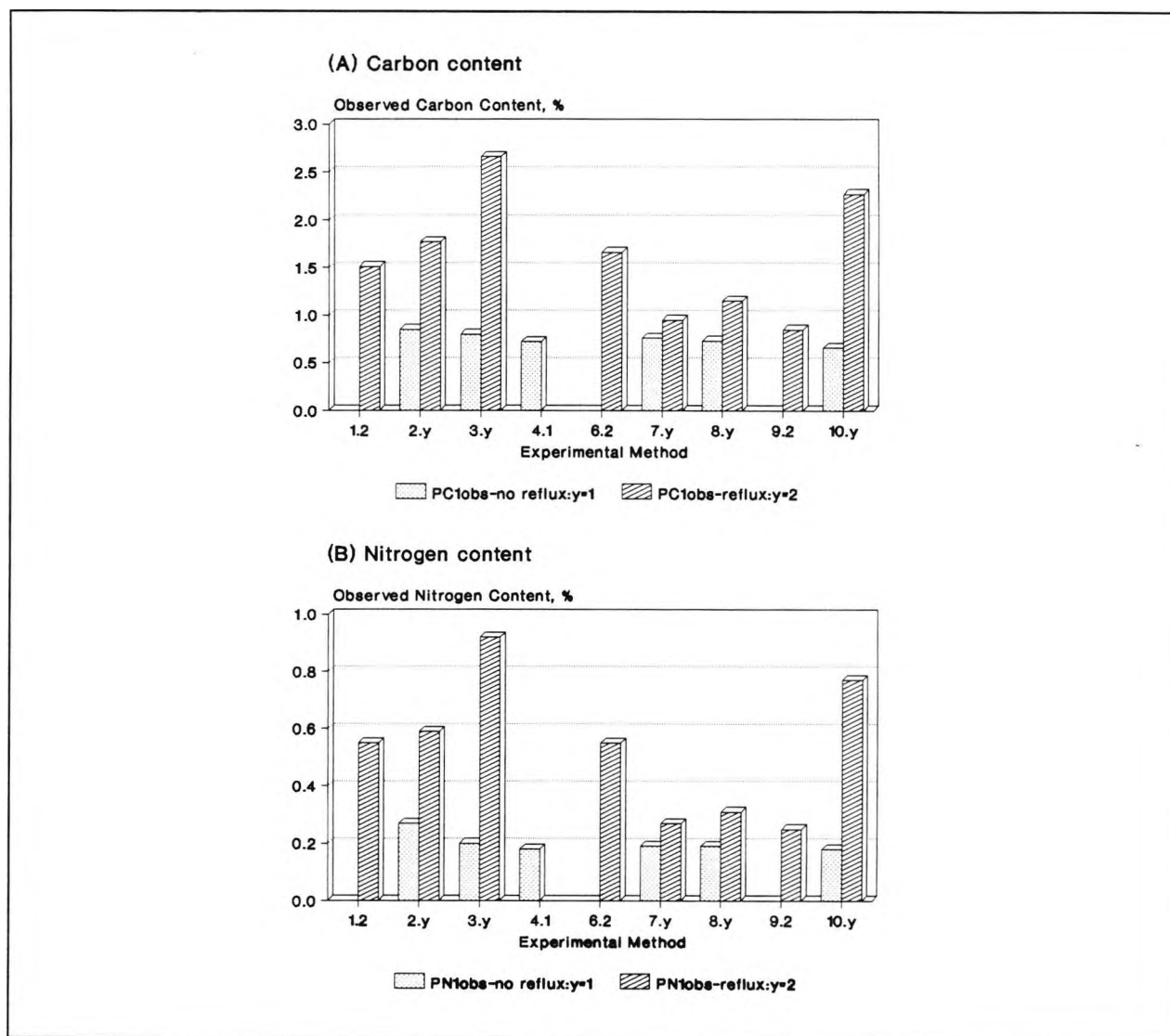


Figure 5.13 Effect of experimental method on stage 1 on a) PC1obs b) PN1obs

5.3.3 FLUORESCENCE ANALYSIS

5.3.3.1 EXCITATION SPECTRA

The excitation spectrum for the derivatised porous glass was measured using the fibre optic link to the spectrophotometer and is compared in figure 5.14 to the spectrum of aqueous FITC ($4 \text{ mg (100ml water)}^{-1}$) which was recorded in the conventional manner. The scales used

have been normalised: in practice the intensity of the fluorescence from the FITC in solution was approximately 300 times greater than that for the derivatised FITC.

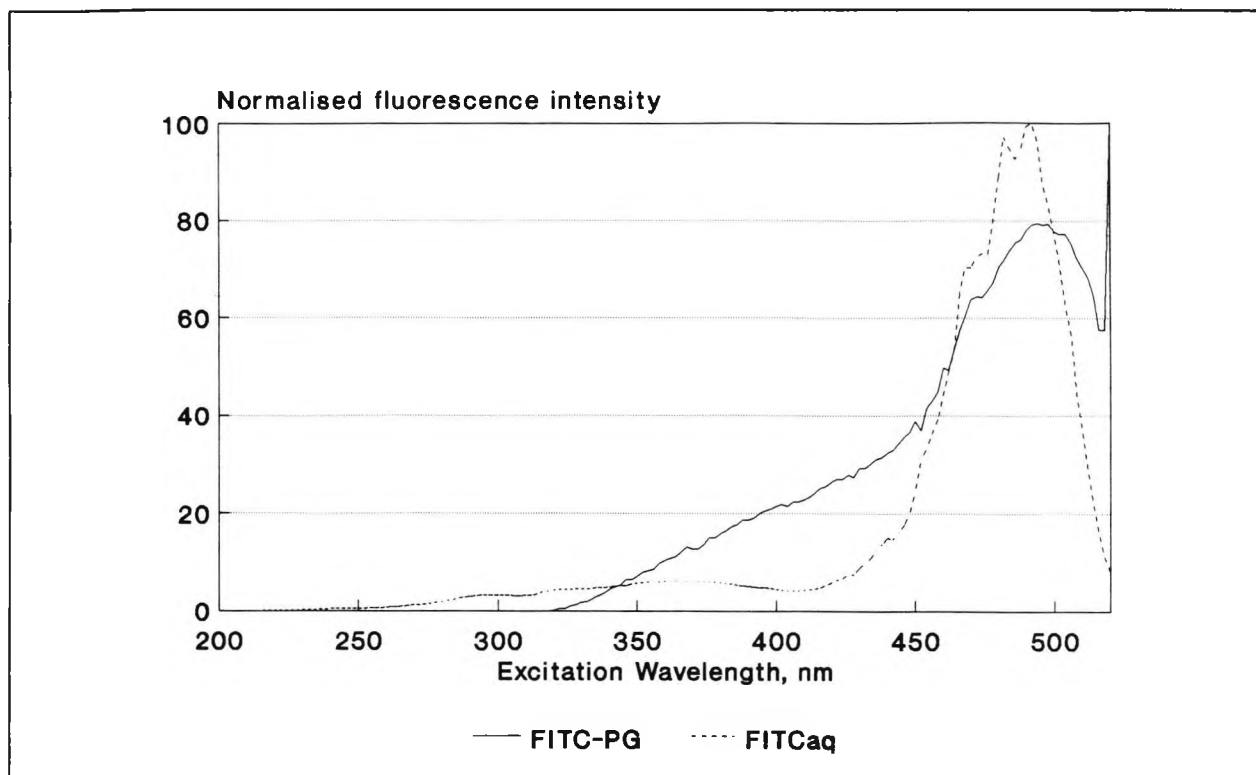


Figure 5.14 Comparison of excitation spectra of PG-FITC and FITCaq.

At wavelengths below about 320 nm, there was no fluorescence observed via the fibre optic probe since the attenuation of the optical fibre in the UV is significant. A slight shift of the absorption band of the immobilised dye as compared to the dye in solution was observed as might be expected⁷⁵ ($\lambda_{\text{ex max}} = 494$).

5.3.3.2 EMISSION SPECTRA

(a) Dry Derivatised Porous Glass

The emission spectrum of dry derivatised porous glass (figure 5.15) exhibits a slight shift to the long wave compared to the dye in solution (see figure 4.4a). The overall effect on the Stokes shift, however, is minimal, and for both the immobilised and solution FITC the difference in excitation and emission maxima is about 50 nm. For many long pass interference filters, a shift of this order will result in effective separation of short and long waves⁹⁴ and in fibre optical chemical sensing this is an important point since it means that more sophisticated wave resolution techniques may not be required.

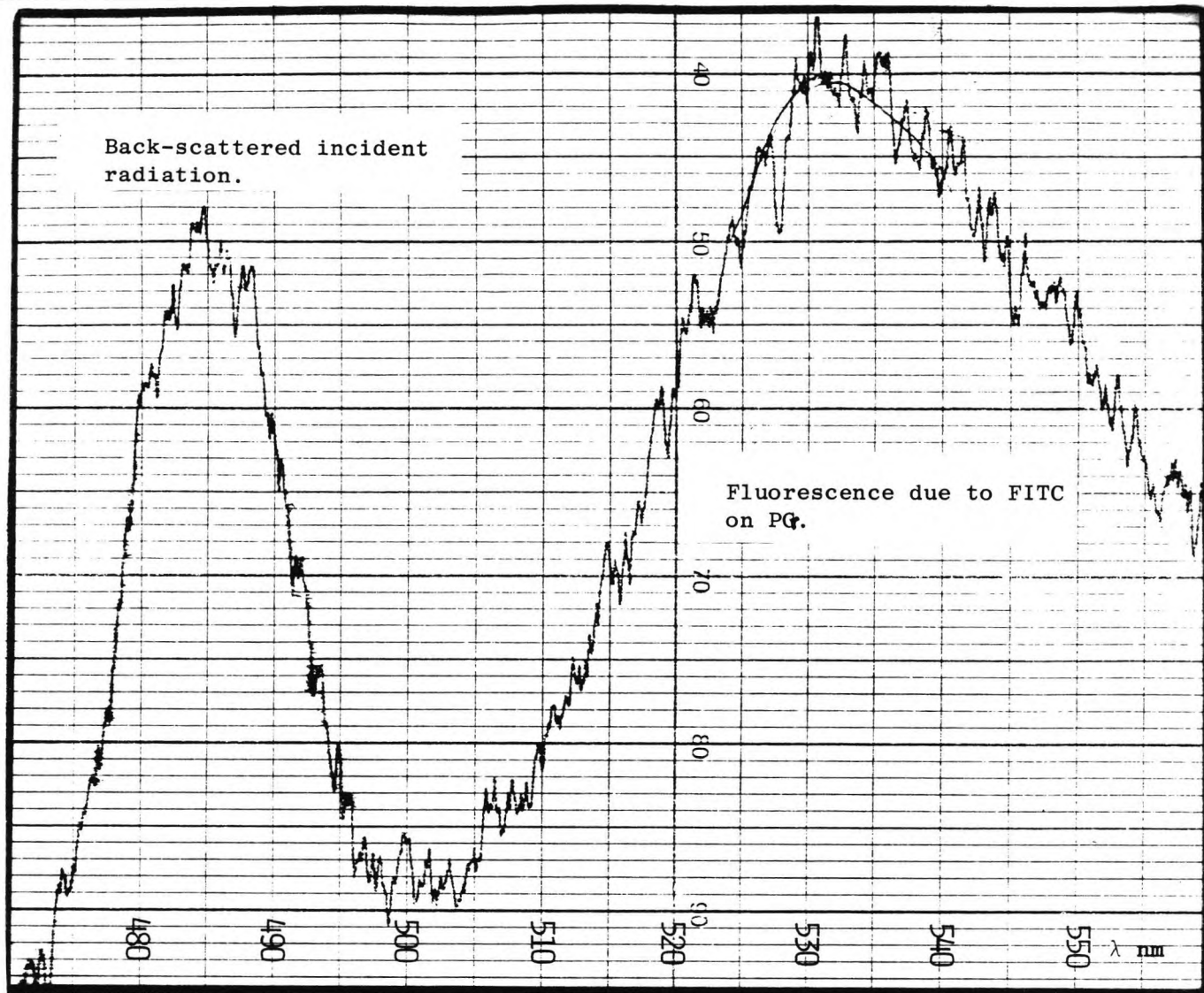


Figure 5.15 Emission spectrum of dry derivatised PG-FITC

(b) Fluorescence Response as a Function of pH

The spectra for the immobilised FITC in solutions of different pH values are shown in figure 5.16.

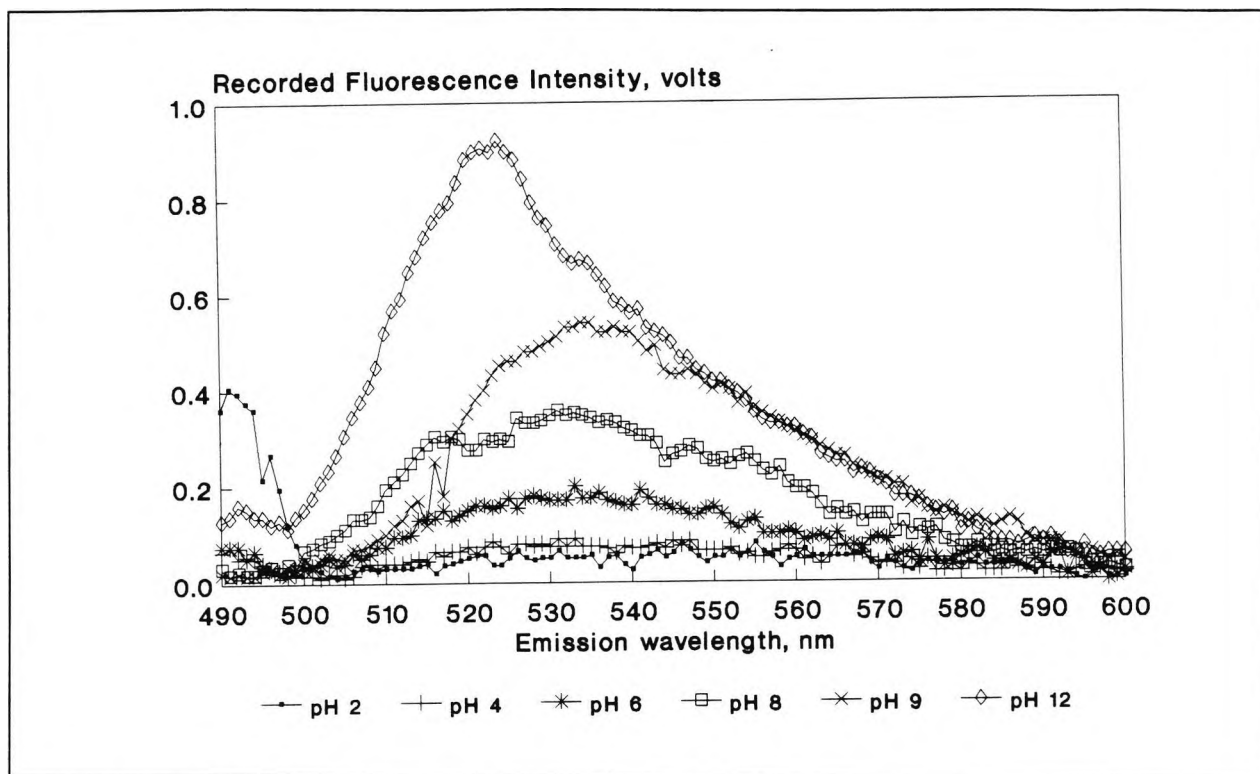


Figure 5.16 Emission spectrum of PG-FITC at different pHs.

The total emission intensities were calculated from the areas under the curves and compared with the measured fluorescence intensity of FITC in solution. For pH values below 8 (figure 5.17a), the total (normalised) emissions are similar for both the immobilised FITC and the dye in solution. The sensitivities in the linear range of the two methods are similar in terms of percentage change (i.e. the slopes across the points of inflexion are nearly the same). In absolute terms, however, the sensitivity of the FITC in solution is much greater although the actual values will depend on the concentration of the solution.

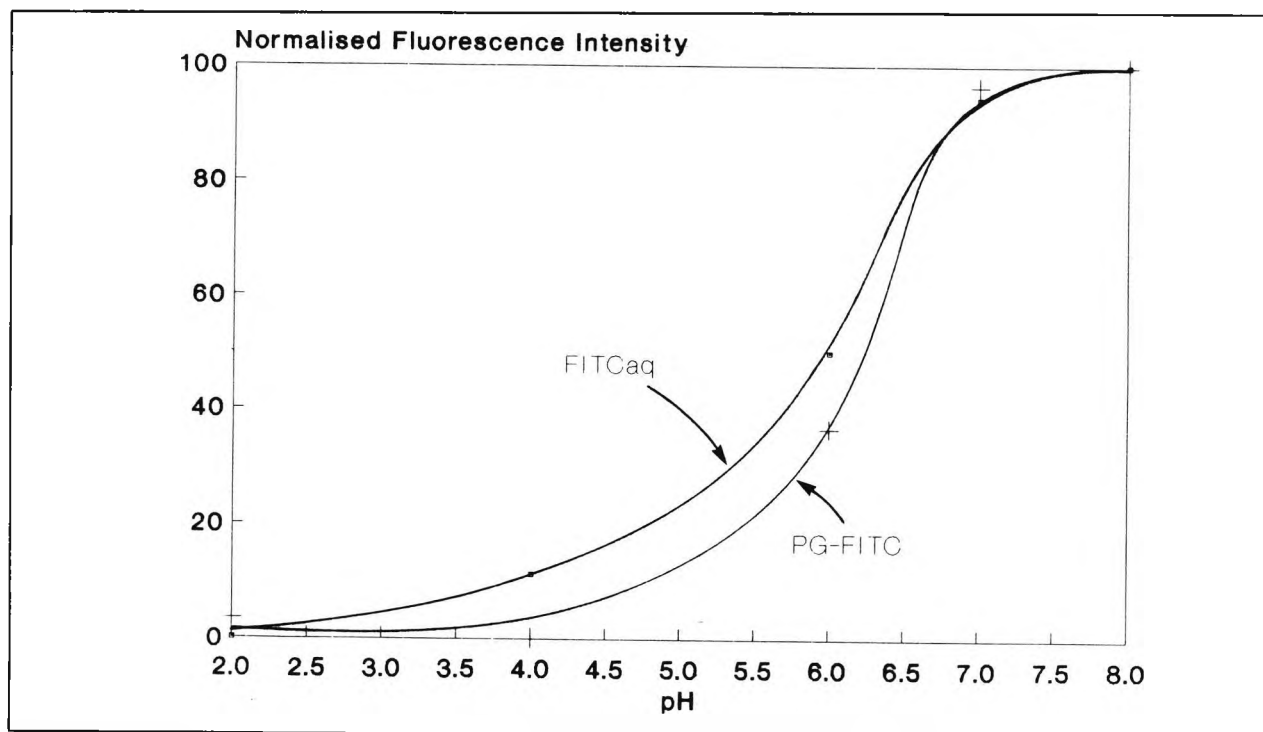


Figure 5.17(a) Fluorescence response of PG-FITC and FITCaq between pH 2 and pH 8

When the fluorescence response of the probe and solution FITC are compared at higher pH values, some marked differences are observed (figure 5.17b). At pH values above 8, the intensity of the probe fluorescence increased in contrast to that of the solution FITC. This observation can be explained by realising that in alkaline environments the siloxane bond undergoes cleavage which results in immobilised dye going into solution and that dye in solution is known to possess higher quantum efficiencies than when it is immobilised⁷¹. The construction of the optical probe was such that any dye which was became unbound was retained in the macroporous membrane and would only slowly diffuse into the surrounding environment.

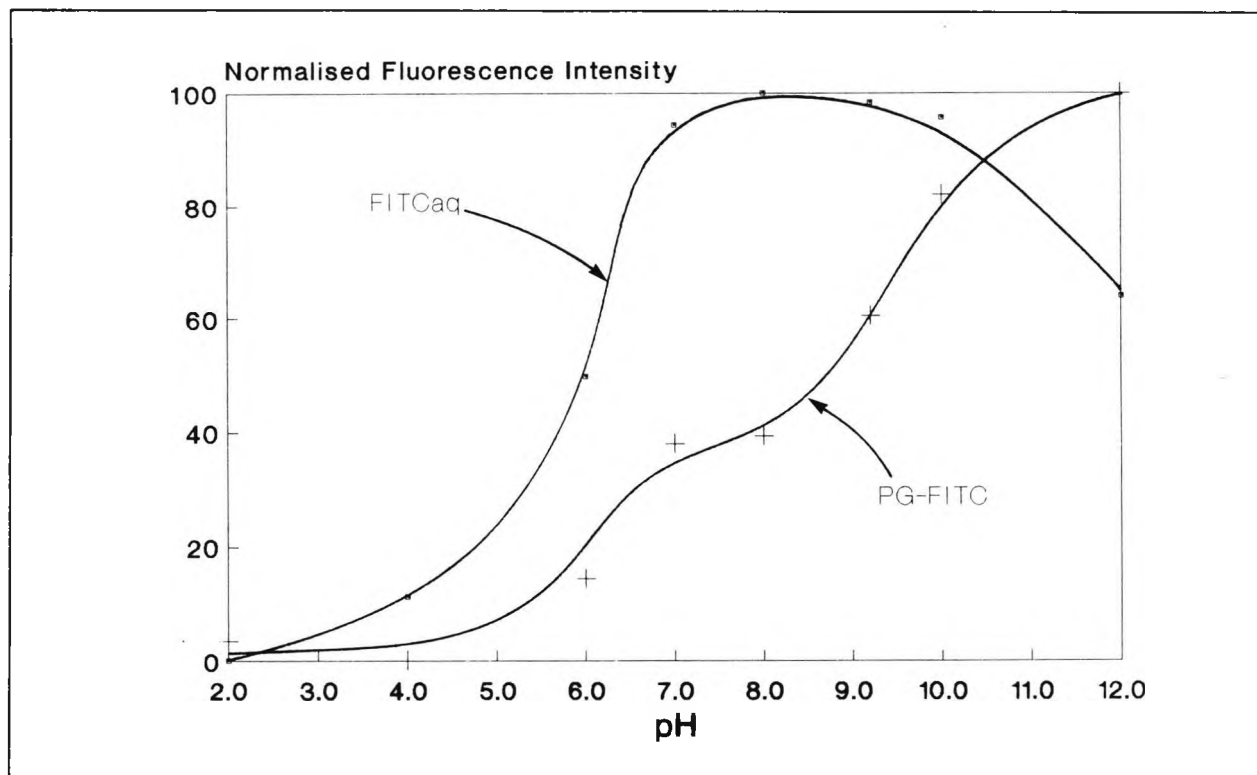


Figure 5.17(b) Fluorescence response of PG-FITC and FITCaq between pH 2 and pH 12

Separate leaching studies in which the absorbance was measured of solutions surrounding known quantities of derivatised PG confirmed that FITC is much more readily leached at higher pH values.

The error of the fibre optic method was calculated on the basis of the variation of the areas under three separately recorded emission curves measured at pH 7 and found to be within 1 per cent. The probe was not moved for the duration of the three measurements. With repeated use, however, the intensity of the response diminishes and the extent of reduction depends mainly on the intensity of radiation and also on the pH of the test solutions. As a result of this variation in reading with time, such a set-up would require calibration prior to use.

(c) Fluorescence Response of the Fibre Optic Probe to a Step Change in pH

The solution surrounding the probe was stirred during this measurement so we would expect that the measured fluorescence intensity was mostly due to the immobilised FITC and not any FITC which leached from the porous glass. An exponential fluorescence response was observed (figure 5.18). The time constant was calculated to 0.285 which equates to 4.38 minutes for the response to achieve 95% of maximum value. This is significantly longer than the response of the pH electrode.

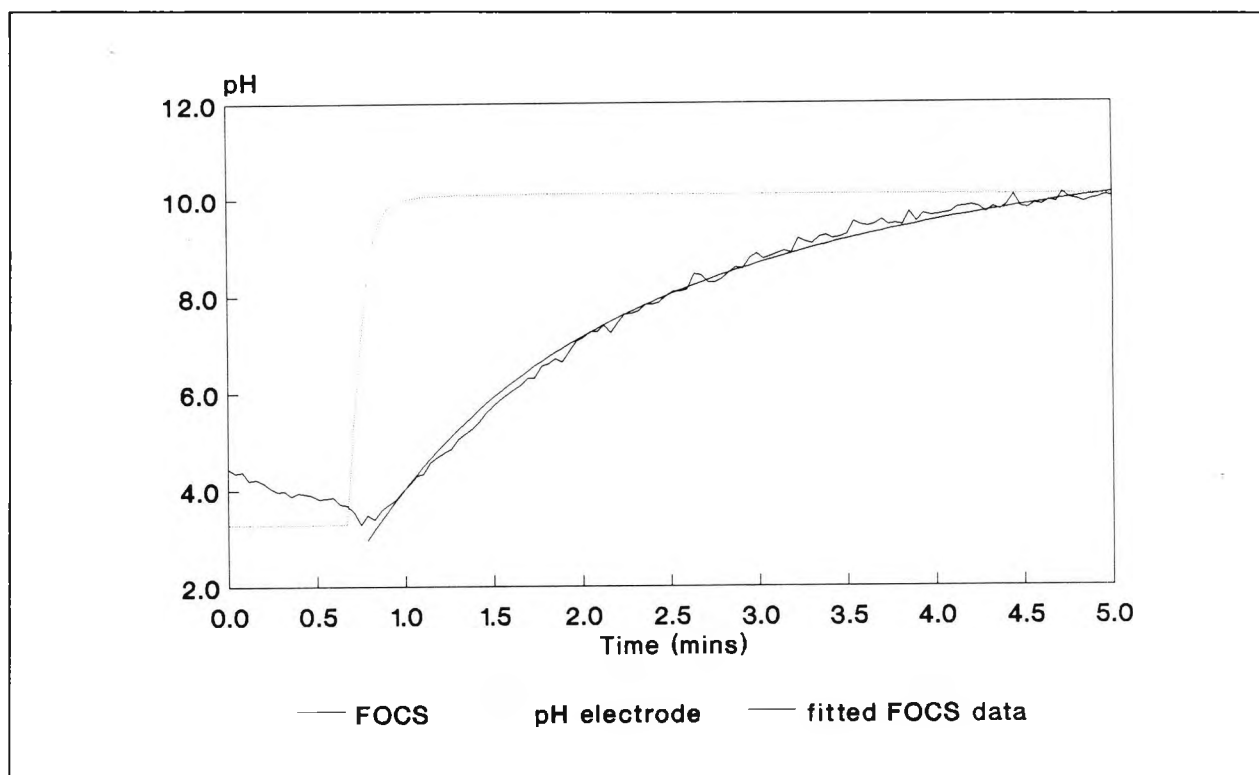


Figure 5.18 Fluorescence response of PG-FITC to a step change in pH.

The reproducibility of this approach was not evaluated, but one would expect it to depend mainly on the way that the probe was prepared.

For some applications, for example ground water monitoring, a response time of the order found would be acceptable. In many instances, however, there is a need for a probe which will react much more rapidly to changes in the analyte concentration. Some workers have managed to achieve this, but their approaches have other drawbacks. Fuh M-R. S. *et al.*³⁴ attached a single sphere of FITC derivatised porous glass to the end of a single fibre optic fluorescence pH probe. Response times of 20 to 35 s were reported, but apart from the limitations owing to the increased susceptibility to loss of dye, the experimental set-up also required the presence of more sensitive detection instrumentations. In another approach³⁵ the FITC was immobilised directly to the distal end of the single fibre optic probe which gave an intrinsic response time of less than 1s. The overall response time of the sensor, however, was determined by the time constant of the lock-in amplifier which was used. In order to achieve adequate signal to noise ratio, the time constant had to be set at 30 s. It is apparent

that there has to be a compromise between signal intensity, ease of measurement and response time and that the optimum balance will depend on the specific application of the probe.

(d) Affect of Method of Immobilisation of FITC on the Fluorescence of Dry Derivatised Porous Glass

Prior to recording the fluorescence spectra of the dry derivatised PG materials, the height of the fibre bundle probe from the surface of the sample was adjusted using a mounted stage until the maximum signal was achieved at 530 nm. It was noticed that for the more deeply coloured samples, the probe tip did not make contact with the material, whereas for the samples which were lighter in colour the tip of the probe was immersed into the bulk of the material.

No correlation could be found between the carbon or nitrogen content and the intensity of the fluorescence response. However, when the fluorescence intensities are plotted against the methods used (figure 5.19), it can be seen that in most cases the fluorescence intensity increases when lower concentrations of FITC solutions are used (see section 5.1.2 for key to sample labelling).

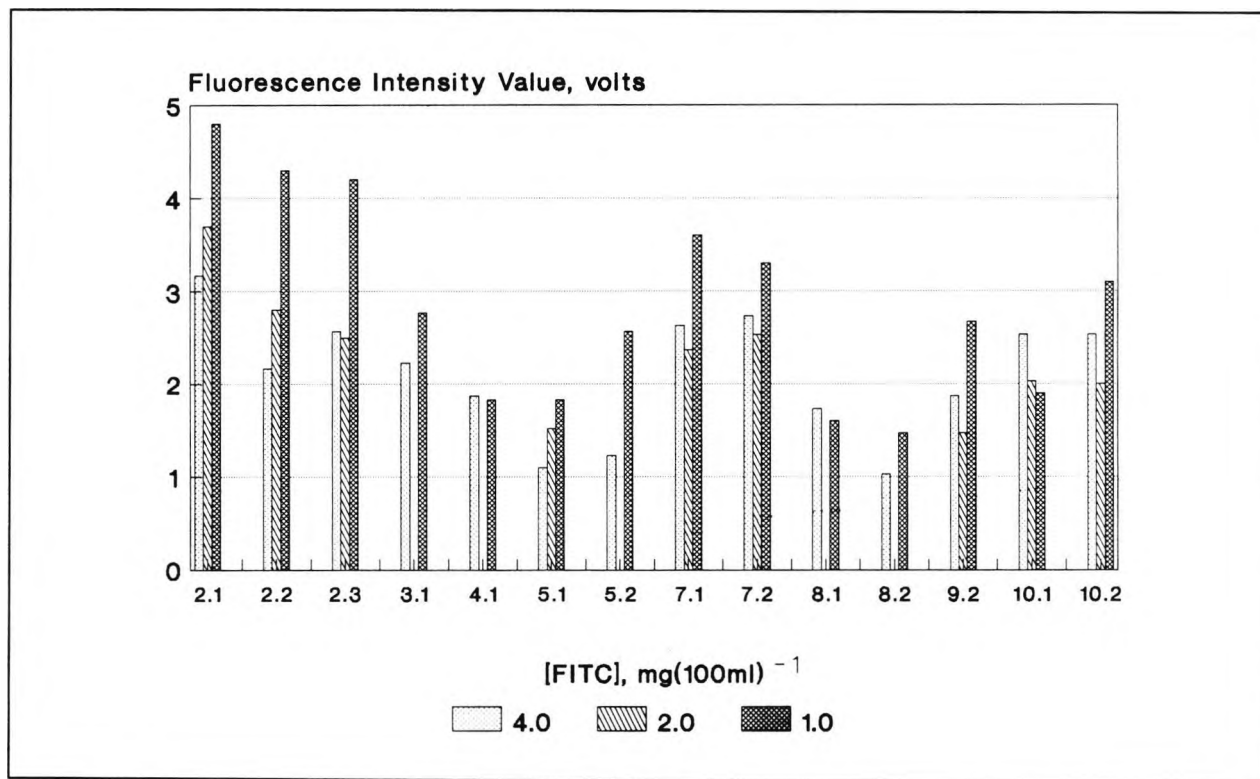


Figure 5.19 Fluorescence response of PG-FITC samples.

The porous glass sample which was neither preheated nor refluxed was not brightly coloured like the other samples and did not exhibit any significant fluorescence.

5.4 SUMMARY AND CONCLUSIONS

It has been shown that porous glass is indeed a useful substrate in fibre optic chemical sensing. Different methods of derivatisation suggest that refluxing has the biggest effect on the loading of the dye onto the porous glass and that thermal pretreatment does not give significant advantages. The concentration of the FITC solution does have an effect on the final dye loading which can be observed by inspection and from the fluorescence responses, but these differences could not be detected by the microanalytical method used.

The fluorescence response of the derivatised porous glass is very similar to that of the dye in solution at the non-alkaline pH range. The reproducibility of the response in this range is, after an initial leaching period, reasonably good. With repeated usage, however, it is expected that the sensitivity of the probe will decrease through additional siloxane bond cleavage and also photobleaching. At pH values greater than pH 7, the hydrolysis of the siloxane bond is accelerated leading to significant loss of the dye from the porous glass surface. When this happens, the fluorescence signal initially increases since the dye in solution gives a higher signal than the immobilised dye.

Although there were exceptions, we found that in general refluxing increases the carbon loading but does not necessarily lead to an increase in the fluorescence intensity and more highly fluorescing samples can generally be prepared using FITC solutions of lower concentrations. From these results one would postulate that highly loaded samples are more prone to a kind of inner filter effect in which the presence of an abundance of the fluorophore acts to absorb the fluorescence produced rather than reradiate it to the surroundings. In conclusion, the preparation of derivatised porous glass for fibre optic chemical sensing is best achieved with relatively low loadings of the dye. In practice, this means that it should not be necessary to reflux preheated porous glass to achieve adequate silylation. Moreover, if the porous glass has been adequately cleaned beforehand, the thermal pretreatment can be limited to dehydration (e.g. N₂ at 150 °C).

The probe configuration used results in a strong fluorescence signal which was readily measurable with the two instrumental set-ups described. It is anticipated that such a signal can also be measured using many of the simpler solid state devices as has been described in the literature. The main limitation of the probe as described is that its response time is too long for many applications. One reason for this is that it is difficult to optimise the granular form of the porous glass for fibre optic sensing. In the next chapter, another approach is investigated which could potentially be used to prepare pH sensitive substrates which could overcome some of the short-comings of porous glass.

Chapter 6

EVALUATION OF SOL-GEL TECHNOLOGY AS A MEANS OF PREPARING MATERIALS USEFUL IN FIBRE OPTIC CHEMICAL SENSING

6.0 ABSTRACT

The sol-gel process is introduced and its potential applicability to preparing glass-like structures which can be used in FOCS is reviewed and further explored.

The main features of sol-gel processing which are potentially relevant to the preparation of a high surface area solid support for use as a sensor substrate are presented. From the literature reviewed it was not possible to clearly define an ideal sol composition which would lead to a material with properties that could best be tailored to FOCS. Nevertheless, there was much evidence that such a material could be prepared and in the subsequent section experimental work is reported which highlights the efforts made to reach that goal.

FITC-containing monoliths are prepared by two routes: impregnation of the FITC into already formed gels and incorporation of FITC into the gel at the sol stage. The properties of these materials are discussed with respect to applicability in FOCS and their stability, both from the point of view of a wet-dry-wet cycle and in terms of storage stability over a number of years.

The preparation of FITC-containing coatings is also discussed and appears to offer the best opportunity for use of this technology in FOCS.

6.1 INTRODUCTION TO SOL-GEL TECHNOLOGY

6.1.1 HISTORICAL BACKGROUND

Although sol-gel synthesis was reported as early as last century, it was not until the mid-seventies that interest in this technology really started to take root. The first workshop "Glasses and Glass Ceramics from Gels" was held in Padua in 1981 and the publication "Journal of Non-Crystalline Solids" is largely devoted to aspects of the sol-gel process. So what exactly is this process and why has it attracted so much attention? The sol-gel process can be described as a chemical phenomenon in which a single or multicomponent metal oxide solution undergoes *gelation* to form a coherent rigid network of the oxides present. The reason it is of interest is that it has the potential to be used to produce "tailor-made" glasses and ceramics with wide-ranging applications and also it allows for lower temperature treatments than is normally possible in the production of conventional glasses. The literature is concerned almost equally with the preparation of bulk glasses, fibres and coatings and industrial applications have been referred to in a number of fields including the coating of glasses to modify their optical properties⁹⁷ and the preparation of high density inorganic oxides used in the production of nuclear fuel^{98, 99}. Sol-gel technology is being considered in a number of other applications including the one which is of interest for the present investigation i.e. its use in the preparation of materials useful in fibre optic probes. Avnir and co-workers have considered the trapping of fluorescent organic molecules in sol-gel glasses since 1984¹⁰⁰ and a recent example of interest focused on the development of an evanescent-wave sensor based on sol-gel derived porous coatings¹⁰¹.

6.1.2 OUTLINE OF SOL-GEL PROCESS

There are three distinct stages to the sol-gel process:-

- (i) Mixing of the precursors in solution to achieve intimacy on a molecular scale.
- (ii) Gelling of the solution in a manner which will retain the chemical homogeneity achieved in step (i).
- (iii) Thermal treatment to further age the gel or to convert the gel to a glass.

The main reaction components in a typical sol-gel process are a metal oxide source, water, solvent and catalyst. The most common source of metal oxides are the corresponding alkoxides although other metal organics as well as inorganic compounds have also been used. Research has also focused on many other species of interest which possess both network modifying and network forming capabilities and in all, over forty elements have been investigated for use in the sol-gel process¹⁰². In order to form the metal oxide networks

which constitute both the gels and the glasses, the metal alkoxides must firstly undergo hydrolysis. Most organoxysilanes are difficult to dissolve in water and alcoholic solvents are typically used in order to achieve complete homogeneity. Nevertheless, when stirred with water (either alone or in the presence of a water-immiscible solvent), and especially when heated, many alkoxysilanes including tetraalkoxysilane undergo profound hydrolysis⁹³. The final component in the reaction mixture is the catalyst. This is normally provided by a mineral acid or base. The preparation of shaped glasses is illustrated below for the system used in the present study: alkoxide = $\text{Si}(\text{OC}_2\text{H}_5)_4$; catalyst = HCl ; solvent = $\text{C}_2\text{H}_5\text{OH}$.

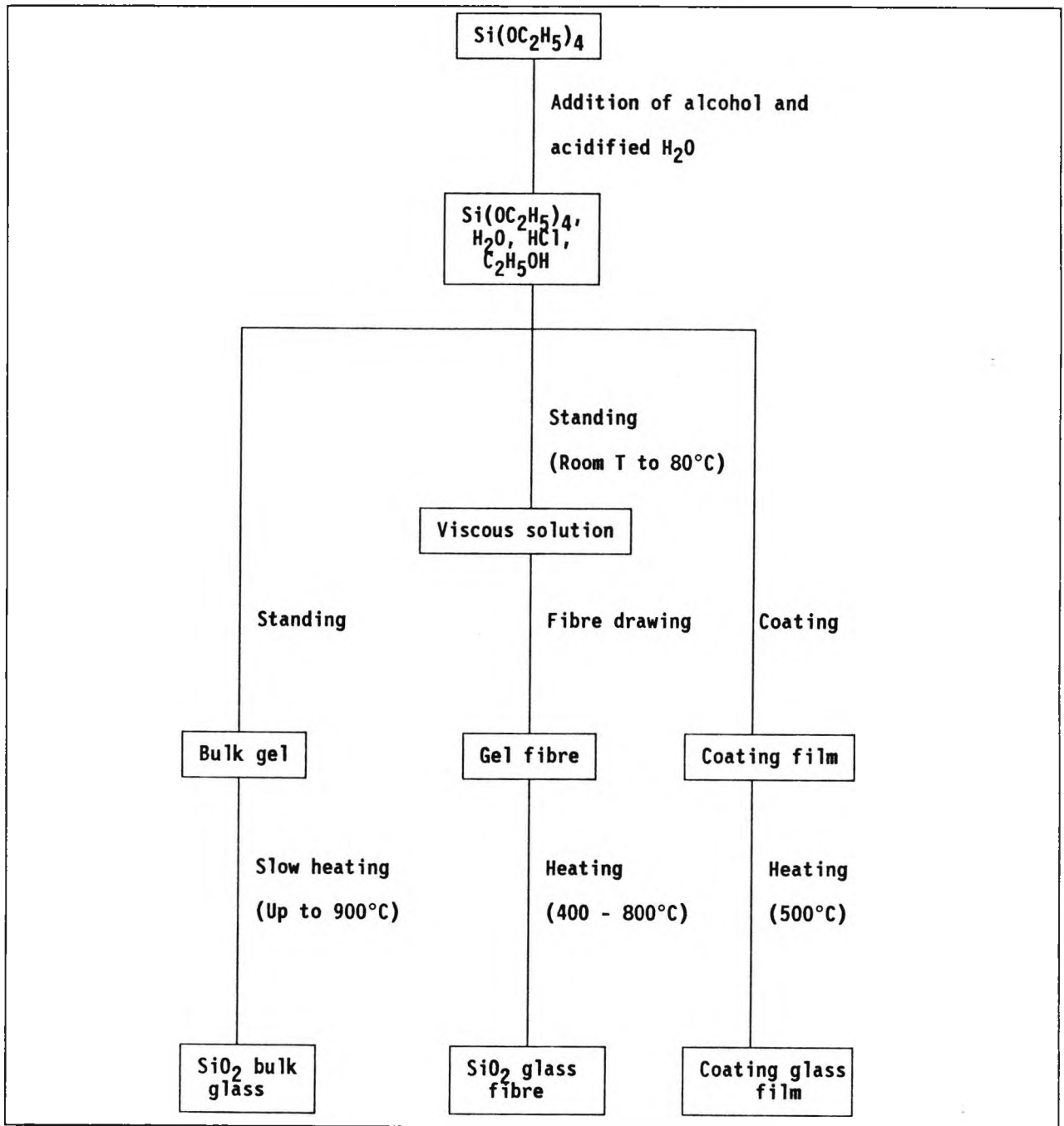


Figure 6.1 Preparation of Shaped Glasses by the Sol-Gel Process¹⁰³

The modification of gel surfaces has received a limited amount of attention. Scholze¹⁰⁴ discusses a new group of vitreous materials, the so-called organically modified silicates ("ORMOSILS"), with a view to improve the possibilities in tailoring new glasses with predetermined properties. In order to develop a reagent that provides an enhanced signal in optical fibre sensors, a similar approach is proposed. Essentially it would involve exploiting certain properties of a gel to produce a substrate which can be derivatised with the required reagent. The properties of an oxide gel that make it useful in this instance are not only its potential to be advantageously shaped, but also the feature of its porosity and hydroxylated surface. Hence, the objective of forming porous glass-like materials seems attainable in principle. In the course of this investigation much work has been carried-out to try and achieve this goal: however certain problems have been identified. In order to appreciate their significance it is necessary to review the details of the chemistry of sol-gel processing and of certain of its inherent limitations.

6.1.3 MIXING

The process parameters that influence the preparation of a solution/sol that subsequently transforms into a wet gel at the gel point are¹⁰⁵:-

- (i) Structure and chemical reactivities and the sequence of adding reactants.
- (ii) Nature of solvents and solubility of reactants in the solvent(s).
- (iii) Concentration of water and the sequence of addition.
- (iv) pH of reaction medium, or the presence of other catalysts influencing hydrolytic polycondensation.
- (v) Time and temperature of reactions.

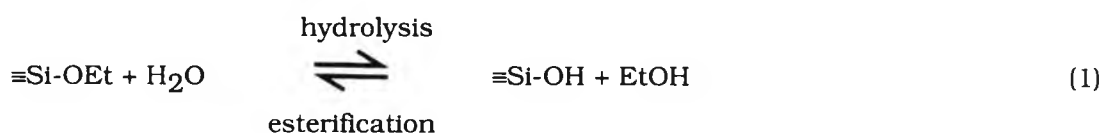
For the simpler single oxide systems such as TEOS:H₂O:EtOH [TEOS ≡ Si(OC₂H₅)₄ ≡ tetraethylorthosilicate, EtOH ≡ C₂H₅OH ≡ ethanol], the most important factor in producing an homogenous solution is the solubility of the reactants. Water and TEOS are essentially immiscible, hence the need to use EtOH. But even in the ternary system described, there is a large liquid-liquid immiscibility zone. As a rule of thumb, equal volumes of TEOS and EtOH normally lead to complete dissolution of all the components involved, though the amount of solvent used has a significant affect on the final gel properties. Miscibility is also affected by the pH of the system.

Although it may be possible to detect if certain compositions of components are immiscible, some forms of inhomogeneity are readily observable. For example, in multicomponent systems the reactivity of the individual metal oxide forming species is very crucial. Brinker¹⁰⁶ suggests that the reaction of mixed alkoxides can be achieved by the partial hydrolysis of the metal alkoxides and their sequential addition in the inverse order of their corresponding rates of

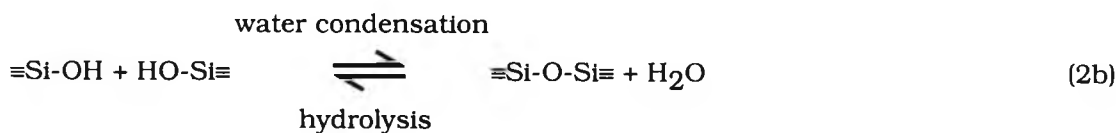
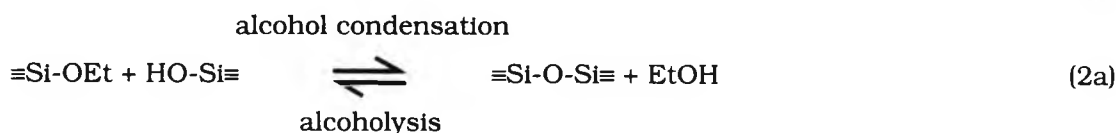
reaction. This is in order to avoid hydrolysis and polymerisation of the more reactive species independently of the rest of the reactants which can lead to precipitation and inhomogeneities at the solution stage. There is also evidence¹⁰⁷ that phase separation can develop in initially homogenous solutions when hydrolysis is carried out under basic conditions. In our work, it was decided not to focus on multicomponent systems partly because some of the difficulties mentioned were also experienced.

6.1.4 HYDROLYSIS AND CONDENSATION

The sol-gel reaction is generally represented as partial hydrolysis of a metal alkoxide $M(OR)_n$, where M is a metal ion and R is an alkyl group. For example, if $M = Si$ and $R = Et$ then,



This is immediately followed by polymerisation:

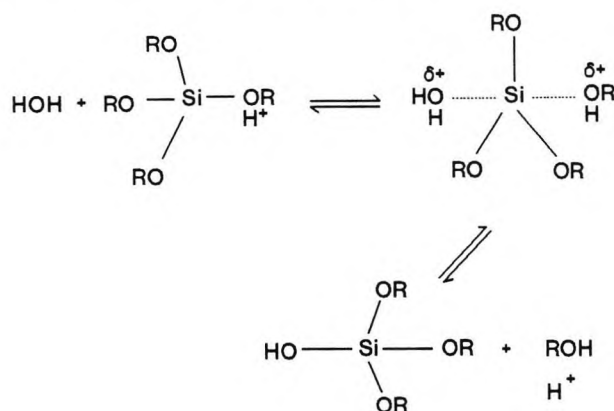


The hydrolysis and condensation polymerisation reactions proceed concurrently. As soon as a silanol group is formed (equation 1) it can react with either ethoxy groups (equation 2a) or other silanol groups (equation 2b). As long as at least 2 moles of water are present per mole of alkoxide the polymerisation reaction will propagate itself and eventually reach a point of gelation. The way in which the oligomers continue to grow depend on many parameters including solvent concentration, pH of the system, water content, processing conditions and environment. When all these effects have to be considered it is evident that generalisations concerning sol-gel parameters can be difficult.

6.1.4.1 HYDROLYSIS

The mechanisms for the hydrolysis of a silicon alkoxide have been widely investigated and depend on the reaction conditions¹⁰⁸. Possible pathways under acidic and basic conditions are given in figure 6.2.

(A) Acid catalysed hydrolysis of silicon alkoxide¹⁰⁸



(B) Base catalysed hydrolysis of silicon alkoxide¹⁰⁷

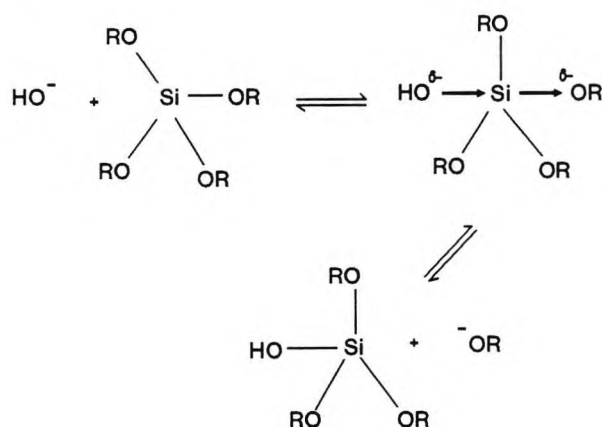


Figure 6.2 Acid- and base- catalysed mechanisms for hydrolysis of a sol-gel mixture.

Consistent with these mechanisms, under acidic conditions, an alkoxide oxygen atom is protonated by H^+ or H_3O^+ in a rapid first step and electron density is withdrawn from silicon atom making more susceptible to attack by water (figure 6.2a). The rate of reaction will not be particularly sensitive to the inductive effect of other groups bonded to the silicon since the flow of charge will be predominantly from the protonated alkoxy to the water molecule. The ease with which electrophiles can approach the silicon complex, on the other hand, will significantly influence the rate of reaction and so steric factors will exert the greatest effect on the hydrolytic stability of the organoxsilanes.

Under basic conditions, water dissociates to produce a nucleophilic hydroxyl anion in a rapid first step. The hydroxyl atom then attacks the silicon atom. Because the silicon atom acquires a formal negative charge in the transition state (figure 6.2b), this mechanism is quite sensitive to inductive as well as steric effects. Electron withdrawing groups ($-OH$ and $-OSi$) should help

stabilise the negative charge on silicon and enhance the hydrolysis rate, whereas electron providing substituents should decrease the rate (figure 6.3).

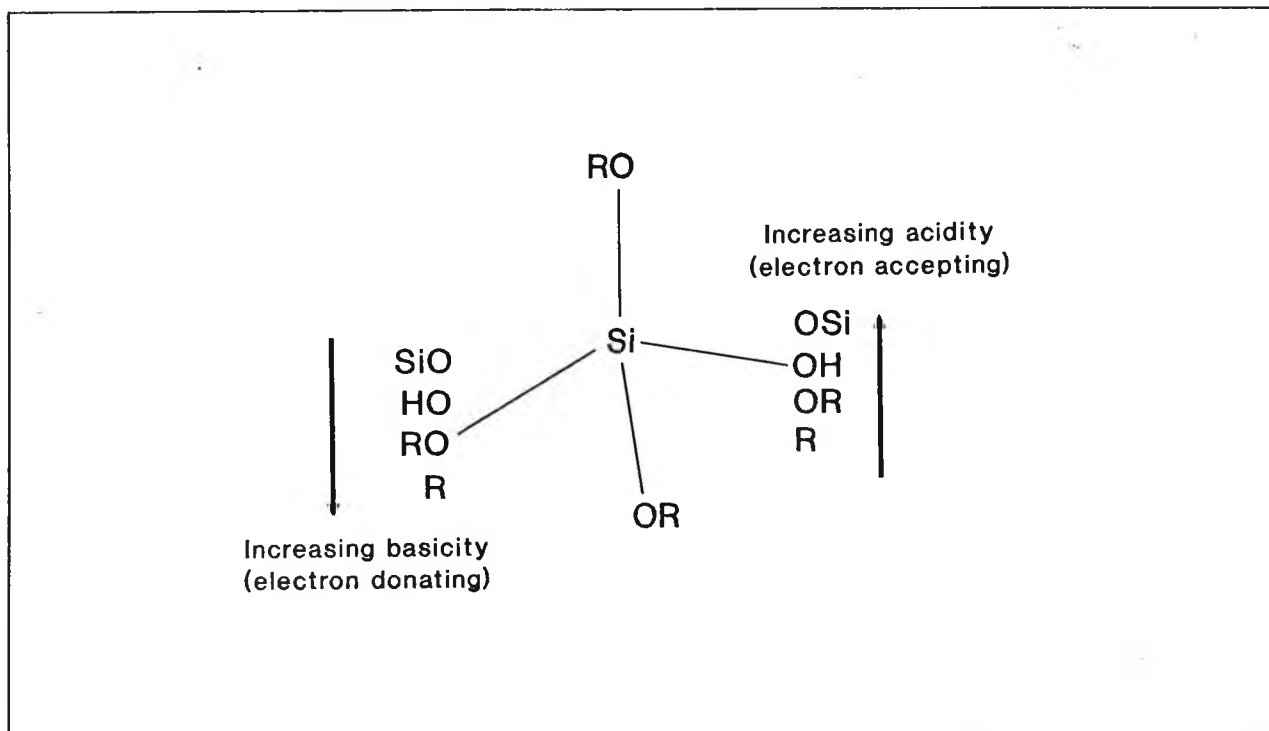


Figure 6.3 Inductive effect of substituents on the silicon atom¹⁰⁸.

6.1.4.2 POLYMERISATION

The most widely accepted mechanism for the condensation reaction involves the attack of a nucleophilic deprotonated silanol on a neutral silicate species:-



This reaction pertains above the isoelectric point of silica (pH ≈ 2.5) where surface silanols may deprotonate according to their acidity. The acidity of a silanol group depends on the inductive effect acting on the silicon atom. When -OR and -OH are replaced with -OSi during the condensation reaction, the reduced electron density on the Si increases the acidity of the remaining silanol protons. Depending on whether the reaction takes place in basic or acidic environments, this will affect how the polymer grows.

6.1.4.3 INFLUENCE OF CATALYST AND pH

Changing the catalyst can have a large influence on the microstructure of the gels formed as well as on the rate of the gelation process. The most commonly reported catalysts are HCl and NH₄OH and it is these two which have been incorporated in the bulk of our experimental work. Due to steric and inductive effects it can be reasoned that under acidic

conditions the rate of hydrolysis decreases with each subsequent hydrolysis step, whereas under basic conditions, the increased electron withdrawing capabilities of -OH and -OSi compared to -OR may establish a condition in which each subsequent hydrolysis step occurs more quickly as hydrolysis and condensation proceed. As a result, in the acid catalysed reaction, condensation is likely to occur before the monomer is fully hydrolysed and the resulting polymer will tend to be lightly cross-linked i.e. primarily linear. In the base catalysed reaction, however, the hydrolysis of the alkoxide molecule tends to go to completion so that the condensation between deprotonated and protonated silanols of the fully hydrolysed monomer will result in a more densely cross linked polymer giving rise to branched clusters. Porosity is one property which can be controlled by the appropriate choice of pH¹¹⁰.

6.1.4.4 INFLUENCE OF SOLVENT

The solvent most commonly reported in sol-gel work is ethanol (EtOH) although studies have also been carried out using so-called drying chemical control additives (DCCAs). The influence of the solvent is important not only because it can take part in the reverse of reactions 1 and 2 but also because its removal during drying determines to a great extent the final morphology of the gel. Esterification (the reverse of hydrolysis) is promoted by large quantities of alcohol under acidic or basic conditions. Therefore hydrolysis may go to completion, but the resulting gel may have a large quantity of SiOR produced during aging and drying of the gel. The retained organics cause difficulty during the heat treatment of the gel and normally it is advantageous to use excess water during hydrolysis. It may also be beneficial to use a solvent, such as tetrahydrofuran, that is not a reactant, although the ability to remove successfully this solvent would also have to be considered. In the present situation, where subsequent reaction to the polymer network is of interest, the presence of alkoxide groups may not be such a disadvantage since they may provide reaction sites which are more suitable than silanols. For example, FITC (the sensor reagent) will react more rapidly with alkoxides than with water or alcohols⁸².

A second and important effect of the solvent is its ability to promote depolymerisation, by the reverse of the equations 2a and 2b. Iler⁸⁸ suggests that under conditions in which depolymerisation is suppressed, condensation may lead to molecular networks, whereas conditions in which depolymerisation can occur allow restructuring ultimately resulting in colloidal sols.

The vapour pressure of the solvent has an important effect on the time required to gel and on the surface area of the resulting gel. When the vapour pressure is low, the solution gels with a larger amount of liquid, so the dried gel has a more open structure.

6.1.4.5 INFLUENCE OF WATER

A high water concentration favours hydrolysis and inhibits condensation (equations 1 and 2b respectively). Therefore, even under acidic conditions, excess water favours hydrolysis and a higher cross link density. Similarly, when the water concentration is low, even at high pH, the condensation may begin before hydrolysis is complete, resulting in more linear structures.

The ratio $R=H_2O/alkoxide$ is one of the most important factors controlling the structure of the gel. The rate of hydrolysis decreases as R increases in acid catalysed tetramethoxyorthosilicate (TMOS) solutions, but the rate increases with R with a basic catalyst. Increasing R also reduces the amount of retained organics in the dried gel since, as mentioned above, it inhibits esterification.

6.1.5 STRUCTURAL EVOLUTION: GELATION AND AGING

The sol-gel transition is usually determined by inspection, for example by noting the point at which cessation of flow occurs. Viscosity is often used as a more quantitative method for determining the gel point, although since no arbitrary values have formally been stipulated as being indicative of the gel point, the use of this parameter is still somewhat subjective. The time-to-gel and the change of viscosity with time is affected by many of the reaction parameters. For example, in acid-catalysed systems low-water concentrations result in a gradual increase in viscosity before losing fluidity, while high water concentrations lose fluidity more abruptly at lower viscosity¹¹². The concentration of TEOS with ethanol, and the R ratio also have a very marked effect. Normally, a higher TEOS concentration leads to a shorter gelation time. Interestingly, the relationship of time to gel versus R exhibits a minimum time for $R=2$ to 4. This can probably be explained in terms of the reverse reactions as discussed above.

The sol-gel transition is reached when the one-phase liquid becomes a two-phase alcogel that can be transformed into a two-phase xerogel or aerogel of a solid and a gas. The transition is irreversible and occurs with no change in volume. (An *alcogel* is a gel in which the pores are filled with alcohol (an *aquagel* is one whose pores are filled with water). A *xerogel* is a gel from which the liquid medium has been removed in such a way that the gel structure is compressed and the porosity is reduced. An *aerogel* is a special type of xerogel from which the liquid has been removed by autoclaving the gel above the critical point of the liquid. This prevents any collapse or change of structure of the gel.) Although the sol-gel transition point is an important indication of the extent of the reaction, it is by no means the end of the gelation process as a whole. Furthermore, the time to gel is influenced by many physical as well as chemical parameters. For example, the gel state can be achieved in both open and closed systems but with different end properties. In a closed system, the gel is formed

within the mother liquor. This leads to the observation of phase separation since the gel normally shrinks from the sides of the container, but we have found even this phenomenon is composition dependant. Klein¹¹² speculates that the gel polymer loses its solubility in the water-ethanol solvent once all of the sites prone to reaction have been used consumed. In an open system, the removal of solvents forces the monomer and polymer species into closer proximity, resulting in a much shorter gelling time and a quite different rheological behaviour¹¹³. Consequently, phase separation under this condition, is less likely to be observed. Figure 6.4 illustrates the difference between open and closed systems.

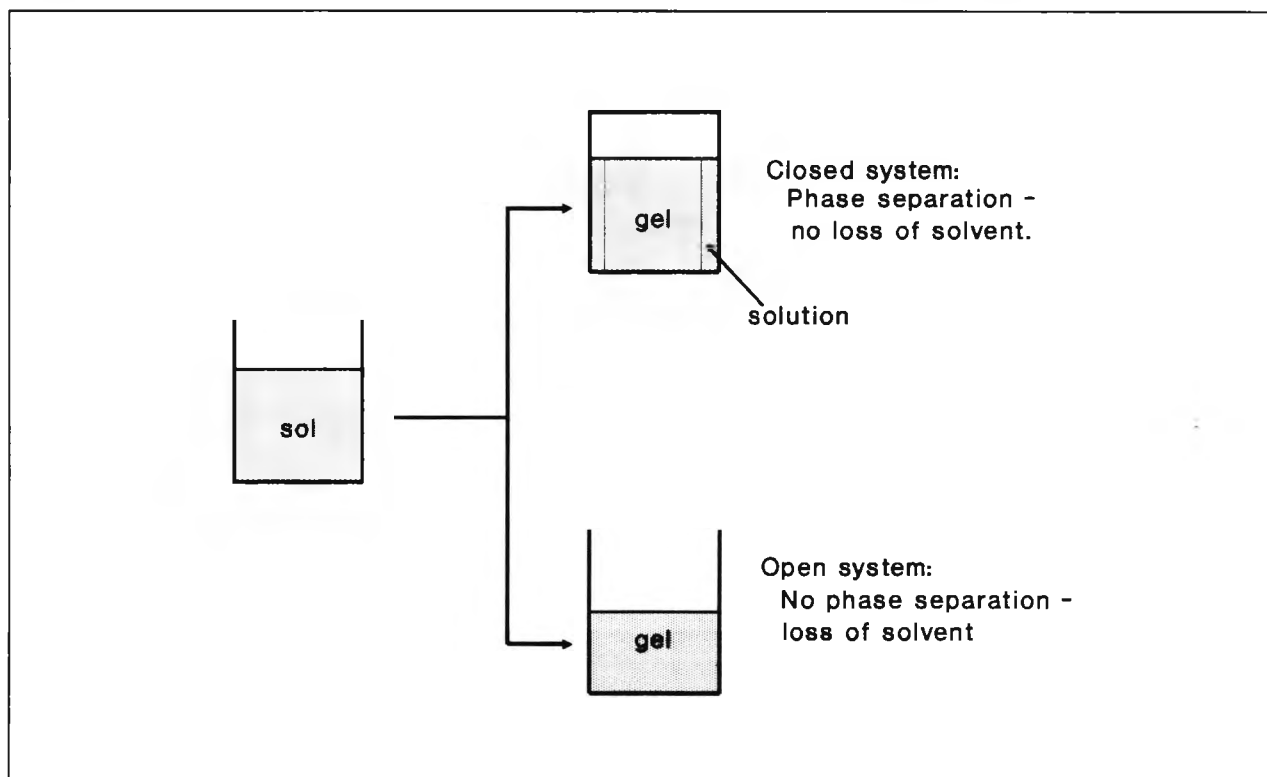


Figure 6.4 Gelation in open and closed systems.

Aging is the term used to indicate the on-going hydrolysis and polymerisation reactions in a sol-gel system both before and after gelation has taken place. During aging, the gel structure is evolved and much work has been carried out in an attempt to model this process. Some of the mechanisms that have been reviewed include treating the system with percolation theory, molecular orbital calculations and molecular dynamic simulations¹⁰⁷. Work is also referred to which considers aspects of fractal modelling to describe the structures which evolve during the polymerisation of acid or base catalysed systems. The reason it is important to consider at least the conclusions of these investigations is that for the sensor substrate produced to be suitable it must have a porous structure which is accessible to the analyte of interest. The structure of the evolving species ultimately forms the back bone of the gel and, as has been demonstrated earlier, the evolution of this structure is dependent on many chemical and physical parameters.

6.1.6 DRYING OF GELS

In many preparations, the removal of solvents from a wet gel is the stumbling block which has prevented sol-gel processing achieving wide commercial application. The method of drying is influenced by the intended use of the dried material, so that bulk monoliths require much more careful approaches than, say, powders. Cooper (referred to in reference 109) finds that permissible drying rates, consistent with the avoidance of fracture, vary inversely with the thickness of the body being dried. In order to prepare a suitable substrate for our sensor reagent, a strong and essentially coherent porous network is required onto which the reagent can be immobilised in a manner in which it will be accessible to the analyte. Consequently it is important to consider how drying effects the morphology and microstructure of the gels.

During the evaporation of the liquid from the gel, large capillary stresses develop in the pores as a result of the small pore size and these can lead to cracking. Scherer¹¹⁴ presents a model that shows that the stress is proportional to the drying rate and to the thickness of the gel; larger pores and a stiffer network are shown to reduce the stress and hence the amount of cracking.

As liquid evaporates from the surface of the gel, the solid-liquid interface is replaced by a solid-vapour interface. Since the energy of the latter is greater than that of the former, the liquid tends to spread over the exposed area. In so doing, tensile stress develops in the liquid and compressive stress is imposed on the solid phase. The magnitude of this stress depends on the difference in interfacial energies and on the specific surface area of the solid phase. If the gel network has a significantly low viscosity, then the stresses which develop will be correspondingly low since the contraction rate of the solid will more easily match the rate of liquid evaporation. A high contraction rate readily leads to cracking, especially if it is anisotropic. Also, if the rate of evaporation is high, or the permeability of the gel is low (so that flow through the pores is difficult), then the exterior of the gel will contract faster than the interior and differential stresses will result. This leads to such phenomena as the warping of a slab of gel and cylindrical gels with smaller radii at one end, both of which we have observed. It also leads to cracking.

The rate of shrinkage of a gel depends on the pressure in the pore liquid, and the pressure distribution depends on the shape of the gel. The stress decreases in the order: plate > cylinder > sphere > film. Basically, the stress is proportional to the evaporation rate and the size of the body, and inversely proportional to the permeability and the bulk modulus ('stiffness'). So, according to this model, in order to prepare a gel monolith the solvent evaporation should be controlled (i.e. slow) and the pore size and hardness of the gel should be maximised.

The use of *drying control chemical additives* (DCCAs) has been shown to lead to the formation of larger pores and smaller pore size distributions^{115,116,117}. Not only does this result in a more reliable method of monolithic gel preparation, but it may also be important in the preparation of a sensor substrate which will afford a relatively fast response time. For this reason the use of DCCAs has been investigated in our experiments.

The danger of cracking during drying can be avoided if the gel is subjected to hypercritical drying to produce *aerogels*^{118,119}. In this method the gel is heated above the critical temperature and pressure of the liquid phase (which for ethanol, for example, is 243°C and 63 atm), at which point there is no interface between the liquid and vapour phases. The vapours are then removed rapidly by venting. The gel dries without significant shrinkage, so that the dried body has a similar volume as the starting wet gel. Silica aerogels produced in this manner are highly porous and have very low densities. Until recently, hypercritical drying was used to prepare powders, but it can now be used to make pieces as large as tens of centimetres. After some initial work we decided not to pursue the route of hypercritical drying because of the specialised equipment which is involved, but given the wide ranging possibilities for this technology it cannot be ruled-out as a potential route to preparing porous substrates for sensors.

6.1.7 HEAT TREATMENT OF DRIED GELS

This section will review aspects of the gel-glass transition. As has been indicated the structure of the dried gel depends very much on the physical and chemical parameters used in its preparation. Generally though, the gel can be thought of as a porous silica body, with some alkoxide residue but mainly a hydroxylated surface. Nitrogen adsorption analysis of gel surfaces have often revealed bimodal pore size distributions. These have been attributed to aggregation of clusters, producing large pores between, and small pores within, the clusters. There is evidence that this porosity is continuous^{114,120} a fact which is of fundamental importance in preparing a useful substrate for sensor applications.

High R ratios reduce the amount of retained organics by promoting the hydrolysis of the alkoxide groups (see earlier discussions) which consequently facilitates drying. Depending on the nature of the gel and conditions of formation, any of the following reactions may occur during the thermal treatment prior to sintering and densification:

1. decomposition of salts
2. carbonisation or combustion of residual organic groups
3. desorption of absorbed solvent from the walls of the micropores
4. dehydration (polymerisation)

5. formation of micropores or even foams from gas generation
6. beginning of collapse of micropores

As in the drying step, if particulate materials are desired, no special attention need be exercised to prevent fragmentation during subsequent thermal treatment although even in these cases, care must be taken to avoid undesirable bloating, foaming or blackening. If monolithic structures are desired, special care must be taken to ensure the complete removal of water or organic groups or decomposition products prior to micropore collapse to avoid discoloration and the development of stresses leading to fragmentation.

Typical differential thermal analysis and thermal gravimetric analysis of a dry gel is shown below.

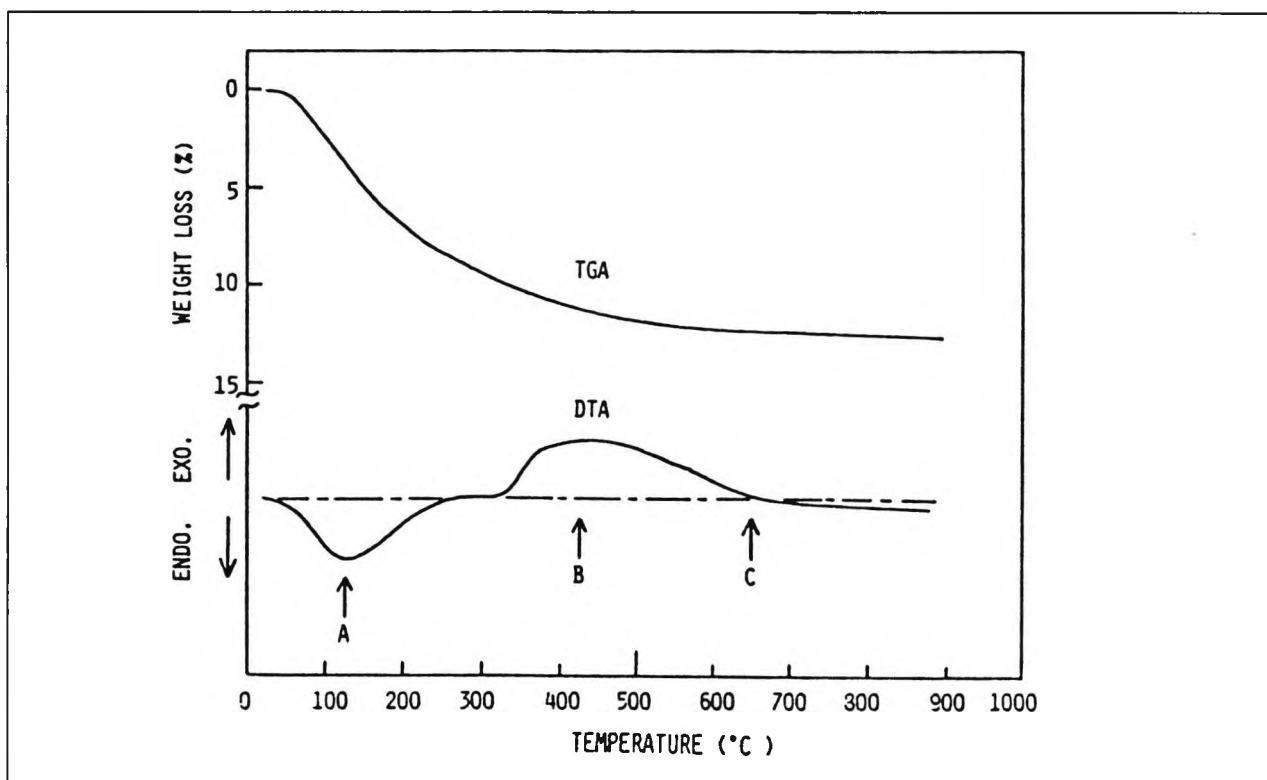


Figure 6.5 TGA and DTA of a dry gel¹²¹

The endotherm at around 100°C (peak A) is attributable to the desorption of water and alcohol from the micropore walls of the gel and the exotherm at B represents combustion of the residual organics. This latter peak is much sharper if the analysis is made under the flow of oxygen gas¹²³. The gradual deviation starting at around 600°C (C) is caused by the release of water generated by the dehydration condensation of silanols. The evaporation and oxidation reactions evolve a large volume of gas. Consequently, not only must heating rates to these temperatures be slow in order to avoid build-up of pressure inside the gel (typically 1°C min⁻¹), the heating schedule must also include isothermal temperatures in order to allow the completion of certain reactions.

For the purpose of developing a suitable substrate for FOCS, the complete sintering of the gel is not desired since there is a dependence on its porosity to provide the area onto which to immobilise the sensor reagent. In fact, as will be discussed later, it may not even be necessary to remove the residual alkoxides. This would present a novel approach to the derivatisation of gels. However, some understanding of the chemical and structural changes which occur during the sintering of dry gels is essential since many of our prepared gel samples have been found to be unstable when immersed in water. This would indicate that these silica structures were not strong enough to withstand the pressures which develop during the penetration of water into the porous structure. Partial sintering may help to overcome this problem. During sintering, further shrinkage and densification of the gel occurs as a result of the collapse and elimination of pores. The temperature used for this stage of the process depends on the size distribution of residual pores (lowest for the smallest) but is always usually below the glass transformation temperature (T_g) and the temperatures used for conventional melted glass. This aspect of low temperature processing has been one of the strongest driving forces in sol-gel research.

6.2 EXPERIMENTAL INVESTIGATION OF SOL-GEL FORMATION

6.2.1 PRELIMINARY INVESTIGATIONS

Preliminary work is reported which indicated that it is possible to derivatise FITC onto the glass-like structures produced by the sol-gel method. The effect of the main reaction components in the preparation of sol-gel monoliths was investigated and so was the use of drying controlled chemical additives. The preliminary work was used as a basis for preparing monoliths and coatings which contain FITC.

6.2.1.1 PREPARATION OF DERIVATISED SOL-GEL GRANULES

(a) Objective

To confirm that porous glass-like granules could be prepared by using the sol-gel method and to determine if it were possible to immobilise FITC onto their surfaces.

(b) Experimental Procedure

A gel of target composition 100 % silica was prepared by dissolving TEOS (50 cm^3) in ethanol (60 cm^3) and then adding a stoichiometric excess of water (60 cm^3 acidified with conc. HCl to

pH2). The mixture was stirred vigorously and heated uncovered at 60°C until all the liquid component had been consumed or evaporated and glass-like granules remained.

Some of the glass-like gels that were formed were further heat treated. The temperature schedule for the heat treatment was as follows: ramp from room temperature at 10°C min⁻¹ to 400°C; hold at 400°C for 2 hours and then ramp at 3°C min⁻¹ to 750°C; soak at this temperature for 15 minutes and then power off and allow to cool to ambient conditions. Specific surface area measurements (Micrometrics Surface Area analyser) were carried out on both thermally treated and untreated granules.

In order to assess whether it was possible to immobilise FITC to the granules formed by the sol-gel process, the same two-step procedure was used that has already been described for the derivatisation of commercial porous glass: silylation was effected by gently warming the samples overnight in a 1% solution of 3APTS in dry toluene after which the samples were filtered and washed in turn with MeOH, H₂O, MeOH, H₂O, MeOH and EtOH and then dried in an oven at 80°C for 8 hours. To each sample was added 50 cm³ FITC solution (22.7 mg FITC in 500 ml pH7 buffer solution) and these were left standing for about 15 hours prior to filtering and washing with water. The effect of water was noted and the fluorescence of the granules was compared with that of commercial porous glass which was derivatised at the same time.

(c) Results and Discussion

After 3 hours at 60°C the alkoxide mixture had become so viscous that the magnetic stirrer could no longer turn and so it was switched off. After 6 hours, most of the mixture had gelled though some liquid still remained. At this stage the mixture was still clear. After 21 hours the gel appeared dry.

In a previous preparation, the stirrer had not been switched off and glass like-granules had formed which were mainly in the order of 3.5 mm in diameter. The particles did not crumble into powder when subjected to manually applied pressure and possessed an optical transparency which ranged from fairly good to poor. Where the stirrer had been disconnected, larger pieces (≈1 cm) had formed. On closer inspection, however, these larger pieces were seen to be in reality a cluster of smaller granules which were readily separated by gentle pressure.

When the samples were covered with water they underwent violent fragmentation. Viewed under an optical microscope (x 25 magnification), it was observed that on exposure to water small bubbles formed around the granules prior to an audible fragmentation taking place. This effect suggests that the material was highly porous and that the capillary forces which developed when water was absorbed into its structure were sufficient to cause the granules to literally 'explode'. The programmed temperature schedule was designed with the intention of strengthening the gel structure by initiating a gel to glass transition. After the treatment, a few granules had become very discoloured, almost black. When viewed under the optical microscope it was possible to confirm that the discoloration originated from within the granules and not on their surfaces. The blackened granules tended to be the smaller ones and it may be that in their cases the porous networks collapsed at temperatures lower than 400°C, leaving isolated pores. Any remaining organic material that would subsequently be converted to carbon would then be trapped and would result in the observed discolouration.

The thermal treatment did not affect the general shape of the glass-like granules, although some shrinkage did appear to have occurred. On the other hand, the vast majority of the heated glass-like granules were slightly clearer than the unheated ones and were also much harder to break.

The effect of wetting with water was also studied. Of three unheated granules which were covered with a drop of water, two cracked within 30 seconds. The third also developed a few bubbles on its surface but did not crack or break apart. Of three heated pieces, two developed flaws but none developed many bubbles and none actually fragmented.

Surface area analysis of the heated and unheated granules gave values of 86.4 m²g⁻¹ and 99.7 m²g⁻¹ respectively. The decrease of surface area with thermal treatment is consistent with the findings of other workers¹²³ but much higher values for the specific surface areas have also been reported¹²⁰.

Both heated and unheated glass granules were derivatised with FITC. After the silylation stage, the unheated glass granules had changed from being clear to white and opaque. When reacted with FITC overnight, they adopted an uneven orange-brown colouring and no fluorescence could be detected when viewed through an optical microscope with appropriate filters. Other than a slight reduction in the average size of the pieces, the heated granules had not undergone a similar transition. Instead, quite evenly coloured, clear granules had been formed. A little fluorescence was detected but this was very slight when compared with derivatised commercial porous glass. The different behaviours of the heated and unheated gel fragments cannot be directly accounted for, although one possible explanation is that residual adsorbed water molecules in the latter caused the 3APTS to polymerise. Not only would this explain for the opaqueness which developed, it would help explain why the FITC was unevenly and inefficiently immobilised.

(d) Conclusions

These initial investigations of the sol-gel process indicated that it was possible to prepare porous glass-like granules without using any specialised equipment and at relatively low temperatures. Furthermore, it was also shown that a chromophore such as FITC could be attached to the surface of these granules, although with much less success than with commercial porous-glass.

6.2.1.2 PREPARATION OF DERIVATISED SOL-GEL COATING

(a) Objective

To coat a microscope slide with a porous silica layer and to subsequently derivatise this porous layer with FITC and compare it with untreated glass slides. At this stage, no attempt was made to optimise the solution or processing conditions.

(b) Experimental Procedure

Standard microscope slides were washed with detergent, dried and then immersed in a 1:1 (v/v) mixture of $\text{H}_2\text{SO}_4:\text{HNO}_3$ (stirred) for about 20 minutes. The slides were then flushed and rinsed with distilled water before finally drying at 90°C .

The metal alkoxide solution was prepared as in the previous case using TEOS (50 cm^3), EtOH (60 cm^3) and water acidified with HCl (60 cm^3). The mixture was stirred vigorously for a few minutes at 40°C until all components were completely dissolved. Four slides were coated to half their length (plus one blank). The slides were simply dipped slowly into the solution and

removed. Where drying was used, this was at 70°C in a convection oven. The following coating methods were used:

Table 6.1 Sol-gel coating methods.

Slide	Procedure
1	Single dip
2	3 dips + drying between each dip
3	5 dips + drying between each dip
4	5 dips + no drying between each dip
5	Blank (no coating applied).

The five slides were transferred to an oven and heated at 300°C for 16 hours and then at 400°C for a further 4 hours.

FITC was immobilised onto the coated glass slides using the method previously described for the glass-like granules.

(c) Results and Discussion

The first dipping resulted in evenly wetted slides. After 1 hour of drying at 70°C, slide 1 had developed a thin-layer iridescent coating. Patches of the coatings exhibited some flaws which when viewed under an optical microscope revealed themselves to consist of a complex array of channels and patterns.

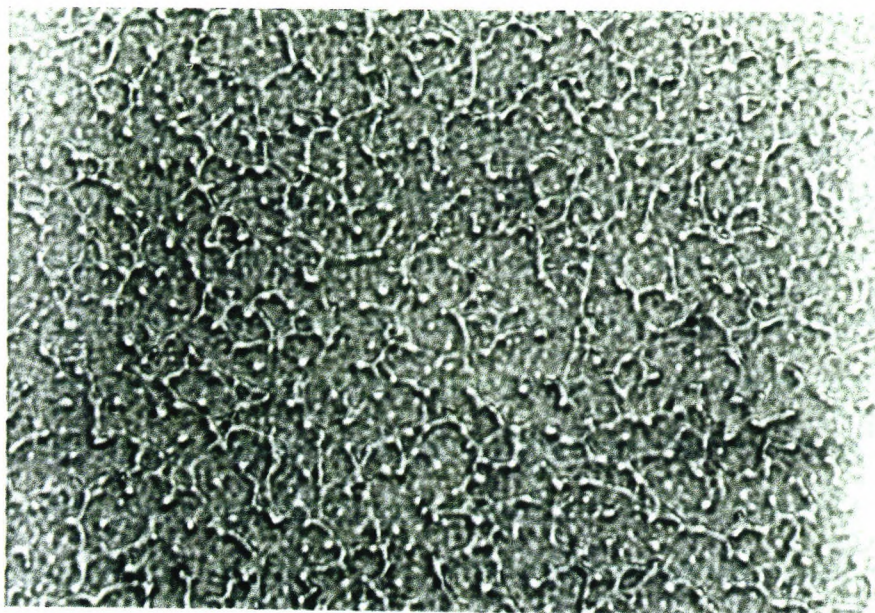


Figure 6.6 Photograph show patterns on sol-gel coated slides.

This effect is known as *crazing*. Careful observation of these patches also indicated the presence of some very fragile glass-like fibres ($\approx 0.05 - 0.5$ mm) which were easily removed.

The second and third slides both became increasingly opaque and patchy after repeated dips. Slide 4 was even more flawed and when observed under the optical microscope ($\times 40$ magnification) it was very clear that a thin coating had not been formed. Instead the surface resembled that of (clear) cracked and flaking paint. Fibral structures similar to slide 1 were also present, but to a much greater degree. The heat treatment did not significantly alter the appearance of the slides other than reduce their slight opacity somewhat.

The slides were silylated using 3APTS and then immersed in FITC solution overnight. The slides were rinsed and wiped to remove any loose particles. The following observations were noted.

Table 6.2 Appearance of sol-gel coated slides.

Slide	Observation
1	Overall brown tinge. Some patchy areas. Iridescence indicating optically thin film.
2	A lot of material removed during the wiping stage indicating that the heat treatment did not sinter the surface glass fibres. Still patchy, but overall more material remained than in slide 1.
3	As for 2. Slightly more material remaining.
4	Practically all surface material removed during wiping. No iridescent behaviour.
5	Clear brownish tinge. Very similar to slide 4.

Absorption spectra recorded of the sol-gel coated and uncoated areas of the slide are shown in figure 6.7.

The absorption peaks in the lower curve are due to the immobilisation of FITC directly onto the glass slide, whereas a much more intense absorption resulted through the derivatised sol-gel coating. Coatings produced by multiple dips did not result in significantly greater absorption maxima.

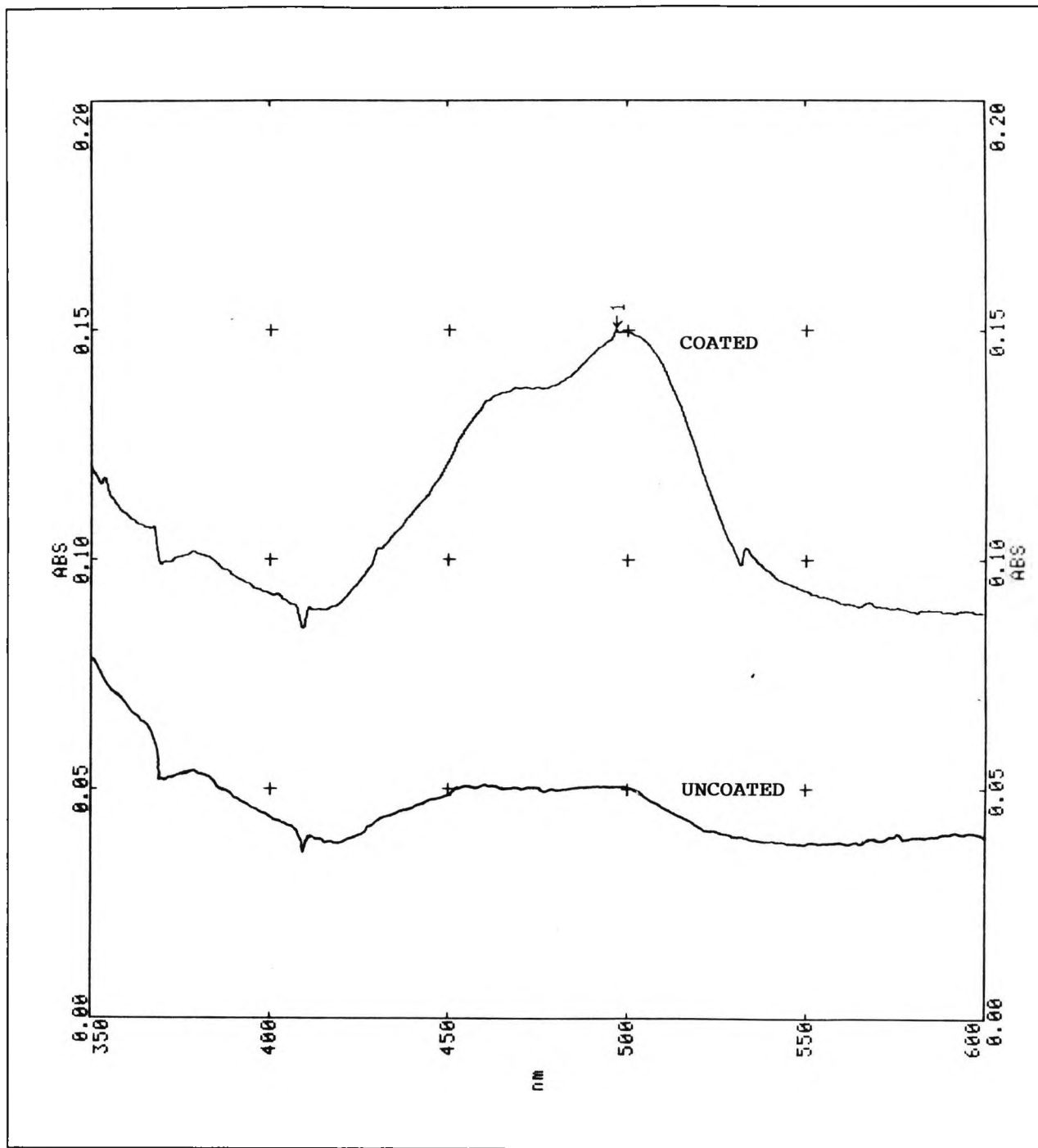


Figure 6.7 Absorption spectra of glass slides through sol-gel coated and uncoated areas.

(d) Conclusions

Although no measurements were made to quantify the coating thickness, the iridescent properties coupled with the areas of obvious patchiness did seem to give the clear impression that the quality of the coated layers was generally poor. Two possible reasons for this are (i) the dipping velocity was haphazard and variable, (ii) the metal oxide mixture was not allowed to age at all which meant that the viscosity was probably much too low to form coatings of appreciable thicknesses.

Notwithstanding these shortcomings, these preliminary investigations did indicate that thin films could be prepared using the sol-gel approach (as in slide 1) and that these films could be subjected to the outlined derivatisation procedure. On the other hand, since one of the overall aims was to prepare relatively thick porous glass-like coatings, the approach described above was not extensively pursued any further.

6.2.1.3 PREPARATION OF SOL-GEL MONOLITHS

(a) Objective

To investigate the influence of the main reaction components in the preparation of monoliths by the sol-gel process.

(b) Experimental Procedure

The preparation of gel monoliths using the ternary system TEOS:H₂O:EtOH was investigated using the compositions indicated in Table 6.3. Three sets of samples were produced, under acid, basic and neutral conditions. The sols were placed in glass vials, sealed and allowed to age first at room temperature and then at 60°C. The gels were dried slowly by piercing an ever increasing number of 1 mm holes in the seals. In some cases where monoliths did develop, they were subjected to subsequent thermal treatment. Observations were made over a period of 25 days.

Table 6.3 Compositions of sol-gel mixtures.

Sample	Molar Ratios (wrt TEOS)			Molar Fractions		
	TEOS	H ₂ O	EtOH	TEOS	H ₂ O	EtOH
1	1	1	1	0.33	0.33	0.33
2	1	5	1	0.14	0.71	0.14
3	1	10	1	0.08	0.83	0.08
4	1	15	1	0.06	0.88	0.06
5	1	20	1	0.05	0.91	0.05
6	1	1	4	0.17	0.17	0.67
7	1	1	8	0.10	0.10	0.80
8	1	5	4	0.10	0.50	0.40
9	1	5	8	0.07	0.36	0.57
10	1	10	4	0.07	0.67	0.27
11	1	10	8	0.05	0.53	0.42
12	1	15	4	0.05	0.75	0.20
13	1	15	8	0.04	0.63	0.33
14	1	20	8	0.04	0.80	0.16
15	1	20	8	0.03	0.69	0.28

If a catalyst was employed, the molar ratio of catalyst:water was 0.01 (HCl for acid, NH_3 for base). The reactants were weighed-out into the vials in the order TEOS, EtOH and catalysed water. The mixture was stirred vigorously and if miscibility was good the samples were stored at room temperature for the first 18 hours. Otherwise the solutions were placed in an ultrasonic bath. A 'fair' solubility was noted if a clear solution was produced after a half hour of ultrasonic agitation. Miscibilities were deemed as 'poor' if only an emulsion could be formed, and as 'very poor' if not even that was possible after about an hour. Where clear solutions were not produced within this time period, the samples were kept in the ultrasonic bath overnight.

(c) Results and Discussion

Table 6.4 summarises the observations for the three sets of sol-gel preparations. In some instances, the vapour pressure which developed during the drying of the gel led to a breaking of the seal and a rapid loss of solvent. This may have caused some samples to fragment unnecessarily, nevertheless, gels were more likely to remain uncracked if prepared using high concentrations of water and ethanol.

It was found that high water contents resulted in shorter gelation times although, as has been previously mentioned, the shortest times probably occur when the water:TEOS ratio is between 2 and 4.

The choice of catalyst has the most significant effect on the final structure of the gel. Acid catalysed system, and to a lesser extent mixtures in which no catalyst was used, resulted in clearer, more monolithic gels than those prepared using the base catalyst. The latter tended to begin by forming particulate suspensions, which on aging occasionally formed very friable gel-like structures. Basic catalysed solutions led to particulate or cloudy suspensions. Some of these mixtures (7,8,11,12,15) subsequently formed coherent structures, that is, they gelled. Solutions in which no catalyst had been incorporated had initially given indications of the shortest gelation times. In fact, none of these mixtures formed a gel monolith, although some did produce clear dry gel fragments. Acid catalysed solutions led to the clearest gel monoliths and fragments. In all the cases which formed monoliths which essentially retained the shape of the containers (9,10,11,14,15), distinct two-phase systems had developed in which the solvent was expelled from the gel network. This had not been observed for the high pH samples. This difference may be due to the particulate versus linear-type structural evolutions that were discussed earlier. The pH of the mixture also greatly effects the miscibility. Generally, it was found that the degree of solvation increases with decreasing pH when comparing solutions of similar compositions.

Table 6.4 Influence of reaction parameters on sol-gel system.

(a) Uncatalysed

H ₂ O:TEOS	Samples	Initial Miscibility	Time to Gel ^a	2 Distinct Phases	Clarity of Gels	Cracking of Gels
1	1,6,7	v.poor at low [EtOH]	long	no	good	yes
5	2,8,9	v.poor at low [EtOH]	short	yes	fair	yes
10	3,10,11	v. poor at l/med[EtOH]	short	yes	fair/poor	yes
15	4,12,13	v.poor	short	yes	fair	yes/no ^b
20	5,4,15	v.poor	short	yes	poor	yes/no

(b) Acid Catalysed

H ₂ O:TEOS	Samples	Initial Miscibility	Time to Gel	2 Distinct Phases	Clarity of Gels	Cracking of Gels
1	1,6,7	good	v.long	no	good	yes
5	2,8,9	fair at low [EtOH]	short	yes	good	yes
10	3,10,11	poor at low [EtOH]	short	yes	fair	no
15	4,12,13	v.poor at low [EtOH]	short	yes	fair	yes/no
20	5,4,15	v.poor low [EtOH]	short	yes	fair	no

(c) Basic Catalysed

H ₂ O:TEOS	Samples	Initial Miscibility	Time to Gel ^c	2 Distinct Phases	Clarity of Gels	Cracking of Gels
1	1,6,7	v.poor at low [EtOH]	v.long	no	v.poor	yes
5	2,8,9	v.poor at low [EtOH]	v.long	no	v.poor	yes
10	3,10,11	v.poor	(v.)long	no	v.poor	yes
15	4,12,13	v.poor	(v.)long	no	v.poor	yes
20	5,4,15	v.poor	(v.)long	no	v.poor	yes

(a) short ≤ 1 week; long ≈ 1 week - 1 month; v.long > 1 month

(b) depended on the volume of EtOH used: higher volume led to less cracking.

(c) particulate suspensions,hence gel point difficult to define

Dried gel monoliths from acid and base catalysed systems were subjected to further thermal treatment at 900°C for 3 hours. Glasses were produced which had undergone significant volume shrinkage. The acid based one was much clearer, but fragmented on immersion in water. The glass/gel produced by basic catalysis was almost completely opaque and stable in water. It was difficult to ascertain whether it had still retained a degree of porosity.

(d) Conclusions

This experiment demonstrated certain differences in the structural evolution of gels which arise from different compositions and catalysts. For the purpose of preparing structures which could find applications in FOCS it was decided to focus on the acid catalysed systems since these readily resulted in clear monolithic structures.

6.2.1.4 USE OF DRYING CONTROL CHEMICAL ADDITIVES TO FACILITATE THE PREPARATION OF GEL MONOLITHS

(a) Objective

One of the most serious problems encountered when one attempts to produce gel monoliths through the sol-gel process is fracture and crack formation during the conversion of wet gel to the dry gel. In the previous set of experiments, the influence of the starting materials was investigated and it was found that acid catalysed systems containing a high H₂O:TEOS ratio were most likely to give coherent, flawless structures. Another approach to facilitate the preparation of crack-free structures is by incorporating so-called drying chemical control additives, "DCCA" (see earlier discussion). The use of DCCA has been shown to lead to larger pores and smaller pore size distributions in the gels produced. These features, coupled with the presence of lower surface tension liquid in the pores at the final stage of drying result in a decrease in the magnitude of the capillary stresses which would otherwise tend to cause the gels to crack. Not only does this result in a more reliable method of monolithic gel preparation, but it may also be important in the preparation of a sensor substrate which will afford a relatively fast response time. The objective of this work was to determine if the use of DCCAs in the system investigated earlier would result in a reduced tendency for the gels to crack.

(b) Experimental Procedure

Based on the work reported in the literature it was decided to use N,N-dimethylformamide (DMF) as the DCCA. The reactants were used in the following ratios:

$$\text{TEOS:H}_2\text{O:EtOH:DMF:HCl} = 1:10:2:1.5:0.1$$

This corresponds to one of the samples (sample 10) referred to in the previous section which resulted in a crack-free gel, except that in this case approximately half of the volume of EtOH was substituted by the DMF.

Five sols were produced as follows. TEOS (16.16 g) and then DMF (8.89 g) were weighed into a plastic beaker and magnetically stirred for about one minute. Ethanol (7.21 g) and acidified water (14.75 g) were added to give a clear mixture. Five sols were also prepared in which the volume of DMF was replaced by ethanol.

Mixing was continued for about 25 minutes and then the sols were transferred into polythene vials which were sealed and placed in an oven at 60°C overnight. By morning, the mixtures had gelled to give two phase systems. The oven temperature was raised to 80°C and the gels allowed to age at this temperature for a further 30 hours. The seals were removed and replaced by aluminium foil which was pierced with five 1 mm holes. The samples were returned to the oven until all the solvent surrounding the gel had evaporated at which point more holes were made in the foil covers. Some gels were prepared in duplicate and these were removed from the oven during the subsequent drying period for closer inspection.

In a separate investigation samples were prepared in the same manner but with varying volumetric EtOH:DMF ratios (1:0, 3:1, 1:1, 1:3, 0:1). These were subsequently subjected to a programmed thermal treatment as follows: 1°Cmin⁻¹ to 120 °C - hold 5 hours; 1°Cmin⁻¹ to 250°C - hold 5 hours; 1°Cmin⁻¹ to 450 °C - hold 5 hours; power-off and allow to cool.

(c) Results and Discussion

After 10 days of drying, 3 of the 5 gels produced using only ethanol showed slight flaws (the others were flaw-free), whereas none of the DMF-based gels exhibited any cracks.

In the separate investigation, mixtures with higher concentrations of DMF gelled first and after about 18 hours, all the samples had gelled. All samples except that containing only ethanol as the solvent consisted of completely uncracked gels surrounded by a liquid phase. The ethanol-only sample was slightly flawed.

The shrinkage rate of the gels during drying was slower the higher the concentration of DMF, although after about 4 days drying all of the gels were more or less the same size. Gels prepared using higher concentration of DMF tended to be less transparent, this could be due to the higher mean pore sizes which arises when using such a DCCA.

A potential disadvantage of using a DCCA was highlighted by the thermal treatment. Following this treatment, only the sample which was prepared without DMF was still clear - all the other

samples had adopted a translucent brown tint, the degree of which increased in line with the original DMF content. The coloration arises as a result of the difficulty in removing all of the DMF prior to the collapsing of the porous network. This effectively traps some of the organic solvent and on combustion discolours the gel. Another major problem that arises using the thermal treatment of gels which have been prepared using DMF is the tendency of the residual formamide to react with the water vapour which will lead to cracking during vitrification. All of the samples were, in fact, cracked. This problem can be circumvented by using organic acid DCCAs, such as oxalic acid¹¹⁵, but for the purpose of the present investigation densification by thermal treatment was not a direct issue and so different types of DCCAs were not studied.

(d) Conclusions

It has been confirmed that the use of DMF as a DCCA enables the preparation of the selected gel compositions in a more reliable manner than with ethanol alone.

6.3 IMPREGNATION OF FITC IN ALREADY FORMED GELS

The sol-gel method was used to prepare gels which were subsequently impregnated with FITC. The use of a silylating agent improved the immobilisation of the dye to the substrate and this significantly reduced the amount of dye which leached from the gel. Nevertheless, dye was lost to the surrounding solution even when a silylating agent was used. The prepared gels were used to obtain fluorescence responses which varied with pH in a manner similar to those obtained for FITC in solution, with an intensity similar to derivatised porous glass but with a response time between 20 to 30 seconds instead of nearly 5 minutes as observed with a previously described configuration using porous glass.

It was found that as the gels became dryer prior to their impregnation with FITC they became harder and more 'glass-like'. If the gels were allowed to dry after impregnation with the dye, however, they would crack and become friable and lose any glass-like qualities. On re-immersion into water the dry gel would fragment and break-down completely.

6.3.1 OBJECTIVE

In preliminary investigations it was found that if aged and partially dried gels were transferred into aqueous solutions of FITC, after a couple of days the dye would completely impregnate the gel and the gel would adopt the characteristic green colour of FITC and clearly fluoresced when illuminated with blue light. Subsequently, however, when the impregnated gel was placed in fresh water it was found that over a period of about 1 week the FITC slowly diffused out of the gel structure into solution. This leaching process was accelerated considerably if the impregnated dye was left to stand under running water. For most of the envisaged applications of fibre optic chemical sensing such a rapid loss of indicator would be unacceptable, so it was necessary to investigate a method in which the dye could be irreversibly bound to the gel network. To this end, it was decided to attempt a two-step reaction similar to the one used to derivatise FITC to porous glass.

6.3.2 EXPERIMENTAL PROCEDURE

A stock solution was prepared as previously described (section 6.2.1.4) with the reactants in the molar ratio TEOS:10H₂O:2EtOH:1.5DMF:0.1HCl. Aliquots of 25 cm³ of the sol were transferred to polythene vials which were sealed and placed in an oven at 80 °C to gel and age. After three days the seals on the first pair of samples were removed and replaced by aluminium foil which was pierced to promote drying. The same procedure was used for the remaining three pairs of samples on consecutive days so that at the beginning of the 5th day the samples had undergone between 4 and 1 days drying. The samples were labelled in the order of drying so that the sample which was set to dry first was labelled "1" and was dried for a total of 4 days. Similarly, the sample which was set to dry last was labelled "4" and was dried for 1 day.

The gels were removed from the vials, immersed in anhydrous DMF, covered with a molecular sieve and left to stand for 2 days with occasional gentle agitation. (This step was performed in order to dehydrate the gels prior to their reaction with 3APTS). One gel of each pair was then transferred into a fresh 1% solution of 3APTS in anhydrous DMF (designated "A") and the other gel was transferred into neat DMF (designated "B"). After 2 days the gels were removed from the DMF solutions and placed in an aqueous solution of FITC (5.1 mg FITC in 100 ml pH 7 buffer) and left to stand for another 2 days so that the dye could fully impregnate the gel structure. Figure 6.8 illustrates the sequence described.

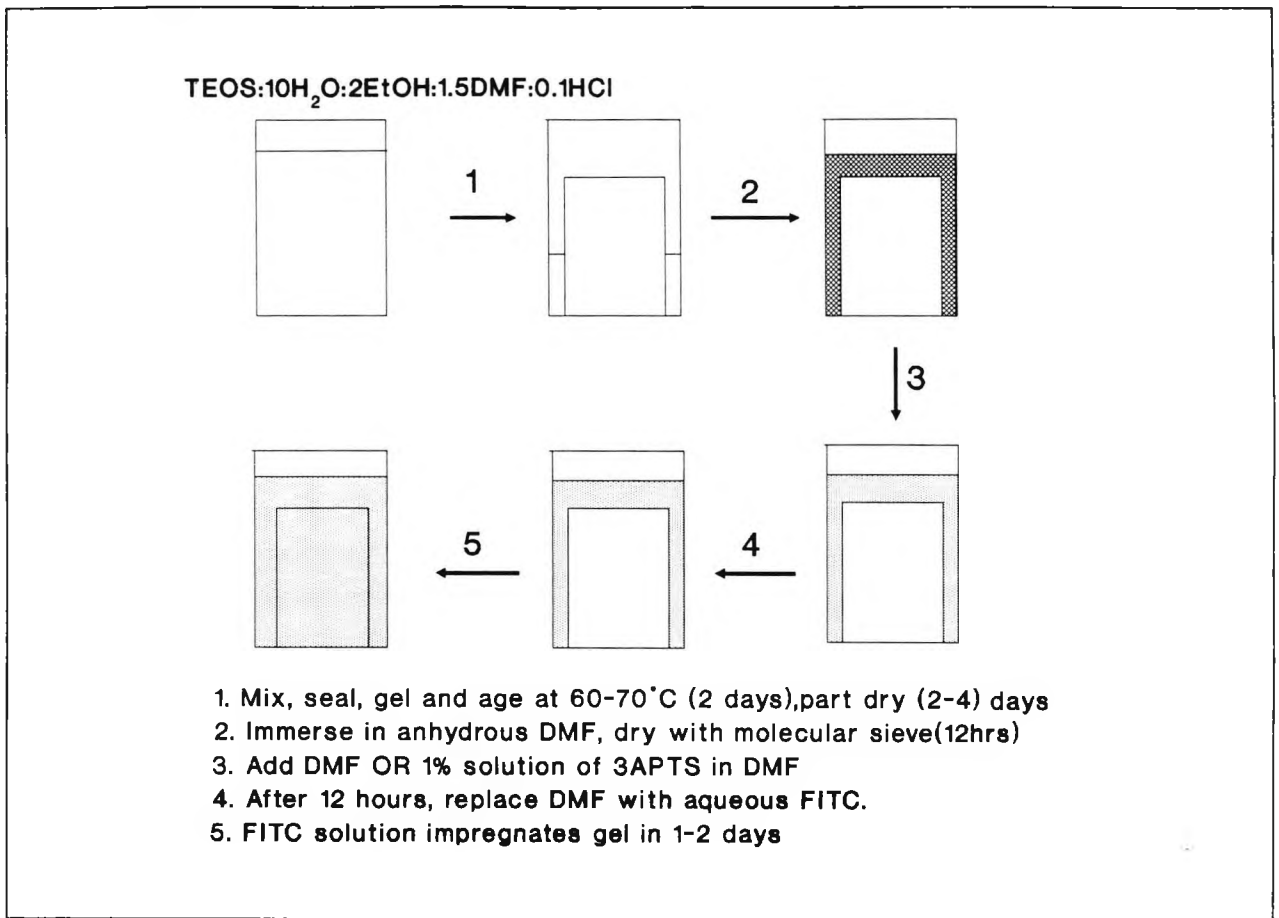


Figure 6.8 Impregnation of FITC into already formed gel.

The gels were weighed during the drying period and photographed before and after impregnating with FITC. The gels were then washed under running water for about 18 hours in order to observe the affect of using 3APTS.

Fluorescence emission spectra of one pair of gels were obtained using the optical fibre link to the spectrophotometer previously described. An excitation wavelength of 488 nm was used and the fluorescence emission at 530 nm was noted for a gel in a solution of varying pH. The fluorescence response the step change in pH was also noted. In all cases, the probe head was fixed just above the gel piece in the position which resulted the maximum response. The gel itself was positioned free standing in a large beaker containing the solution of choice. Gentle stirring was effected by a magnetic stirrer. The analyses were performed at room temperature.

The influence of the extent of drying of a gel after it had been impregnated with FITC was investigated.

6.3.3 RESULTS AND DISCUSSION

6.3.3.1 GELATION AND DRYING STAGES

The mixtures gelled overnight to give the characteristic two distinct phases, with the gel clearly separated from the sides of the container. During the aging period the gels underwent significant reduction in volume and weight loss due to solvent evaporation. This is illustrated in figure 6.9.

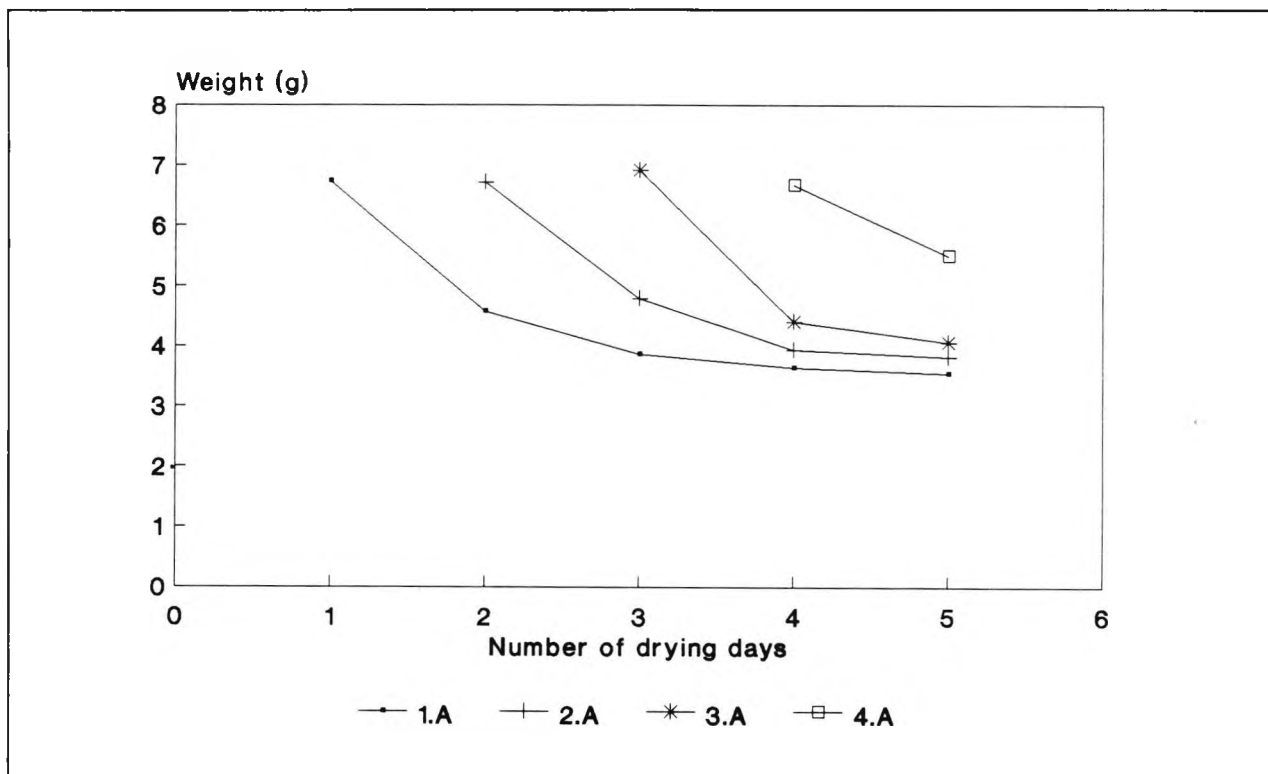


Figure 6.9 Graph of weight changes during drying of gel prior to impregnation with FITC solution.

6.3.3.2 IMMERSION IN DMF SOLUTION

The DMF solutions containing 3APTS developed white precipitates during the time that the gels were immersed in them. This was probably due to polymeric reactions involving the silylating agent and traces of remaining water or water which was produced as result of continued sol-to-gel transformation.

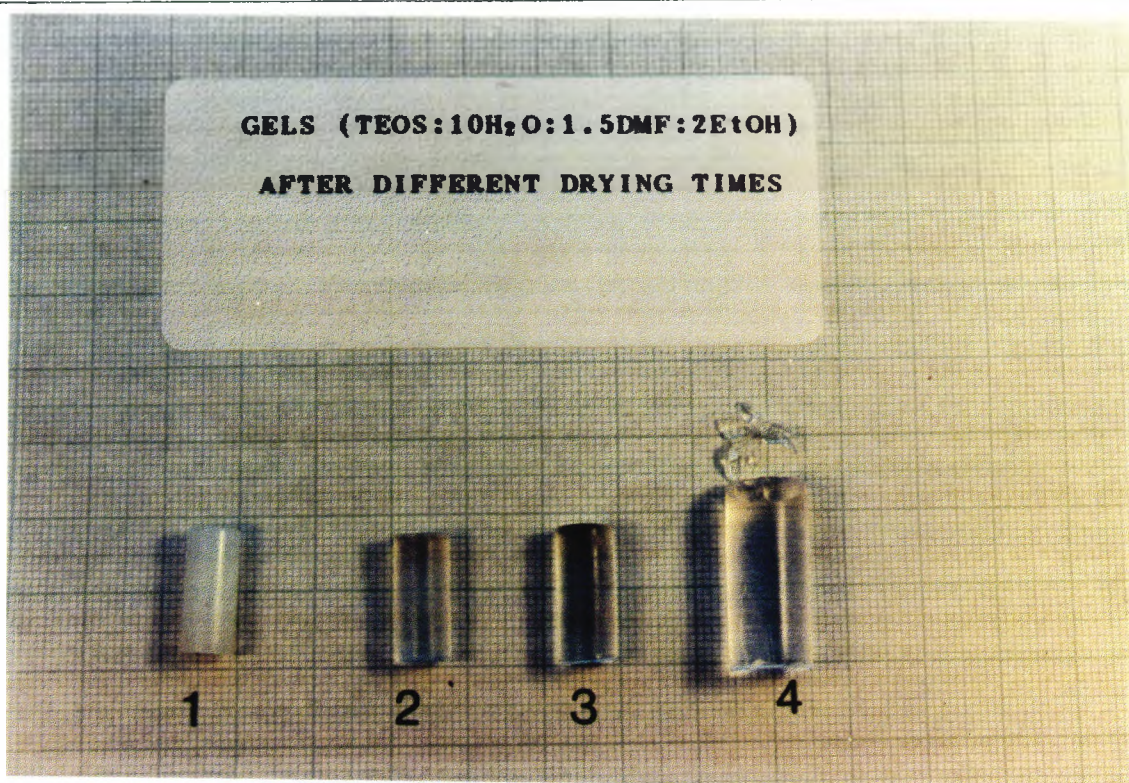
6.3.3.3 IMPREGNATION OF FITC INTO GEL

As the FITC impregnated the pores of the polymeric network, the gels developed a strong green fluorescent appearance. In a separate preparation, gels which had been prepared in the same manner were cut by pressing a scalpel on their cylindrical side and it was clear that

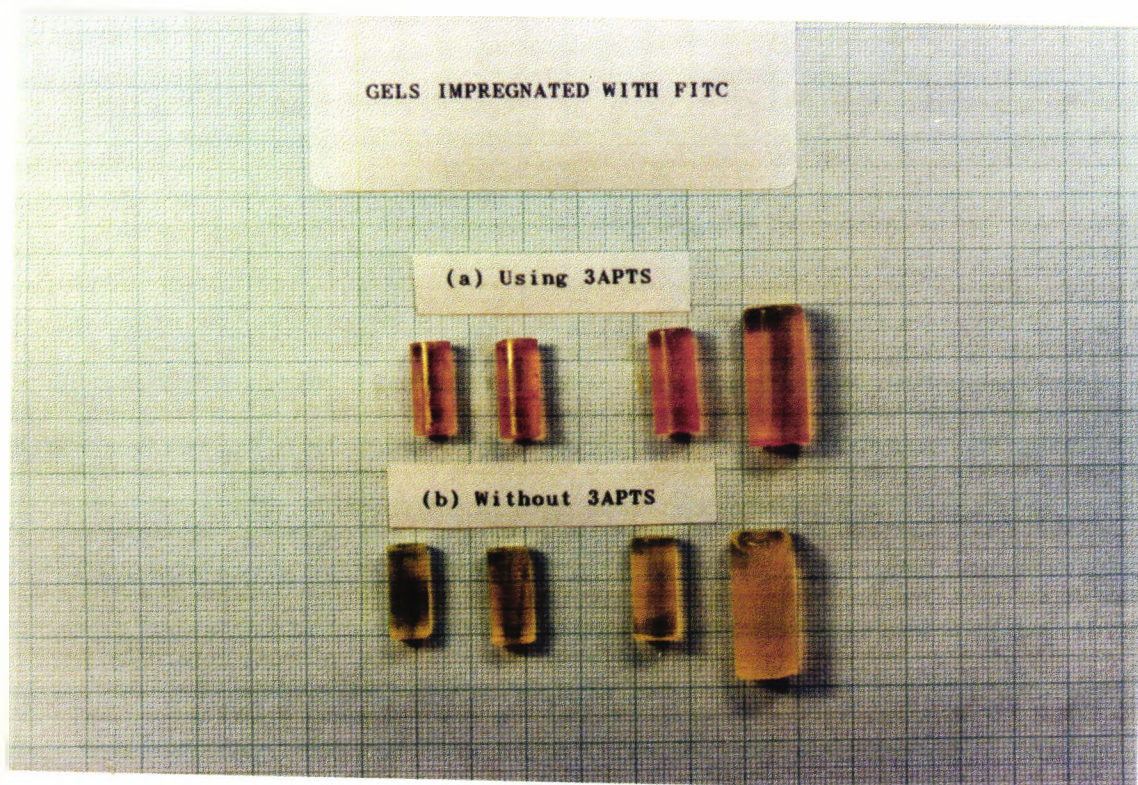
the FITC had obviously penetrated throughout the gel structure. The gels which had been prepared using the silylating agent appeared slightly darker at the edges and did not demonstrate the intensity of fluorescence of their counterparts prepared without using 3APTS.

6.3.3.4 EFFECT OF EXTENT OF DRYING PRIOR TO IMPREGNATION OF FITC INTO GEL

The extent to which the gels were dried prior to impregnation with the dye greatly affected both the appearance and the properties of the gel. Those which had undergone very little drying were soft and easily cut. Gels which had been allowed to dry for a number of days, became denser and harder and when a scalpel was pressed on their side a flaw would form which would propagate across the axis of the gel. If the gels were allowed to become very dry, then they would become opaque and difficult to cut without cracking in all directions. This suggests that as the gel becomes drier, the three dimensional polysiloxane network becomes stronger, which is what one would expect. Figure 6.10 shows gels at different stages of drying before and after impregnation.



(A) Before impregnating with FITC: "1" = 4 days drying, "2" = 3 days drying, "3" = 2 days drying, "4" = 1 day drying (only one from each pair of gels shown).



(B) After impregnating with FITC (both gels from each pair shown).

Figure 6.10 Photograph of gels at different stages of drying.

In one example of a similar preparation a sample had been left to dry at 65°C for 6 days. It was heterogeneous in appearance possessing a lower opaque region and an upper clearer region (gel C in figure 6.11).

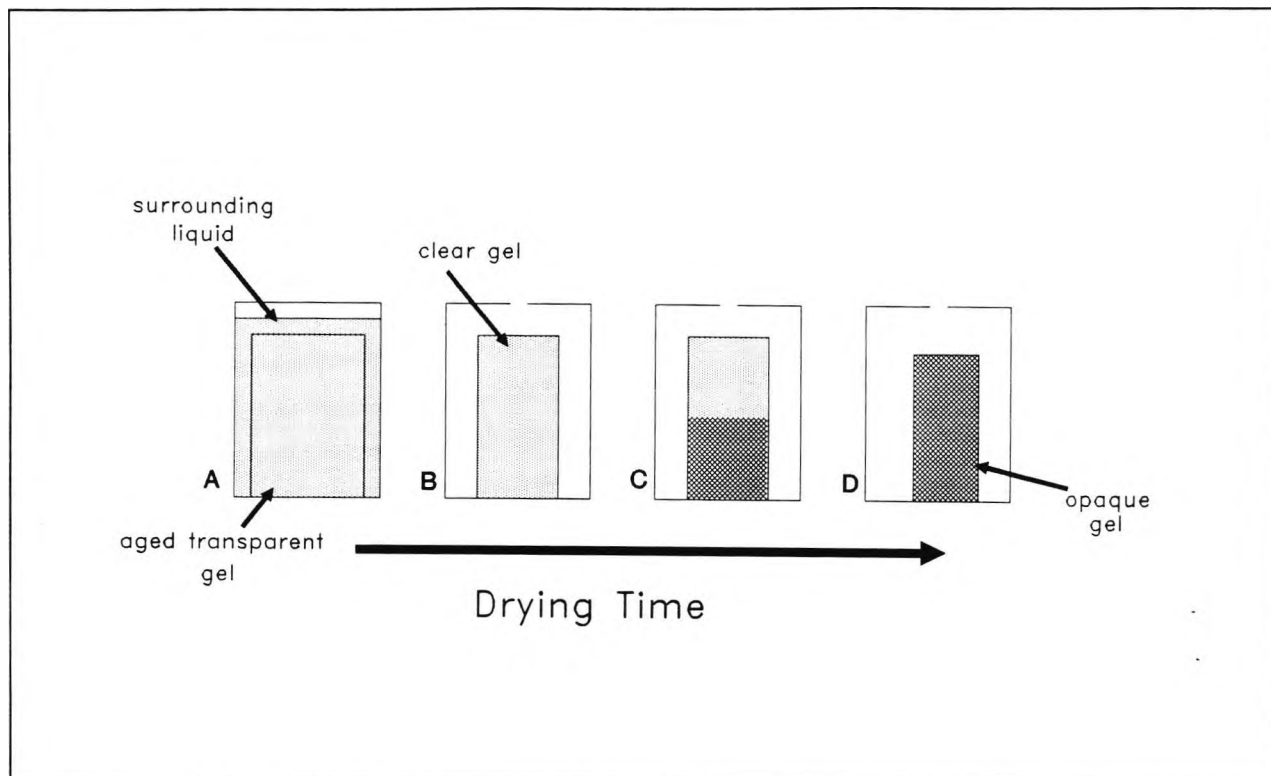


Figure 6.11 Schematic representation of drying of gel.

When immersed in DMF it immediately cracked along the line dividing the opaque region from the clear one. Furthermore, after about 10 minutes, the opaque region had become clear. This suggests that the lower area was dry and porous and that the DMF was able to impregnate into the porous network. The presence of the opaque zone below a clear region can be explained by assuming that it was formed as the solvent in the gel evaporated upwards through the network. It also indicates that the porous network is continuous, and that the mean pore diameters are equal or greater than the wavelength of visible light.

6.3.3.5 LEACHING OF FITC FROM GEL

When the gels were kept under running water it was found that the FITC had a tendency to wash-out much more quickly and to a much greater degree from the gels that had not been treated with the silylating agent. This seems to indicate that FITC can be irreversibly bound to a gel by a method similar to that used for its immobilisation onto a conventional silica surface. Fluorescence spectra are shown of the two types of gels after running under water for several hours and the difference in the amount of remaining FITC is clearly illustrated (figure 6.12). Moreover, when similarly prepared gels were reduced to powder, immersed first in ethanol then pH 7 buffer solution and finally filtered and thoroughly rinse with distilled

water, the characteristic orange colour of FITC was much stronger on the sample prepared using 3APTS.

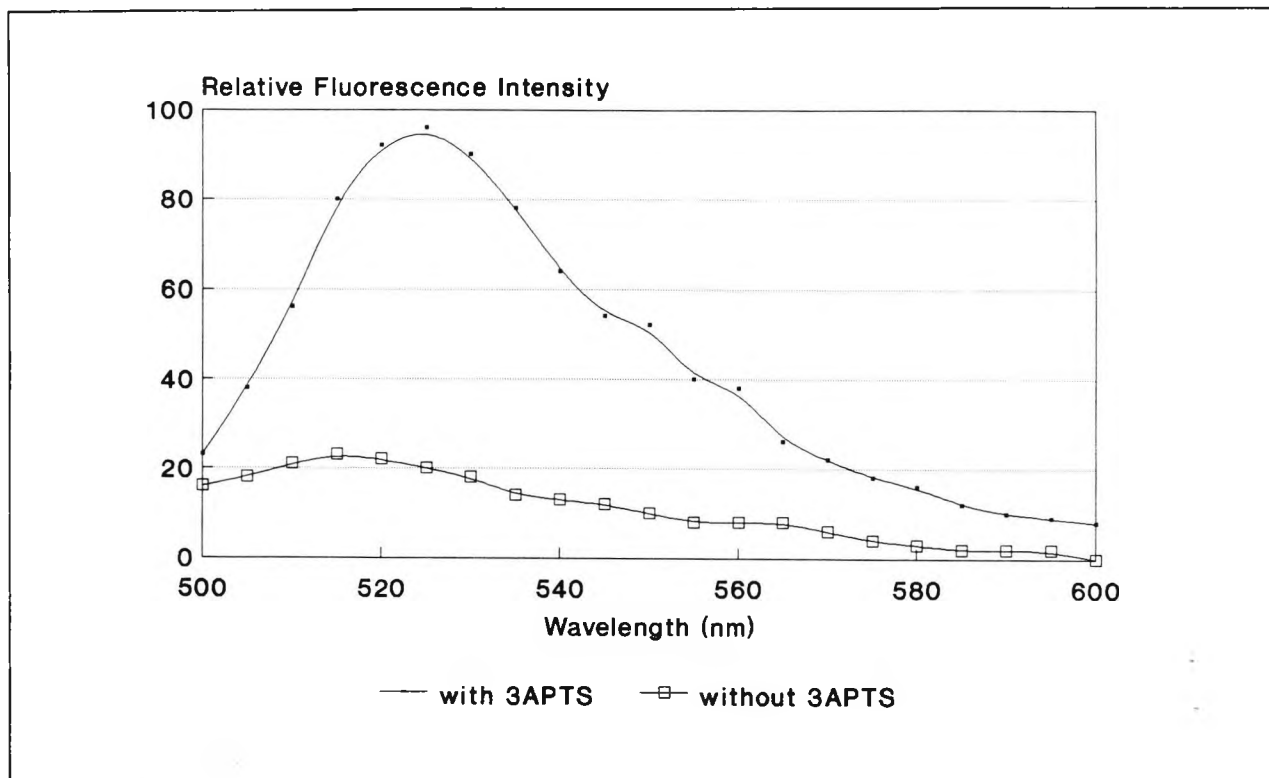


Figure 6.12 Emission spectra of gels prepared with and without 3APTS.

The influence of the extent of drying prior to dye impregnation on fluorescence response and rate of leaching of dye was not studied in detail. In terms of the absolute values of fluorescence intensity measured, these would depend very much on the concentration of the FITC solution used to impregnate the gel. In the cases investigated, the fluorescence intensity was in the order of that of observed for derivatised porous glass.

6.3.3.6 FLUORESCENCE RESPONSE TO VARYING pH

The fluorescence response of an impregnated gel under conditions of varying pH is shown in fig 6.13. The curve is very similar to that expected for FITC in solution. The gel had been washed under running water for a number of hours prior to analysis. As usual, care was taken to fix the probe in the position which resulted in the largest response for the given wavelength of 488 nm. The reproducibility of this response was dependent on a number of factors. Generally, reproducibility was best for a sample prepared using 3APTS which had undergone significant prewashing to remove excess dye and where the pH range was limited to below about pH 8.

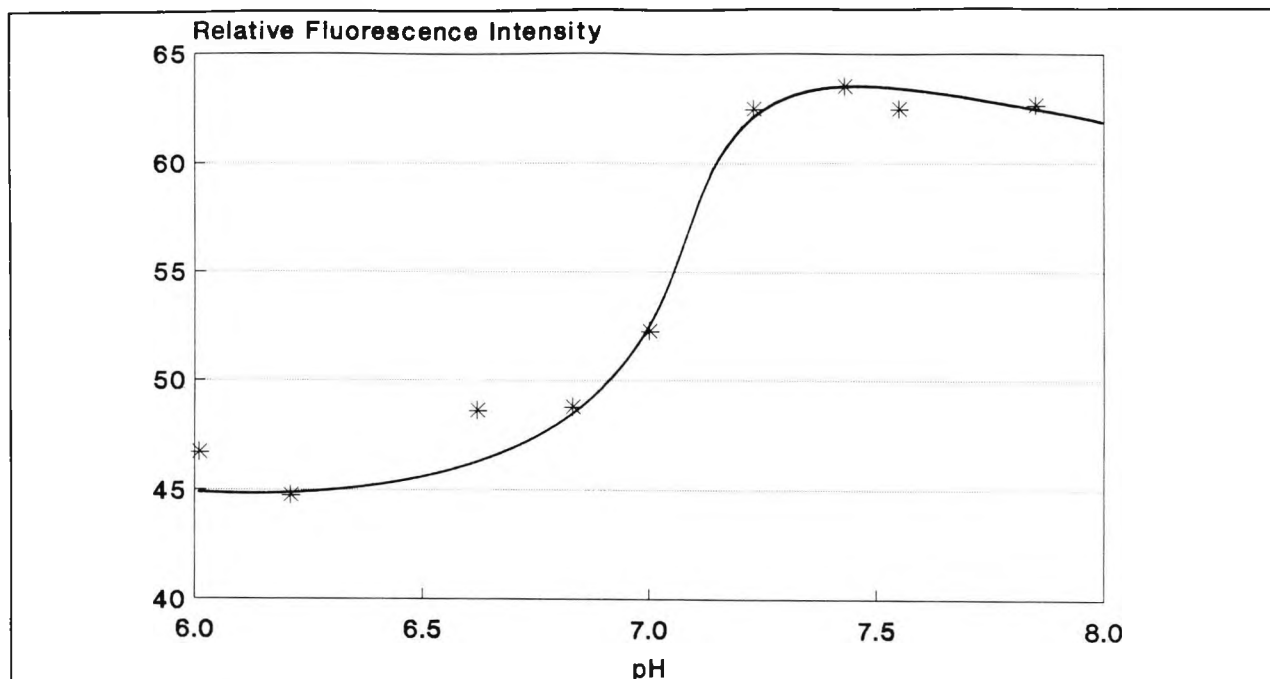


Figure 6.13 Fluorescence vs pH.

6.3.3.7 FLUORESCENCE RESPONSE TO A STEP CHANGE IN pH

During the measurement of the fluorescence response to varying pH it was observed that the maximum response was reached after approximately 20 to 30 seconds. This is considerable faster than the time recorded for the configuration using the porous glass (see section 5.3.3.2).

6.3.3.8 EFFECT OF DRYING GELS AFTER IMPREGNATION WITH FITC

The effect of drying gels which had been impregnated with FITC was investigated. It was found that on exposure to air, the gels would dry and crack in the space of a few hours. Even if the samples had previously possessed some glass-like qualities prior to immersion in DMF solution, after impregnating with the dye and a second drying stage these properties would no longer be present. On the contrary, the gels would be opaque and quite friable and if reimmersed in water they would fragment and in some cases (especially for the wet, soft gels) they would be reduced to powder. On the other hand, if the gels are stored in a saturated environment (e.g. in a sealed vial) they retain their coherent structures for a very long time. One gel was kept in this manner for over four years. Notwithstanding this example, the inability of the gels to survive changes of environment highlights a serious limitation for application in FOCS.

6.3.4 SUMMARY

The approach as presented is not suitable for preparing substrates for FOCS, and alternative methods are discussed which have more potential.

6.4 INCORPORATION OF FITC INTO GEL AT SOL STAGE

Uncracked gel monoliths were prepared incorporating FITC by adding the dye to the liquid sol. The procedure which was developed also enabled 3APTS to be added to the sol without any precipitation. Gels were also prepared using lower concentrations of H₂O than commonly recommended in the literature.

As the gels incorporating FITC dry, shrinkage and weight loss occurs due to solvent evaporation. Gels which are insufficiently aged when immersed in water will tend to crack and fragment, and the dye leaches into solution. It was found that this leaching process is retarded but not stopped by the presence of 3APTS.

If stored in a sealed container, aged and partially dried gels will be stable for a number of years and can withstand being immersed in water, dried and re-immersed in water without fragmenting. Such gels exhibit strong fluorescence behaviour suggesting their potential usefulness for some FOCS applications. Although this is a significant improvement toward preparing sol-gel monoliths suitable for FOCS, some changes in the gel structure do take place as exemplified by microhardness and DSC measurements.

The effect on the stability of gels immersed into solutions of different pHs was shown by atomic absorption measurements to be related to dissolution of the polysiloxane structure and is considered an intrinsic limitation to this approach.

6.4.1 OBJECTIVE

One of the reasons that sol-gel technology has created so much interest in recent years is that it offers the potential to tailor the composition of gels and glasses simply and directly by controlling the composition of the mixture at the sol stage. Hence there is a great body of work devoted to the preparation of multicomponent glasses which contain oxides other than that of silicon^{e.g.120,102} or to the inclusion of other species such as transition metals¹²⁴. A few authors have also reported the inclusion or entrapment of dye materials in sol-gel coatings^{125,126}. The work reported in this section discusses attempts at preparing monoliths in which FITC is incorporated at the sol stage, rather than impregnated into an already formed gel. A further objective of the work reported in this section was to include 3APTS into the gel structure since we have already indicated that there is evidence that the inclusion of 3APTS retards any subsequent leaching of FITC from the gel. Some of the problems associated with

this procedure are also presented. To the best of our knowledge the approach described in this section is novel and many details have not been reported elsewhere.

6.4.2 EXPERIMENTAL PROCEDURE

In a separate experiment it was found that FITC could be derivatised onto PG by gently heating the PG in an anhydrous ethanolic solution of FITC and 3APTS. Subsequent inspection and leaching studies suggested that this approach is not as effective as the two-step method previously described, nevertheless, the intensity of the colour of the derivatised PG where 3APTS was present was much greater than that where the silylating agent was absent. It was anticipated that such a reagent could also be used in the present investigation and hence the following solutions were prepared in ethanol which had been dried over NaPb alloy and then distilled:

$\text{EtOH}_{\text{FITC}}$	=	42mg FITC in 100g EtOH
$\text{EtOH}_{3\text{APTS}}$	=	2g 3APTS in 100g ethanol
$\text{EtOH}_{\text{FITC}/3\text{APTS}}$	=	2g 3APTS in 100g $\text{EtOH}_{\text{FITC}}$

Aliquots of TEOS, DMF and $\text{H}_2\text{O}_{\text{HCl}}$ in the molar ratio of 1:1.5:10_{0.01} were mixed together in a polypropylene or teflon beaker and until no more heat was evolved. The mixture was left to stand for 1 hour at room temperature and then 4 samples were prepared by adding either neat ethanol or one of the above ethanolic solutions to give a final EtOH:TEOS = 2. The clear solutions were cast in polythene vials, sealed and gelled in an oven at 65 °C.

After aging for 48 hours the seals were replaced with singly pierced foil and the samples allowed to dry slowly in the oven. Photographs were taken of the aged and partially dried gels. Figure 6.14 summarises the procedure used.

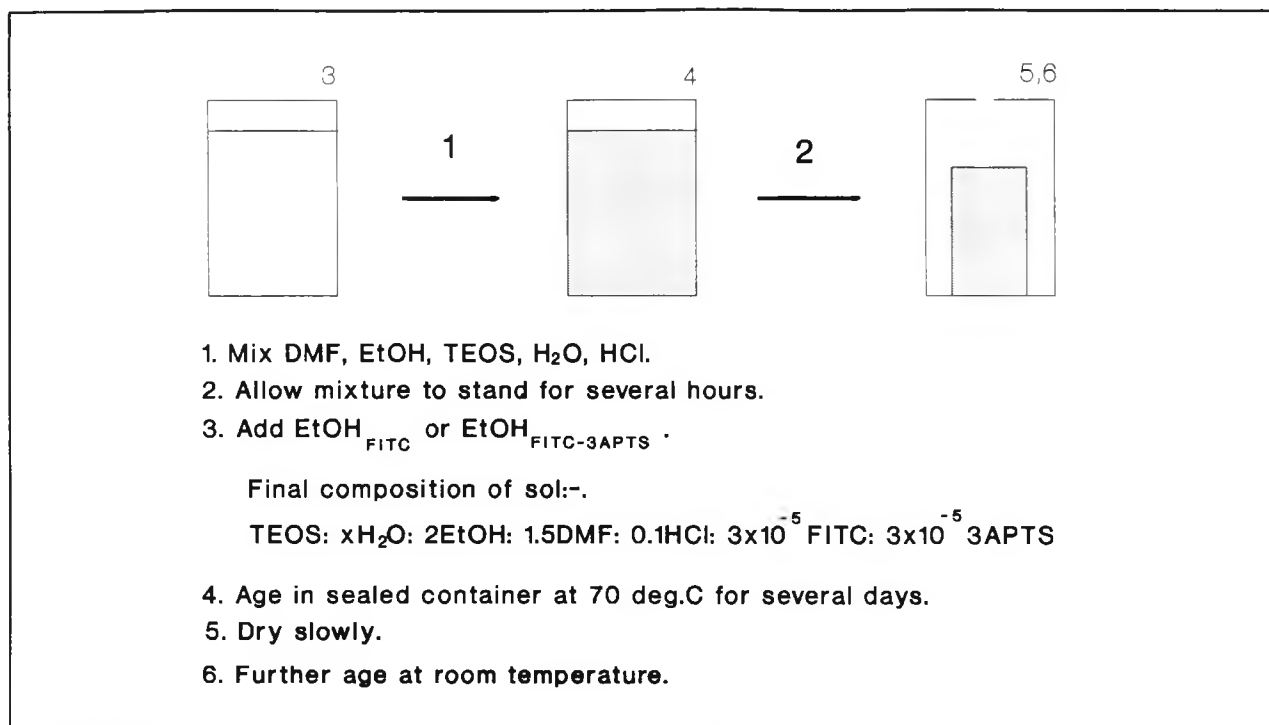


Figure 6.14 Incorporation of FITC into gel network.

Gels were also prepared using H₂O:TEOS ratios of 1, 2 and 4 (TEOS:HCl constant at 0.1) in order to investigate the effect of using lower concentrations of water.

In a separate preparation, the effect of drying rate as measured by weight loss was compared to the appearance of the gels. The effect of immersion in water of the partially dried gels was also investigated, and photographs were taken to illustrate the observations.

The extent of leaching of FITC from gels was investigated by grinding two samples (2.0 g) prepared with and without 3APTS and transferring them to pH 7 buffer solutions (50 cm³). Absorption spectra were run after 48 hours.

Samples of gels 1.A,B and 4.A,B (reported in the previous section) which had been impregnated with FITC were weighed and added to buffer solutions of either pH 7 or pH 9.2 (20.0g). The concentration of Si in the surrounding solutions was measured by atomic absorption after 1 and 2 days.

6.4.3 RESULTS AND DISCUSSION

6.4.3.1 GELATION

The initial pH of the sols was about 1.5 and gelation occurred within 6 hours to form 2 distinct phase systems. The gels were completely separated from the sides of the container, although

quite often it was noted that in the samples which contained 3APTS the separations were not 'clean'.

The refractive indices of the gels and surrounding liquids were very similar since the two were difficult to distinguish from each other, which suggests as expected that the gels consist of porous networks filled with the same solution as that which surround them. This feature is later illustrated (figure 6.18). Figure 6.15 show the gels after aging in sealed containers for a number of days.

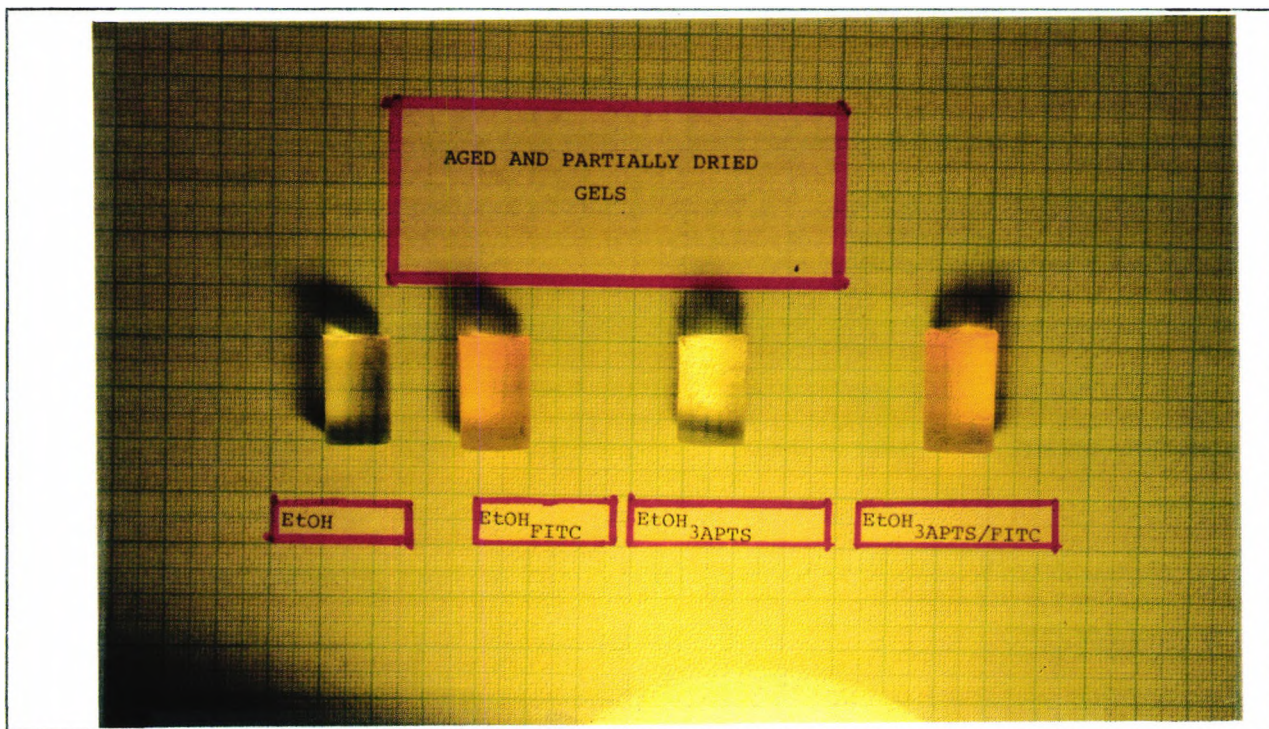


Figure 6.15 Photograph of aged and partially dried gels.

6.4.3.2 DIFFICULTIES ASSOCIATED WITH THE INCORPORATION OF 3APTS.

Many attempts to incorporate 3APTS into a sol-gel failed as a result of the precipitation which occurred on addition of water (a similar problem exists if alkoxides of different metals are used¹⁰⁷). It is well known that 3APTS is sensitive to hydrolysis and normally, as in the case where FITC is impregnated into an already formed gel, anhydrous conditions should be employed. In this approach, however, it was postulated that the ethoxy groups of the 3APTS could undergo hydrolytic polycondensation reactions with the silanols resulting from the hydrolysis of the ethoxy groups of the TEOS. In this manner, the 3APTS should be incorporated directly into the polysiloxane structure. By limiting the amount of 3APTS used, only a small effect should be observed on the overall properties of the gel. If FITC is added after hydrolysis and partial condensation has occurred then reaction between the pendant amine group of the incorporated 3APTS and the isocyanate group of the FITC should take place to give the strong thiourea linkage. Alternatively, since in the procedure described in the previous section the

FITC and 3APTS are firstly dissolved in ethanol and only subsequently added to the sol mixture, the reaction between the FITC and the free 3APTS might take place in the ethanol. Reaction between the silanol groups and ethoxy groups of the TEOS and the isothiocyanate groups of the FITC might also take place⁸² so that the final structure might be represented as shown in figure 6.16.

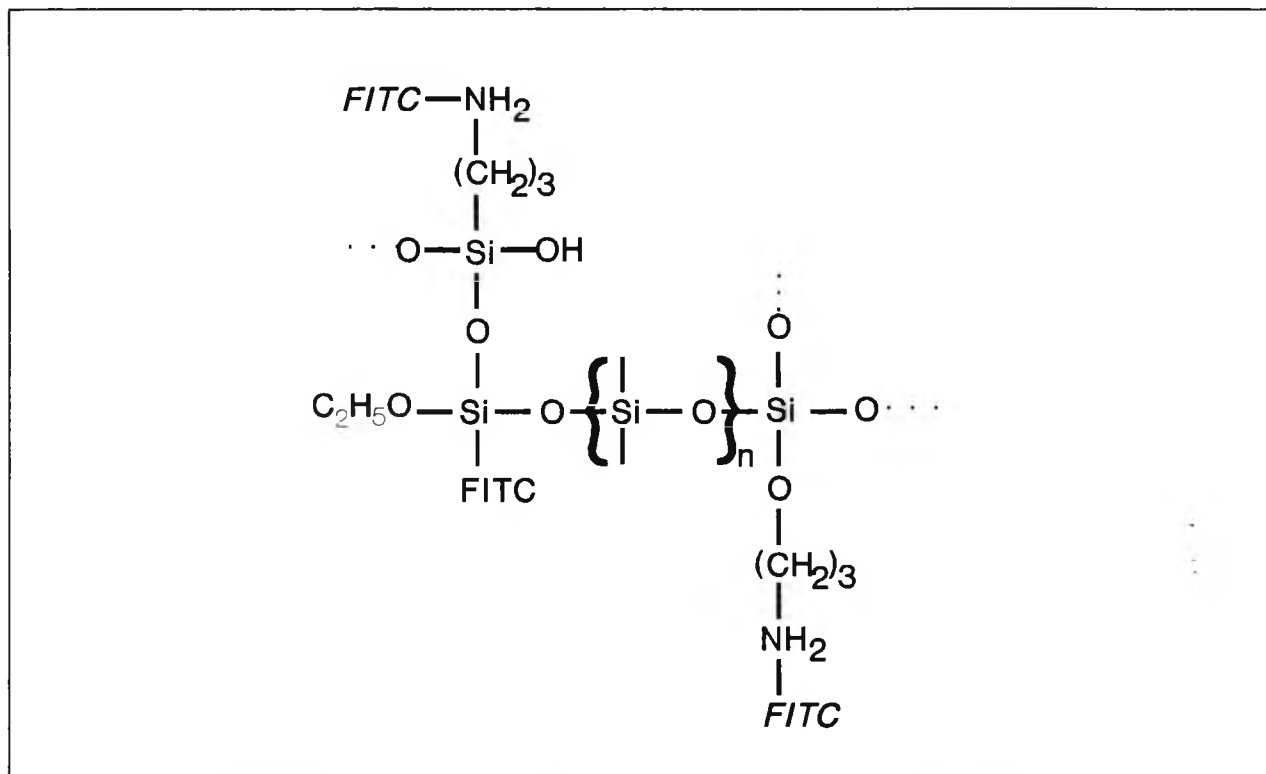


Figure 6.16 Postulated structure of FITC incorporated into gel network.

In the earlier attempts, neat 3APTS had been added before the addition of H₂O. It was found that as soon as the molar ratio of H₂O:TEOS > 3-4, a loose polymer was formed which remained suspended in the sol mixture. On vigorous or ultrasonic agitation, the polymer formation could be disintegrated but subsequent gels often possessed thin layer of more opaque material indicating that the polymer dispersion settled-out during aging. This feature was also observed when 3APTS was added very soon after forming the TEOS-H₂O mixture.

These observations suggest that the presence of H₂O in concentrations exceeding the initial stoichiometric requirement of the H₂O-TEOS reaction will cause the 3APTS to undergo rapid polycondensation. The problem was overcome by firstly adding the H₂O to the ethanolic solution of TEOS and allowing sufficient time for the hydrolysis reaction to reach a satisfactory equilibrium and then adding the ethanolic solution 3APTS or FITC/3APTS.

A possible explanation for the success of this approach might be that in acidic environments the protonation of the amine will take place preferentially to the protonation of the oxygen in an alkoxy group.(section 6.1.4.1) making the Si atom more susceptible to attack from a water

molecule. Subsequent condensation and hence polymerisation is consequently more likely to occur than that of the TEOS. If H_2O is added to a mixture of 3APTS and TEOS where, as in the example described above, the TEOS is very much in molar excess then it would be expected that the H_2O would react initially with the TEOS. If the stoichiometric requirement for H_2O is exceeded, however, the hydrolysis and subsequent polycondensation reaction of the 3APTS will take place rapidly. On the other hand, if H_2O is added before the 3APTS and enough time is allowed to elapse, much of the H_2O will be consumed either by its direct reaction with the TEOS or by its adsorption of molecules on the newly formed silanol molecules¹²⁷. Moreover, if the 3APTS is then added in the form of a low ethanolic concentration then the probability of rapid 3APTS polymerisation is reduced.

6.4.3.3 PREPARATION OF GELS WITH LOWER CONCENTRATIONS OF H_2O - LONG TERM OBSERVATIONS

Even though it was possible to include 3APTS into a sol containing a stoichiometric excess of H_2O , the risk of separate-polymerisation of 3APTS would be even more reduced if less H_2O was used to begin with. One problem which was envisaged by using low concentration of H_2O was that according to a number of other investigations^{e.g. 112,124} and as reported earlier, high H_2O :TEOS ratios were recommended in order to achieve unbroken monoliths. Nevertheless, three sols were prepared as described above except that the H_2O :TEOS ratios used were 1, 2 and 4. (HCl was added separately in order to maintain a constant HCl :TEOS = 0.1). On addition of the ethanolic solutions containing 3APTS, no precipitation was observed. The sols were aged in at 65°C for 7 days (longer than in the previous example) and the drying operation was performed at room temperature over a period of several weeks. Crack-free gels were formed using molar ratios of TEOS: H_2O as low as 2 (figure 6.17).

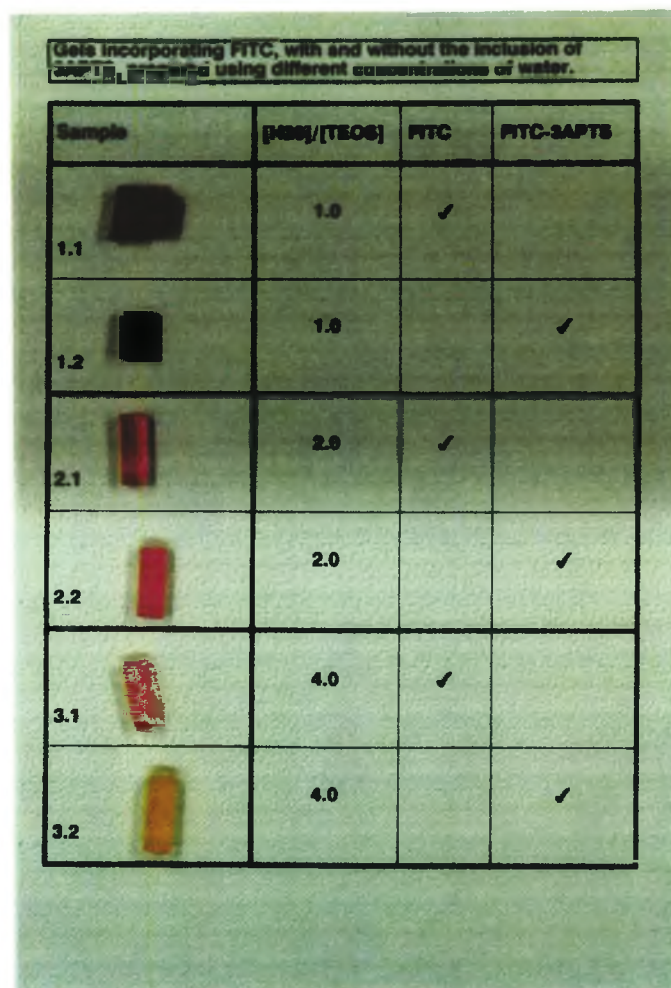


Figure 6.17 Photographs of gels prepared with different H₂O concentrations

It can be seen from photograph 6.17 that the gel prepared with H₂O:TEOS = 1 is markedly different from the other gels. This reflects the critical value of H₂O:TEOS = 2 as defined by the sol-gel reaction equations given earlier (section 6.1.4) Also, these gels are generally transparent and glass-like in their appearance which is not the case when insufficient aging or too-rapid drying is allowed to take place (see next section).

The gels shown in figure 6.17 were stored in semi air-tight conditions for a number of years. On subsequent immersion in water the gels did not fragment and exhibited a strong fluorescence. Figure 6.18 illustrates such a gel.

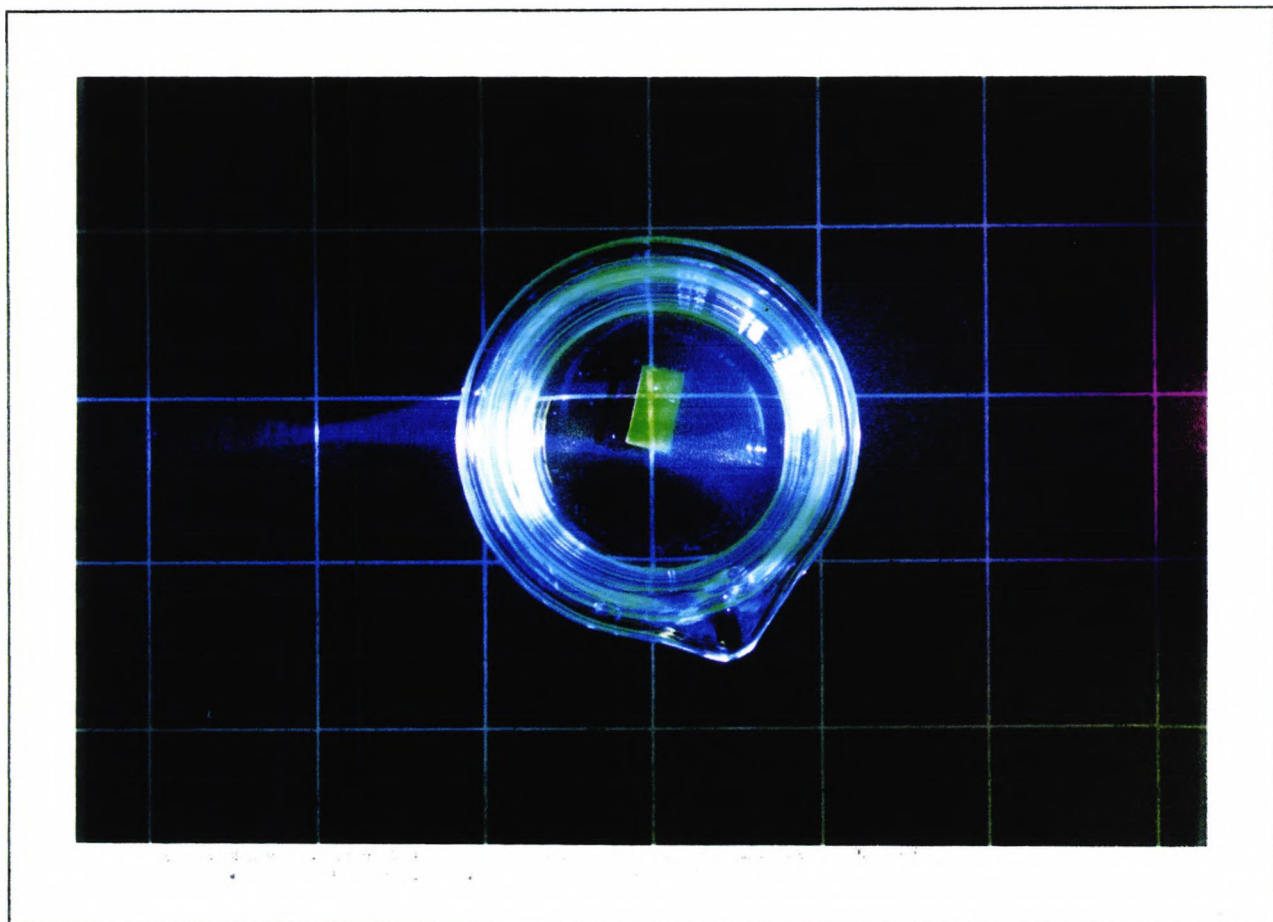


Figure 6.18 Photographs of a gel immersed in water (illuminated under blue light).

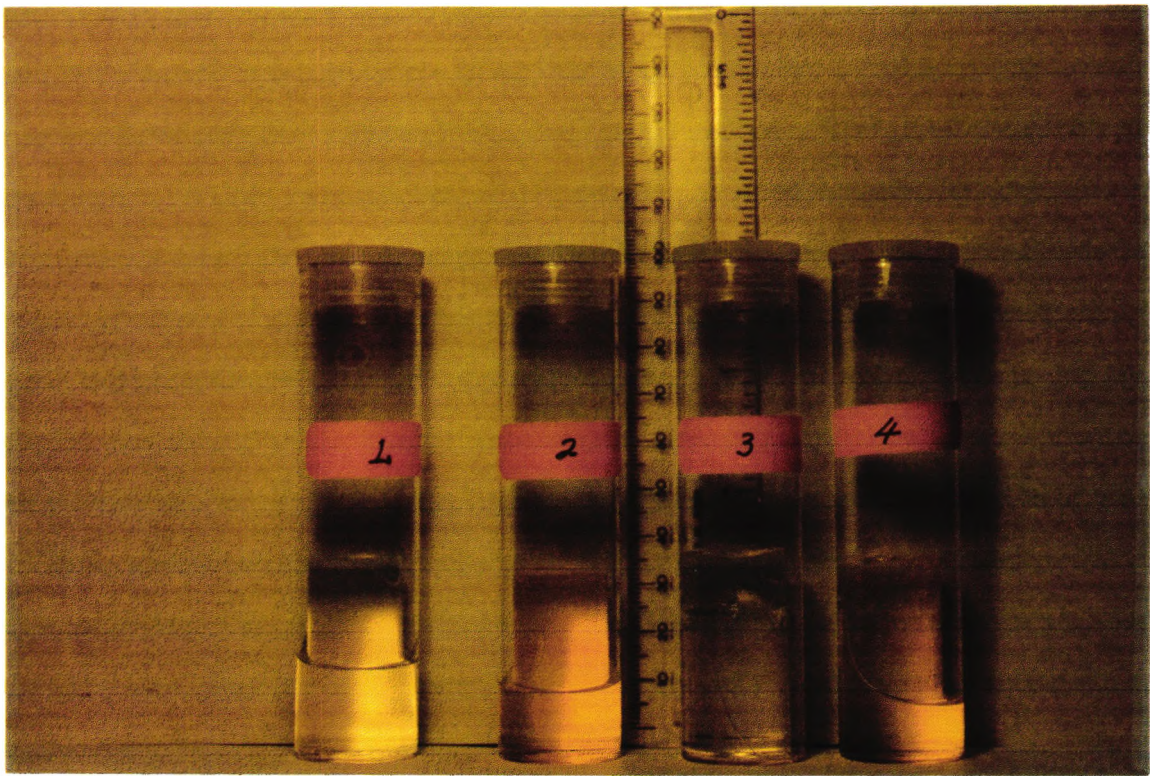
The minimum aging time to achieve such stable gel structures could not be systematically investigated in detail over the period of study due to the long time scale involved but from other work conducted in course of this investigation it is believed to be in the order of several weeks or even months. Similarly stored gels which had been prepared using higher H₂O to EtOH ratios (10:1) were also found to be stable and highly fluorescing. Significantly, however, the gels prepared with high H₂O were less stable if 3APTS had been included in the composition. Some of these latter gels were also heterogeneous suggesting some precipitation or phase separation due to the presence of 3APTS.

So it is apparent that for the conditions described, storage-stable and water-stable gels can be formed with a range of water concentrations. If 3APTS is to be incorporated, hydrolysis and partial polycondensation appears to be necessary prior to the addition of this component, although if high concentrations of H₂O are employed, subsequent problems may nevertheless occur. Aging of the sol as it undergoes the sol-gel transition is important and needs to be done over a sufficient period of time (we found 2 to 4 days, at least, although this is also dependent on the size of the gel). Even with the presence of DMF in the sol composition great care has to be taken with the subsequent drying of the gel. For best results, we found that drying/aging should be conducted over many weeks or months in semi-sealed conditions.

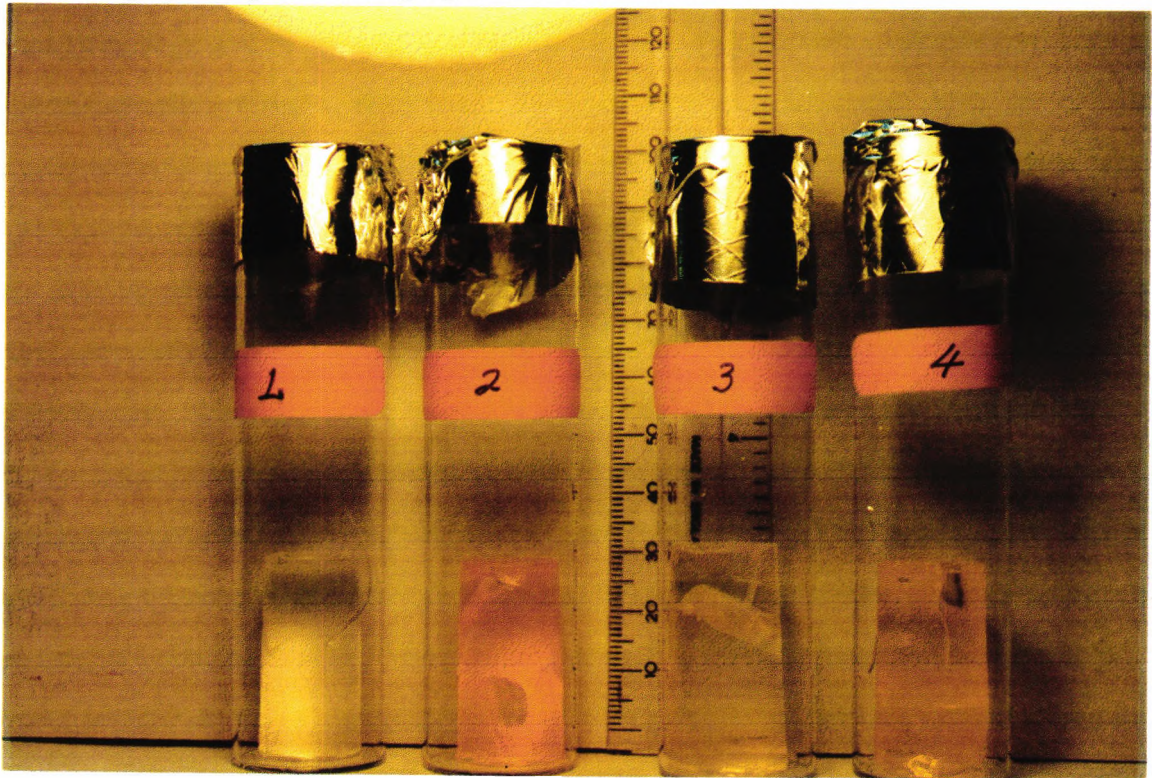
Without further investigations, it is difficult to state what the optimum sol composition and preparation procedure should be. Suffice it to say that in the past others have also commented on the fact that an optimum ratio for the formation of gels from H₂O, TEOS and EtOH-mixtures was yet been established¹³⁸ and this simply reflects the complexity of the interrelated parameters which influence gel formation as indicated in the introductory remarks on sol-gel processing. In the following sections, some of the potential problems and limitations of the use of sol-gel techniques to prepare substrates for FOCS are discussed.

6.4.3.4 POTENTIAL PROBLEMS ASSOCIATED WITH INSUFFICIENT AGING OR TOO-RAPID DRYING

As already indicated (section 6.1.6), gels have to be dried carefully in order to avoid the development of flaws during the removal of the solvent phase. In photographs 6.19(a), gels prepared using a TEOS:H₂O ratio of 1:10 had just been transferred from sealed polythene vials (after aging for 2 days) in order to enable better inspection. Drying was performed at 70°C and after 24 hours most of the surrounding solvent had evaporated and all but one gel was severely cracked (photograph 6.19(b)). The poor stability of the gels in this case is almost certainly due to the insufficient aging time employed which did not allow the gel structure to be sufficiently developed.



(A) Photograph of gels after aging in sealed containers.



(B) Photographs of gels after 24 hours drying at 70°C.

Figure 6.19 Effect of extent of drying on some gels.

In a separate evaluation, FITC-containing gels were also prepared as described above but were allowed to age for 6 days prior to drying rather than for only 2 days. The gels were much harder and could be dried (at 70°C) without breaking. The appearance of the partially dried gels after a

number of days (photographs 6.20a) can be related to their percentage weight losses (graph 6.20b):

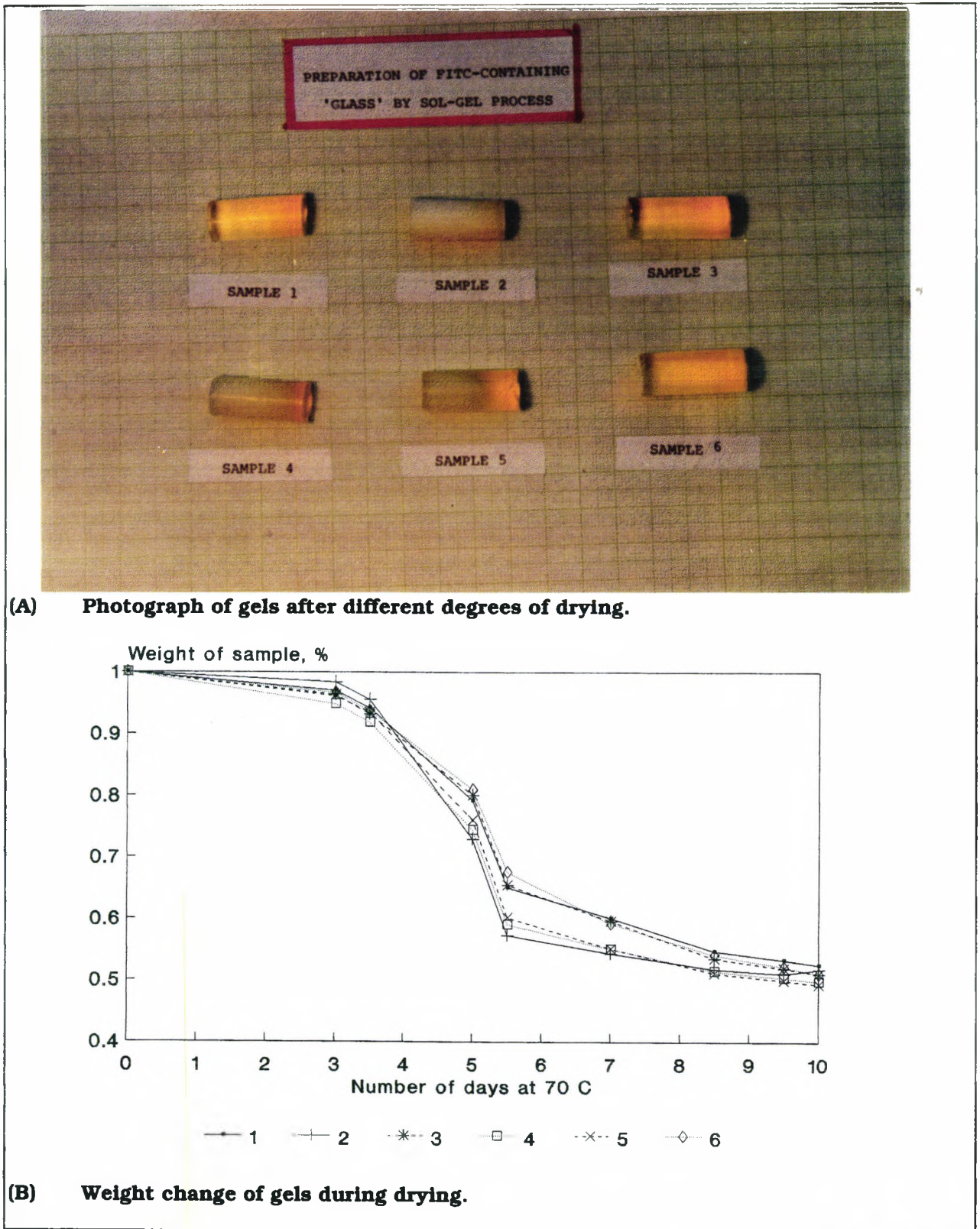


Figure 6.20 Photographs of gels incorporating FITC after different degrees of drying.

Samples 2, 4 and 5 underwent the greatest degree of weight loss and in the photograph these gels appear mainly white and opaque. This effect is very similar to that described earlier for the

gels prepared prior to their subsequent impregnation with dye material. The reason the drier gels incorporating FITC do not appear more orange in colour is probably due to the low concentration of the FITC relative to its volume. Where sols were gelled in non-sealed containers, the resulting materials were much darker in colour. They were also transparent and much harder, suggesting a much smaller mean pore size, but large gel pieces could not be produced - only fragments.

6.4.3.5 IMMERSING GELS IN H₂O

So far, it has been show that it is possible to prepare gels which incorporate FITC both with and without 3APTS. The next step was to see how these gels behaved in H₂O. If the gels were not dried to opaqueness then they could generally be immersed in H₂O without cracking as already illustrated in figure 6.18.

The case of the result of a drier gel (such as "sample 2" in photograph 6.20) being covered with water is worth considering. After just under 2 minutes in water, the gel is severely cracked (photograph 6.21a). Water penetrates the porous structure, making the gel transparent. After nearly 4.5 minutes the gel is completely cracked and will soon after be reduced to fragments (photograph 6.21b). It is believed that this structural instability is due to a combination of insufficient pre-aging of sol, too-rapid drying, and insufficient aging *after* drying.



(A) After nearly 2 minutes immersion in water.



(B) After nearly 4.5 minutes immersion in water.

Figure 6.21 Photographs showing severe cracking of dry gel on immersion in water.

6.4.3.6 EFFECT OF DRY-WET-DRY CYCLES ON GEL STRUCTURES

A major problem with the samples prepared by impregnating the dye into an already formed gel was that on drying after immersion in the FITC solution and then subsequent immersion in water the gels would lose all glass-like properties and even be reduced to powder (section 6.3.3.8). Some of the storage-stable and water-stable gels described in section 6.4.3.3 (high and low water content) were initially immersed in water for a number of days and then dried under ventilated air overnight at room temperature. After drying it was noticed that the surface of the gels had become fragile and could easily be removed. On subsequent re-immersion of the gels in water some fragmented but some remained whole and exhibited the same fluorescence properties as before drying. Although this represents a significant improvement over the previously described materials some changes in the nature of the gels did occur as is exemplified by the change in microhardness.

The Fischerscope microhardness test involves the indentation of a diamond-headed probe into the surface of a sample. The relationship between force of penetration and the penetration depth is measured and, since the surface area of the diamond is known, the microhardness (in N/mm^2) can be related to the penetration depth (μm). This evaluation was performed on gels which had been immersed in water and gels which had not. The evaluations were repeated a number of times and although the reproducibility for a given gel was rather low (probably due to the cylindrical shape of the samples), the gel which had been immersed in water exhibited a maximum microhardness of around $10 \text{ N}/\text{mm}^2$ (figure 6.22a), whereas the dry gel reached values of at least around $80 \text{ N}/\text{mm}^2$ (figure 6.22b). Clearly, immersion in water results in a much softer gel. [By way of comparison, microscope glass slides exhibited a microhardness of around $5000 \text{ N}/\text{mm}^2$].

Further indication that structural change occurs on immersion in water is evidenced by thermal analysis in which the DSC and TGA traces are significantly different for the two samples (figure 6.23). Both samples demonstrate endotherms below 150°C primarily due to removal of physically adsorbed water. At above 200°C , however, the dry sample exhibited energy peaks and weight loss which can be attributed to residual condensation reactions and combustion of residual organic material. (The gel had been prepared with a TEOS: H_2O ratio of 1:2 so some residual reaction might be expected). The wet sample, on the other hand, exhibited no such peaks suggesting that immersion in water leads to a loss of unreacted alkoxy groups and so alters the structure of the gel at the molecular level.

It was not investigated if the hardness of the gel which had been immersed in water could be re-developed, for example, by storage at elevated temperatures. Practically, this would of little value in FOCS applications. Nevertheless, the tendency of a number of samples to fragment on

re-wetting and the general change in the appearance of the gels leads us to believe that some irreversible changes occur in the gel structure. This topic is expanded upon in a later section.

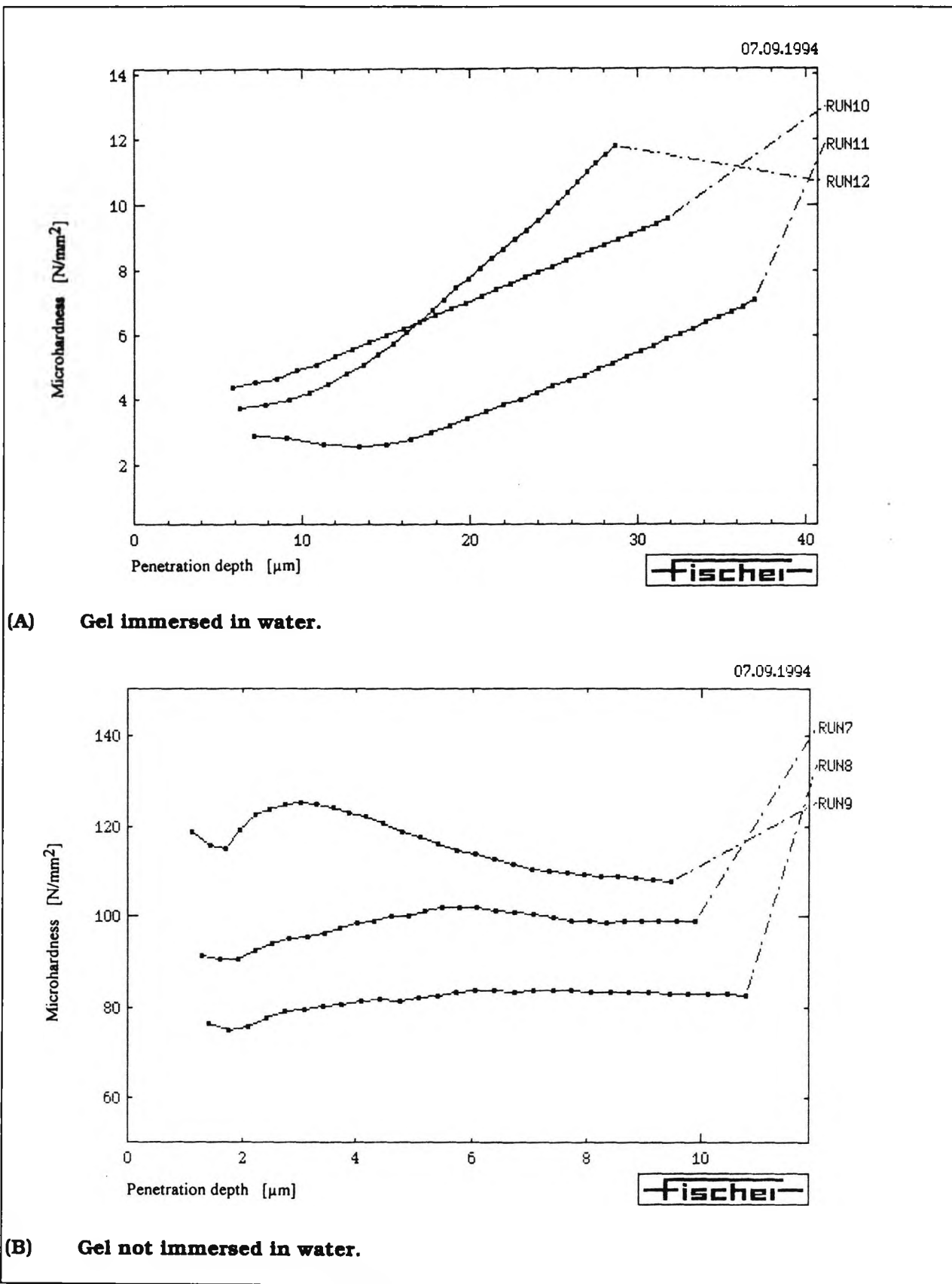
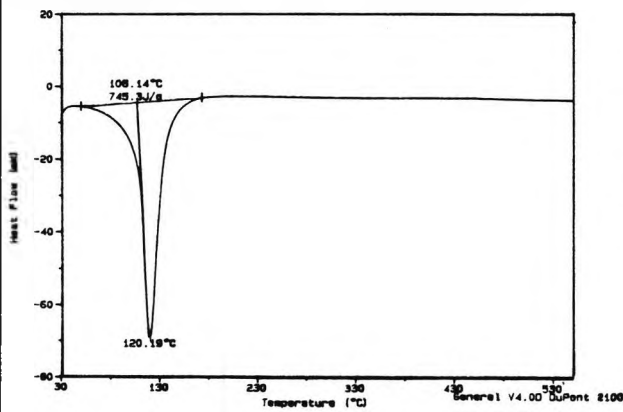


Figure 6.22 Microhardness of gels.

Sample: S.BAGDINI SOL. GEL. 2.2H
 Size: 11.9100 mg
 Method: RAMP 30C- 800C /10C
 Comment: R 940801

DSC

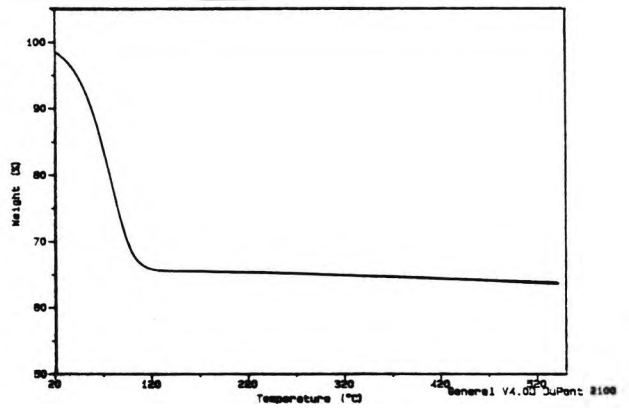
File: DS40801-1.01
 Operator: SJ
 Run Date: 8-Sep-94 10:58



Sample: S.BAGDINI SOL. GEL. 2.2H
 Size: 14.5200 mg
 Method: VOLATILES 30 -500 C
 Comment: PLOM 3L/H AIR REG S40801

TGA

File: TS40801-1.01
 Operator: SJ
 Run Date: 8-Sep-94 08:08

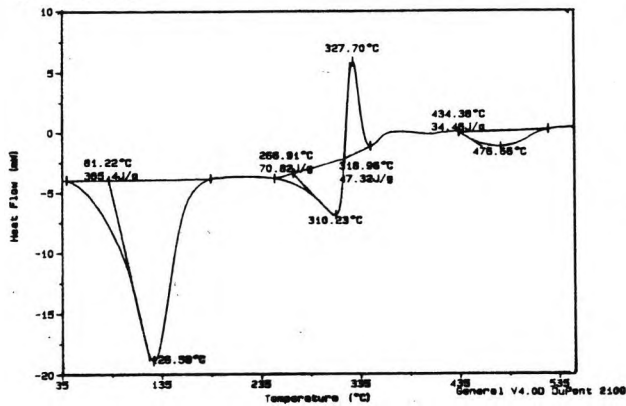


(A) Gel immersed in water.

Sample: S.BAGDINI SOL. GEL. 2.2H
 Size: 12.3600 mg
 Method: RAMP 30C- 550C /10C
 Comment: R 940801

DSC

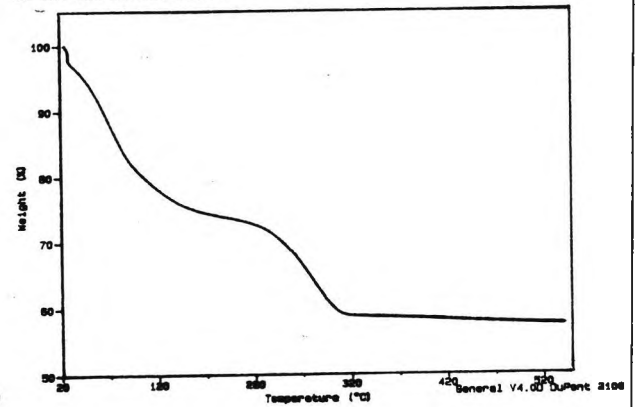
File: DS40801-2.01
 Operator: SJ
 Run Date: 8-Sep-94 12:51



Sample: S.BAGDINI SOL. GEL. 2.2H
 Size: 15.7048 mg
 Method: VOLATILES 30 -500 C
 Comment: PLOM 3L/H AIR R 940801

TGA

File: TS40801-2.01
 Operator: SJ
 Run Date: 8-Sep-94 10:01



(B) Gel not immersed in water.

Figure 6.23 Thermal analysis of gels.

6.4.3.7 LEACHING OF FITC FROM GEL

In some of the above photographs, it is very obvious that dye from the gels leaches into the surrounding solutions. For gels which had not been properly aged and dried, visual inspection of gels incorporating FITC after immersion in large quantities of water for a period of time suggests that most of the dye in the gel is eventually leached out. This evidence, however, also indicates that the leaching out process occurs significantly more slowly where the gel had been prepared with 3APTS. Figure 6.24 shows visible absorption spectra of the pH 7 buffer solutions surrounding small amounts of sol-gel samples which had been reduced to powder, measured after 24 hours of immersion. The smaller absorbance of the solution surrounding the gel prepared using 3APTS in addition to FITC further indicates that the 3APTS retards the leaching of the dye.

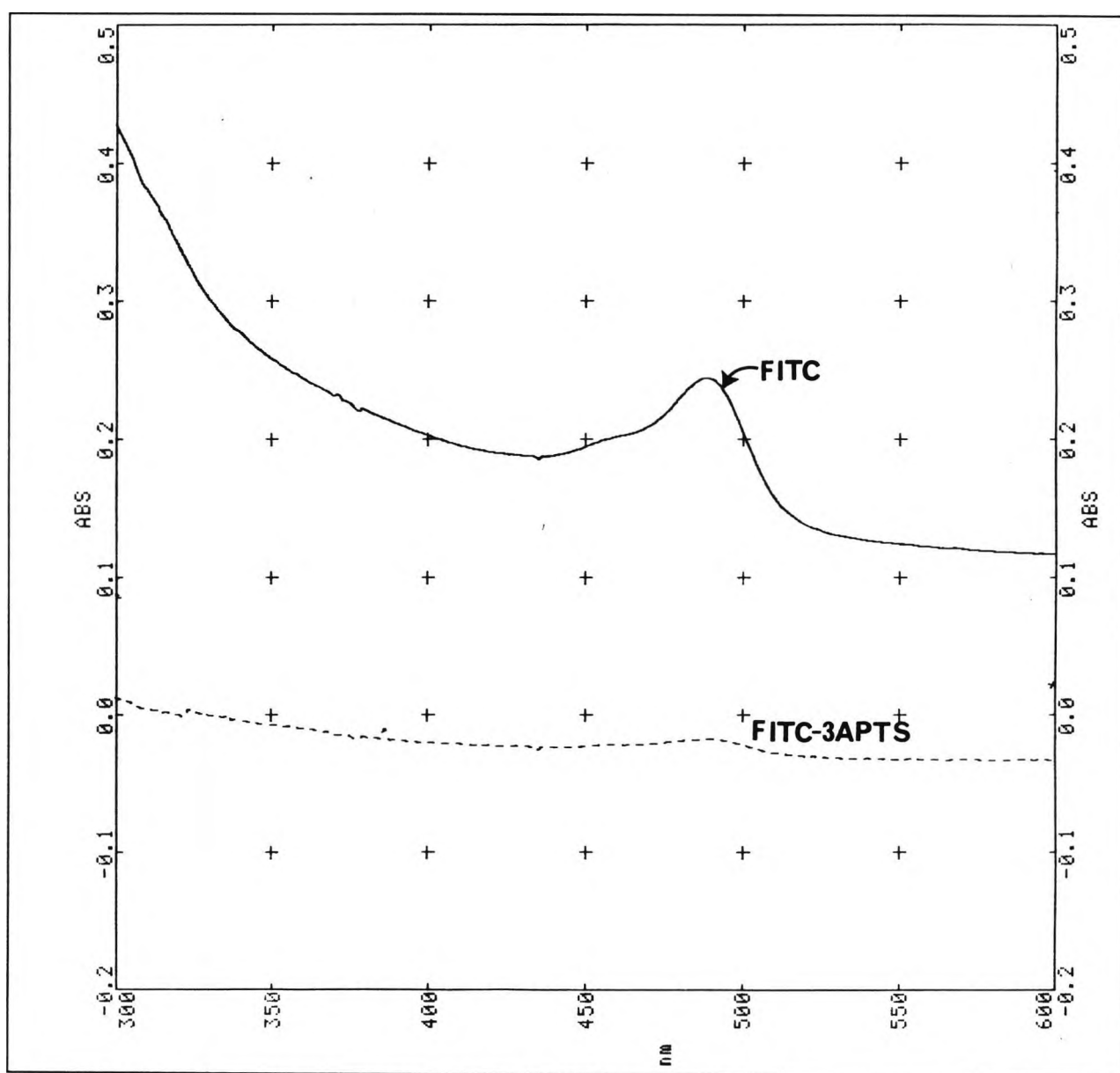


Figure 6.24 Absorbance spectra for pH 7 buffer solution surrounding powdered sol-gel samples impregnated with FITC prepared with and without 3APTS.

The gels which had undergone proper aging and drying, on the other hand, were found to have a much lower tendency to lose FITC to the surrounding water. Some loss was observed as soon as the gels are immersed in water, probably due to FITC which is not 'bound' within the porous polysiloxane network, but the subsequent loss of dye was very slow and practically indistinguishable by inspection.

Gel samples were also reduced to fine granules by grinding and washed with copious quantities of acetone (which is a good solvent for FITC) and then left immersed in acetone for 2 weeks. The distinctive colour due to FITC was still very much present in the granulated material and the surrounding solvent was colourless. This confirms that the dye does not readily go into solution as in some previous examples.

Interestingly, this lack of tendency of the FITC to leach out into solution was demonstrated by gels which had been prepared with and without 3APTS. This indicates that 3APTS may not be bringing significant advantage for gels prepared using the methods described. More extensive evaluations would be needed, however, before this tentative conclusion can be more fully corroborated.

6.4.3.8 DISSOLUTION OF GELS IN H₂O

Even where 3APTS was present in the gels which had *not* undergone proper aging and drying, the extent to which dye was lost to the solutions surrounding the gels suggested that a more complex process was occurring than a simple leaching of entrapped FITC from the pores within the gel. In fact, this was especially pertinent where 3APTS was used. It was suspected that some dissolution of the gels might be taking place and this was investigated by atomic absorption spectroscopy. The gels used were described in an earlier section (6.2.2.1)). Figure 6.25 shows the concentration of Si in the solutions surrounding the gels. The gels are labelled as in figure 6.10 where the first digit indicates the number of days that the gel had been dried prior to impregnation with 3APTS (1 = 4 days, 4 = 1 day). An additional third digit was used to differentiate gels immersed in pH 7 buffer (".1") or pH 9.2 buffer (".2).

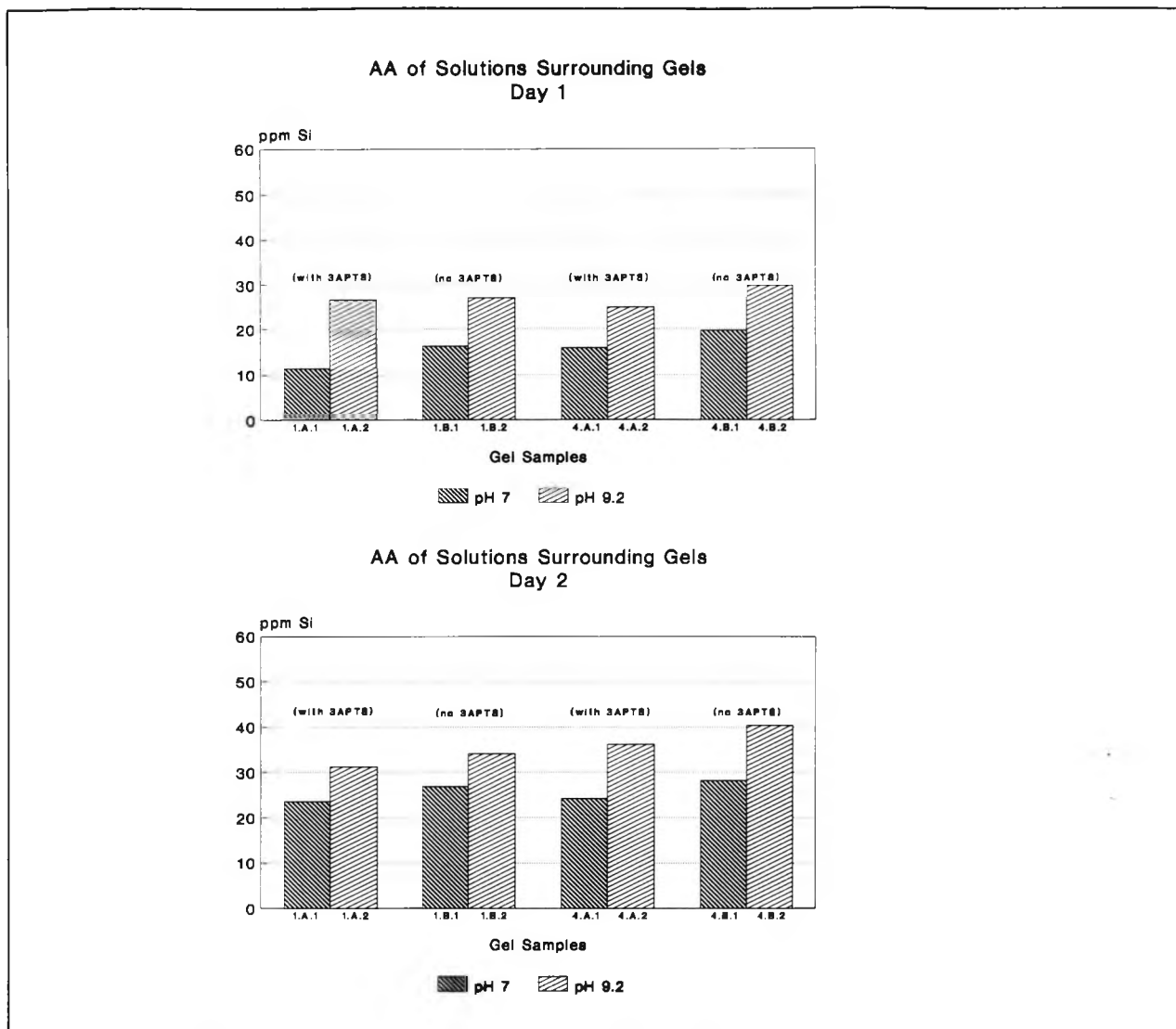


Figure 6.25 Graph of AA of solutions surrounding gels.

It is clear from these results that the gels dissolve much more readily in solutions of high pH (when comparing x.y.2 with x.y.1), which is line with previous observations (figure 5.17b) . Since the rate of dissolution of silica in aqueous solutions depends on the area of the surface of the solid silica phase⁸⁸, it is difficult to reach clear conclusions regarding the other parameters where the differences observed are not as great as in the case of the effect of pH. Nevertheless, there does appear to be a tendency for the gels which underwent a shorter drying period prior to impregnation with FITC to dissolve more readily than the corresponding gels which were dried for longer (compare 4.y.z with 1.y.z). Once again, this is expected given that the dryer gels form much harder and stronger networks. A similar tendency in dissolution is also apparent for gels prepared using 3APTS compared to those prepared without 3APTS (compare x.A.z with x.B.z). This observation is a little more difficult to explain but where 3APTS has been incorporated into the gel structure (i.e. added at the sol stage) there is further evidence which supports this. For example, photograph 6.26 shows a number of samples in which the FITC was incorporated into the gel structure at the sol stage and the concentration of 3APTS used in the ethanol was increased from 0 to 1 wt% (corresponding to left to right in the photograph). The photograph

was taken about 3 hours after covering aged and partially dried gels with pH 7 buffer solution and it is just clear from the pictures that the resulting gel pieces become smoother (their edges less jagged) with increasing concentration of 3APTS. This suggests a greater degree of dissolution.



Figure 6.26 Photographs of gels prepared with different concentrations of 3APTS immersed in pH 7 buffer solution.

At first sight these data might appear to contradict the fact that after a number of days the remaining gels prepared using 3APTS always appeared more coloured than those prepared without 3APTS. However, the extent of leaching need not be related to the stability of the polysiloxane structure and the observations indeed suggest that these are two different processes.

6.4.5 SUMMARY AND CONCLUSIONS

It is possible to prepare gels containing a pH sensitive dye such as FITC by incorporating the dye at the sol stage. If stored under sealed conditions, partially dried gels have been shown to be stable over a number of years. If subsequently immersed in water, the gels are seen to be brightly fluorescing, suggesting their continued usefulness as materials for FOCS. Fragmentation of the gels may occur on wetting but this depends on the extent of prior aging and drying, as well as the initial composition used.

These observations have significant positive implications for the long term storage of FOCS using such materials. The gels can be used to record fluorescence spectra as a function of pH but the reproducibility of such measurements is limited by the fact that dye material is slowly-but-surely lost to the environment. The use of 3APTS retards but does not prevent the leaching out of the dye material from poorly aged gel structure since the gels themselves undergo some dissolution. This effect is greater in solutions of higher pH.

For properly aged and dried gels, however, the use of 3APTS does not seem to reduce significantly the leaching process, which is in any case very slow. The dissolution of these improved gels was not measured using atomic absorption spectroscopy but given what has been observed in this work, it is to be expected that this dissolution will be pH dependent but much slower than that previously discussed.

The properties of the gels prepared are very close to those that could be expected to find general usage in FOCS. Indeed, assuming that the same approach could be used to measure analytes other than pH, such gels could find use in certain applications where a strong signal is required (e.g. for cost reasons) but where prolonged service is not a pre-requisite and probe tip disposability tolerated. One example might be the detection of harmful gases. These results have significant implications for the choice of materials for FOCS, clearly showing under which circumstances they could and could not be used. In general, it would appear that they are best suited to disposable sensors, and with cheap materials and compatible optical couplings, this is a strong possibility for many markets. The long term storage capabilities of some of these systems enhances this feature.

6.5 PREPARATION OF FITC CONTAINING COATINGS

Microscope slides were mechanically dipped into FITC-containing silica sols of different compositions and at different stages during the aging of the mixtures. The ability of the sol to wet the glass substrate and clarity of the subsequent coating depends mainly on the H₂O:TEOS ratio, but also on the extent of aging and the level of catalyst used. The incorporation of DMF as a DCCA leads to thicker coatings.

6.5.1 OBJECTIVE

In work leading up to this investigation, FITC was immobilised directly onto microscope slides by the two step procedure involving 3APTS (previously described for porous glass in section 5.1.2.2). Although the FITC could be detected by UV-VIS analysis and also by fluorescence emission spectroscopy, the intensity of the measured signals was very weak since the procedure only resulted in the immobilisation of a monolayer of fluorophore on the glass surface. Sol-gel coatings, on the other hand, have high specific surface areas¹²⁰ and therefore should enable the deposition of a higher concentration of dye material.

Coatings derived from the sol-gel process are extensively described in the literature. A number of very diverse potential applications have been reported for such coatings including coatings for anti-reflection systems, opto-electronic films and protective coatings^{97,128,129}. Sol-gel derived dip coatings date from 1939 with respect to single-oxides and thirty years later with respect to multicomponent oxide coatings. Avnir¹²⁵ reported the entrapment of organic fluorescent dyes in sol-gel produced silica hosts and this was extended by Knobbe¹²⁶ specifically for the preparation of biosensor probe material. In this section, some of the critical processing parameters in the preparation of the doped sol-gel films are considered and the applicability of this approach to FOCS is indicated.

6.5.2 EXPERIMENTAL PROCEDURE

Five mixtures were prepared with the following molar compositions:

Table 6.5 Composition of FITC-containing sol-gel coating mixtures.

Mixture	TEOS	H ₂ O	DMF	EtOH	HCl	EtOH* _i
2	1	2	-	2	0.02	2
3	1	8	-	2	0.08	2
4	1	2	-	2	0.002	2
5	1	2	1.5	-	0.02	2

Two forms of EtOH* were prepared:

EtOH*_a = FITC (110 mg) in dry distilled EtOH (100 g).

EtOH*_b = EtOH*_a (15 g) + 3APTS (0.01 cm³).

The mixtures were prepared in a fashion very similar to that described for the monoliths: H₂O and EtOH were added to TEOS and the solution stirred until no more heat was evolved. This was followed by the addition of the EtOH*. The coatings were deposited on microscope slides previously cleaned by washing with water and detergent followed by thorough rinsing with distilled water then acetone and finally dried in an oven at 80 °C. The microscope slides were mechanically dip-coated by withdrawing the glass slips from the alkoxide mixtures at a constant rate of 0.29 cm s⁻¹ (a modified chart recorder was used for this purpose). The faster the rate of withdrawal, the thicker the coating¹³¹ but when rates faster than the 2 cm s⁻¹ were used, difficulty was experienced in obtaining initially clear coatings or coatings which did not readily crack. The coating procedure was repeated on new slides after the mixtures had been allowed to age at 30 °C in sealed containers for set times.

6.5.3 RESULTS AND DISCUSSION

6.5.3.1 APPEARANCE OF COATINGS

The following table summarise the observations of the coatings.

Table 6.6 Appearance of Coatings on Microscope Slides.

Mixture	Time (hours)			
	0	3	22	46
1.a	CLR/GRNY	CLR/GRY	CLR/GRNY	CLR/GRNY
b	CLR/GRNY	>CLR	>CLR	CLR
2.a	CLR-CLDY	CLR-CLDY	CLR	CLR
b	CLR-CLDY	CLR-CLDY	CLR-CLDY	CLR/PWT
3.a	>PWT	PWT	PWT	<PWT
b	>PWT	PWT	CLR	CLR
4.a	>CLDY	CLDY	CLR	CLR
b	>CLDY	<CLDY	CLR	CLR
5.a	CLR/FLWPT	CLR/FLWPT	CLR/FLWPT	<PWT
b	CLR/FLWPT	CLR/FLWPT	CLR/FLWPT	CLR/FLWPT

CLR - clear
 GRNY - grainy
 PWT - poorly wetted
 CLDY - cloudy
 FLWPT - flow patterns

It is not clear from the literature what, if any, is the ideal composition of a system in order to result in a good coherent coating¹¹². In this work it was found that the initial wetting ability of the FITC-containing coatings were very dependent on the concentration of the water used. The importance of this has also been reported by others¹³⁰ and can be partly explained by considering the type of networks which can develop during the polycondensation stage. In environments of lower pH and lower water concentration linear polymers are

formed preferentially, whereas at higher pHs or water concentrations the tendency is for branched polymers to be developed¹⁰⁷. It is not unreasonable to suppose that the linear polymers, with their lower initial viscosities¹³³ would lead to better coatings than the branched clustered structures of the high water concentration solutions, but a full explanation of this phenomenon would require a much more thorough investigation of the chemrheology of these systems and is beyond the scope of this work. The grainy appearance of some of the coatings prepared using low water concentrations is probably due to the precipitation of the dye material (FITC is insoluble in TEOS at room temperature).

The use of DMF appears to lead to thicker coatings as typified by the flow marks or sagging observed. The thicker parts of these coatings tended to crack and craze (figure 6.27).

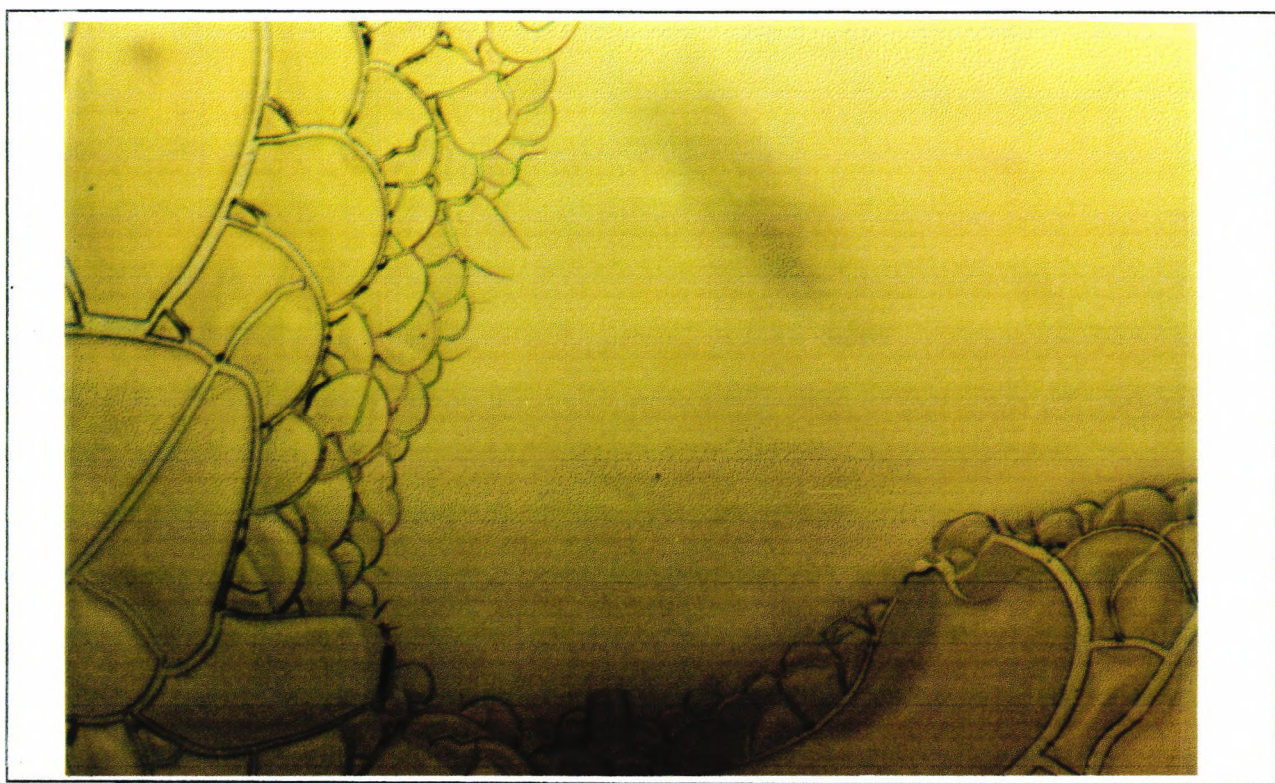


Figure 6.27 Photograph of thick coatings showing cracks.

At room temperature most of the coatings did not exhibit any cracks: however, if heated to 70°C cracks readily developed within a short period of time (figure 6.28) in most of the samples. This feature was not systematically investigated but it is known from other workers that it is possible to subject sol gel coatings to some thermal treatment without it leading to cracking or crazing of the coatings^{108,110}. However, the thickness of the coating is a limiting factor.

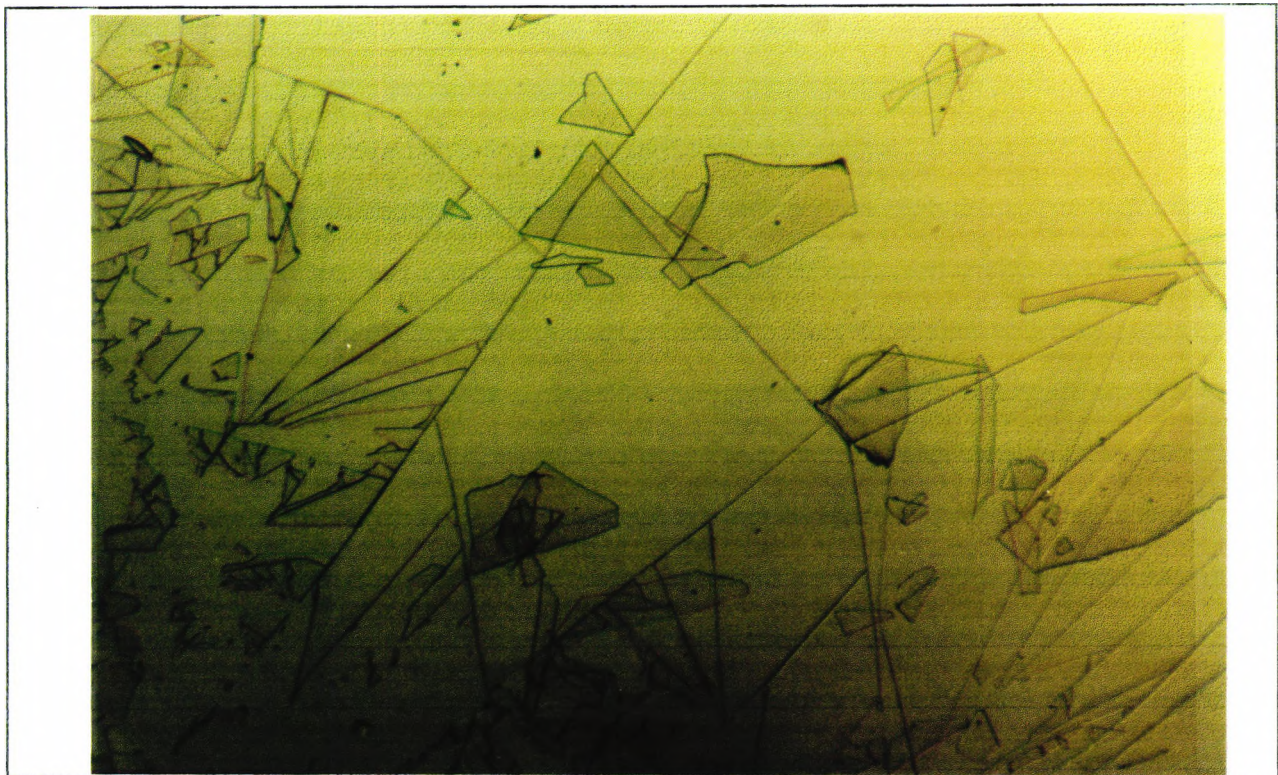


Figure 6.28 Photograph of cracked coating after heating.

The use of 3APTS resulted in better wetting of coatings produced with mixtures containing the highest concentration of water (all other mixtures resulted in good wetting to begin with). This is quite likely a manifestation of the flow control properties of silicon-based materials which are widely recognised in the paint industry¹³³. It is further anticipated that better coatings with fewer surface flaws could be produced by the addition of the types of surface active agents described by some workers¹²⁵.

In a separate investigation, multiple coatings were prepared by re-dipping coatings which had been deposited and allowed to dry at room temperature for a number of hours. Crack free coatings were realised with some difficulty and only at room temperature.

6.5.3.2 VISIBLE SPECTRA

Spectra taken of coatings produced at different times during the aging process have been reported elsewhere¹³⁴. Changes in the shape of the characteristic FITC absorptions were observed and these are probably due to variations of the pH as the mixture ages. This observation was also noted during the gelation of a number of gels containing other pH sensitive dyes.

The influence of pH on the absorption spectrum of a sol-gel coating was evaluated by immersing the slide in a solution of given pH for 5 minutes prior to making the measurement. The results are shown in figure 6.29.

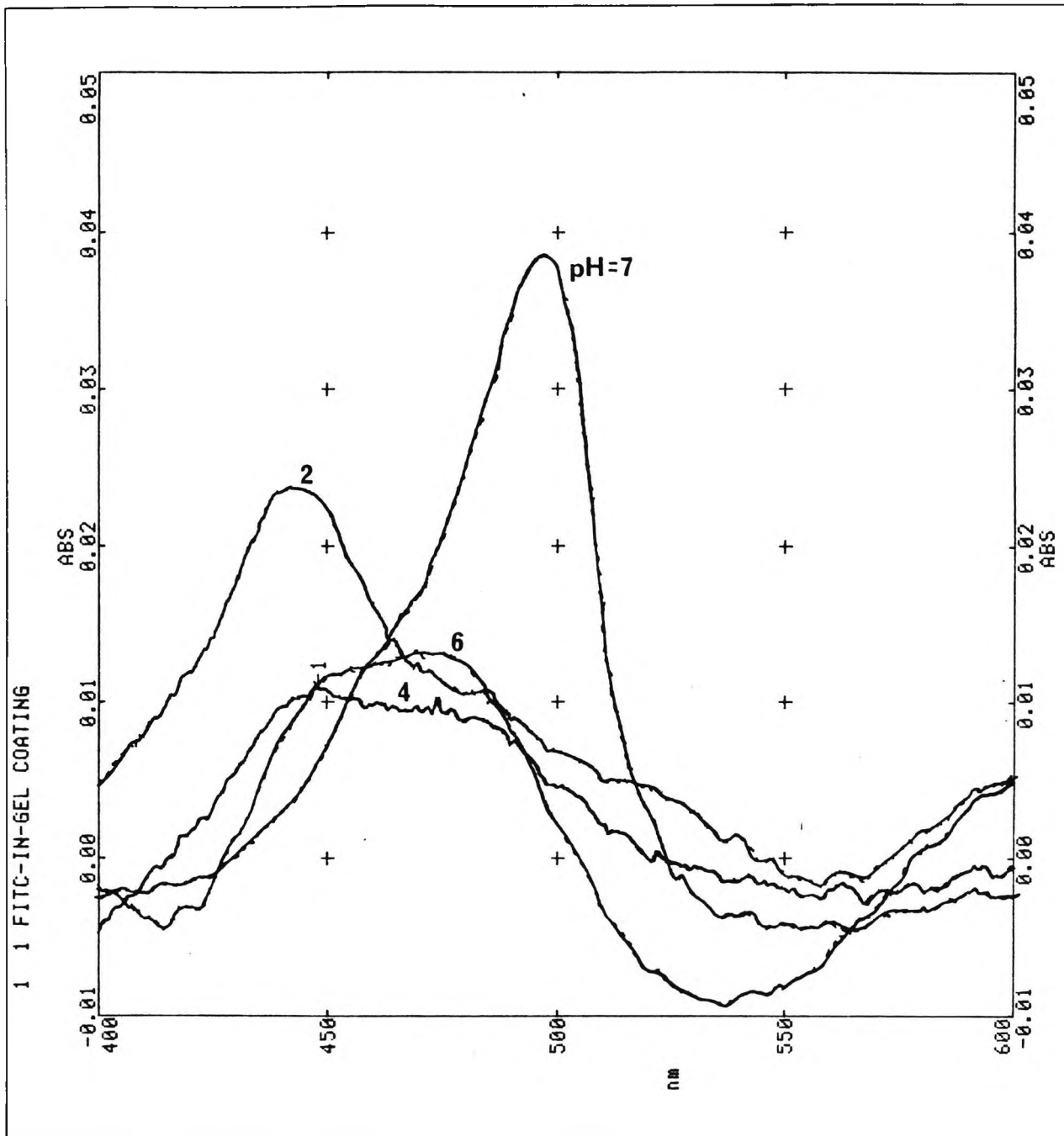


Figure 6.29 Absorption spectra of FITC-in-gel coatings after soaking in solutions of different pHs.

These results are in good agreement with pH effects on the absorption characteristics of FITC in solution (see figure 4.5) and provide a sound basis further investigations.

6.5.4 SUMMARY AND CONCLUSIONS

The results confirm that the sol-gel approach is indeed useful for the entrapment of organic dye material and that it can be used to form analyte sensitive coatings. The composition of the starting sol influences the final coating performance and the use of DMF as a DCCA leads to thicker coatings which could prove an advantage for some FOCS applications. 3APTS can also

be incorporated into the coatings and leads to coatings which have a better general appearance. It is likely that the presence of 3APTS will also help to prevent leaching from the coatings of the dye, although we did not carry out any investigations toward this end.

In order for the described coatings to remain coherent, they needed to be protected from drying out too rapidly. The visible absorbance of coatings which contained FITC suggests that under such controlled conditions the coatings could find use in FOCS applications. In our opinion, however, in order for more general usage there are a number of issues which still need to be addressed and some of these are highlighted in the final chapter: *Suggestions for future work*.



Chapter 7

GENERAL CONCLUSIONS

The outcome of this work has been to take a broad look at factors related to FOCS development and then to consider in more detail a number of aspects involved in the immobilisation of the indicator of choice (FITC) onto a traditional substrate (porous glass) and a much more recently developed support (sol-gel matrix). The goal of a FOCS for pH which exhibited a combination of the following features: fast response time, high signal intensity, physical and chemical storage stability remains to be achieved, after one decade of study by a number of research groups worldwide, as is evidenced by the literature. As a result of our investigations, however, we have reached the following conclusions which are important in relation to future developments in FOCS, and which are the result of a detailed study of the materials involved:

- (1) The development of FOCS can be divided into a number of distinct research areas, each of which can be addressed quite separately from the other as long as the correct boundary conditions and final project objectives are known, to lead to advances in the field.
- (2) Simple modification of commercial equipment can enable the study of certain important aspects of FOCS (e.g. indicator behaviour) without the need to consider many of the opto-electronic features that these systems require. This is a vital step in material characterisation and improvement.
- (3) FITC is indeed a suitable indicator for a fluorescence-based FOCS to measure pH, although it was found that its most useful dynamic range is limited to between pH 5.4 to pH 6.6.
- (4) The immobilisation of FITC onto porous glass was considered in detail and microanalysis was used to identify a number of the features which influence the final loading of the dye. This analytical method was not sensitive enough to relate the indicator loading with the fluorescence intensity of the derivatised PG, although trends were seen.
- (5) The use of a macroporous membrane enables the design of a fibre-probe which contains a relatively large quantity of derivatised PG. This leads to a strong fluorescence signal which it is believe could allow the use of a relatively unsophisticated opto-electronic systems, thereby reducing the ultimate cost of a sensor system.

- (6) For pH measurement (and likely for other analytes of interest) it is not envisaged that a single approach which would find universal applicability. The choice of indicator, substrate and immobilisation chemistry, as well as what type of opto-electronic and probe configuration are used will depend on the end application.
- (7) Monolithic sol-gel structures containing FITC were prepared by a number of routes but demonstrated to have only limited potential for FOCS in aqueous environments. Although we were able to prepare gels which had properties very close to those which could find general use in FOCS, the main problems with the gels studied, which were all based on acid-catalysed reaction mechanisms, was that their physical and chemical storage stability could not at all be proven.
- (8) The preparation of FITC containing coatings by the sol-gel route was studied and the work confirmed the pH dependence of the absorption spectra as reported by others. Although we acknowledge that recent publications^{101,135} and presentations^{136,137} also reinforce the applicability of this approach in FOCS, in our opinion continued work is required to demonstrate clearly that this method offers distinct advantages over other currently employed systems. Moreover, when analyte sensitive-coatings are used in FOCS they tend to require more sophisticated opto-electronic arrangements which may prove an economic limitation for some applications.
- (9) In our opinion, derivatisation of an analyte sensitive dye onto a porous glass-like substrate offers a realistic opportunity to develop extrinsic FOCS which could find success in areas where conventional approaches have major limitations (technical or economic). For this success to be realised for applications where disposability is not an option, however, the long term reproducibility of the sensor under practical conditions needs to be demonstrated and we present a number of proposals which might lead to this desired outcome.



Chapter 8

RECENT ADVANCES IN SOL-GEL DERIVED PROCESSING

The bulk of the practical work reported in this thesis was conducted in the period 1987 - 1990. Since that time, advances have been made with respect to the preparation of gel-based silica optics and this section attempts to summarise the most important of these. Because one of the main conclusions reported in this thesis relates to the problematic storage stability of analyte-sensitive sol-gel structures, particular emphasis will be given to this topic. This section is based on reports contained in a single work¹⁴³ edited by L. Klein and published in 1994. Reference to specific chapters will be made in the ensuing text.

Hench and Noguès (chapter 3) describe two primary sol-gel processing methods to produce silica optics which have reached commercialisation: (1) hydrolysis and condensation of a silica alkoxide precursor and (2) gelation of colloidal alkali silicate powder suspensions. The silicas resulting from these sol-gel processes are termed *Type V* when the final product is fully dense and *Type VI* if the densification process is purposely not completed and the resulting material retains a degree of porosity. Type V materials can be prepared by both of the methods described above, Type VI materials are prepared primarily from the alkoxide method i.e. method 1. (Types I to IV are related to fused quartz and synthetic fused silica and do not involve organic polycondensation reactions).

The driving force for the development of sol-gel silica are mainly related to the advantages of net-shape processing (i.e. casting) versus the traditional methods. For example, sol-gel techniques enable the preparation of complex geometries with a reduced requirement for grinding and polishing. Improved properties can also be achieved in the final products such as, for Type V silicas, higher optical transmission, no absorption due to H₂O or OH bands and fewer defects. The advantages claimed for the transparent porous structures (i.e. Type VI silicas) include the potential for impregnation with organic polymers and controlled chemical doping.

Scaleup of sol-gel processing to manufacture net shape optics with high reliability was eventually made possible by paying particular attention to drying control (in particular during the transition between filled pores and pore emptying), defect control (for example, the elimination of bubbles in the precursor) and atmosphere control (the use of halogen-containing gases to enhance the dehydroxylation process). A range of Gelsil[®] gel-silica optical components are now available from Geltech, Inc..

Chapter 3 deals mainly with the fully densified Type V gel-silica optics, since these are designed to replace the traditionally available optical components. Few details are given regarding the Type VI gel silicas which, by virtue of their porosity, would be most useful in FOCS. What is noteworthy, however, is that a processing temperature of over 600°C is indicated for the preparation of the porous material (exposure time not detailed). This implies that incorporation of an sensing indicator at the precursor stage is probably not possible but it does potentially permit the impregnation and immobilisation of an indicator in a manner to that described in this thesis for porous glass.

In Chapter 23, Avnir et al. review past results and recent work related to chemical sensing applications of doped sol-gel glasses. One of the notable drawbacks of sol-gel technology relates to the fracture of monolithic glasses during gelation or drying or upon immersion in aqueous solutions. Doping of sol-gel glasses with a few percent of quaternary ammonium compounds prevents most of the gelation fracture, improves the leaching stability and reduces the risk of fracture even after repeated wet-dry-wet cycles. The incorporation of fracture prevention agents, however, narrows the window of optical transparency of the sensors and may limit some applications.

The advantages of chemical doping (i.e. incorporation of the organic indicator at the liquid precursor stage) has found popularity mainly as a result of its high versatility enabling, for example, a wide number of reagents to be included in the sol-gel matrix. Another advantage is that doping has less of an impact on the spectral properties of the entrapped reagent because the reagent retains a high degree of mobility as compared to when it is covalently immobilised. The penalty for these advantages is paid by increased leaching of organic reagents from doped glasses placing the long term stability of a doped silica sensor somewhere between absorption (impregnated) and chemically immobilised sensors.

Shahriari and Ding (Chapter 13) consider the stability and chemical durability of silica gel films entrapped with pH indicators at different drying stages on immersion in water, anhydrous ethanol, acetone and benzene. The leaching experiments were performed at room temperature and at 60°C by monitoring the absorption spectra of the surrounding solvents. The preliminary results show that the stability of fully dried silica gel films in all the solvents tested are excellent which highlights a significant difference between the behaviour of films and monoliths. No data are presented relating the stability of the coatings in aqueous solutions of varying pHs.

To summarise, the recent advances made in sol-gel processing indicate that the doping of coatings with analyte-sensitive dyes is much closer to providing useful substrates for

FOCS than the doping of monoliths, since the leaching of indicator from the latter appears to be still unresolved even though the structural and chemical stability of the monoliths may be sufficient. On the other hand, stable porous gel silicas are now commercially available and covalent immobilisation of an indicator should be achievable. Add to this the advantage of being able to prepare optics of relatively complex shapes and the indications are that the immobilisation approach could indeed be very useful in preparing suitable substrates for FOCS. Further advances in reducing the leachability of reagents from monoliths may be possible by using functionalised indicator reagents and structural stability improvements may also be realisable by preparing organic-inorganic polymer blends. Both these ideas are discussed briefly in the next chapter.



Chapter 9

SUGGESTIONS FOR FUTURE WORK

Despite the substantial effort devoted towards the development of optically based sensors there still remains a need for further improvements. In our opinion, the main technical challenges which need to be overcome in order to be able to facilitate the introduction of extrinsic-type FOCS into targeted industrial settings include improved signal-to-noise ratio, stability, longevity, reproducibility, ease of use and cost competitiveness. Below are some suggestions and recommendations.

9.1 The identification and use of analyte sensitive dyes which exhibit a high quantum yield and low photofading ratio.

The aspects of high quantum yield and low photofading ratio are important properties related to the choice of a suitable fluorescing agent since they will greatly impact the sensitivity and longevity of a FOCS respectively. Possibilities which have not been reported in the context of FOCSs include dichlorotriazinylaminofluorescein (DTAF) [51306-35-5]⁸⁴ and fluorescein succinimido ester. The latter compound has been described in work conducted at City University (London) under the supervision of Prof. S. Davidson. It was prepared as follows: a solution of carboxyfluorescein (1g; 2.65 mmole), dicyclohexylcarbodiimide (546 mg; 2.65 mmol) and N-hydroxysuccinimide (305 mg; 2.65 mmole) in 50% dichloromethane in dry THF (30 ml) was left to stand overnight at room temperature. The precipitate of urea was filtered off and the filtrate evaporated to dryness to leave a soft orange powder, melting point 216-218°C. The rate of photofading of a dye is related to the intensity of the excitation light. Consequently, the identification of suitable dyes will enable less intense (lower cost) excitation sources as well as increasing the life-time of sensor as a whole.

9.2 Preparation of true glass substrate using sol-gel method, followed by subsequent immobilisation of sensor reagent.

The main desired outcome of this study was to develop an optimally shaped microporous substrate which is chemically and optically inert in the sensing environment, storage stable and rugged so that it can be handled easily in realistic working conditions and readily derivatisable with the sensing reagent of choice. Although the sol-gel approaches that were considered did not fully achieve this goal, this route still warrants further investigation. In fact,

recent reports indicate that dye-impregnated sol-gel glasses continue to be investigated^{136,137} although it is not clear from these sources whether the sol-gel materials could be re-used after repeated wetting and drying.

After further consideration, it is our opinion that adequate stability will be best achieved if the gels are converted to *true* glasses (i.e. undergo significant gel-to-glass transition). For monoliths and thick coatings this would require thermal treatment at temperatures significantly higher¹¹¹ than the drying procedures described in this and other commonly reported sensor work and would probably prevent the incorporation of an organic reagent at the sol-stage.

The advantage of this approach is that it combines two well known and tested methods i.e. the preparation of a porous glass substrate (coating or monolith) and the derivatisation of a sensing reagent onto porous glass. Stable porous glass monoliths prepared by the sol-gel are now commercially available (Gelsil[®] - see previous chapter), consequently, this approach is quite practicable.

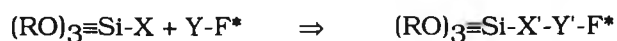
9.3 Organic-Inorganic Polymer Blends to Improve Structural Stability

Novak¹⁴⁴ describes a number of recent advances in the preparation of simultaneous interpenetrating networks by the synchronous formation of both organic polymer and inorganic glass network and the development of "non-shrinking" sol-gel composite formulations. The resultant materials are less likely to fracture during processing and possess mechanical properties which surpass those of other glass-polymer composites. It is unclear if these materials retain a high degree of porosity so their use in liquid media may be limited. On the other hand, the permeation coefficient toward specific gases differs considerably for different polymers¹⁴⁰ and, assuming that appropriate indicator reagents can also be incorporated into these structures, it may be possible to develop gas phase optical sensing materials with unique mechanical properties.

9.4 Alternative routes to immobilise analyte sensing reagents in thin films prepared using sol-gel technology.

The use of analyte sensitive thin films in FOCS will probably be most useful in evanescent wave sensing techniques. Since glassy thin films can be prepared after relatively low heat treatment⁹⁷ the incorporation of an organic sensing reagent is feasible. In the work reported in this thesis, only one route for organically modifying the polysiloxane network (using FITC and 3APTS) was evaluated but many other routes are possible and further investigation into alternative possibilities is justified. A number of the readily available silanes have functional

groups and reactivity profiles which will enable them to be linked to an appropriate sensing agent leading to a general structure which can be represented as follows:-



where R is an alkyl group e.g. CH_3 - or CH_2CH_3 -
X is a group which will react with Y
Y is a group which will react with X
F* is the chromophore containing group, the optical properties of which change with the concentration of the analyte of interest.

The work we carried out focussed on one possibility ($\text{X} = \text{NH}_2$, $\text{Y} = \text{NCO}$ and $\text{F}^* = \text{fluorescein}$) which gave some encouraging results. But given the wide variety of X, Y and F* compounds available it is recommended that a systematic study to be made to identify those groups which when reacted as shown above result in a product, $(\text{RO})_3\text{SiX'Y'-F}^*$, which can be readily incorporated into a solution of $\text{Si}(\text{RO})_4$ and transformed into a gel. Care should be taken to match the hydrolytic reactivities of the two silane products in order to ensure the formation of an homogenous gel. The chemical stability of the organic-inorganic linkages should also be investigated and optimised in order to reduce any tendency of the sensing reagent to leach out of the coating. In this manner it is anticipated that an suitable reagent (F*) will be successfully incorporated into the polysiloxane structure.

This concept can be taken a step further by functionalising the fluorescence reagent itself with appropriate tialkoxysily moieties, $-\text{CH}_2\text{Si}(\text{OR})_3$ and then covalently incorporating these species into the polysiloxane structure of the final gel. For example, in a modification of the 2-step process described in this thesis, FITC could be linked to 3APTS in a *separate* reaction prior to the addition to a sol-gel precursor. Organosilanes with optical properties have already reported for the sol-gel synthesis of components for non-linear optics [Chapter 2 in reference 143].

9.5 Investigate the effect of different pore sizes and particle size distributions of porous glass on fluorescence response.

The rate of reaction and the light scattering properties will be influenced by these two parameters. Since the concentration of reactive groups on the glass surface depends on pore size (figure 5.5), the response to changes in analyte concentrations of an immobilised reagent will also depend on the size of the pores. Further optimisation is therefore likely.

9.6 Optimisation of optical fibre configuration.

One of the limitations of evanescent wave sensing techniques is that the sensing zone is relatively small resulting in a weak signal which consequently requires relatively expensive detection equipment for accurate measurement. In more recent reports, bare porous glass fibres impregnated with analyte sensitive sol-gel coatings have led to increased sensitivity^{9,44}. In our opinion, the sensitivity of these configurations could be further enhanced if a *porous* cladding could be developed which possessed a suitable refractive index such that the analyte sensitive signal in the porous fibre core could undergo total internal reflection. In principle, such a cladding could be prepared using sol-gel techniques since it is known that refractive index can be controlled¹³⁰, although the final cladding porosity would also need to be tailored toward allowing rapid transfer of the analyte from the sensing zone to the fibre core. In the ideal case, the cladding would be itself optically modified to act as a dichroic filter which would be transparent to the excitation light but reflective to the resulting analyte sensitive signal. This would 'trap' that part of the signal which would have been lost because of its angle of incidence to the fibre-cladding interface and would increase the signal-to-noise ratio. Again, sol-gel techniques have been reported which in principle could enable the development of such edgefilters⁹⁷ and the use of reflective coatings to enhance signals in FOCS has also been reported³⁰.

9.7 Above all, focus on developing FOCSs for applications where they are most needed.

Deciding how best to deploy limited resources is a problem which can be tackled in a number of different ways. One approach which is often used in industry is to focus efforts in areas where the perceived 'opportunity' is highest. The mechanism for reaching such a conclusion is quite complex but hinges on identifying where there is a distinct 'need' for a product or service. A 'need' is loosely defined as something which is in demand but cannot be met with existing technology and would, if provided, command a financial premium. Bearing this in mind, it is suggested that future work should focus on the development of FOCS for applications where FOCS can offer distinct and value added advantages over conventional sensing techniques. These applications will be the ones which benefit most from the unique advantages that FOCS can provide such as the ability to be used invasively and remotely, selectivity (e.g. evanescent wave sensing in immunological assaying techniques¹⁵) and safe handling potential (see also section 2.3.1). Specifically, it is recommended that further investigations be concentrated in the areas of immunosensors for medical diagnostics, industrial chemical hazard and process monitoring and environmental monitoring.



REFERENCES

1. Hampartsoumian E. and Williams A. *J. Inst. Energy*, 159(1985).
2. Jones B. E. *J. Phys. E: Sci. Instrum.* **18**, 770(1985).
3. Kawahara F. K. and Fiutem R. A. *Anal. Chim. Acta* **151**, 315(1983).
4. Newby K., Reichert W.M., Andrade J.D. and Benner R.E. *Appl. Optics* **23**, 1812(1984).
5. Badini G.E., Grattan K.T.V. and Tseung A.C.C. *Conference on Lasers and Electro-Optics (CLEO)*, 1989.
6. *New Scientist* **25.4.92**.
7. Wilson J. and Hawkes J.F.B. *Optoelectronics: An Introduction* (Prentice Hall, New Jersey, 1983).
8. Rhines T.D. and Arnold M.A. *Anal. Chem.* **60**, 76(1988).
9. Shahriari M.R., Zhou Q. and Sigel G.H. Jr. *Opt. Letters* **13**, 407(1988).
10. Siemens Research Laboratories, Munich, Data Sheet B3-B3314-x-x-7600.
11. Benaim Nira, Grattan K.T.V. and Palmer A.W. *Analyst* **111**, 1095(1986).
12. Schulze J.E., *EU PAT 252 578 1988*.
13. *New Scientist* **14.12.91**.
14. *Quartz & Silice*, Promotional Leaflet "F1".
15. Bluestein B.I., Walczak I.M. and Chen S.Y. *Trends Biotechnol.* **8**, 161(1990).
16. Love W.F., Walczak I.M. and Slovacek R.E. *Springer Proc. in Physics* **44**, 431(1989).
17. Wolfbeis O.S. *Molecular Luminescence Spectroscopy 1988*, **2**, 129 (Schulman S.G. Ed., John Wiley & Sons, New York).
18. Smardzeski R.R. *Talanta* **35**, 95(1988).
19. Kirkbright G.F., Narayanaswamy R. and Welti N.A. *Analyst*, **109**, 1025(1984).
20. Promotional Literature, Technologies Incorporated, P.O. Box 325, New Jersey USA.
21. Wolfbeis O.S. *Analytical Uses of Immobilised Biological compounds for Detection, Medical and Industrial Uses* **17**, 219(1988) (Guilbault G.G. and Mascinin M. Eds., Reidel).
22. Angel S.M. *Spectroscopy* **2**, 38(1987).
23. Cowles T.J., James N.M., Desiderio R.A. and Angel S.M. *Appl. Optics* **28**, 595(1989).
24. Roe J.N. and Hirschfeld T. *Int. J. Optoelect.* **3**, 289(1988).
25. Mouaziz Z. *et al. Sens. Actuators*, **B11**, 431(1993).
26. Zung J.B., Woodlee R.L., Fuh M-R.S. and Warner I.M. *SPIE (Chemical, Biochemical and Environmental Applications of Fibers)*, **990**, 49(1988).
27. Perihan Ç and Narayanaswamy R. *Analyst* **112**, 1285(1987).
28. Guthrie A.J., Narayanaswamy R. and Welti N.A. *Talanta*, **35**, 157(1988).
29. Klainer S.M., *WO PT 90/09602 1990*.
30. Milo C.S., *EU PAT 529 247 A2 1993*.
31. Arakawa Y., Fukunaga H. and Inaba H. *Proc. Optical Fibre Sensors OFS'86*, 127(1986).
32. Zhujun Z. and Seitz W.R. *Anal. Chim. Acta* **160**, 305(1984).
33. East Ger. Pat. 106,086 (from 17).
34. Fuh M-R. S., Burgess L.W., Hirschfeld T., Christian G.D. and Wang F. *Analyst* **112**, 1159(1987).
35. Kawabata Y., Imasaka T. and Ishibashi N. *Proc. Optical Fibre Sensors OFS'86*, 139(1986).
36. Macedo P.B. *et al. SPIE (Fiber Optic Smart Structures and Skins 986)*, 200(1988).
37. Shahriari M.R., Zhou Q. and Sigel G.H. Jr. *Opt. Letters* **5**, 407(1988).
38. Tromberg B.J. and Dinh T.V. *SPIE (Optical fibers in Medicine III)* **906**, 30(1988).
39. Lieberman R.A. and Brown K.E. *SPIE (Chemical, Biochemical and Environmental Applications of Fibers)* **990**, 104(1988).
40. Narayanaswamy R. and Sevilla F. III *J. Phys. E:Sci. Instrum.* **21**, 10(1988).
41. Bacci M., Baldini F., Cosi F., Conforti G. and Scheggi A.M. *Springer Proc. in Physics* **44**, 425(1989).
42. Zhujun Z. and Seitz W.R. *Anal. Chem.* **58**, 220(1986).
43. Çaglar P. and Naryanaswamy R. *Analyst* **112**, 1285(1987).
44. Zhou Q., Shahriari R.S., Kritz D. and Sigel G.H. Jr. *Anal. Chem.* **60**, 2318(1988).
45. Willard H.H., Meritt L.L. Jr., Dean J.A. and Settle F.A. *Instrumental Methods of Analysis*, 6th Edition, Wadsworth (California), 1981.
46. Lee E.D., Werner T.C. and Seitz W.R. *Anal. Chem.* **59**, 279(1987).
47. Shulze J.E., *EU PAT 252 578 1988*.

48. Yuan P. and Walt D.R. *Anal. Chem.* **59**, 2391(1987).
49. Wolfbeis O.S. and Posh H.E. *Anal. Chem.* **57**, 2556(1985).
50. Petrea R.D. and Sepaniak M.J. *Talanta* **35**, 139(1988).
51. Tuan V.D., Nolan T., Cheng Y.F. and Sepaniak M.J. *Proc. SPIE-Int. Soc. Opt. Eng. (Chemical, Biochemical, Environmental Fiber Sensors)* **1172**, 266(1990).
52. Papkovsky D.B., Olah J. and Kurochkin I.N. *Sens. Actuators* **B11**, 525(1993).
53. Varineau P.T., Duesing R. and Wangen L.E. *Appl. Spectrosc.* **45**, 1652(1991).
54. Thompson R.B. and Lakowicz J.R. *Anal. Chem.* **65**, 853(1993).
55. Lieberman S.H., Inman S.M. and Theriault G.A. *Proc. SPIE-Int. Soc. Opt. Eng. (Chem. Biochem. Environ. Fiber. Sens)* **1172**, 94(1990).
56. Reichert W.M., Suci O.A., Ives J.T. and Andrade J.D. *Appl. Spectrosc.* **41**, 503(1987).
57. Love W.F., Walczak I.M. and Slovacek R.E. *Springer Proc. in Physics* **44**, 431(1989).
58. Newby K., Reichert W.M., Andrade J.D. and Benner R.E. *Appl. Optics* **23**, 1812(1984).
59. DeGradpre M.D. *Diss. Absr. Int. B 1991* **51**, 1990.
60. Conzen J.P., Buerck J. and Ache H.J. *Appl. Spectrosc.* **47**, 753(1993).
61. Bhatia S.K., Thomspson R.B., Shriver-Lake L.C., Levine M. and Ligler F.S. *SPIE (Fluorescence Detection III)* **1054**, 184(1989).
62. Jordan D.M., Walt D.R. and Milanovich F.P. *Anal. Chem.* **59**, 437(1987).
63. Meadows D. and Schultz J.S. *Talanta* **35**, 145(1988).
64. Meadows D. and Schultz J.S. *Anal. Chim. Acta* **280**, 21(1993).
65. Peterson J.I. *SPIE (Chem. Biochem. Environ. Appl. Fibers)* **990**, 2(1988).
66. Bacci M., Baldini F., Cosi F., Conforti G. and Scheggi A.M. *SPIE (Micro-Optics)* **1014**, 73(1988).
67. Wolfbeis O.S., Furlinger E., Krenais H. and Marsoner H. *Fresenius Z Anal. Chem.* **314**, 119(1983).
68. Besar S.S.A., Kelly S.W. and Greenhalgh P.A. *Int. J. Optoelect.* **3**, 381(1988).
69. Harper G.B. *Anal. Chem.* **47**, 348(1975).
70. Johnson J.I., Goldstein S.R. and Fitzgerald R.V. *Anal. Chem.* **52**, 864(1980).
71. Saari L.A. and Seitz W.R. *Anal. Chem.* **54**, 821(1982).
72. Hirschfeld T. *EU PAT 247 261*, 1987.
73. Sharma B., Bailey L.F. and Messing R.A. *Angew. Chem. Int. Ed. Engl.* **21**, 837(1982).
74. Bacci M., Baldini F. and Scheggi A.M. *Anal. Chim. Acta* **207**, 343(1988).
75. Zemskii V.I., Kolesnikov Y.L. and Meshkovskii I.K. *Opt. Spectrosc. (USSR)* **60**, 574(1986).
76. Wolfbeis O.S. and Offenbacher H. *Sens. Actuat.* **9**, 85(1986).
77. P.C.G. Danby *Electronic Engineering January 1970* (Brookdeal Electronics (now part of EG&G))
78. Wolfbeis O.S. *Springer Proc. Physics* **44**, 416(1989).
79. C Technologies Incorporated, P.O. Box 325, Short Hills, NJ 07078.
80. Adams A.P. and Hahn C.E.W. *Principles and practice of Blood-Gas Analysis* (Churchill Livingstone, New York, 1982)
81. Weetall H.H., *US PAT 3,652,761 1972*
82. Jones N. *Comprehensive organic Chemistry* (Pergamon Press, 1979).
83. Martin M.M and Lindqvist L. *J. Luminesc.* **10**, 381(1975)
84. Blakeslee D. *J. Immun. Methods* **17**, 361(1977).
85. Rendell D. *Fluorescence and Phosphorescence* (John Wiley & Sons, Chichester, 1987).
86. Hood H.P. and Nordberg M.E., *U.S. PAT 2,106,744 1938*
87. Haller W., *US PAT 3,549,524, 1970*
88. Iler R.K. *The Chemistry of Silica* (John Wiley & Sons, New York, 1979).
89. Gilpen R.K. and Burke M.F. *Anal. Chem.* **45**, 1383(1973).
90. Matlin S.A., Lloret,A., Lough W.J., Bryan D.G., Browne T. and Mehani S. *J. HRC & CC* **4**, 81(1981).
91. Davidson R.S., Lough W.J., Matlin S.A. and Morrison C. L. *J.C.S. Chem. Comm.* 517(1981).
92. Leyden D.E. and Dollins W.T. (Eds) *Silylated Surfaces 1980*, (Gordon & Breach Science Publishers, 1980)
93. Voronkov V.G., Mileshekevich and Yuzhelvski Yu A. *The Siloxane Bond*, (Consultants Bureau, New York, 1978)
94. Ealing Electro-Optics *Product Guide*, 232(1981-1988).
95. Matlin S.A., Tinler J.S., Lloret A.T., Lough W.J., Chan L. and Bryan D. *Proc. Analyt. Div. chem. Soc.* **16**, 354 (1979).

96. Moses P.R., Wier L.M., Lennox J.C., Finklea H.O., Lenhard J.R. and Murray R.C. *Anal. Chem.* **50**, 576(1978).
97. Dislich H. *Sol-Gel Technology for Thin Films, Fibers, Preforms, Electronics and Speciality Shapes 1988*, (Klein L. C. Ed., Noyes Publications, New Jersey).
98. Woodhead J.L and Segal D.L. *Chem. Britain*, 310(1984).
99. Fletcher J.M. and Hardy C.J. *Chem. Industry*, 48(1968).
100. Avnir D., Levy D. and Reisfeld R. *J. Phys. Chem.* **88**, 5956(1984).
101. MacCraith B.D., McDonagh C.M., O'Keeffe G., Keyes E.T., Vos J.G., O'Kelly B. and McGilp J.F. *Analyst* **118**, 385(1993).
102. Dislich H. *J. Non-Cryst. Solids* **73**, 599(1985).
103. Sakka S. *Am. Ceram. Soc. Bull.* **64**, 463(1985).
104. Scholze H. *J. Non-Cryst. Solids* **73**, 669(1985).
105. Mukherjee S.P. *J. Non-Cryst. Solids* **63**, 35(1984).
106. Brinker C.J. and Scherer G.W. *J. Non-Cryst. Solids* **70**, 301(1985).
107. Scherer G.W. *Yogyo-Kyokai-Shi* **95**, 21(1987).
108. Brinker C.J. *J. Non-Cryst. Solids* **100**, 31(1988).
109. Zelinski B.J. and Uhlmann D.R. *J. Phys. Chem. Solids* **45**, 1069(1984).
110. MacCraith B.D., Ruddy V., Potter C., O'Kelly B. and McGilp J.F. *Electr. Letters* **27**, 1247(1991).
111. Jones N. *Comprehensive Organic Chemistry 1979* (Pergamon Press).
112. Klein L.C. *Ann. Rev. Mater. Sci.* **15**, 227(1985).
113. Kozuka H., Kuroki H. and Sakka S. *J. Non-Cryst. Solids* **101**, 120(1988).
114. Scherer G.W. *J. Non-Cryst. Solids* **99**, 324(1988)
115. Hench L.L. *Science of Ceramic Chemical Processing 1986*, (Hench L.L and Ulrich D.R. Eds., Wiley, New York).
116. Adachi T. and Sakka S. *J. Non-Cryst. Solids* **99**, 118(1988).
117. Grimmer A.-R., Rosenberger H., Bürger H. and Vogel W. *J. Non-Cryst. Solids* **99**, 371(1988).
118. Gesser H.D. and Goswami P.C. *Chem. Rev.* **89**, 765(1989).
119. Hrubesh L.W. *Chem. Industry*, 824(1990).
120. Brinker C.J. and Mukherjee S.P. *Thin Solid Films* **77**, 141(1981).
121. Yamane M. *Sol-Gel Technology for Thin Films, Fibers, Preforms, Electronics and Speciality Shapes 1988*, (Klein L. C. Ed., Noyes Publications, New Jersey).
122. Kawaguchi T., Hishikura H., Iura J. and Kokubu Y. *J. Non-Cryst. Solids* **63**, 61(1984).
123. Osaka A. *et al. J. Non-Cryst. Solids* **100**, 409(1988).
124. Wang S.H. and Hench L.L. *Science of Ceramic Chemical Processing 1986*, (Hench L.L and Ulrich D.R. Eds., Wiley, New York).
125. Avnir D., Kaufman V.R. and Reisfeld R. *J. Non-Cryst. Solids* **74**, 395(1985).
126. Knobbe E.T., Dunn B. and Gold M. *SPIE (Optical Fibers in Medicine III)* **90**, 39(1988).
127. Kaufman V.R., Avnir D., Rojanski-Pines D. and Huppert D. *J. Non-Cryst. Solids* **99**, 9(1988).
128. Mukherjee S.P. and Lowdermilk W.H. *J. Non-Cryst. Solids* **48**, 177(1982).
129. Debsikdar J.C. *J. Non-Cryst. Solids* **91**, 262(1987).
130. Yoldas B.E. *Appl. Optics* **21**, 2960(1982).
131. Mohallem N.D.S. and Aegerter M.A. *J. Non-Cryst. Solids* **100**, 526(1988).
132. Pettit R.B., Ashley C.S., Reed S.T. and Brinker C.J. *Sol-Gel Technology for Thin Films, Fibers, Preforms, Electronics and Speciality Shapes 1988*, (Klein L. C. Ed., Noyes Publications, New Jersey).
133. Payne H. F. *Organic Coating Technology Volume 1 1954*, (John Wiley and Sons).
134. Grattan K.T.V., Badini G.E., Palmer A.W., Tseung A.C.C. *Sens. Actuators A26*, **483(1991)**.
135. Ding J., Tong J., Shahriari M.R. and Sigel G.H., Jr. *SPIE* **1761**, 175(1992).
136. O'Keeffe G. *et al.*, "Development of an intrinsic phase fluorimetric oxygen sensor using a high intensity blue LED", *Optical Fibre Sensors Conference - Glasgow 11th - 13th October 1994*.
137. Wallace P.A., Yang Y. and Cambell M. "Application of sol-gel processes for fibre optic chemical sensor development", *Optical Fibre Sensors Conference - Glasgow 11th - 13th October 1994*.
138. Shukla B.S. and Johari G.P. *J. Non-Cryst. Solids* **101**, 263(1988).
139. Ruddy V., McCraith B. and McCabe S. *SPIE (Fiber Optic Sensors IV)* **1267**, 97(1990).
140. Wolfbeis O.S. *Fiber Optic Chemical Sensors and Biosensors* **1**, CRC Press, 1991.

141. McGlip J., O.Kelly B., McCraith B. and Ruddy V. WO PAT 92/15862, 1992.
142. Turner A.P.F., Karube I. and Wilson G.S. (Eds) *Bioensors - Fundamentals and Applications* **1987**, Oxford University Press, Oxford.
143. Klein L.C. (Ed) *Sol-Gel Optics: Processing and Applications* **1994**. Kluwer Academic Publishers, Massachusetts.
144. Novak B.M. *Adv. Mater.* **5(6)**, 422(1993).



APPENDIX

optical fibre characteristics

APPENDIX III.1

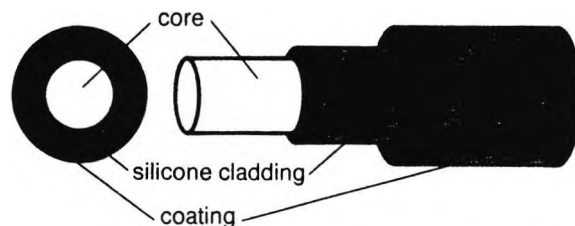
STEP INDEX
MULTIMODE
FIBRES

PCS fibres

plastic clad silica

PCS fibres consist of:

- a silica core
- a silicone resin optical cladding
- an ETFE protective coating



Range:

Fibres PCS 200 A PCS 300 A PCS 600 W
 PCS 200 W PCS 300 W PCS 1000 W

Characteristics		PCS 200 A PCS 200 W	PCS 300 A PCS 300 W	PCS 600 W	PCS 1000 W
Core diameter	μm	200 ± 8	300 ± 12	600 ± 24 $r = 300$	1000 ± 40 $r = 500$
Cladding diameter	μm	380 ± 30	440 ± 35	750 ± 60 $t_1 = 75$	1260 ± 100 $t_1 = 130$
Core-cladding excentricity	μm	20	20	30	mini thickness 80
Coating diameter	μm	600 ± 48	650 ± 52	1060 ± 85 $t_2 = 155$	1550 ± 155 $t_2 = 145$
Numerical aperture (theoretical maximum)		0.4	0.4	0.4	0.4
Guaranteed attenuation at 0.85 μm	dB/km	PCS 200 A : 8 PCS 200 W : 12	PCS 300 A : 8 PCS 300 W : 12	12	
Mechanical strength (screen test)	GPa kpsi	0.32 45	0.32 45	0.32 45	
Bandwidth	MHz.km	14			
(typical value at 0.85 μm)	MHz.300 m	40			

Bandwidth measurement conditions:

- The fibre is wound unto the transit reel which may effect the measured value (cabled fibre might display a slightly different bandwidth)
- $\lambda = 0.85 \mu\text{m}$
spot diameter \geq fibre diameter
source N.A. = equilibrium N.A.
lambertian source

N.B. - With the source N.A. < equilibrium N.A., bandwidth rather higher than the typical values indicated is obtained, e.g. using an edge-LED

Delivery Standard lengths	PCS 200 A : 2200 m 1100 m	1100 m other lengths on request	600 m 400 m 200 m	5 to 200 m
	PCS 200 W : 1100 m other lengths on request			
Transit reel	SD 300	SD 300	PE 500	PE 500

Appendix III.2

- D1. Screen print of program DATALOG.
- D2. Program listing for DATALOG.
- M1. Screen print of program MANUALOG.
- M2. Program listing for MANUALOG.
- A1. Screen print of program AUTOLOG.
- A2. Program listing for AUTOLOG.

A1: READY

File: DATALOG

A B C D E F G H

WELCOME TO "DATALOGGER"

G. E. Badini 1988

21-Nov-93 11:15 AM

A21: MENU

1 2 123
Manual mode

A B C D E F G H

DATALOGGER will record any measurements that are made using a device which complies with the IEEE-488 standard.

There are two main modes of operation:-

1- Manual mode

2- Automatic mode

In the former mode (1), an "x-parameter" has to be entered manually (possible uses include calibration of instruments).

When the program is used in its automatic mode (2), the sampling rate (to the nearest 10 seconds) and the total run time have to be entered. (Possible applications include monitoring of experimental voltage outputs).

<<Move cursor over required option and press return.>>

21-Nov-93 11:16 AM CMD

D1.1

I1: READY

I J K L M N O P

1
2 \O /XCset-up-
3 \A /XCintro-
4 {IF choicel=2}/XG\D-
5 \C /XCmanualog-
6 \D /XCautolog-
7
8
9
10
11
12
13
14
15
16
17
18
19
20

21-Nov-93 03:03 PM

I26: READY

I J K L M N O P

21 set-up: {APPL}NRDVM2-Q
22 (\O) {GOTO}page1-{WAIT @NOW+@TIME(00,00,05)}
23
24 intro: {GOTO}page2-/XMJ25-
25 (\A) 1 2 123
26 Manual moAutomaticLeave macro and go to READY mode.
27 {LET choi{LET choi/XQ
28 /XR
29 choicel= 2
30
31
32
33
34
35
36

37 snglin: /FRmanualog-
38 (\C)
39 multiin: /FRautolog-
40 (\D)
21-Nov-93 03:03 PM

D1.2

```

P1: '-
I2: '\0
J2: '/XCset-up-
I3: '\A
J3: '/XCintro-
J4: '{IP choice1=2}/XG\D-
I5: '\C
J5: '/XCmanualog-
I6: '\D
J6: '/XCautolog-
C8: \-
D8: \-
E8: \-
F8: \-
C9: '
G9: '
C10: '
D10: 'WELCOME TO "DATALOGGER"
G10: '
C11: '
G11: '
C12: '
D12: ' G. E. Badini 1988
G12: '
C13: '
G13: '
C14: \-
D14: \-
E14: \-
F14: \-
I21: 'set-up:
J21: '{APP1}NRDVM2-Q
B22: 'DATALOGGER will record any measurements that are made
I22: '\0
J22: '{GOTO}page1-,WAIT @NOW+@TIME(00,00,05)}
B23: 'using a device which complies with the IEEE-488 standard.
I24: 'intro:
J24: '{GOTO}page2-/XMJ25-
B25: 'There are two main modes of operation:-
I25: '\A
J25: 1
K25: 2
L25: '123
J26: 'Manual mode
K26: 'Automatic mode
L26: 'Leave macro and go to READY mode.
B27: *1-
C27: 'Manual mode
J27: '{LET choice1,1}
K27: '{LET choice1,2}
L27: '/XQ
J28: '/XR
B29: *2-
C29: 'Automatic mode
K29: 'choice1=

```

```

B32: 'In the former mode (1), an "x-parameter" has to be entered
B33: 'manually (possible uses include calibration of instruments).
B35: 'When the program is used in its automatic mode (2), the
B36: 'sampling rate (to the nearest 10 seconds) and the total run
B37: 'time have to be entered. (Possible applications include
B38: 'monitoring of experimental voltage outputs).
I38: 'snqlin:
J38: '/FRmanualog-
I39: '\C
B40: '<<Move cursor over required option and press return.>>
I41: 'multiin:
J41: '/FRautolog-

```

A1: [W10] '

READY

File: MANUALOG

A B C D E F G H

1
2
3
4
5
6
7
8
9
10
11
12
13
14
15
16
17
18
19
20

Manual Sampling Routine

21-Nov-93 11:33 AM

CAPS

A21: [W10]

MENU

1 2

Use only the HP 3478A Multimeter.

A B C D E F G H

21
22
23
24
25
26
27
28
29
30
31
32
33
34
35
36
37
38
39
40

The routines have been written for use with one or both of the following IEEE compatible Digital Multimeters:-

1. Hewlett-Packard 3478A
2. Hewlett-Packard 3438A

The above have both been installed and configured to be used with Lotus Measure. Any other suitable instruments can be used as long as the appropriate software setting-up procedure is performed. Furthermore, the first line of the \0 macro in the program DATALOG will also have to be changed.

If only one of the above Digital Multimeters is used, it is assumed to be the first one.

Please use the cursor indicate how many multimeters you will use and then press RETURN.

21-Nov-93 11:33 AM

CMD

CAPS

11,1

A57: [W10] '

MENU

Procede Change

No parameter changes required.

A B C D E F G H

41
42
43
44
45
46
47
48
49
50
51
52
53
54
55
56
57
58
59
60

MULTIPLE READINGS MODE

Date: 21-Nov-93
Title of experiment:EXAMPLE EXPERIMENT (max. 35 chars)
File name:EXAMPLE2
Title of first Y parameter: Y11
Title of second Y parameter (RETURN if none): Y22
Title of X parameter (manual input): X11

Comments (do not type off the screen; max 3 lines):

THIS IS ANOTHER EXAMPLE FOR THE REPORT

21-Nov-93 11:35 AM

CMD

CALC

CAPS

A77: [W10]

READY

A B C D E F G H

61
62
63
64
65
66
67
68
69
70
71
72
73
74
75
76
77
78
79
80

EXAMPLE EXPERIMENT

21-Nov-93

File : EXAMPLE2

THIS IS ANOTHER EXAMPLE FOR THE REPORT

X11 Y11 Y22 Sample Number : 0

21-Nov-93 11:35 AM

CAPS

11,2

MANUAL 100

I1: READY

```

I      J      K      L      M      N      O      P
1
2 \O      /XCtitles-
3 \R      /XCranges-
4 \A      /XCchoose-
5 \B      /XCinfoin-
6 \C      /XCcheck-
7 \D      /XCinit-
8 \E      /XCmenu-
9 \P      /XCdatain-
10
11
12
13
14
15
16
17
18
19
20
21-Nov-93 03:04 PM

```

I21: READY

```

I      J      K      L      M      N      O      P
21
22
23
24
25
26
27
28
29
30
31
32
33 titles: (APP1)NRDVN2-Q
34 (\O)    {GOTO}page1-
35         (WAIT @NOW+@TIME(00,00,05))
36         /XR
37
38 ranges: /RNCstart-A80-
39 (\R)    /XR
40
21-Nov-93 03:04 PM

```

M1.3

I41: READY

```

I      J      K      L      M      N      O      P
41
42
43
44
45
46
47
48 choose: {BLANK info1}{BLANK comms}{BLANK a75..c3280}      2
49 (\A)    (LET flag,0){GOTO}page2-
50         /XNJ52-
51
52         1      2
53         Use only Use both the HP 3478A and HP 3438A Multimeters.
54         (LET choi(LET choice2,2)
55
56
57
58
59
60
21-Nov-93 03:05 PM

```

I61: 'infoin: READY

```

I      J      K      L      M      N      O      P
61 infoin: {GOTO}page3-
62 (\B)    {GOTO}C46-{GETLABEL "Enter the title of the experiment: ",C46}/
63         {GOTO}B47-{GETLABEL "Enter file name (8 chars max.): ",B47}/RMC
64         {GOTO}D49-{GETLABEL "",D49}/RMCcell-D49-/XCerr1-
65         {GOTO}P50-{GETLABEL "",P50}{IP choice2=2}/RMCcell-P50-/XCerr1-{
66         {GOTO}E51-{GETLABEL "",E51}/RMCcell-E51-/XCerr1-
67         {GOTO}A55-{GETLABEL "",A55}
68         {GOTO}A56-{GETLABEL "",A56}
69         {GOTO}A57-{GETLABEL "",A57}
70         /XG\C-
71
72
73
74 check:  (LET flag,1)/XNJ75-
75         (\C)    Procede Change
76         No parameChange one or more of the parameters.
77         /XR      /XNK78-
78         All      Title      File      1-Y1      2-Y2      X
79
80         (LET flag/XGJ62- /XGJ63- /XGJ64- /XGJ65- /XGJ66-
21-Nov-93 03:06 PM

```

M1.4

I81: READY

```

      I      J      K      L      M      N      O      P
81          /XG\A-
82
83      flag =      0
84
85
86
87  init: {INIT}
88  (\D)  {CLEAR 3478A}
89        {IF choice2=2}{CLEAR 3438A}
90        {GOTO}page4-
91        {GOTO}start-
92        /XR
93
94
95  menu: {GOTO}page4-{GOTO}A80-/XNJ96-
96  (\E)  Go      Repeat Save      Plot      123
97        Begin theRepeat thSave the Plot an rReturn to READY mode.
98        /XR      /XG\A- {GOTO}A61{GOTO}A75/XQ
99                /FXV      0
100
21-Nov-93 03:06 PM

```

I101: READY

```

      I      J      K      L      M      N      O      P
101          -(PGDM){ETP{ESC}
102          /XG\E-      0
103          -LA{ESC}
104          0
105          ~
106          LB{ESC}
107          0
108  datain: /WGRM      -QQ
109  (\F)  {GOTO}A75-      {GRAPH}/XG\E-      75 counter
110        {POR counter,76,3075,1,routine2}
111        {LET counter,75}
112        /XG\E-
113
114        ERR
115        {IF A75=9999}{BLANK A75}{GOTO}start-/XGJ111-
116        {NREAD 3478A,B75,1}
117        {IF choice2=2}{TRIGGER 3438A}{NREAD 3438A,C75}
118        {CALC}
119        {GOTO}A75-
120        {RETURN}
21-Nov-93 03:06 PM

```

M1.5

I121: 'err1: READY

```

      I      J      K      L      M      N      O      P
121  err1: {IF (@LENGTH(cell)>0#AND#@LENGTH(cell)<35#AND#flag<>1)}/XR
122        {IF (@LENGTH(cell)>0#AND#@LENGTH(cell)<35#AND  $C$46 /XGj62-
123        {BEEP 2}      $B$47 /XGj63-
124        /XGj66-      $D$49 /XGj64-
125        $E$51      $F$50 /XGj65-
126        0      $E$51 /XGj66-
127        ERR      ?      32323.68 /XGJ80-
128        ?      $B$87 /XGJ81-
129        ?      $D$89 /XGJ82-
130
131
132
133
134
135
136
137
138
139
140
21-Nov-93 03:07 PM

```

M1.6

```

A1: [W10] '
I2: '\0
J2: '/XCtitles-
I3: '\R
J3: '/XCranges-
I4: '\A
J4: '/XCchoose-
I5: '\B
J5: '/XCinfoin-
I6: '\C
J6: '/XCcheck-
I7: '\D
J7: '/XCinit-
I8: '\E
J8: '/XCmenu-
I9: '\F
J9: '/XCdatain-
C10: \-
D10: \-
E10: \-
F10: \-
B11: [W10] "
C11: ' Manual Sampling Routine
G11: [W7] '|
C12: \-
D12: \-
E12: \-
F12: \-
B22: [W10] 'The routines have been written for use with one or both of
B23: [W10] 'the following IEEE compatible Digital Multimeters:-
B25: [W10] ' 1. Hewlett-Packard 3478A
B26: [W10] ' 2. Hewlett-Packard 3438A
B28: [W10] 'The above have both been installed and configured to be
B29: [W10] 'used with Lotus Measure. Any other suitable instruments
B30: [W10] 'can be used as long as the appropriate software setting-up
B31: [W10] 'procedure is performed. Furthermore, the first line
B32: [W10] 'of the \0 macro in the program DATALOG will also have to be
B33: [W10] 'changed.
I33: 'titles:
J33: '{APP1}NRDVM2-Q
I34: '\0
J34: '{GOTO}page1-
B35: [W10] 'If only one of the above Digital Multimeters is used, it is
J35: '{WAIT @NOW+@TIME(00,00,05)}
B36: [W10] 'assumed to be the first one.
J36: '/XR
B38: [W10] 'Please use the cursor indicate how many multimeters you will
I38: 'ranges:
J38: '/RNCstart-A80-
B39: [W10] 'use and then press RETURN.
J39: '/XR
B42: [W10] 'MULTIPLE READINGS MODE
B43: [W10] \-
C43: \-
D43: '---
A45: [W10] 'Date:
B45: (D1) [W10] @DATEVALUE(@NOW)
A46: [W10] 'Title of experiment:
C46: 'EXAMPLE EXPERIMENT
G46: [W7] '(max. 35 chars)

```

```

A47: [W10] 'File name:
B47: [W10] 'EXAMPLE2
I48: 'choose:
J48: '(BLANK info1){BLANK comms}{BLANK a75..c3280}
O48: 1
A49: [W10] 'Title of first Y parameter:
D49: 'Y11
I49: '\A
J49: '{LET flag,0}{GOTO}page2-
A50: [W10] 'Title of second Y parameter (RETURN if none):
F50: 'Y22
J50: '/XWJ52-
A51: [W10] 'Title of Y parameter (manual input):
E51: 'X11
J52: 1
K52: 2
J53: 'Use only the HP 3478A Multimeter.
K53: 'Use both the HP 3478A and HP 3438A Multimeters.
A54: [W10] 'Comments (do not type off the screen; max 3 lines):
J54: '{LET choice2,1}
K54: '{LET choice2,2}
A55: [W10] '
A56: [W10] 'THIS IS ANOTHER EXAMPLE FOR THE REPORT
A57: [W10] '
I61: 'infoin:
J61: '{GOTO}page3-
B62: [W10] \-
C62: \-
D62: \-
E62: \-
F62: \-
G62: [W7] \-
I62: '\B
J62: '{GOTO}C46-(GETLABEL "Enter the title of the experiment: ",C46)/RNCcell-C46-/XCerr1-
A63: [W10] "
B63: [W10] @REPEAT(" ",(55-@LENGTH(@INDEX(INP01,1,0)))/2)&@INDEX(INP01,1,0)
B63: '|'
J63: '{GOTO}B47-(GETLABEL "Enter file name (8 chars max.): ",B47)/RNCcell-B47-/XCerr1-
B64: [W10] \-
C64: \-
D64: \-
E64: \-
F64: \-
G64: [W7] \-
J64: '{GOTO}D49-(GETLABEL "",D49)/RNCcell-D49-/XCerr1-
J65: '{GOTO}F50-(GETLABEL "",F50){IF choice2=2}/RNCcell-F50-/XCerr1-{IF flag=1}/XG\C-
B66: (D1) [W10] +B45
F66: +* File : "%&@INDEX(INP01,0,1)
J66: '{GOTO}E51-(GETLABEL "",E51)/RNCcell-E51-/XCerr1-
J67: '{GOTO}A55-(GETLABEL "",A55)
J68: '{GOTO}A56-(GETLABEL "",A56)
J69: '{GOTO}A57-(GETLABEL "",A57)
A70: [W10] +A55
J70: '/XG\C-
A71: [W10] +A56
A72: [W10] +A57
A74: [W10] @INDEX(INP01,3,5)
B74: [W10] @INDEX(INP01,2,3)
C74: @INDEX(INP01,4,4)
E74: +*Sample Number : "%&@STRING(COUNTER-75,0)

```

M2,7

M2,2

```

I74: 'check:
J74: '{LET flag,1}/XNJ75-
I75: '{\C)
J75: 'Procede
K75: 'Change
J76: 'No parameter changes required.
K76: 'Change one or more of the parameters.
J77: '/XR
K77: '/XMK78-
K78: 'All
L78: 'Title
M78: 'File
N78: '1-Y1
O78: '2-Y2
P78: 'X
K79: +""
L79: +""
M79: +""
N79: +""
O79: +""
K80: '{LET flag,0)
L80: '/XGJ62-
M80: '/XGJ63-
N80: '/XGJ64-
O80: '/XGJ65-
P80: '/XGJ66-
K81: '/XG\A-
J83: 'flag =
K83: 1
I87: 'init:
J87: '{INIT)
I88: '{\D)
J88: '{CLEAR 3478A)
J89: '{IF choice2=2){CLEAR 3438A)
J90: '{GOTO}page4-
J91: '{GOTO}start-
J92: '/XR
I95: 'menu:
J95: '{GOTO}page4-(GOTO)A80-/XNJ96-
I96: '{\E)
J96: 'Go
K96: 'Repeat
L96: 'Save
M96: 'Plot
N96: 123
J97: 'Begin the data acquisition procedure.
K97: 'Repeat the procedure from the beginning.
L97: 'Save the data.
M97: 'Plot an xy graph of the data.
N97: 'Return to READY mode.
J98: '/XR
K98: '/XG\A-
L98: '{GOTO}A61-
M98: '{GOTO}A75-/GTXXA75..A3075-AB75..B3075-BC75..C3075-OFALBSQTX(ESC)
N98: '/XQ
L99: '/FXV
M99: @INDEX(INF01,3,5)
L100: @INDEX(INF01,0,1)
M100: '-
L101: '-{PGDN}{END}{DOWN}{RIGHT 7}{?}-/XCmenu-

```

```

M101: 'TF(ESC)
L102: '/XG\E-
M102: @INDEX(INF01,1,0)
M103: '-LA(ESC)
M104: @INDEX(INF01,2,3)
M105: '-
M106: 'LB(ESC)
M107: @INDEX(INF01,4,4)
I108: 'datain:
J108: '/WGRM
M108: '-QQ
I109: '{\F)
J109: '{GOTO}A75-
M109: '{GRAPH}/XG\E-
O109: 75
P109: 'counter
J110: '{FOR counter,76,3075,1,routine2)
J111: '{LET counter,75)
J112: '/XG\E-
J114: +'{GETNUMBER "Enter "&A74&" value (or 9999 to end) and press RETURN: "",A"&@STRING(COUNTER,0)&"}"
J115: +'{IF A"&@STRING(COUNTER,0)&"-9999){BLANK A"&@STRING(COUNTER,0)&"}{GOTO}start-/XGJ111-"
J116: +'{NREAD 3478A,B"&+@STRING(COUNTER,0)&,1)"
J117: +'{IF choice2=2){TRIGGER 3438A}{NREAD 3438A,C"&+@STRING(COUNTER,0)&"}"
J118: '{CALC)
J119: +'{GOTO}A"&+@STRING(COUNTER,0)&"}"
J120: '{RETURN)
I121: 'err1:
J121: '{IF (@LENGTH(cell)>0#AND#@LENGTH(cell)<35#AND#flag<1)}/XR
J122: '{IF (@LENGTH(cell)>0#AND#@LENGTH(cell)<35#AND#flag=1)}/XG\C-
O122: "$CS$46
P122: '/XGj62-
J123: '{BEEP 2)
O123: "$BS$47
P123: '/XGj63-
J124: @VLOOKUP({@CELL("address",CELL)},LKUPTABLE1,1)
O124: "$DS$49
P124: '/XGj64-
O125: "$FS$50
P125: '/XGj65-
J126: @CELL("address",CELL)
O126: "$ES$51
P126: '/XGj66-
J127: +K84
N127: '?'
O127: 32323.680625
P127: '/XGJ80-
J128: @LENGTH(+CELL)
N128: '?'
O128: "$BS$87
P128: '/XGJ81-
N129: '?'
O129: "$DS$89
P129: '/XGJ82-

```

A1: [W10]

READY

File AUTOLOG

```

A      B      C      D      E      F      G      H
1
2
3
4
5
6
7
8
9
10
11      -----
12      | Automatic Sampling Routine |
13      -----
14
15
16
17
18
19
20
21-Nov-93 11:55 AM                                CAPS

```

A21: [W10]

READY

```

A      B      C      D      E      F      G      H
21
22      The routines have been written for use with one or both of
23      the following IEEE compatible Digital Multimeters:-
24
25      1. Hewlett-Packard 3478A
26      2. Hewlett-Packard 3438A
27
28      The above have both been installed and configured to be
29      used with Lotus Measure. Any other suitable instruments
30      can be used as long as the appropriate software setting-up
31      procedure is performed. Furthermore, the first line
32      of the \O macro in the program DATALOG will also have to be
33      changed.
34
35      If only one of the above Digital Multimeters is used, it is
36      assumed to be the first one.
37
38      Please use the cursor indicate how many multimeters you will
39      use and then press RETURN.
40
21-Nov-93 11:55 AM                                CAPS

```

A1.1

A41: [W10]

READY

```

A      B      C      D      E      F      G      H
41
42      MULTIPLE READINGS MODE
43      -----
44
45      Date:      21-Nov-93
46      Title of experiment:EXAMPLE1 EXPERIMENT
47      File name:EXAMPLE1
48
49      Title of first Y parameter: Y1
50      Title of second Y parameter (RETURN if none): Y2
51      Total sampling time (HH:MM:SS):      00:10:00
52      Time interval between each sample (HH:MM:SS): 00:00:01 *
53
54      Comments (do not type off the screen; max 3 lines):
55
56      THIS IS JUST AN EXAMPLE FOR THE REPORT
57
58
59      * (Enter EITHER 1 second OR time to the nearest 10 seconds)
60
21-Nov-93 11:55 AM                                CAPS

```

A61: [W10]

READY

```

A      B      C      D      E      F      G      H
61
62
63      -----
64      | EXAMPLE1 EXPERIMENT |
65      -----
66
67      21-Nov-93                                File : EXAMPLE1
68
69      Total sampling Time : 00:10:00
70      Interval between each sample : 00:00:01
71      Total number of samples : 600
72
73
74
75      THIS IS JUST AN EXAMPLE FOR THE REPORT
76
77
78      Sample Number : 0
79      Time      Y1      Y2
80
21-Nov-93 11:56 AM                                CAPS

```

A1.2

I1:

READY

```

      I      J      K      L      M      N      O      P
1
2 \O      /XCtitles-
3 \R      /XCranges-
4 \A      /XCchoose-
5 \B      /XCinfoin-
6 \C      /XCcheck-
7 \D      /XCinit-
8 \E      /XCmenu-
9 \F      /XCdatain-
10
11
12
13
14
15
16
17
18
19
20
21-Nov-93 03:08 PM

```

I21:

READY

```

      I      J      K      L      M      N      O      P
21
22
23
24
25
26
27
28
29
30
31
32
33 titles: {APP1}WRDVM2-Q
34 {\O}    {GOTO}page1-
35         {WAIT @NOW+@TIME(00,00,05)}
36         /XR
37
38 ranges: /RMCdata-A80..C3080-
39 {\R}    /RMCfirstdata-A200..C3200-
40         /RMCstart-A80-
21-Nov-93 03:08 PM

```

A1.3

I41:

READY

```

      I      J      K      L      M      N      O      P
41      /RNCxvalues-A80..A3080-
42      /RNCy1values-B80..B3080-
43      /RNCy2values-C80..C3080-
44      /XR
45
46
47
48 choose: {BLANK info1}{BLANK comms}{BLANK a80..c3280}      2
49 {\A}    {GOTO}page2-
50         /XMJ52-
51
52         1      2
53         Use only Use both the HP 3478A and HP 3438A Multimeters.
54         {LET choi{LET choice2,2}
55
56
57
58
59
60
21-Nov-93 03:09 PM

```

I61: 'infoin:

READY

```

      I      J      K      L      M      N      O      P
61 infoin: {GOTO}page3-
62 {\B}    {GOTO}C46-{GETLABEL "Enter the title of the experiment: ",C46}/
63         {GOTO}B47-{GETLABEL "Enter file name (8 chars max.): ",B47}/RNC
64         {GOTO}D49-{GETLABEL "",D49}/RNCcell-D49-/XCerr1-
65         {GOTO}F50-{GETLABEL "",F50}{IF choice2=2}/RNCcell-F50-/XCerr1-{
66         {GOTO}E51-{GETLABEL "",hold}/RNCcell-E51-/XCerr2-
67         {GOTO}F52-{GETLABEL "",hold}/RNCcell-F52-/XCerr2-      00:00:01
68         {GOTO}A55-{GETLABEL "",A55}
69         {GOTO}A56-{GETLABEL "",A56}
70         {GOTO}A57-{GETLABEL "",A57}
71         /XG\C-
72
73
74 check:  {LET flag,0}/XMK75-
75 {\C}    Proceed Change
76         No paramChange one or more of the parameters.
77         /XR      /XMK78-
78         All      Title      File      1-Y1      2-Y2      Time
79
80         /XG\A- {LET flag{LET flag{LET flag{LET flag{LET flag
21-Nov-93 03:09 PM

```

A1.4

I81:

READY

```

      I      J      K      L      M      N      O      P
81          /XGJ62- /XGJ63- /XGJ64- /XGJ65- /XGJ66-
82
83
84      flag=      0
85
86
87  init:  {INIT}
88  (\D)  {CLEAR 3478A}
89        {IF choice2=2}{CLEAR 3438A}
90        {GOTO}page4-
91        {GOTO}start-
92        /XR
93
94
95  menu:  {GOTO}page4-{GOTO}A80-/XMJ96-
96  (\E)  Go      Repeat  Save  Plot      123
97        Begin theRepeat thSave the Plot an rReturn to READY mode.
98        /XR      /XG\A- {GOTO}A61{GOTO}A80/XQ
99                /FXV  Time
100       0 -SXFDT3QLA{ESC}
21-Nov-93 03:10 PM

```

I101:

READY

```

      I      J      K      L      M      N      O      P
101          -{PGDN}{E      0
102          /XG\E-      -
103          LB{ESC}
104          0
105          -
106          QQ
107          {GRAPH}/XG\E-
108  datain: /WGRM      32322.64 start tim
109  (\F)  {LET 0127,@NOW}      200 counter
110        ERR      ERR 200+sampl
111        {LET counter,200}
112        /M{ESC}{END}{DOWN}.{RIGHT 2}{END}{DOWN}--/WGRA
113        /RNCstart-A80-/XG\E-
114
115        {LET A200,@NOW-0127}
116        {NREAD 3478A,B200,1}
117        {IF choice2=2}{TRIGGER 3438A}{NREAD 3438A,C200}
118        {IF @TIMEVALUE(@INDEX(info1,4,6))>@TIME(00,00,09)}{WAIT @NOW+@T
119        {CALC}
120        {RETURN}
21-Nov-93 03:10 PM

```

A1.5

I121: 'err1:

READY

```

      I      J      K      L      M      N      O      P
121  err1: {IF (@LENGTH(cell)>0#AND#@LENGTH(cell)<55#AND#flag<>1)}/XR
122        {IF (@LENGTH(cell)>0#AND#@LENGTH(cell)<55#AND  $C$46 /XGj62-
123        {BEEP 2}      $B$47 /XGj63-
124        ERR      $D$49 /XGj64-
125        ?      $F$50 /XGj65-
126        $F$52      ?      $C$51 /XGj66-
127        0      ?      32323.68 /XGJ80-
128        ERR      ?      $B$87 /XGJ81-
129        ?      $D$89 /XGJ82-
130  err2:  {CALC}
131        {IF @ISERR(@TIMEVALUE(hold))<1#AND#flag<>1}{LET cell,hold}/XR
132        {IF @ISERR(@TIMEVALUE(hold))<1#AND#flag=1}{LET cell,hold}/XG\C
133        {BEEP 2}      $E$51 /XGJ66-
134        0 /XGJ67-      $F$52 /XGJ67-
135        0
136
137
138
139
140
21-Nov-93 03:10 PM

```

A1.6

```

A1: [W10] '
I2: '\0
J2: '/XCtitles-
I3: '\R
J3: '/XCranges-
I4: '\A
J4: '/XCchoose-
I5: '\B
J5: '/XCinfoin-
I6: '\C
J6: '/XCcheck-
I7: '\D
J7: '/XCinit-
I8: '\E
J8: '/XCmenu-
I9: '\F
J9: '/XCdatain-
C10: \-
D10: \-
E10: \-
F10: \-
B11: [W10] "
C11: ' Automatic Sampling Routine
G11: [W7] '|
C12: \-
D12: \-
E12: \-
F12: \-
B22: [W10] 'The routines have been written for use with one or both of
B23: [W10] 'the following IEEE compatible Digital Multimeters:-
B25: [W10] ' 1. Hewlett-Packard 3478A
B26: [W10] ' 2. Hewlett-Packard 3438A
B28: [W10] 'The above have both been installed and configured to be
B29: [W10] 'used with Lotus Measure. Any other suitable instruments
B30: [W10] 'can be used as long as the appropriate software setting-up
B31: [W10] 'procedure is performed. Furthermore, the first line
B32: [W10] 'of the \0 macro in the program DATALOG will also have to be
B33: [W10] 'changed.
I33: 'titles:
J33: '{APP1}NRDVM2-Q
I34: '\0
J34: '{GOTO}page1-
B35: [W10] 'If only one of the above Digital Multimeters is used, it is
J35: '{WAIT @NOW+@TIME(00,00,05)}
B36: [W10] 'assumed to be the first one.
J36: '/XR
B38: [W10] 'Please use the cursor indicate how many multimeters you will
I38: 'ranges:
J38: '/RMCdata-A80..C3080-
B39: [W10] 'use and then press RETURN.
J39: '/RMCfirstdata-A200..C3200-
J40: '/RMCstart-A80-
J41: '/RMCxvalues-A80..A3080-
B42: [W10] 'MULTIPLE READINGS MODE
J42: '/RMCyvalues-B80..B3080-
B43: [W10] \-
C43: \-
D43: '---
J43: '/RMCy2values-C80..C3080-
J44: '/XR

```

```

A45: [W10] 'Date:
B45: (D1) [W10] @DATEVALUE(@NOW)
A46: [W10] 'Title of experiment:
C46: 'EXAMPLE1 EXPERIMENT
A47: [W10] 'File name:
B47: [W10] 'EXAMPLE1
I48: 'choose:
J48: '{BLANK info1}{BLANK comms}{BLANK a80..c3280}
O48: 1
A49: [W10] 'Title of first Y parameter:
D49: 'Y1
I49: '\A
J49: '{GOTO}page2-
A50: [W10] 'Title of second Y parameter (RETURN if none):
F50: 'Y2
J50: '/XWJ52-
A51: [W10] 'Total sampling time (HH:MM:SS):
E51: (D8) '00:10:00
A52: [W10] 'Time interval between each sample (HH:MM:SS):
F52: (D8) '00:00:01
G52: [W7] '*
J52: 1
K52: 2
J53: 'Use only the HP 3478A Multimeter.
K53: 'Use both the HP 3478A and HP 3438A Multimeters.
A54: [W10] 'Comments (do not type off the screen; max 3 lines):
J54: '{LET choice2,1}
K54: '{LET choice2,2}
A55: [W10] '
A56: [W10] 'THIS IS JUST AN EXAMPLE FOR THE REPORT
A57: [W10] '
A59: [W10] '**
B59: [W10] '(Enter EITHER 1 second OR time to the nearest 10 seconds)
I61: 'infoin:
J61: '{GOTO}page3-
B62: [W10] \-
C62: \-
D62: \-
E62: \-
F62: \-
G62: [W7] \-
I62: '\B
J62: '{GOTO}C46-{GETLABEL "Enter the title of the experiment: ",C46}/RNCcell-C46-/XCerr1-
A63: [W10] "
B63: [W10] @REPEAT(" ",(55-@LENGTH(@INDEX(INF01,1,0)))/2)&@INDEX(INF01,1,0)
H63: '
J63: '{GOTO}B47-{GETLABEL "Enter file name (8 chars max.): ",B47}/RNCcell-B47-/XCerr1-
B64: [W10] \-
C64: \-
D64: \-
E64: \-
F64: \-
G64: [W7] \-
J64: '{GOTO}D49-{GETLABEL " ",D49}/RNCcell-D49-/XCerr1-
J65: '{GOTO}F50-{GETLABEL " ",F50}{IF choice2=2}/RNCcell-F50-/XCerr1-{IF flag=1}/XG\C-
B66: (D1) [W10] +B45
J66: '{GOTO}E51-{GETLABEL " ",hold}/RNCcell-E51-/XCerr2-
F67: +' File : "%@INDEX(INF01,0,1)
J67: '{GOTO}F52-{GETLABEL " ",hold}/RNCcell-F52-/XCerr2-
P67: '00:00:01

```

```

B68: [W10] +"Total sampling Time : "%@INDEX(INF01,3,5)
J68: '{GOTO}A55-(GETLABEL "",A55)
B69: [W10] +"Interval between each sample : "%@INDEX(INF01,4,6)
J69: '{GOTO}A56-(GETLABEL "",A56)
B70: [W10] +"Total number of samples : "%@STRING(SAMPLES-200,0)
J70: '{GOTO}A57-(GETLABEL "",A57)
J71: '/XG\C-
A74: [W10] +A55
I74: 'check:
J74: '{LET flag,0}/XWJ75-
A75: {W10} +A56
I75: '{\C)
J75: 'Procede
K75: 'Change
A76: [W10] +A57
J76: 'No parameter changes required.
K76: 'Change one or more of the parameters.
J77: '/XR
K77: '/XMK78-
E78: +"Sample Number : "%@STRING(COUNTER-200,0)
K78: 'All
L78: 'Title
M78: 'File
N78: '1-Y1
O78: '2-Y2
P78: 'Time
Q78: 'Interval
A79: [W10] 'Time
B79: [W10] @INDEX(INF01,2,3)
C79: @INDEX(INF01,4,4)
K79: +""
L79: +""
M79: +""
N79: +""
O79: +""
K80: '/XG\A-
L80: '{LET flag,1}
M80: '{LET flag,1}
N80: '{LET flag,1}
O80: '{LET flag,1}
P80: '{LET flag,1}
Q80: '{LET flag,1}
L81: '/XGJ62-
M81: '/XGJ63-
N81: '/XGJ64-
O81: '/XGJ65-
P81: '/XGJ66-
Q81: '/XGJ67-
J84: 'flag=
K84: 0
I87: 'init:
J87: '{INIT}
I88: '{\D)
J88: '{CLEAR 3478A}
J89: '{IF choice2=2}{CLEAR 3438A}
J90: '{GOTO}page4-
J91: '{GOTO}start-
J92: '/XR
I95: 'menu:
J95: '{GOTO}page4-{GOTO}A80-/XWJ96-

```

```

I96: '{\E)
J96: 'Go
K96: 'Repeat
L96: 'Save
M96: 'Plot
N96: 123
J97: 'Begin the data acquisition procedure.
K97: 'Repeat the procedure from the beginning.
L97: 'Save the data.
M97: 'Plot an xy graph of the data.
N97: 'Return to READY mode.
J98: '/XR
K98: '/XG\A-
L98: '{GOTO}A61-
M98: '{GOTO}A80-/GTXX.{END}{DOWN}-A{RIGHT}.{END}{DOWN}-B{RIGHT}{RIGHT}.{END}{DOWN}-OFALBSQTX{ESC)
N98: '/XQ)
L99: '/FXV
M99: 'Time
L100: @INDEX(INF01,0,1)
M100: '-SXFDPT3QLA{ESC)
L101: '-{PGDN}{END}{DOWN}{RIGHT 7}{?}-
M101: @INDEX(INF01,2,3)
L102: '/XG\E-
M102: '-
M103: 'LB{ESC)
M104: @INDEX(INF01,4,4)
M105: '-
M106: 'QQ)
M107: '{GRAPH}/XG\E-
I108: 'datain:
J108: '/WGRM
O108: 32322.643519
P108: 'start time
I109: '{\F)
J109: '{LET O127,@NOW}
O109: 200
P109: 'counter
J110: +"{FOR counter,201,"@STRING(SAMPLES,0)&","1,routine2}"
O110: 200+@TIMEVALUE(@INDEX(INF01,3,5))/@TIMEVALUE(@INDEX(INF01,4,6))
P110: '200+samples
J111: '{LET counter,200}
J112: '/M{ESC){END}{DOWN}. {RIGHT 2}{END}{DOWN}--/WGRA
J113: '/RNCstart-A80-/XG\E-
J115: +"{LET A"@STRING(COUNTER,0)&","@NOW-O127}"
J116: +"{NREAD 3478A,B"@STRING(COUNTER,0)&","1}"
J117: +"{IF choice2=2}{TRIGGER 3438A}{NREAD 3438A,C"@STRING(COUNTER,0)&"}"
J118: '{IF @TIMEVALUE(@INDEX(inf01,4,6))>@TIME(00,00,09)}{WAIT @NOW+@TIMEVALUE(@INDEX(inf01,4,6))}
J119: '{CALC)
J120: '{RETURN)
I121: 'err1:
J121: '{IF (@LENGTH(cell)>0#AND#@LENGTH(cell)<55#AND#flag<1)}/XR
J122: '{IF (@LENGTH(cell)>0#AND#@LENGTH(cell)<55#AND#flag=1)}/XG\C-
O122: *$C$46)
P122: '/XGj62-
J123: '{BEEP 2}
O123: *$B$47)
P123: '/XGj63-
J124: @VLOOKUP({@CELL("address",CELL)},LKUPTABLE1,1)
O124: *$D$49)
P124: '/XGj64-

```

M125: '?'
O125: "\$F\$50
P125: '/XGj65-
J126: @CELL("address",CELL)
M126: '?'
O126: "\$C\$51
P126: '/XGj66-
J127: +FLAG
M127: '?'
O127: 32323.680625
P127: '/XGJ80-
J128: @LENGTH(+CELL)
M128: '?'
O128: "\$B\$87
P128: '/XGJ81-
M129: '?'
O129: "\$D\$89
P129: '/XGJ82-
I130: 'err2:
J130: '{CALC}
J131: '{IF @ISERR(@TIMEVALUE(hold))<>1/AND(flag<>1)}(LET cell,hold)/YR
J132: '{IF @ISERR(@TIMEVALUE(hold))<>1/AND(flag=1)}(LET cell,hold)/XG\C-
J133: '{BEEP 2}
M133: "\$E\$51
P133: '/XGJ66-
I134: @ISERR(@TIMEVALUE(+P47))
J134: @VLOOKUP(@CELL("address",CELL),LKUPTABLE2,1)
M134: "\$F\$52
M134: '/XGJ67-
I135: +P54

20876 UV

Appendix IV.1



Sadtler Research Laboratories, Inc.
Subsidiary of Bock Engineering, Inc.

© 1974

IR 9792

FLUORESCEIN

 $C_{20}H_{12}O_5$

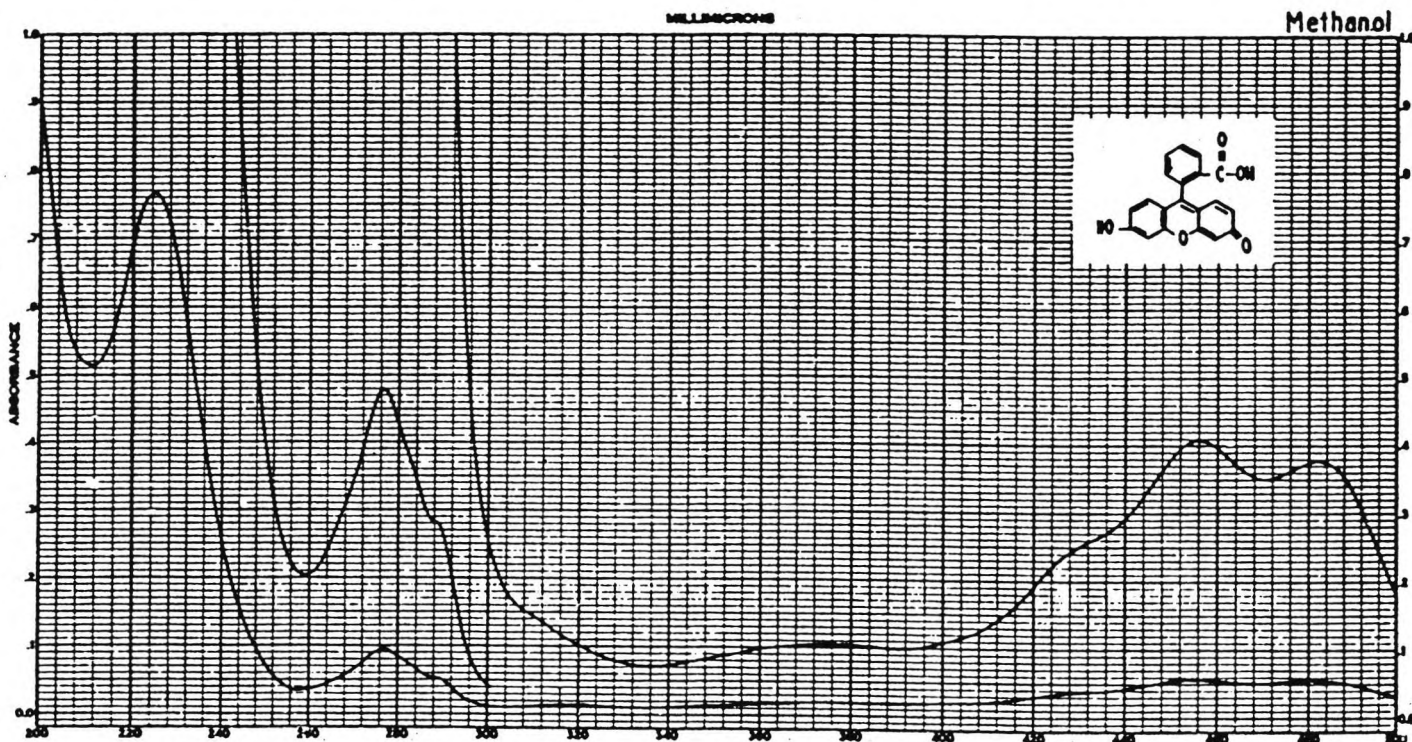
Mol. Wt. 332.32

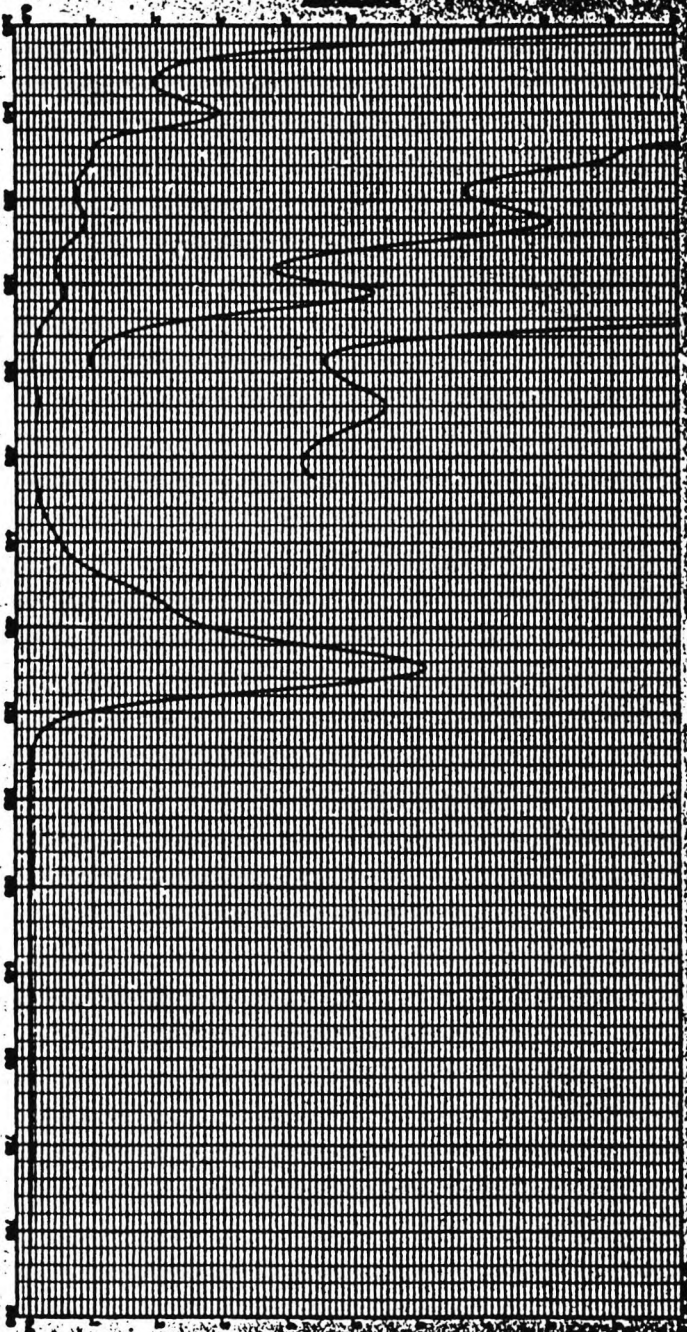
Source: E. Merck AG, Darmstadt, Germany

		A	B	C	D	E
Methanol vis/UV	Conc. g/L	0.100	0.100	0.100	0.100	0.0200
	Cell mm	10	10	10	2	2
	ϵ_m	1260	1370	350	8000	63900
	λ Max. $m\mu$	482	456	376	276.5	225

Methanol KOH vis/UV	Conc. g/L	0.0200	0.100	0.100	0.100	0.0200
	Cell mm	1	10	2	2	1
	ϵ_m	101700	1830	8850	13500	49200
	λ Max. $m\mu$	499	376	324	290	240

	Conc. g/L					
	Cell mm					
	ϵ_m					
	λ Max. $m\mu$					





20876 UV

11526 UV



IR 11918

5-ISOTHIOCYANATOFLUORESCEIN

 $C_{21}H_{11}NO_5S$

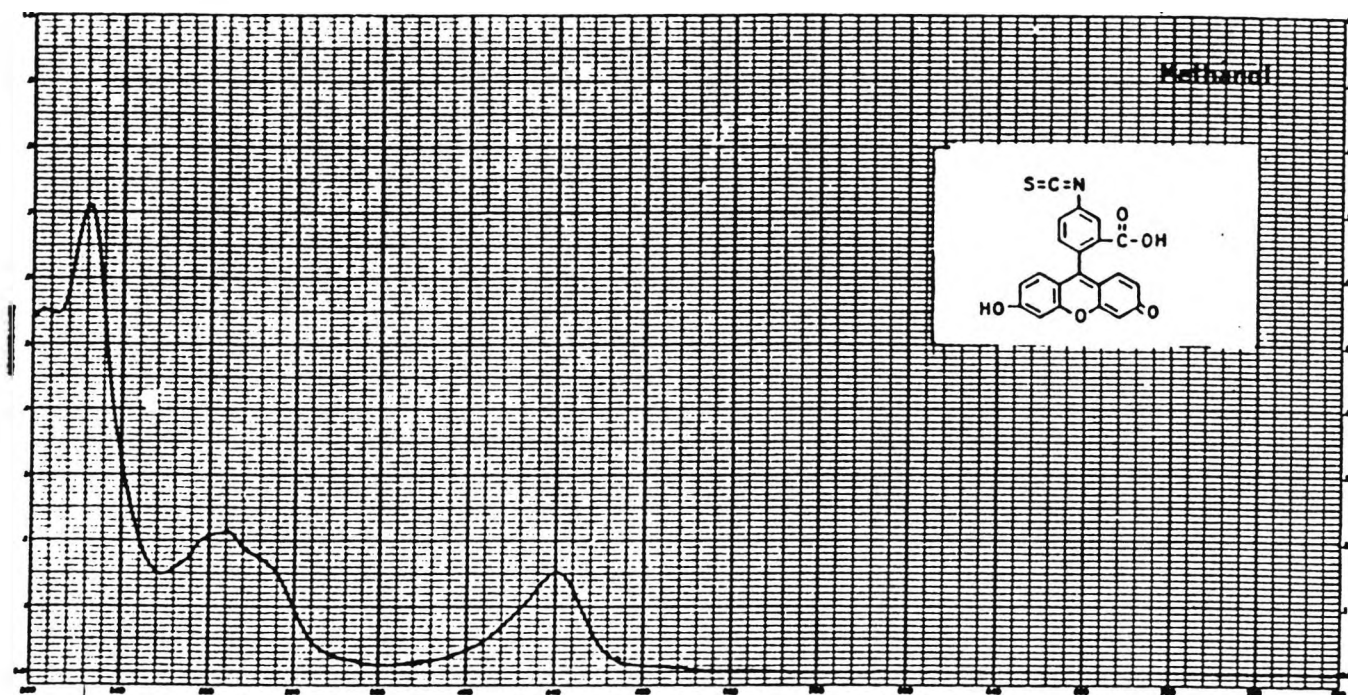
Mol. Wt. 389.39

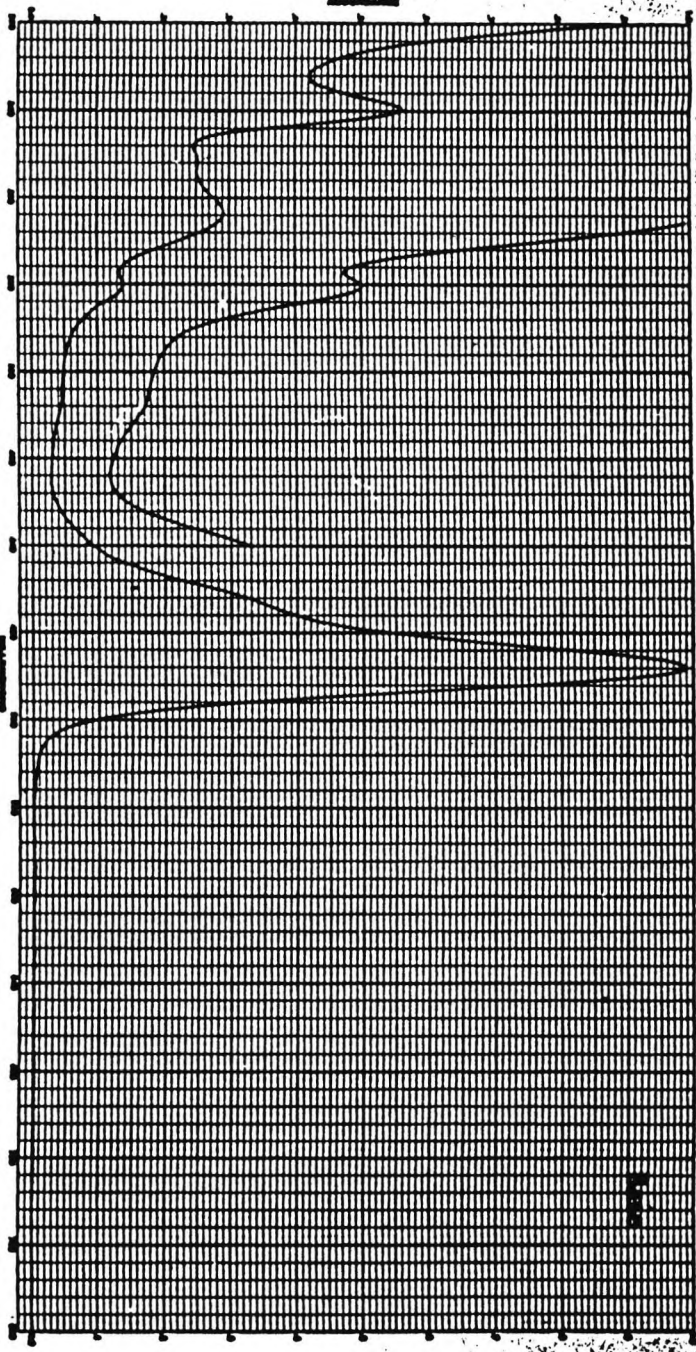
Source: Fluka AG, Buchs, Switzerland

		A	B	C	D	E
Methanol	Conc. g/L	0.0500	0.0500	0.0500		
	Cell mm	1	1	1		
	a_m	11800	16600	55400		
	λ Max. $m\mu$	440	289	225		

Methanol KOH	Conc. g/L	0.0500	0.100	0.0500	0.0500	0.0500
	Cell mm	1	2	1	1	1
	a_m	77100	9770	22700	19600	43800
	λ Max. $m\mu$	496	321	287	263	239

	Conc. g/L					
	Cell mm					
	a_m					
	λ Max. $m\mu$					

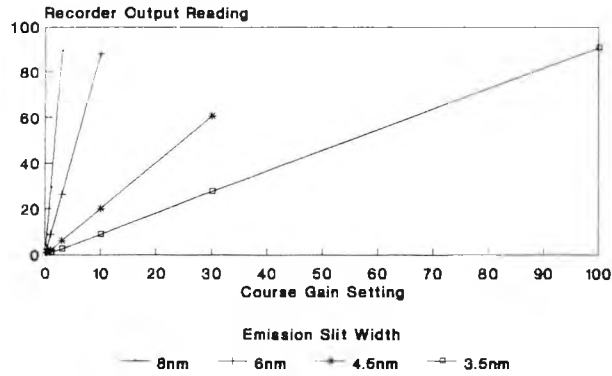




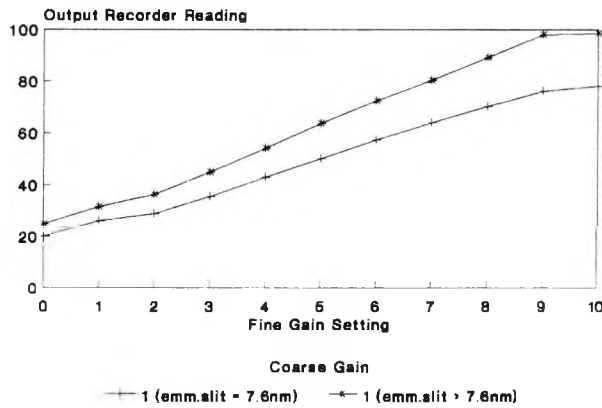
11526 UV

Analysis of the Effect of Gain Adjustments of the Spectrophotometer Amplifier

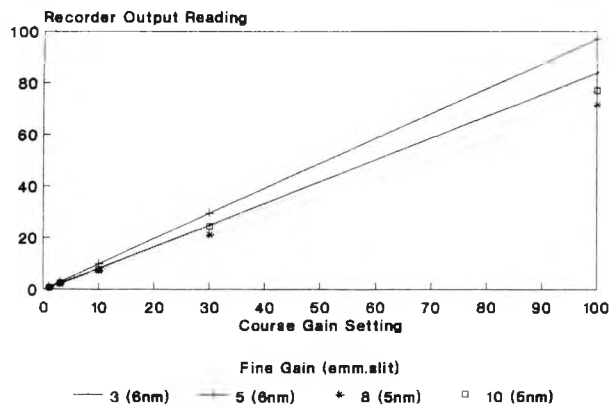
1) Variation of Emission Slit Width and Course Gain Adjustment



2) Fine Gain Adjustment



3) All Parameters



Appendix IV.3

BUFFER SOLUTIONS (Continued)

SOLUTIONS GIVING BOUND VALUES OF pH AT 25°C

Reproduced from "Electrolyte Solutions" by permission from Robinson and Stokes, authors, and Butterworth's Scientific Publications.

A*		B*		C*		D*		E*	
pH	z	pH	z	pH	z	pH	z	pH	z
1.00	67.0	2.20	49.5	4.10	1.3	5.80	3.6	7.00	46.6
1.10	52.8	2.30	45.8	4.20	3.0	5.90	4.6	7.10	45.7
1.20	42.5	2.40	42.2	4.30	4.7	6.00	5.6	7.20	44.7
1.30	33.6	2.50	38.8	4.40	6.6	6.10	6.8	7.30	43.4
1.40	26.6	2.60	35.4	4.50	8.7	6.20	8.1	7.40	42.0
1.50	20.7	2.70	32.1	4.60	11.1	6.30	9.7	7.50	40.3
1.60	16.2	2.80	28.9	4.70	13.6	6.40	11.6	7.60	38.5
1.70	13.0	2.90	25.7	4.80	16.5	6.50	13.9	7.70	36.6
1.80	10.2	3.00	22.3	4.90	19.4	6.60	16.4	7.80	34.5
1.90	8.1	3.10	18.8	5.00	22.6	6.70	19.3	7.90	32.0
2.00	6.5	3.20	15.7	5.10	25.5	6.80	22.4	8.00	29.2
2.10	5.1	3.30	12.9	5.20	28.8	6.90	25.9	8.10	26.2
2.20	3.9	3.40	10.4	5.30	31.6	7.00	29.1	8.20	22.9
		3.50	8.2	5.40	34.1	7.10	32.1	8.30	19.9
		3.60	6.3	5.50	36.6	7.20	34.7	8.40	17.2
		3.70	4.5	5.60	38.8	7.30	37.0	8.50	14.7
		3.80	2.9	5.70	40.6	7.40	39.1	8.60	12.2
		3.90	1.4	5.80	42.3	7.50	41.1	8.70	10.3
		4.00	0.1	5.90	43.7	7.60	42.8	8.80	8.5
						7.70	44.2	8.90	7.0
						7.80	45.3	9.00	5.7
						7.90	46.1		
						8.00	46.7		
F*		G*		H*		I*		J*	
pH	z	pH	z	pH	z	pH	z	pH	z
8.00	20.5	9.20	0.9	9.60	5.0	10.90	3.3	12.00	6.0
8.10	19.7	9.30	3.6	9.70	6.2	11.00	4.1	12.10	8.0
8.20	18.8	9.40	6.2	9.80	7.6	11.10	5.1	12.20	10.2
8.30	17.7	9.50	8.8	9.90	9.1	11.20	6.3	12.30	12.8
8.40	16.6	9.60	11.1	10.00	10.7	11.30	7.6	12.40	16.2
8.50	15.2	9.70	13.1	10.10	12.2	11.40	9.1	12.50	20.4
8.60	13.5	9.80	15.0	10.20	13.8	11.50	11.1	12.60	25.6
8.70	11.6	9.90	16.7	10.30	15.2	11.60	13.5	12.70	32.2
8.80	9.6	10.00	18.3	10.40	16.5	11.70	16.2	12.80	41.2
8.90	7.1	10.10	19.5	10.50	17.8	11.80	19.4	12.90	53.0
9.00	4.6	10.20	20.5	10.60	19.1	11.90	23.0	13.00	66.0
9.10	2.0	10.30	21.3	10.70	20.2	12.00	26.9		
		10.40	22.1	10.80	21.2				
		10.50	22.7	10.90	22.0				
		10.60	23.3	11.00	22.7				
		10.70	23.8						
		10.80	24.25						

*A. 25 ml of 0.2 molar KCl + x ml of 0.2 molar HCl.

*B. 50 ml of 0.1 molar potassium hydrogen phthalate + x ml of 0.1 molar HCl.

*C. 50 ml of 0.1 molar potassium hydrogen phthalate + x ml of 0.1 molar NaOH.

*D. 50 ml of 0.1 molar potassium dihydrogen phosphate + x ml 0.1 molar NaOH.

*E. 50 ml of 0.1 molar tris(hydroxymethyl) aminomethane + x ml of 0.1 M HCl.

*F. 50 ml of 0.025 molar borax + x ml of 0.1 molar HCl.

*G. 50 ml of 0.025 molar borax + x ml of 0.1 molar NaOH.

*H. 50 ml of 0.05 molar sodium bicarbonate + x ml of 0.1 molar NaOH.

*I. 50 ml of 0.05 molar disodium hydrogen phosphate + x ml of 0.1 molar NaOH.

*J. 25 ml of 0.2 molar KCl + x ml of 0.2 molar NaOH.

Final Volume of Mixtures = 100 ml

Appendix IV.4

[This is an example of output from the MANUAL DATA LOG routine.]

DATE: 16-05-88

EXPERIMENT: Fluorescence of FITC solution versus pH.

FILE: R16058_C

(subsequently calculated values:-)

Reading	Fluorescence (I)	pH (volts)	pH (using calibration values)
1	3.315	0.069	6.929
2	1.2832	0.049	4.979
3	1.239	0.049	4.919
4	1.2189	0.048	4.848
5	1.1518	0.047	4.707
6	1.1123	0.046	4.636
7	1.0586	0.045	4.515
8	1.0071	0.044	4.384
9	0.9637	0.042	4.252
10	0.925	0.0416	4.192
11	0.924	0.0421	4.242
12	0.926	0.0423	4.262
13	0.933	0.0426	4.293
14	0.944	0.0429	4.323
15	0.949	0.0432	4.353
16	0.950	0.0435	4.384
17	0.955	0.0437	4.404
18	0.960	0.0440	4.434
19	0.965	0.0442	4.454
20	0.976	0.0444	4.474
21	0.990	0.0449	4.525
22	0.998	0.0453	4.565
23	1.004	0.0458	4.616
24	1.021	0.0463	4.666
25	1.030	0.0468	4.717
26	1.034	0.0470	4.737
27	1.046	0.0471	4.747
28	1.091	0.0483	4.868
29	1.164	0.0497	5.010
30	1.228	0.0509	5.131
31	1.265	0.0515	5.192
32	1.293	0.0519	5.232
33	1.312	0.0522	5.262
34	1.353	0.0525	5.293
35	1.385	0.0530	5.343
36	1.406	0.0533	5.373
37	1.457	0.0538	5.424
38	1.509	0.0543	5.474
39	1.555	0.0548	5.525
40	1.628	0.0554	5.585
41	1.683	0.0560	5.646
42	1.801	0.0568	5.727
43	2.062	0.0586	5.909
44	2.219	0.0599	6.040
46	2.773	0.0639	6.444
47	3.025	0.0691	6.969
48	2.935	0.0964	9.726
49	2.911	0.1037	10.464
50	2.874	0.1067	10.767
51	2.859	0.1086	10.959
52	2.827	0.1098	11.080
53	2.769	0.1107	11.171
54	2.771	0.1115	11.252
55	2.643	0.1139	11.494
56	2.536	0.1153	11.635
57	2.410	0.1170	11.807

Example of commercially available
controlled-pore glass

Fluka 

sFr. 357

Controlled-Pore Glass

Controlled-Pore Glass (CPC) is a column packing material which offers substantial advantages over gels for permeation chromatography. Derivatized CPG is used for ion-exchange chromatography and as a carrier for affinity chromatography. It is an inert, rigid material having a large internal surface of controlled pores with free access. Its porous structure is unaffected by changes in flow rate, pH, ionic strength or pressure. Pore size are manufactured to specific mean diameters within the range of 75 to 3000 Ångströms Å.

Free booklet about Controlled-Pore Glass, its specifications and uses is available on request.

a) for permeation chromatography

Controlled-Pore Glass is effective for separating and characterizing a variety of compounds of biological interest like e.g. cell components, viruses, nucleic acids, proteins, polysaccharides, antibiotics etc. and synthetic polymers, ranging in molecular weight from 10^3 to 10^{10} and beyond.

CPG, uncoated

Uncoated CPG is immune to biological attack. Used CPG may be cleaned by treating with concentrated sodium chloride solution, 1% sodium lauryl sulfate (SDS) or diluted ammonia. Tenacious impurities may be removed by hot nitric acid.

Operating range for globular proteins and particles in water are listed below

CPG-10-75 Å				
operating range: M, $3-30 \times 10^3$				
27704	120-200 mesh; $d_p^{\circ} 0.4$	1 l \approx 0.40 kg	50 ml	505.—
27705	200-400 mesh; $d_p^{\circ} 0.4$	1 l \approx 0.40 kg	50 ml	505.—
CPG-10-120 Å				
operating range: M, $7-130 \times 10^3$				
27707	120-200 mesh; $d_p^{\circ} 0.4$	1 l \approx 0.40 kg	50 ml	505.—
27708	200-400 mesh; $d_p^{\circ} 0.4$	1 l \approx 0.40 kg	50 ml	505.—
CPG-10-170 Å				
operating range: M, $12-400 \times 10^3$				
27710	120-200 mesh; $d_p^{\circ} 0.4$	1 l \approx 0.40 kg	50 ml	505.—
27711	200-400 mesh; $d_p^{\circ} 0.4$	1 l \approx 0.40 kg	50 ml	505.—
CPG-10-240 Å				
operating range: M, $22-1200 \times 10^3$				
27713	120-200 mesh; $d_p^{\circ} 0.4$	1 l \approx 0.40 kg	50 ml	459.10
27714	200-400 mesh; $d_p^{\circ} 0.4$	1 l \approx 0.40 kg	50 ml	505.—
CPG-10-350 Å				
operating range: M, $40-5000 \times 10^3$				
27716	120-200 mesh; $d_p^{\circ} 0.4$	1 l \approx 0.40 kg	50 ml	505.—
27717	200-400 mesh; $d_p^{\circ} 0.4$	1 l \approx 0.40 kg	50 ml	505.—
CPG-10-500 Å				
operating range: M, $70-10000 \times 10^3$				
27719	120-200 mesh; $d_p^{\circ} 0.4$	1 l \approx 0.40 kg	50 ml	505.—
27720	200-400 mesh; $d_p^{\circ} 0.4$	1 l \approx 0.40 kg	50 ml	505.—
CPG-10-700 Å				
operating range: M, $130-30000 \times 10^3$				
27721	120-200 mesh; $d_p^{\circ} 0.4$	1 l \approx 0.40 kg	50 ml	505.—
27724	200-400 mesh; $d_p^{\circ} 0.4$	1 l \approx 0.40 kg	50 ml	505.—
CPG-10-1000 Å				
operating range: M, $250-100000 \times 10^3$				
27722	120-200 mesh; $d_p^{\circ} 0.4$	1 l \approx 0.40 kg	50 ml	505.—
27723	200-400 mesh; $d_p^{\circ} 0.4$	1 l \approx 0.40 kg	50 ml	505.—
CPG-10-1400 Å				
operating range: M, $400-300000 \times 10^3$				
27725	120-200 mesh; $d_p^{\circ} 0.4$	1 l \approx 0.40 kg	50 ml	505.—
27726	200-400 mesh; $d_p^{\circ} 0.4$	1 l \approx 0.40 kg	50 ml	505.—
CPG-10-2000 Å				
operating range: M, $700-900000 \times 10^3$				
27728	120-200 mesh; $d_p^{\circ} 0.4$	1 l \approx 0.40 kg	50 ml	505.—
27729	200-400 mesh; $d_p^{\circ} 0.4$	1 l \approx 0.40 kg	50 ml	505.—

Results of Thermal Analysis

METHOD	WEIGHT PERCENTS		
	C	H	N
1.2	0.51	0.47	0.55
1.2.1	0.17	0.68	0.36
1.2.2	0.12	0.67	0.34
2.1	0.85	0.61	0.27
2.2	0.77	0.76	0.59
2.3	0.45	0.70	0.48
2.1.1	0.69	0.63	0.21
2.1.2	0.67	0.63	0.21
2.1.4	0.64	0.62	0.22
2.2.1	0.21	0.74	0.38
2.2.2	0.17	0.69	0.38
2.2.4	0.15	0.74	0.38
2.3.1	0.02	0.70	0.34
2.3.2	0.08	0.70	0.34
2.3.3	0.07	0.76	0.35
2.3.4	0.12	0.75	0.34
3.1	0.80	0.38	0.20
3.2	0.66	0.83	0.92
3.1.1	0.58	0.44	0.16
3.1.4	0.61	0.45	0.18
3.2.1	0.66	0.67	0.53
4.1	0.72	0.44	0.18
4.1.1	0.53	0.49	0.15
4.1.4	0.58	0.48	0.16
4.2.1	0.49	0.71	0.49
5.1.1	0.62	0.42	0.16
5.1.2	0.60	0.45	0.14
5.1.4	0.59	0.40	0.14
5.2.1	0.29	0.53	0.34
5.2.4	0.19	0.50	0.39
6.2	0.66	0.53	0.55
6.2.1	0.16	0.53	0.36
7.1	0.76	0.32	0.19
7.2	0.95	0.32	0.27
7.1.1	0.60	0.38	0.15
7.1.2	0.58	0.38	0.16
7.1.4	0.60	0.36	0.15
7.2.1	0.83	0.36	0.21
7.2.2	0.70	0.36	0.21
7.2.4	0.75	0.37	0.22
8.1	0.73	0.35	0.19
8.2	0.15	0.41	0.31
8.1.1	0.72	0.46	0.16
8.1.4	0.61	0.44	0.15
8.2.1	0.94	0.48	0.26
8.2.4	0.90	0.46	0.23
9.2	0.85	0.40	0.25
9.2.1	0.93	0.44	0.21
9.2.2	0.73	0.42	0.20
9.2.3	0.70	0.38	0.19
9.2.4	0.92	0.43	0.19
10.1	0.66	0.30	0.18
10.2	0.27	0.65	0.77
10.1.1	0.62	0.37	0.15
10.1.2	0.60	0.37	0.15
10.1.4	0.58	0.37	0.14
10.2.1	1.45	0.53	0.43
10.2.2	1.29	0.51	0.42
10.2.4	1.37	0.53	0.41
Blank	0.03	0.53	0.00

Derivation of expression for the weight percent of C, H or N contained in a sample of porous glass which has undergone the two-stage derivatization reaction.

Summary of notation used:-

L_i	=	loading of species i per nm^2
n_i	=	number atoms of species i present in the average surface group.
N_A	=	Avogadro constant ($= 6.023 \times 10^{23}$).
A	=	specific surface area of porous glass ($= 32.4\text{m}^2\text{g}^{-1}$).
X_{FITC}	=	mole ratio of FITC present on the surface ($= [\text{FITC}]/[\text{3APTS}]$)
L_G	=	loading of the average surface group per nm^2 .
M_i	=	relative molecular weight of species i .
P_G	=	calculated weight percent of theoretical group = $P_i M_i / (n_i M_i)$

and the subscripts denote:-

1	=>	values after stage 1 of immobilisation reaction.
2	=>	values after stage 2 of immobilisation reaction.
2'	=>	values arising from components added during stage 2 of immobilisation reaction.
G	=>	average surface group = $G_1 + X_{\text{FITC}} \cdot G_2$
i	=>	a surface species i.e. carbon (C), hydrogen (H), nitrogen (N), FITC, 3APTS or G.

$$\begin{array}{l} \text{Number of groups present per } \text{m}^2 \\ \text{of the substrate surface} \end{array} = 10^{18} L_G$$

There are n atoms of the species i in the surface group, hence:

$$\begin{array}{l} \text{Number of atoms of species } i \text{ present} \\ \text{per } \text{m}^2 \text{ of the substrate surface} \end{array} = n_i 10^{18} L_G$$

$$\begin{array}{l} \text{Number of moles of species } i \\ \text{per } \text{m}^2 \text{ of the substrate surface} \end{array} = \frac{n_i 10^{18} L_G}{N_A}$$

$$\begin{array}{l} \text{Mass of species } i \text{ present per g} \\ \text{of substrate} \end{array} = \frac{n_i 10^{18} L_G M_i}{N_A}$$

Now, what we call the *sample* consists of the *substrate + surface material*, hence,

Mass of *sample* present per g of substrate

$$= \frac{n_i 10^{18} L_G M_i}{N_A} + 1$$

Now consider the situation after stage 1 of the reaction (section 5.3.2.1) such that the only group immobilised onto the surface of the porous glass is group 1 (i.e. 3APTS), hence:

Weight percent of species *i* present in the sample, P_i :

$$= \frac{100 \times n_{i1} 10^{18} L_{G1} M_i}{N_A \left(\frac{n_{i1} 10^{18} L_{G1} M_i}{N_A} + 1 \right)}$$

This simplifies to:

$$P_i = \frac{10^{20} L_{G1} n_{i1} M_i A}{N_A + 10^{18} L_{G1} M_{G1} A}$$

If the species of interest is carbon, then for the above expression:

n_{i1}	=	3	(i.e. 3 C atoms in 3APTS)
L_{G1}	=	no. of 3APTS per nm^2 on the surface of the PG	
M_i	=	12.011	(rel. mol. wt. of C)
M_{G1}	=	58.096	(rel. mol. wt. of the detectable fraction of 3APTS)

Now consider the addition of group 2 (i.e. FITC) to the surface of the substrate as occurs in stage 2 of the derivatisation reaction and assume that one group of FITC reacts with each and every group of 3APTS present from stage 1 of the reaction. It follows that:

$$P_i = \frac{10^{20} (L_{G1} + L_{G2}) (n_{i1} + n_{i2}) M_i A}{N_A + 10^{18} (L_{G1} + L_{G2}) (M_{G1} + M_{G2}) A}$$

where,

n_{i2}	=	21	(i.e. 21 C atoms in FITC)
L_{G2}	=	no. of FITC per nm^2 on the surface of the PG	
		(note: $L_{G2} = L_{G1}$ when FITC adds to all 3APTS groups)	
M_i	=	12.011	(rel. mol. wt. of C)
M_{G2}	=	389.37	(rel. mol. wt. of the detectable fraction of FITC)

However, if only partial addition occurs, $X_{\text{FITC}} = [\text{FITC}]/[\text{3APTS}]$, then:

$$P_i = \frac{10^{20} L_G (n_{i1} + X_{\text{FITC}} \cdot n_{i2}) M_i A}{N_A + 10^{18} L_G (M_{G1} + X_{\text{FITC}} \cdot M_{G2}) A}$$

Calculation of the loading average surface group

We have defined the *loading* as the number of atoms of a species or molecules (groups) present per m^2 of the substrate surface.

Now, 1 g of sample contains $0.01P_i$ g of species i ,

Hence, $(1 - 0.01P_G)$ substrate carries $0.01P_i$ g of species i ,

Hence, 1 g of substrate carries $0.01P_i/(1 - 0.01P_G)$ g of species i ,

Since $P_G = P_{G1} + X_{FITC} \cdot P_{G2'}$, it follows that loading of species i is given by:

$$L_i = \frac{0.01P_i N_A}{(1 - 0.01(P_{G1} + X_{FITC} \cdot P_{G2'})) M_i A 10^{18}}$$

Furthermore, since on average the number of atoms of species i in the surface group is given by:

$$n_{iG} = n_{i1} + X_{FITC} \cdot n_{i2'}$$

It follows that the loading of the average surface group is expressed by:

$$L_G = \frac{L_i}{n_{iG}}$$

or

$$L_G = \frac{0.01P_i N_A}{(1 - 0.01(P_{G1} + X_{FITC} \cdot P_{G2'})) M_i A 10^{18} (n_{i1} + X_{FITC} \cdot n_{i2'})}$$

Use of calculated P_G versus observed P_G to
calculate loading values.

P_G is the total weight percent of all the species on the surface of the glass, in other words, the weight of percent due to the average surface group.

P_G can readily be calculated if the empirical formula of the average surface group is assumed. For example, a surface group which contains only C, H and N has a relative molecular weight which is given by:

$$M_G = \frac{n_C M_C + n_N M_N + n_H M_H}{\sum (n_i \cdot M_i)}$$

Since M_G is known, P_G can be calculated if the weight percent of a single species i is known:

$$P_{G,i} = \frac{P_i \cdot M_G}{n_i \cdot M_i}$$

where

P_i	=	observed weight percent of species i .
G	=	surface group
M	=	Molecular or atomic mass
n_i	=	number of atoms of species i in the surface group

The loading of an individual species, L_i , is calculated from expression 2 given in section 5.3.2. Consequently there are two ways to calculate the loading values for each of the surface species, from the *observed* weight percents:

$$L_i = f(P_{G,obs})$$

or from the *calculated* weight percents:

$$L_i = f(P_{G,i})$$

By definition, the values of P_G calculated from each of the observed weight percents of the individual surface species should, *in the ideal case*, be identical to each other and should be equal to the sum of the individual P_i recordings, *viz*:

$$P_{G,C} = P_{G,H} = P_{G,N} (= P_{G,i})$$

and

$$P_{G,i} = \sum P_i$$

But in order to calculate L_i the molecular formula of the surface group must be known or assumed. However, the difference (error) between L_i and L_i is small enough to ignore (see tables V.5a and V.5b) so the *observed* total weight percent was used in loading calculations throughout.

Stage 1 values. The loading values are calculated using observed data.

Assumptions :- Specific surface area of support, A: 32.4 m²/g

Empirical formula of surface group :

C :	3
H :	8
O :	0
N :	1
S :	0
MOL WTS:	58.1029

Table 5.3 Stage 1 Loading Values: using PGlobs.
(empirical formula of surface group not used in the calculation of the loading values).

PClobs = percentage carbon (stage 1) recorded by CHN analysis.

LC1 = calculated carbon loading using equation 2 (Stage 1: XFITC = 0).

PGlobs = total percentage weight loss recorded by CHN analysis.

PG1(C1) = calculated percentage total weight loss due to surface group based on PClobs data.

[For "N" or "H" instead of "C", read "nitrogen" or "hydrogen" respectively in place of "carbon"]

Exp	PClobs	PNlobs	PHlobs	LC1	LN1	LH1	PGlobs
1.2	1.51	0.47	0.55	23.98	6.40	104.07	2.53
2.1	0.85	0.27	0.61	13.39	3.65	114.49	1.73
2.2	1.77	0.59	0.76	28.28	8.08	144.69	3.12
2.3	1.45	0.48	0.70	23.05	6.54	132.59	2.63
3.1	0.80	0.20	0.38	12.55	2.69	71.07	1.38
3.2	2.66	0.92	0.83	43.07	12.77	160.15	4.41
4.1	0.72	0.18	0.44	11.29	2.42	82.25	1.34
6.2	1.66	0.55	0.53	26.42	7.51	100.51	2.74
7.1	0.76	0.19	0.32	11.91	2.55	59.78	1.27
7.2	0.95	0.27	0.32	14.93	3.64	59.94	1.54
8.1	0.73	0.19	0.35	11.44	2.55	65.38	1.27
8.2	1.15	0.31	0.41	18.14	4.19	77.06	1.87
9.2	0.85	0.25	0.40	13.36	3.37	74.90	1.50
10.1	0.66	0.18	0.30	10.33	2.42	55.97	1.14
10.2	2.27	0.77	0.65	36.48	10.61	124.48	3.69
Avg	1.253	0.388	0.503	19.91	5.29	95.16	2.14
Ratio	3.23	1.00	1.30	3.76	1.00	17.98	

PC1 vs PN1:-

Regression Output:

Constant	0.23039802
Std Err of Y Est	0.04801489
R Squared	0.99438384
No. of Observations	15
Degrees of Freedom	13
X Coefficient(s)	2.63471
Std Err of Coef.	0.05491

Use of calculated P_G versus observed P_G to
calculate loading values.

P_G is the total weight percent of all the species on the surface of the glass, in other words, the weight of percent due to the average surface group.

P_G can readily be calculated if the empirical formula of the average surface group is assumed. For example, a surface group which contains only C, H and N has a relative molecular weight which is given by:

$$M_G = \frac{n_C M_C + n_N M_N + n_H M_H}{\sum (n_i \cdot M_i)}$$

Since M_G is known, P_G can be calculated if the weight percent of a single species i is known:

$$P_{G,i} = \frac{P_i \cdot M_i}{n_i \cdot M_i}$$

where

P_i	=	observed weight percent of species i .
G	=	surface group
M	=	Molecular or atomic mass
n_i	=	number of atoms of species i in the surface group

The loading of an individual species, L_i , is calculated from expression 2 given in section 5.3.2. Consequently there are two ways to calculate the loading values for each of the surface species, from the *observed* weight percents:

$$L_i = f(P_{G,obs})$$

or from the *calculated* weight percents:

$$L_i = f(P_{G,i})$$

By definition, the values of P_G calculated from each of the observed weight percents of the individual surface species should, *in the ideal case*, be identical to each other and should be equal to the sum of the individual P_i recordings, viz:

$$P_{G,C} = P_{G,H} = P_{G,N} (= P_{G,i})$$

and

$$P_{G,i} = \sum P_i$$

But in order to calculate L_i , the molecular formula of the surface group must be known or assumed. However, the difference (error) between L_i and L_i' is small enough to ignore (see tables V.5a and V.5b) so the *observed* total weight percent was used in loading calculations throughout.

Table V.5a Loading values, L_i' , calculated from the values of the weight percent of the surface group, $P_{G,i}$, deduced assuming the empirical formula of the surface group.

	E	F	G	H	I	J	K
33	LC1	LN1	LH1	PG1obs	PG1(C1)	PG1(N1)	PG1(H1)
34							
35	23.99	6.40	103.87	2.53	2.58	2.60	2.34
36	13.35	3.64	115.51	1.73	1.45	1.49	2.60
37	28.25	8.09	144.86	3.12	3.03	3.26	3.24
38							
39	Empirical formula of surface groups :					Average obs wt	
40	1st grp			1st grp			
41	C :			3.76496	0.104293	1.252666	
42	H :			18.0277	0.499388	0.503333	
43	O :			0	0		
44	N :			1	0.027701	0.388	
45	S :			0	0		
46	MOL WTS:			77.3978	2.144		
47	OPEN						
48	10.33	2.41	56.05	1.14	1.13	0.99	1.28
49	36.55	10.67	123.30	3.69	3.89	4.25	2.77
50							
51	<u>19.91</u>	<u>5.30</u>	<u>95.10</u>	2.14	2.14	2.14	2.14
52	3.7554	1.0000	17.9346				

Table V.5b Loading values, L_i' , calculated from the observed weight percent values of the surface group, $P_{G,obs}$. No assumption made of surface group.

	E	F	G	H	I	J	K
30	LC1	LN1	LH1	PG1obs	PG1(C1)	PG1(N1)	PG1(H1)
31							
32	23.98	6.40	104.07	2.53	ERR	ERR	ERR
33	13.39	3.65	114.49	1.73	ERR	ERR	ERR
34	28.28	8.08	144.69	3.12	ERR	ERR	ERR
35							
36	Empirical formula of surface group :					Average obs wt	
37	C :			0	1.253		
38	H :			0	0.503		
39	O :			0	0		
40	N :			0	0.388		
41	S :			0	0		
42	MOL WTS:			0	2.144		
43	OPEN						
44	10.33	2.42	55.97	1.14	ERR	ERR	ERR
45	36.48	10.61	124.48	3.69	ERR	ERR	ERR
46							
47							
48	<u>19.91</u>	<u>5.29</u>	<u>95.16</u>	2.14	ERR	ERR	ERR
49	3.76	1.00	17.98				

7.2.4	0.75	0.22	0.37	11.77	2.96	69.17	1.34
8.1.1	0.72	0.16	0.46	11.29	2.15	85.99	1.34
8.1.4	0.61	0.15	0.44	9.56	2.01	82.14	1.20
8.2.1	0.94	0.26	0.48	14.80	3.51	90.04	1.68
8.2.4	0.9	0.23	0.46	14.15	3.10	86.21	1.59
9.2.1	0.93	0.21	0.44	14.62	2.83	82.46	1.58
9.2.2	0.73	0.2	0.42	11.45	2.69	78.52	1.35
9.2.3	0.7	0.19	0.38	10.97	2.55	70.99	1.27
9.2.4	0.92	0.19	0.43	14.46	2.56	80.55	1.54
10.1.1	0.62	0.15	0.37	9.71	2.01	69.03	1.14
10.1.2	0.6	0.15	0.37	9.39	2.01	69.02	1.12
10.1.4	0.58	0.14	0.37	9.08	1.88	68.99	1.09
10.2.1	1.45	0.43	0.53	23.00	5.85	100.17	2.41
10.2.2	1.29	0.42	0.51	20.42	5.70	96.20	2.22
10.2.4	1.37	0.41	0.53	21.70	5.57	100.06	2.31
10.2.4	1.37	0.41	0.53	21.70	5.57	100.06	2.31

Avg	0.907	0.263	0.518	14.298	3.563	97.281	1.688
Ratios	3.44	1.00	1.97	4.0134	1.00	27.31	

Ratio $LC2/LN2 = (PC.M_N)/(PN.M_C)$ 4.0151

PC2 vs PN2:-

Regression Output:

Constant	0.19193226
Std Err of Y Est	0.07368978
R Squared	0.94524739
No. of Observations	45
Degrees of Freedom	43

X Coefficient(s) 2.71418

Std Err of Coef. 0.09961

Stage 2 values. The loading values are calculated using observed data.

Assumptions :- Specific surface area of support, A: 32.4 m²/g

Empirical formula of surface groups :	X_FITC:	0.00926	
	1st grp	2nd grp	Stage 2 grp
C :	3	21	3.19446
H :	8	11	8.10186
O :	0	5	0.0463
N :	1	1	1.00926
S :	0	1	0.00926
MOL WTS:	58.103	389.382	61.709

Table 5.3 Stage 2 Loading Values: use PG2obs.
(empirical formula of the surface group not used in
the calculation of the loading values).

PC2obs = percentage carbon (stage 2) recorded by CHN analysis.
LC2 = calculated carbon loading using equation 2 (Stage 2: XFITC = as above).
PG2obs = total percentage weight loss recorded by CHN analysis.
PG(C2) = calculated percentage total weight loss due to surface group based on
PC1obs data and assumed empirical formula for surface group.

[For "N" or "H" instead of "C", read "nitrogen" or "hydrogen" respectively in place of "carbon"]

Exp	PC2obs	PN2obs	PH2obs	LC2	LN2	LH2	PG2obs
1.2.1	1.17	0.36	0.68	18.52	4.89	128.25	2.21
1.2.2	1.12	0.34	0.67	17.71	4.61	126.26	2.13
2.1.1	0.69	0.21	0.63	10.85	2.83	118.00	1.53
2.1.2	0.67	0.21	0.63	10.53	2.83	117.98	1.51
2.1.4	0.64	0.22	0.62	10.05	2.96	116.07	1.48
2.2.1	1.21	0.38	0.74	19.17	5.16	139.74	2.33
2.2.2	1.17	0.38	0.69	18.52	5.16	130.18	2.24
2.2.4	1.15	0.38	0.74	18.21	5.16	139.65	2.27
2.3.1	1.02	0.34	0.7	16.12	4.61	131.82	2.06
2.3.2	1.08	0.34	0.7	17.08	4.61	131.90	2.12
2.3.3	1.07	0.35	0.76	16.93	4.75	143.30	2.18
2.3.4	1.12	0.34	0.75	17.73	4.61	141.45	2.21
3.1.1	0.58	0.16	0.44	9.08	2.15	82.12	1.18
3.1.4	0.61	0.18	0.45	9.56	2.42	84.04	1.24
3.2.1	1.66	0.53	0.67	26.45	7.24	127.21	2.86
4.1.1	0.53	0.15	0.49	8.30	2.01	91.44	1.17
4.1.4	0.58	0.16	0.48	9.09	2.15	89.62	1.22
4.2.1	1.49	0.49	0.71	23.70	6.68	134.57	2.69
5.1.1	0.62	0.16	0.42	9.71	2.15	78.40	1.20
5.1.2	0.6	0.14	0.45	9.40	1.88	84.00	1.19
5.1.4	0.59	0.14	0.4	9.24	1.88	74.62	1.13
5.2.1	1.29	0.34	0.53	20.41	4.61	99.91	2.16
5.2.4	1.19	0.39	0.5	18.81	5.29	94.18	2.08
6.2.1	1.16	0.36	0.53	18.33	4.88	99.80	2.05
7.1.1	0.6	0.15	0.38	9.39	2.01	70.89	1.13
7.1.2	0.58	0.16	0.38	9.08	2.15	70.88	1.12
7.1.4	0.6	0.15	0.36	9.39	2.01	67.14	1.11
7.2.1	0.83	0.21	0.36	13.03	2.83	67.34	1.40
7.2.2	0.7	0.21	0.36	10.97	2.82	67.25	1.27

LIST OF PUBLICATIONS AND PRESENTATIONS

1. Badini G.E., Grattan K.T.V., Tseung A.C.C. and Palmer A.W. *Conference on Lasers and Electro-Optics (CLEO)*, 1989.
2. Badini G.E., Grattan K.T.V., Tseung A.C.C. and Palmer A.W. *The Sixth International Conference on Optical Fibre Sensors*, 1989.
3. Grattan K.T.V., Badini G.E., Palmer A.W. and Tseung A.C.C. *Sens. Actuators A26*, **483(1991)**.
4. Badini G.E., Grattan K.T.V. and Tseung A.C.C. "Sol-Gel Substrates for Fibre-Optic Chemical Sensors - Effects of preparation, aging and long-term storage" *Submitted for Review Prior to Publication, 1994*.
5. Badini G.E., Grattan K.T.V. and Tseung A.C.C. "Impregnation of pH-Sensitive Dye into Sol-Gels for Fibre Optic Chemical Sensors" *Submitted for Review Prior to Publication, 1994*.



LIST OF PUBLICATIONS AND PRESENTATIONS

1. Badini G.E., Grattan K.T.V., Tseung A.C.C. and Palmer A.W. *Conference on Lasers and Electro-Optics (CLEO)*, 1989.
2. Badini G.E., Grattan K.T.V., Tseung A.C.C. and Palmer A.W. *The Sixth International Conference on Optical Fiber Sensors*, 1989.
3. Grattan K.T.V., Badini G.E., Tseung A.C.C. and Palmer A.W. *Sens. Actuators* **A26**, 483(1991).
4. Badini G.E., Grattan K.T.V., Tseung A.C.C. "Sol-Gel Substrates for Fibre-Optic Chemical Sensors - Effects of Preparation, Aging and Long-Term Storage" *Submitted for Review Prior to Publication*, 1994.
5. Badini G.E., Grattan K.T.V., Tseung A.C.C. "Impregnation of pH-Sensitive Dye into Sol-Gels for Fibre-Optic Chemical Sensors" *Submitted for Review Prior to Publication*, 1994.